

CHAPTER ONE

INTRODUCTION AND LITERATURE REVIEW

1.0 INTRODUCTION

Oil is the life blood of any modern industrial society. It fuels the machineries and lubricates the wheels of the world's production. It is one of the most important energies and raw material sources for synthetic polymers and chemicals worldwide (Hussein *et al.*, 2008; Annunciado *et al.*, 2005).

Whenever oil is explored, transported and stored and its derivatives are used, there is risk of spillage with potential to cause significant environmental impact (Hussein *et al.*, 2008).

Due to its destructive properties, once an area has been contaminated with oil, the whole character of the place is damaged and when it encounters something to cling to, whether it be a beach, a rock, the feathers of a duck or a bathers hair, it does not readily let go (Aynechi, 2004). Hence, pollution by petroleum oils affects sea life, economy, tourism and leisure activities because of the coating properties of these materials (Hussein *et al.*, 2008).

The adverse impact to ecosystems and the long term effect of environmental pollution call for an urgent need to develop a wide range of materials for cleaning-up oil from oil impacted areas especially as the effectiveness of oil treatment varies with time, the type of oil and spill, the location and weather conditions (Adebajo *et al.*, 2003).

Huge amounts of agricultural wastes (corn cob and mango kernel) are produced in many countries of the world. However, only a fraction of these materials are reused. One of the features of these organic materials is that it can absorb by capillary forces an amount of oil and/or water greater than its own weight (Bodirlau and Teaca, 2009). In addition this natural material can be completely degraded in nature by biological, physical, chemical and

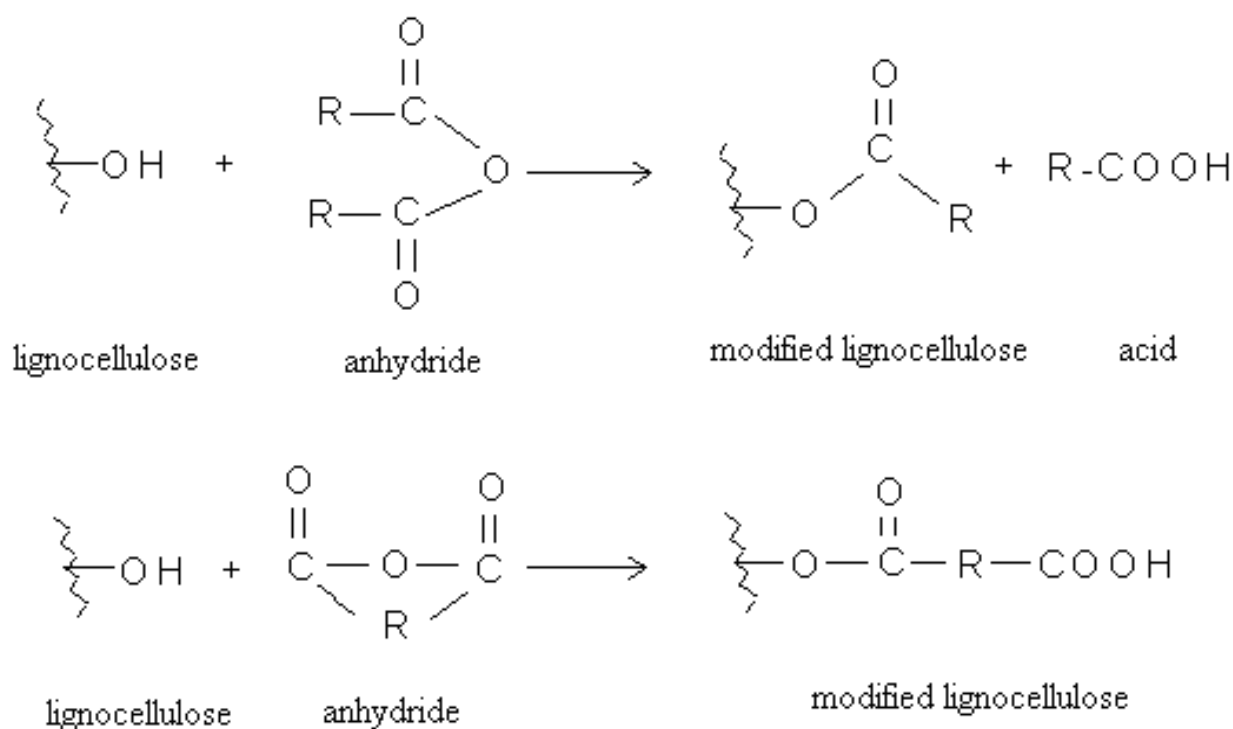
photochemical processes (Tronc *et al.*, 2006). In the past two decades, the reuse of agricultural byproducts as oil sorbents has received growing attention due to their low cost and biodegradability (Adebajo *et al.*, 2003). Most agricultural byproducts derived from plants such as bagasse, coir, kenaf, rice straw, sisal and saw dust have been investigated for oil spill cleanup application (Choi and Cloud, 1992). The main drawbacks of these plant-derived sorbents are a relatively low oil sorption capacity, low hydrophobicity and poor buoyancy compared to synthetic sorbents such as polypropylene (Bayat *et al.*, 2005; Anunciado *et al.*, 2005).

Once plant-derived sorbents are applied to saturated environments, preferential water sorption is favoured over the sorption of oil because the sorbents are generally hydrophilic in nature. A better understanding of the chemical composition of these natural fibers is necessary for developing natural fiber sorbents. Agricultural byproducts can be considered polymeric composites made up primarily of cellulose, hemicellulose and lignin (Kumar, 1994; Homan *et al.*, 2000). These polymers make up the cell wall and are responsible for most of the physical and chemical properties exhibited by these materials (Bodirlau and Teaca, 2009). Agricultural byproducts have a well-documented problem of water sorption and lack of dimensional stability, due to associated hydroxyl functionality. These groups are abundantly available in all the three major chemical components of plant based materials and are responsible for their hydrophilicity (Bodirlau and Teaca, 2009).

Hydrophobicity (oleophilicity) is one of the major determinants of sorbents properties influencing the effectiveness of oil sorption in the presence of water. The effectiveness of the sorbents in saturated environments would be enhanced if the density of the hydroxyl functionality is decreased (Bodirlau and Teaca, 2009). This functional group (hydroxyls) is

the most reactive and abundant site in the cell wall polymers of the lignocellulosic materials. The hydroxyl functionality of these fibers can be reduced by chemical modification such as acetylation, methylation, cyanoethylation, benzylation, acrylation and acylation (Hofle *et al.*, 1978; Sun *et al.*, 2004; Breitenbeck *et al.*, 2007).

The acetylation reaction is one of the most common techniques used for hydrophobic treatment of lignocellulosic materials (eg. wood) by a substitution reaction of a hydroxyl group (hydrophilic) into an acetyl group (hydrophobic) as shown in Figure 1.1. This reaction is usually carried out by heating lignocellulosic material in the presence of acetic anhydride with or without catalyst (Rowel *et al.*, 1994). Various catalysts have been used for enhancing the efficiency of acetylation reactions. Pyridine and 4-dimethyl amino pyridine (DMAP) have been commonly applied for acetylation for many years (Hofle *et al.*, 1978). However, they are too toxic and/or expensive for commercial use. Sun *et al.*, (2004), recently reported that acetylation of sugarcane bagasse with N- bromosuccinimide (NBS) as catalyst in a solvent-free system was a convenient and effective method. In addition, they claimed modified bagasse applied in oil-water system presented an enhanced oil sorption capacity exceeding that of commercial synthetic sorbents.



Source: Bodirlau and Teaca, 2009

Figure 1.1. Scheme of reaction of acetic anhydride with lignocellulose

1.1 Justification for the Research

Residents of wetlands like the Nigeria's Niger delta are concerned about the environmental impact of residual oil spill into receiving surface waters and land. The adverse effect of oil spill to the ecosystem and the long term effect of environmental pollution call for an urgent need to develop a wide range of materials for cleaning up oil from oil impacted areas (Adebajo and Frost, 2004a). Absorbent materials are attractive for some applications because of the possibility of collection and complete removal of the oil from the oil spill site. The possibilities of cleaning oil pollution by sorbent on the basis of fibres, polymers and wood products, however, have not yet been sufficiently investigated (Nenkova *et al.*, 2004).

No known work has been done on the acetylation of corn cob and mango kernel and its application in oil spill cleanup application. The potential input of this research, to the environment includes;

1. Treatment of water resources from oil spillage, thereby conserving the natural mangroves, water supply and reducing the incidence of forest wildfires which occurs as a result of accumulated crude oil residue in the mangroves
2. Conversion of undervalued agricultural waste residues, such as corn cobs and mango kernel to valuable sorption media which has the potential of providing economic incentives.
3. Application of the chemistry of the modification procedure in the development and improvement of other agro-based residues for several other applications.
4. Utilization of biodegradable materials for oil spill clean-up to provide sustainable operations and development.
5. Reduction of over dependence on imported products.

1.2 Aim and Objectives

The purpose of this study broadly consists of modifying corn cob and mango kernel by acetylation using N-bromosuccinimide as catalyst, under mild reaction conditions, so as to enhance the hydrophobic character of these wastes, for subsequent application as sorbents for oil spill cleanup. Specific objectives of this work include;

1. Kinetics and therefore the mechanism of acetylation.
2. Thermodynamics of acetylation.
3. The effect of catalyst on acetylation.

4. The effect of acetylation on water absorption water absorption capacity of modified materials.
5. The effect of acetylation on the structure of the modified materials
6. Kinetics and therefore mechanism of crude oil sorption.
7. Statistical determination of significant variables.

1.3 Scope of Study

This study is limited to chemical modification by acetylation and subsequent trial in oil spill cleanup application. Techniques used in this study are Fourier Transform-Infrared spectrometry, X-ray Diffractometry, X-ray Fluorescence and Gravimetry. These techniques enabled the determination of structural changes, extent of acetylation, % crystallinity, elemental and physical composition of the materials and oil sorption capacity. Variables (time and temperature) used in this study enabled the investigation of the mechanisms of reaction and thermodynamics of the study. Statistical tools used enabled the determination of the statistical differences.

1.4 LITERATURE REVIEW

1.4.1 Oil Spillage

Whenever oil is explored, transported and stored, and its derivate are used, there is a risk of oil spillage with the potential to cause significant environmental impact (Hussein *et al.*, 2008). Pollution by petroleum oils affects sea life, economy, tourism and leisure activities because of the coating properties of these materials. Oil spills harm the beauty of polluted sites; the strong odour can be felt miles away and excessive growth of green algae alters

the sea colour and the landscape (Annunciado *et al.*, 2005). The nature and magnitude of oil spills on water habitats depend on the rate of water flow and the habitat's specific characteristics. Where there is proximity of high density human population, when these spills occur, human health and environmental quality are put at risk (Frost *et al.*, 2007).

1.4.2 Oil spillage in the Nigerian Niger-Delta

Nigeria boasts of over 21 billion barrels of proven oil reserves. Nigeria is Africa's largest oil producer and the world's sixth most important exporter of crude oil with the bulk of its export going to the United States. Today, the Niger Delta is best known as the region that sustains much oil exploration and exploitation by the agents of western economic powers. The Niger-Delta basin is considered the mainstay of the Nigerian economy to its significantly high level of oil reserves. The region is also naturally endowed with viable deposits of hydrocarbons and gas reserves. Petroleum and derivatives dominate the Nigerian economy making about 98 percent of government annual revenue, 80 percent of foreign exchange revenue and 70 percent of budgetary expenditure (Friends of the Earth Netherlands, 2009; UNDP, 2006).

For decades, oil spill have devastated the fertile environment of the Niger-Delta. According to available statistics (SPDC, 2006), in the last 30 years, more than 400,000 tons of oil have been spilled into creeks and soils of southern Nigeria. Some 70 percent of the oil has not been recovered (UNDP, 2006). The vast majority of the spill are consequently of aging facilities and human errors. In January 2008, the Nigerian National Oil Spill Detection and Response Agency (NOSDRA) declared that it had so far located more than 1130 oil spill sites abandoned by various oil companies within the Niger Delta (Anonymous, 2008).

The Niger Delta is situated in the south of Nigeria and is a huge fertile wetland.

Subsistence farming and fishing is the mainstay of the people. Inhabited by more than 3000 long settled communities, the present population figures of the Niger Delta is estimated to be 27million, but its air, water, soil and forest resources have been devastated by the exploitation of oil and gas resources, particularly from gas flares and oil spills (UNDP, 2006). In the period of 1997-2006, according to its own report, Shell Nigeria experienced about 250 oil spills each year (SPDC, 2006). Shell claims some 60 percent are consequences of sabotage.

Oil spill incidences have occurred in various parts and at different times along the Niger Delta coast. According to the Departments of Petroleum Resources (DPR), between 1976 and 1996, a total of 4647 incidents resulted on the spill of approximately 2,369,470 barrels of oil into the environment (Badejo and Nwilo, 2004). Some major spills in the coastal zones are the COCON's Escravos terminal tank failure in 1978 of about 580,000 barrels and Texaco funiwa-5 blow out in 1980 of about 400,000 barrels. Other oil spill incidences are those of Abudu pipeline in 1982 of about 18,818 barrels, the Jesse fire incidence which claimed about a thousand lives and the Idaho oil spill of January 1998. The most publicized of all oil spills in Nigeria occurred on January 17 1980 when a total of 37 million liters of crude oil got spilled into the environment. The spill occurred as a result of a blow out at funiwa-5 offshore station (Badejo and Nwilo, 2004). Table 1.1 shows a summary of some major oil spill incidences in the Niger Delta from 1979 to 2004.

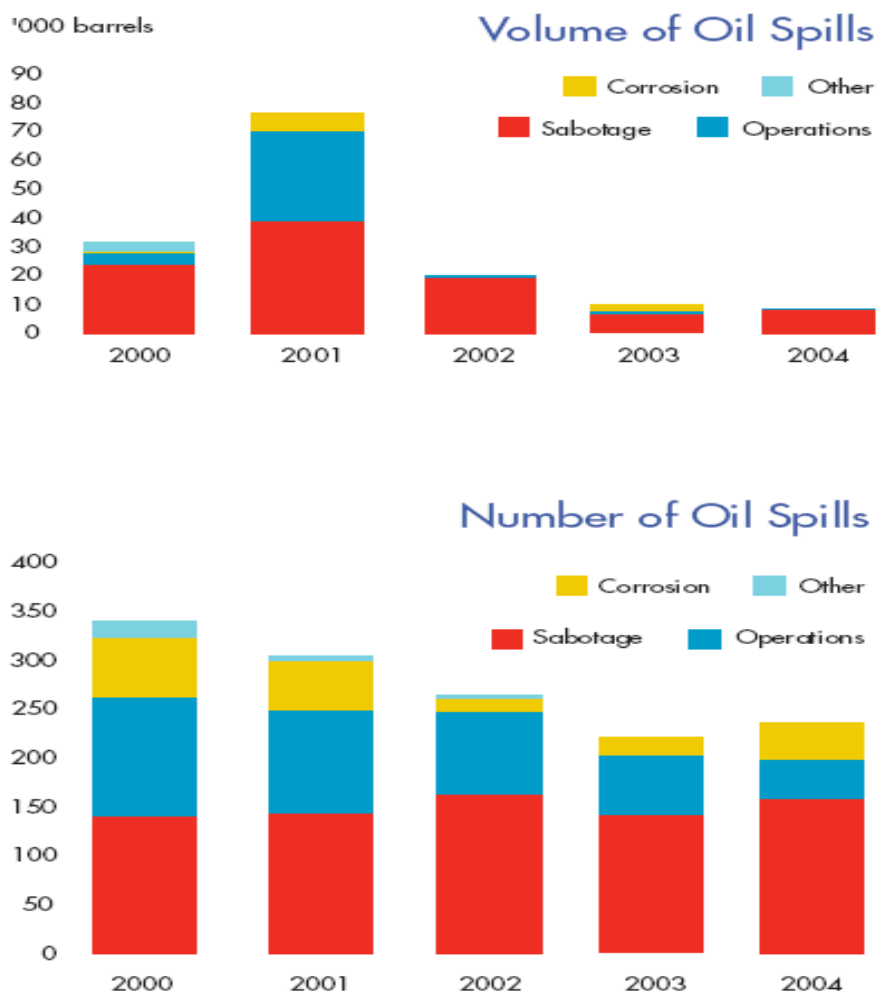
Table 1.1: Summary of some major oil spills in the Niger Delta

Date	Episode	State	Quantity (Barrels)
July, 1979	Forcados terminal oil spillage	Rivers	570,000
Jan, 1980	Funiwa No. 5 well blowout	Rivers	400,000
May, 1980	Oyamaka oil spillage	Rivers	10,000
	System 2c pipeline rupture at Abudu		
Nov, 1982	Edo	Warri-Kaduna	18,000
Aug, 1983	Osika oil spill	Rivers	10,000
Jan, 1998	Idoho oil spill	Akwa Ibom	40,000
Jan, 1998	Jones creek	Delta	21,548
Oct, 1998	Jesse oil spill	Delta	10,000
May, 2000	Etiama oil spill	Bayelsa	11,000
Dec, 2003	Aghada oil spill		
Aug, 2005	Ughelli oil spill	Delta	10,000
Aug, 2004	Ewan oil spill	Ondo	

Source: Eka and Udoyong (2003); UNDP (2006).

With the expansion of oil production, the incidences of oil spills have increased considerably in the region. Available records show that a total of 6817 oil spills occurred between 1976 and 2001 with a loss of approximately 3million barrels of oil. More than 70 percent was not recorded. Approximately 6 percent spilled on land and 25 percent in swamps and 69 percent in offshore environments. In recent times, oil spill appears to be caused more by willful damage to facilities than by accidents (UNDP, 2006). Figure 1.2

shows the causes of oil spills, the influence, the quantity and number of oil spills.

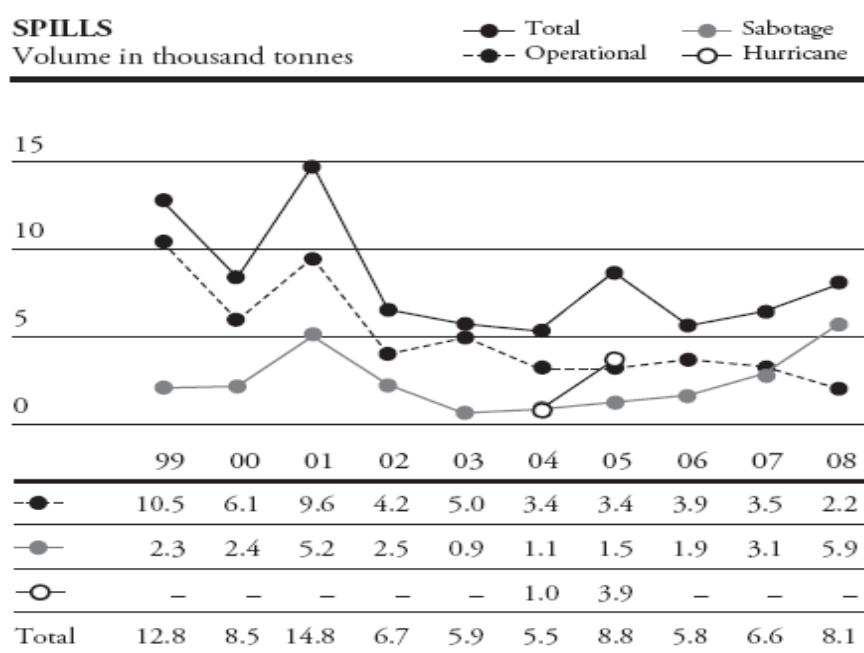


Source: Shell Petroleum Development Company Annual Report 2004.

Figure 1.2: Quantities and Causes of Oil Spills from SPDC Operations in the Niger Delta, 2000-2004

According to Badejo and Nwilo, (2004), fifty percent of oil spills is due to corrosion, twenty eight percent to oil productions operations, One percent to oil drill is due to engineering drills, inability to effectively control oil wells, failure of machines and inadequate care in loading and unloading oil vessels. Shell Petroleum Development Company (SPDC), in their 2009 annual report (Royal Dutch Shell Petroleum Plc, 2009) went further to project an increase in oil spill incidences in Nigeria as shown in Figure 1.3. This shows that spill incidences from production operations are more than other causes but an oil spill trend

from sabotage is gradually increasing over operational spills.



Source: Royal Dutch Shell Petroleum Plc. annual report, 2009

Figure 1.3: Trends in oil spill incidences in the Niger Delta

1.4.3 Nigerian Law on Oil Spillage

Nigerian law concerning oil spill is fairly clear. One significant intervention was the establishment of the Federal Environmental Protection Agency (FEPA) in 1988 to enforce environmental regulations and ameliorate environmental degradation (UNDP, 2006). The Nigerian Federal Environmental Protection Agency act of 1988 orders that following an oil spill, oil companies should “begin immediate cleanup operations following the best available cleanup practice and removal methods”.

The oil pipelines act of 1990 states that oil companies should pay compensation to any person suffering damage as a consequence of any breakage or a leakage from the pipeline or and ancillary installation (except when the spill is the result of the malicious act of a third person (Friends of the Earth Netherlands, 2009).

The Nigerian Petroleum Act of 1969 states that oil and gas production shall conform to good oilfield practice, according to American standards.

1.4.4 Effect of Oil Spillage in the Environment

Depending on its form and chemistry, oil can cause an array of physiological and toxic effects for example; benzene is a carcinogen and is toxic to humans and wildlife (USACE, 2005). Some hydrocarbons are toxic to organisms but less persistent in the environment, while others tend to be less toxic, but more persistent and more likely to result in long term environmental effects (UNDP, 2006).

The environmental effects of oil spillage are well known. They include the degradation of forest and the depletion of aquatic fauna. Long term impacts are also possible, as in the case where mangrove swamps and ground water resources are harmed (Lee *et al.*, 1999).

Although the situation is improving with more stringent environmental regulations for the oil industry, marine pollution is still a serious problem. The harmful effects on the environment are many. Oil kills plants and animals in the estuarine zones. Oil settles on beaches and kills organisms that lie there. It also settles on ocean floors and kills benthic (bottom dwelling) organisms such as crab (Badejo and Nwilo, 2004; UNDP, 2006).

Oil poison algae, disrupts major food chain and decreases the yield of edible crustaceans. It also coats birds, impairing their flight and reducing the insulative properties of their feathers, thus making the birds more vulnerable to cold. Oil endangers fish hatcheries in coastal areas as well as contaminates the flesh of commercially valuable fish (Badejo and Nwilo, 2004).

The spilled oil contributes an undesirable taste and odor to drinking water and causes severe environmental damage. Contaminated water cannot be used for municipal water

supply, for industry nor irrigation. Public concern for sustaining a healthy environment has resulted in stronger environmental regulations regarding water quality and use of hazardous chemicals and substances (Lee *et al.*, 1999).

The implication of these findings is frightening given that human health is tied to the food web. Udoette, (1997) reported, that ingestion of hydrocarbon directly or indirectly through contaminated food, leads to poisoning. Some researchers such as Kanoh *et al.*, (1990), Snyder and Hedlim, (1996) and Eyong *et al.*, (2004) have documented toxic and carcinogenic effects of exposures to high concentrations of hydrocarbons (UNDP, 2006).

Soil and water contamination by hydrocarbons from leaking storage tanks and improper disposal of hazardous waste are of concerns worldwide. Petroleum hydrocarbons are responsible for 65% of all contaminated groundwater sites (Ramos Vianna *et al.*, 2004). If proper remediation measures are not taken, the organic pollutants released from gasoline spills can lead to surface and ground water contamination, which can be potentially toxic to biota and humans.

Oil spill cleanup in wetlands is problematic because of the limited remediation techniques that can be applied in such environments (Chung and Venosa, 2008). Remediation of wetland ecosystems impacted by crude oil spills is a challenging task because often times, the response can be more destructive than the spill itself (Venosa *et al.*, 2002).

Implications of these findings are important for the cleanup of oil contaminated wetlands.

Also, it is clear from spills and also field and laboratory studies (Wardrop *et al.*, 1996; Duke *et al.*, 2000; Shigenaka, 2002), that at least in many circumstances, oil harms or kills mangroves. What is less obvious is how that harm occurs and the mechanism of toxicity. Although there are some consensus that oil causes physical suffocation and toxicological or physiological impacts, researchers disagree as to the relative contribution of each

mechanism which may vary with type of oil and time since the spill (Proffitt *et al.*, 1997). Investigations from many spill events around the world have shown that mangroves suffer both lethal and sub lethal effects from oil exposure.

One of the universal challenges faced by researchers when dealing with oil impacts is the fact that oil is a complex mixture of many kinds of chemicals. The oil spilled in one incident is almost different from that spilled in another. In addition, oils within broad categories like "crude oil" or diesel can be vastly different, depending on the geological source of the original material, refining processes and additives incorporated from transportation in barges or tankers. Even if we could somehow stipulate that all spilled oil was to be of a single fixed chemical formulation, petroleum products released into the environment are subjective to different processes of weathering that immediately begin altering its original physical and chemical characteristics. As a result, samples of oil of exactly the same source can be different in composition after being subjected to a different mix of environmental influences.

Similar to the oil toxicity situation for many other intertidal environments, the mangrove-related biological resources at risk in a spill situation can be affected in at least two principal ways: First from physical effects; second, the true toxicological effects of the petroleum (Shigenaka, 2002). As the crude oil is a very complex mixture of many different chemicals, consequently the effect of an oil spill on the marine environment is dependent on the exact nature and quantity of the oil spilled as well as such other factors as the prevailing conditions and the ecological characteristics of the effected region (Sayed *et al.*, 2004). Many oil products are highly viscous. In particular, crude oils and heavy fuels oils can be deposited on shorelines and shoreline resources in thick, stick layers that may either disrupt or completely prevent normal biological process of exchange with the

environment. These hydrocarbon spills damage marine ecosystem and cause wide spread contamination of the surrounding environment. The contamination of shorelines generally has the greatest environmental and economic impact due in part to the difficulties of cleanup measures (Frost *et al.*, 2007).

Even if a petroleum product is not especially toxic in its own right, when oil physically covers plant and animals they may die from suffocation, starvation or other physical interferences with normal physiological function. The lighter or lower molecular weight aromatic hydrocarbons often are major components of oil mixtures and are also known to damage the cellular membranes in subsurface roots: this in turn could impair salt exclusion in those mangroves that have the root filters. Genetic damage is a more subtle effect of oil exposure but can cause significant impact at the population level. For example, researchers have linked the presence of polynuclear aromatic hydrocarbons (PAH) in soil to an increased incidence of a mangrove mutation in which chlorophyll is deficient or absent (Shigenaka, 2002).

1.4.5 The Toxic Content of Crude Oil

It has been noted by some people assisting in the clean-up operations that their health has been affected. The obvious effect of the spill is odour (many of these compounds have very low odour threshold), however, the other effects noted such as headaches or fatigues are all symptoms of the exposure of compounds such as polynuclear aromatic hydrocarbons (PAH) (Mobbs, 1996). Eyong *et al.*, (2004) reported that the ingestion of crude oil directly or indirectly, results in toxicity targeted at the hematopoietic system. There are a number of toxic compounds which are of concern since they are present in significant quantities within the oil (Mobbs, 1996). For example:

Toluene: Toluene is a known constituent of crude oil (Mobbs, 1996). Crude oil is by far the largest source of toluene (USEPA, 1994). The most important health concern for humans from either intentional or occupational exposures to toluene is its harmful effects on the nervous system. These effects of toluene depend on both the amount and length of exposure. Short term exposure to moderate amount of toluene, such as in elevated workplace exposures can produce fatigue, confusion, general weakness, drunken type actions, memory loss, nausea and loss of appetite, these symptoms disappear when exposure is stopped (ATSDR, 2008a). Teratological and epidemiological evidence relating toluene exposures to reproductive issues have also been reported (Louise, 1997; Bukowski, 2001). Effects on fertility such as abortion were reported in rabbits by inhalation (Vee Gee scientific, 2004). Phenolic compounds generated by petroleum and petrochemicals, coal conversion and phenol producing industries are common contaminants in wastewater (Ramos-Vianna, 2004).

Benzene: The major sources of benzene in water are at atmospheric deposition, spills from petroleum and other petroleum products and chemical plant effluents. Benzene is known to be a human carcinogen based on sufficient evidence in humans (IARC, 2005). Case report and case series have reported leukemia in individuals exposed to benzene. Benzene is harmful, especially to the tissues that form blood cells. In addition, human and animal studies indicate that benzene is harmful to the immune system, increasing the chance for infections and perhaps lowering the body's defense against tumor (Mobbs, 1996). Later studies reported that when administered, benzene by gavage, mice developed head and neck, thoracic cavity and subcutaneous sarcomas (French *et al.*, 2001; Hulla *et al.*, 2001). The United States Agency for Toxic Substance and Disease Registry (ATSDR) (1997) listed benzene as one of its top twenty toxic chemicals.

Cresols (a group of Phenolic compounds): When cresols are breathed, ingested or applied to the skin at very high levels, they can be very harmful. The US ATSDR (1997) has determined that cresols are possible carcinogens. Effects observed in people include irritation and burning of skin, eyes, mouth, and throat; abdominal pain and vomiting; heart damage; anemia; liver and kidney damage; facial paralysis; coma and even death (Mobbs, 1996). It is not known what the effects are from long-term ingestion or skin contact with low levels of cresols (ATSDR, 2008b).

Polynuclear Aromatic Hydrocarbons (PAH): The quantities of PAH's in crude oil is uncertain as there are particular types of PAH. As a pollutant, they are of concern because some have been identified as carcinogenic mutagenic and teratogenic (European Commission, 2002). Drinking water or swallowing food, soil or dust particle that contain PAH are other routes for these chemicals to enter the body. Under normal conditions of environmental exposure, PAH's could enter the body if skin comes into contact with soils that contains high level of PAH's. The department of health and human services had determined that PAH's may reasonably be anticipated to be carcinogens (ATSDR, 1996). Several of the PAH's are reported to have caused tumors in laboratory animals when they ate them, when they were applied to skin and when they breathed them in air for long periods of time (Adonis *et al.*, 2003; Armstrong *et al.*, 2004). Similar effects occur in humans.

The effect of these compounds may be showing up in those people most exposed to the oil slick and the accompanying air pollution – for example problems of fatigue, headache, nausea and skin rashes. It is important to note also that these substances are not only harmful by ingestion or inhalation, if the skin is exposed, they can be absorbed into the body – an obvious problem for those coming into direct contact with the oil (Mobbs, 1996).

1.4.6 Oil Spill Response Techniques

The serious environmental consequences of oil spills have long been recognized and considerable research and technological development has been carried out to develop appropriate remediation techniques (Sun *et al.*, 2004; Ventikos *et al.*, 2004). The objective of spill response in any habitat is to minimize the damage caused by the accidental and released oil (Yender, 2002). In clean-up operations, after oil spills, the first requirement is to contain the spills in as small an area as possible and prevent it from reaching water courses and thus contaminating their environment (Greene *et al.*, 1975). When significant deposits of oil were discovered in the 19th century, this fossil fuel appeared to offer a limitless source of energy to drive development. Oil spills and leaks along coastline pose risk to marine life and fishes and can threaten the livelihood of human communities (Burgeir *et al.*, 2002). Each year, 0.75-1.8 billion gallons of crude oil are unintentionally released into the environment (Burgeir *et al.*, 2002). Variables such as oil types whether location and availability of response equipment will determine initial spill response options. In the best case scenario, oil is prevented from moving into and contaminating mangrove areas. Promising on-water responses that can help prevent oil from reaching mangrove forest include chemical dispersant and in-situ burning. Potential benefits of oil removal must be weighed against the risk of potential harmful impacts from the clean-up techniques (Yender, 2002). There are five major options for responding to oil spills as shown in Figure 1.4: Mechanical containment, chemical treatment methods, in-situ burning, bio remediation and, natural removal (Mullin and Champ, 2003)

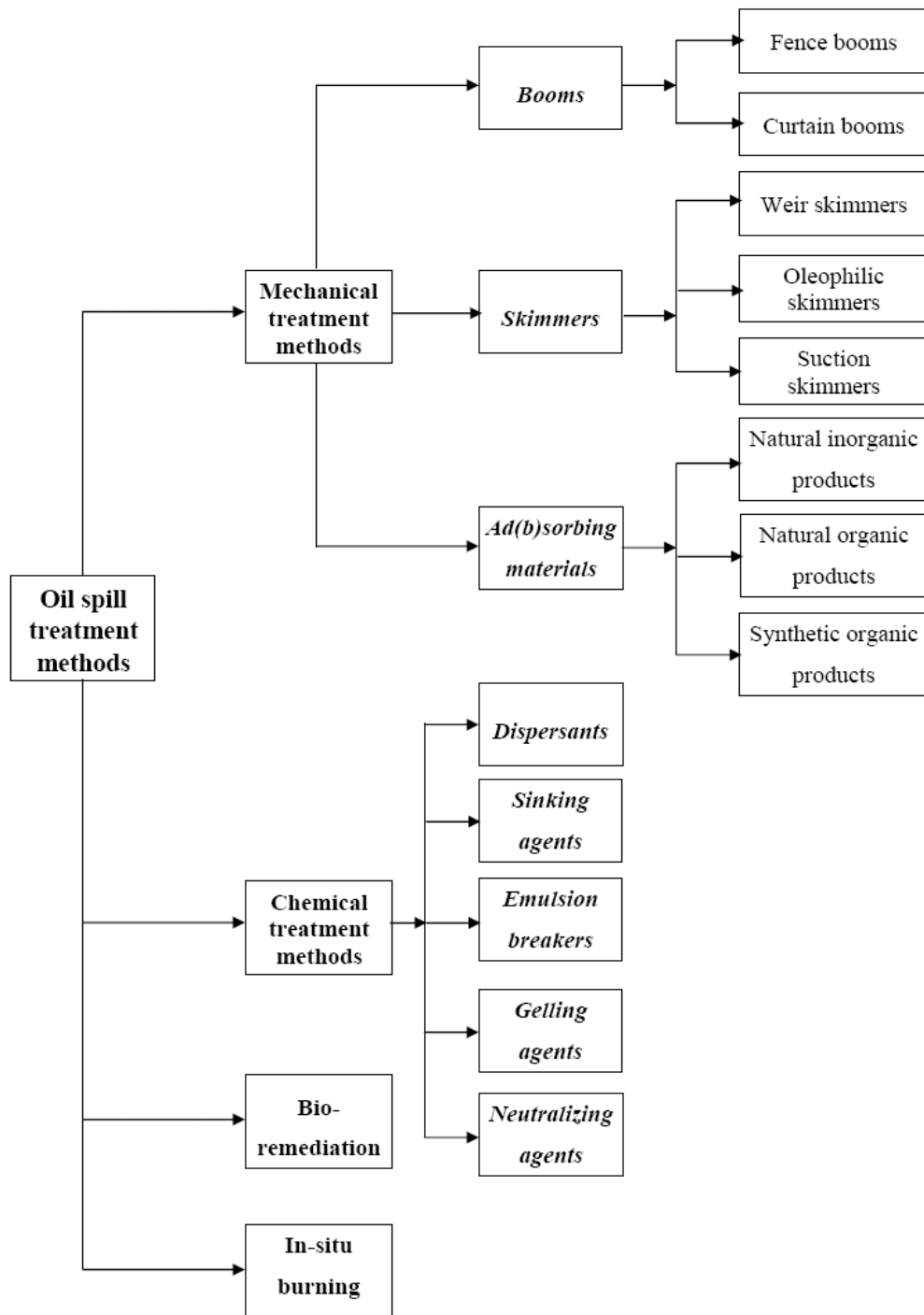


Figure 1.4: Oil spill treatment techniques

1.4.6.1 Mechanical recovery

Mechanical recovery is the transfer of oil from the water surface to some transportable form of temporary storage by the help of booms to contain or divert oil, skimmers or solvents to recover or remove it from the water surface, hoses and pumps (Yender, 2002). Mechanical containment and collection of spilled oil on water using equipment such as booms and skimmers cleanup methods is used at many spills (Yender, 2002). Mechanical methods for oil spill remediation have been utilized for a long time with varying degrees of success (Wei *et al.*, 2003). Booms are employed to prevent oil from spreading on the water's surface and surround the spill close to the source (ITOPF, 2004). However, different from booms, skimmers are designed to recover oil from the surface of water. There are different skimming techniques such as weir skimmer, oleophilic skimmer and suction skimmer (USEPA, 2004a). The use of booms and skimmers is still a primary option for combating marine oil spills (Mullin and Champ, 2003) since it is fairly quick and easy. Barriers can be used along mangrove shorelines and inlets to prevent oil entry. Proper strategic booms deployment in sheltered lagoon areas may be highly effective in trapping large quantities of mobile oil and reducing oil impacts to interior mangroves. To be effective, barriers must be deployed immediately after a spill before oil moves into mangrove areas (Yender, 2002).

Manual removal, using hand tools and manual labor, is often conducted to remove bulk oiling by heavier oils such as crude oil or bunker oil stranded in mangroves. Manual removal help prevent other areas from becoming contaminated as the oil moves around and helps limit long term sediment contamination (Yender, 2002). Performance of any of these however can be severally limited by oceanic conditions and weather, including currents, waves and wind and by the nature of oil slick. Research has shown that

mechanical recovery alone usually cannot adequately deal with very large spills offshore. Weather and sea conditions, the nature of the oil and other factors may limit the effectiveness of mechanical recovery.

Another important method is the use of sorbents. There are numerous compounds and materials available as sorbents to collect oil slicks. Today the sorbents in use can be classified as either: natural organic products such as saw dust, rice husks or maize husk, synthetic organic products such as plastic or polyurethane foam or natural inorganic products such as zeolite and goethite (Deschamps *et al.*, 2003). Sorbent booms or other sorbent materials can be placed at the fringe of oiled mangroves forest to passively recover any mobile oil including sheens. Sorbents are oleophilic and either absorb or adsorb oil. They can be composed of either synthetic or natural materials and they come in variety of forms, including sausage boom, "pom-pom" or snare boom, sheet rolls and loose particulates. Sorbents vary in their effectiveness depending upon type, degree of oil weathering and absorption capacity. Sorbent materials must be placed and removed (when they are saturated and no longer needed) carefully to minimize disturbance of sediments and injury to mangrove roots (Yender, 2002).

1.4.6.2 Chemical methods

Chemical Methods are best methods for removing small spills; widely spread thin layers of oil, oil rough seas and oil spills immediately threatening damage to property and life. Chemical methods involve the use of dispersants, sinking agents, demulsifiers, gelling agents and neutralization agents. Chemical shoreline cleaners are sprayed on oil coated surfaces to loosen the oil from the surface so that it can be flushed off with ambient water. Tidal waters or water sprays alone cannot effectively wash away heavy oil. Shore line

cleaning products vary in their toxicity and recoverability of the treated, mobilized oil. Chemical shoreline cleaners loosen to dissolve heavy oil deposits (Yender, 2002).

Chemical dispersants are products applied to oil on the water surface to enhance formation of tiny oil droplets, which mix into the water column and are dispersed by currents. Dispersants break spilt oil into tiny particles, of different sizes that can be easily degraded by bacteria (Sun, 2010). Most oil physically disperses naturally to some degree due to agitation created by wave action and ocean turbulence. The key components of a chemical dispersant are one or more surface-active agents, or surfactant, sometimes called "detergents". They contain molecules with both water-compatible (hydrophilic) and oil compatible (hydrophobic) portions. Most chemical dispersants also contain a solvent that reduces viscosity and facilitates dispersal.

Chemical dispersants enhance and speed up this natural dispersion process, minimize impact on wildlife at the water surface (e.g. birds and marine mammals) and reduce the amount of floating oil that reaches sensitive near shore and shoreline habitats (Yender, 2002). Moreover, using dispersant in oil spill remediation does not create any waste (NOAA, 2004).

Typical sinking agents include sand, brick dust, fly ash, china clay, coal dust and cement. However, sinking is seldom completely effective initially, and some oil tends to surface. Other chemical materials have also been used in the combat against oil spills on a less extensive scale. They include emulsion breakers (Nordvik *et al.*, 1996; Buist *et al.*, 1999) and gelling agents or solidifiers (Delaune *et al.*, 1999; Reynolds *et al.*, 2001; USEPA, 2004b) and neutralizing agents (Ventikos *et al.*, 2004).

1.4.6.3 In-situ burning

In-situ burning is an oil spill response technique that involves the controlled ignition of the oil at or near the spill site on the surface of the water or in marsh (Mullin and Champ, 2003). In-situ burning involves the ignition and controlled combustion of the spilled oil (USACE, 2005). In order for oil on water to burn, the slick must be relatively fresh and at least 3mm thick. In-situ burning is a response technique in which spilled oil is burned in a place, when viewed appropriately, in-situ burning can remove large quantities of oil quickly and efficiently with minimal logistical support. Like dispersants, in-situ burning can help minimize impacts to wildlife at the water surface and reduce the amount of oil that reaches sensitive near shore and shoreline habitats including mangroves (Yender, 2002).

Since volatile components in the oil begin to evaporate as soon as the spill occurs, the potential for burning decrease with time. Burning is usually 95-98% efficient, but does cause black smoke. The smoke is not more toxic than if the oil were burned as intended in fuels. However, burning oil is not an environmentally friendly method as it causes air pollution and leaves residual unburnt particles (Christodoulou, 2002). One gallon of oil burned this way creates the same pollutions as tree logs in fire place and woodstove. Burning can also be dangerous for the personnel conducting operations (Buist *et al.*, 1999).

1.4.6.4 Bioremediation

Constituents of oil degrade naturally when attacked by bacteria, algae, protozoa and marine fungi. Enhancement of biological degradation has been proposed using specially bioengineered microbes. However, microbes that degrade hydrocarbons are readily available everywhere in nature, except in polar waters where the rates of breakdown are

very slow and variable. It does not appear necessary in most cases to enhance their action. Nutrient addition can enhance biodegradation of oil under nutrient-limited conditions. Microbes and essential nutrients for oil degradation generally are not limited to mangrove habitats, so enrichment may not offer much benefit. Burns *et al.*, (1999) concluded that aeration of contaminated sediments may be effective in enhancing biodegradation of oil in the mangrove sediments, since mangrove sediments are usually anaerobic below surface layers. The researchers suggest a bioremediation strategy that employs selective aeration to promote the survival of trees vital to maintaining the structural integrity of the mangrove forest. Burns *et al.*, (1999), points out that aeration is not necessarily a strategy to be used over large areas.

Bioremediation methods have also been studied by Tsutsumi *et al.*, (2000). Bioremediation is time consuming (USEPA, 2004c) since the rate is normally equal to the half lives of the hydrocarbons (Wang *et al.*, 2001). Another method is the use of plants and their associated microorganisms for remediation. This is known as phytoremediation. Phytoremediation is proving effective for a wide variety of contaminants including petroleum and hydrocarbons (Fingas and Charles, 2001).

1.4.6.5 Natural removal

Natural process will eventually remove oil. Tidal actions and precipitation can help physically flush sanded oil out of contaminated mangrove areas. Weathering processes degrade the oil, gradually reducing quantity and toxicity. There are several circumstances under which it is appropriate to do nothing. When no cleaning is conducted, oil will slowly degrade and can be removed naturally, assisted by natural and storm generated flushing.

Other natural processes that result in the removal of oil from the natural environment include evaporation, oxidation, biodegradation and flushing (USEPA, 1999).

Spills of light oils, which will naturally evaporate and break down very rapidly, do not require clean up. Such light oils are usually gone within five days. Furthermore, light fuel oils such as gasoline and jet fuels typically impart their toxic impact immediately and clean up can do little to reduce the damage. The only light refined product that might warrant some clean up is diesel (if sediment could be contacted) (Yender, 2002) Clean-up is not recommended for small accumulation of oil regardless of product type. Impacts caused by light accumulations, regardless of product type, generally do not warrant the tradeoffs associated with cleanup activities. Even for major oil spills, there may be cases for which it is best to take no action, depending on the nature of oiling and characteristics of the mangrove forest affected (Yender, 2002).

1.4.7 Sorbent for Oil Spillage Treatment

One of the most economic and efficient means of cleaning up hydrocarbon spill on the shoreline and on water is the use of sorbents (Frost *et al.*, 2007). The use of sorbents to clean-up oil spill presents nearly many advantages due to simplicity of approach and the inexpensive nature of the materials (Chung and Venosa, 2008). Recently, increasing concerns about pollution of ground water by organic chemicals has led to research on the use of various sorbents (Ramos-Vianna *et al.*, 2004). Once a sorbent is applied to an impacted wetland, it absorbs the contaminating oil. It retains the oil for a sufficient length of time to allow biodegradation of hydrocarbon by indigenous bacteria under aerobic conditions (Chung and Venosa, 2008).

Sorbents for oil spill in water are materials that soak up the oil. Sorbents work by either absorption or adsorption (Ghalambor, 1995). Absorbents operate like sponges and collect oils by capillary action or suction. They rely on large surface area, the chemical affinity of the sorbent for the spilled oil and chemical constituents including their porosity, molecular structure and changes in volume. Absorbents work best on light, less viscous oil. In some cases, a sorbent material may utilize both techniques for oil recovery (Aboul-Gheit *et al.*, 2006). From literature and field experiences (Choi *et al.*, 1993; Teas *et al.*, 2001; Adebajo *et al.*, 2003), one of the most efficient means of cleaning hydrocarbon spill on the shoreline (on land) is the use of sorbents. They can be used to recover oil through the mechanism of absorption and adsorption or both. Absorbents allow oil to penetrate into pore spaces in the material they are made of, while adsorbent attract oil to their surfaces but do not allow it to penetrate into the material (Aboul-Gheit *et al.*, 2006).

Once sorbents have been used to recover oil, they must be removed from water and properly disposed on land or cleaned for reuse. Any sorbent that is removed from the sorption system must also be disposed off or recycled (Aboul-Gheit *et al.*, 2006).

1.4.8 Types of Sorbents

Sorbents can be natural organic substances, synthetic organic substances and natural inorganic substances or a mixture of the three (Ventikos *et al.*, 2004; Bayat *et al.*, 2005; Frost *et al.*, 2007).

1.4.8.1 Natural organic sorbents

This first category include peat moss (Balternas and Vaisis, 2005), straw (Sun *et al.*, 2002), hay, sawdust, bark (Haussard *et al.*, 2003), grown corn cobs, wool (Choi and Moreau, 1993; Choi, 1996), feathers (Coxeter, 1994) and other wood based products. They are

relatively inexpensive and generally readily available. Organic sorbents can absorb three to fifteen times their weight of oil but they also present some disadvantages. Some organic sorbents are loose particles such as sawdust and are difficult to collect after they spread on water (Ghalambor, 1995). In addition, plant derived organic sorbents are biodegradable thus leaves no permanent residue. Choi and Cloud, (1992) conducted further studies on milkweed and cotton fibers. The results showed that milkweed and cotton sorb oil more efficiently but cannot be reused as often as polypropylene.

The disadvantage of organic sorbents is that organic sorbent are loose particles and are difficult to collect after they have spread on water (Sayed *et al.*, 2004). The use of sorbents combined with bioremediation represents an environmentally friendly, simple and cost effective remediation technology for the cleanup of oil from wetlands. The idea is to sorb or wick the oil from the anaerobic sub-surfaces for hydrocarbon biodegradation (Chung and Venosa, 2008). Organic substances are inexpensive and readily available. Most organic materials can only be used on land and not adaptable to water use for oil spill cleanup.

1.4.8.2 Natural inorganic sorbents

These sorbents include clay (Alther, 2001; Sayed, *et al.*, 2003), perlite (Teas *et al.*, 2001; Roulia *et al.*, 2003), vermiculite (Hitzman and Okia, 1968), glass wool (Smith, 1983) and volcanic ash. They can absorb four to twenty times their weight of oil. These products are used in the oil spill cleanup in the light of the fact that they are inexpensive and are available in large quantities. One of their advantages is that they have low sorption capacity for non-polar hydrocarbons (Ribeiro *et al.*, 2000).

1.4.8.3 Synthetic organic sorbents

Synthetic organic sorbents include man-made, polymeric materials such as polypropylene (Wei *et al.*, 2003), nylon fibers and polyurethane foams (Teas *et al.*, 2001) which are commonly used sorbents in oil spill clean-up due to their oleophilic and hydrophobic characteristics. Most synthetic sorbents can absorb as much as seventy times their weight of oil (Adebajo and Frost, 2004b). Synthetic sorbents that cannot be cleaned after use can present difficulties because they must be stored temporarily until they can be disposed of properly. They are best suited to absorb lighter viscosity oils that can penetrate or wick into its fiber (Aboul-Gheit *et al.*, 2006). Organo-clays and coal/mineral complex were used by Ramos-Vianna, (2004) and found out that organo-clays can be utilized effectively as liners for controlling pollution from petroleum contaminated waters. Aboul-Gheit *et al.*, (2006) conducted adsorption studies on waste plastics (polyethylene and propylene powder) and concluded that they absorb heavier crude oil more strongly than lighter crude oil and have the property of reusability. Synthetic products have high oleophilic and hydrophobic properties and are the most widely used sorbents in the remediation of oil spills. However these materials degrade very slowly relative to mineral and vegetable products (Lee *et al.*, 1999).

1.4.9 Properties of Sorbents

Absorbent materials are attractive for some application because of the possibility of collection and complete removal of the oil from the spill site. The addition of absorbents to oil spill areas facilitate a change from liquid to semi solid phase and once this change is achieved, the removal of the oil by the removal of the absorbent structure then becomes easier. Some properties of good absorbents materials include hydrophobicity and

oleophilicity, buoyancy, high uptake retention over time, oil recovery from absorbents and reusability of the absorbent (Adebajo *et al.*, 2003). These properties affect the sorption capacity of the sorbents. Some of the factors that influence these properties however are;

1. *Density*: There are two types of density relative to absorption; true density and bulk density. The density is a measure of solids only regardless of any internal voids or interstitial areas and once determined, can be considered constant for a given material. To determine density, both mass and volume must be known, it can be determined by the formula

$$D_s = D_l(M_s/M_l + M_l - M_2) \quad (1.1)$$

D_s = density of solid, D_l = density of wetting liquid, M_s = mass of solid, M_l = mass of liquid required to fill the measuring container without fiber and M_2 = mass of liquid required to fill the measuring container without M_s in the container (English, 1997).

Bulk density is a measure of density including void pores and interstices and may vary depending on compaction. Bulk density is a simple measure of mass per unit volume.

2. *Porosity*: porosity or void volume is a measure of how much volume is available in a system for absorption like bulk density, porosity may vary depending in compaction and can be expressed as

$$P_R = V_1 - V_2 / V_1 \quad (1.2)$$

Where, P_r = porosity, V_1 = total volume and V_2 = volume of solid (English, 1997).

3. *Selectivity*: selectivity is the ability of a sorptive material to preferentially absorb one material over another. For instance most agro based materials will, to varying degree, selectively absorb oil over water (Rowell *et al.*, 1999). This makes these materials attractive sorbents in oil spills caused by tanker and offshore oil rig leaks.

The degree of selectivity is influenced by the sorbents pore size wettability and capillary pressure (English, 1997).

4. *Retention*: Retention is the ability of a saturated sorptive material to retain fluid when conditions are conducive to drainage (English, 1997). Adsorbents will release varying amount of oil and organic liquids, depending on the viscosity of the liquid, during the retrieval operations. Consequently, the retention ability of absorbents is absolute (USDOA, 2008). Retention is important because, in practice, retention levels are based largely on conditions related to capillary actions (English, 1997).
5. *Sorbent application*: Agro-based sorbents are seeing commercial use as oil absorbent socks and booms from oil spill cleanup (English, 1997). The use of sorbents for oil spill cleanup work varies in different areas of the country (USDOA, 2008).

The sorption capacity of a given sorbent may depend also on a series of other properties which are grain size distribution, specific surface area, cation exchange capacity , pH, organic matter or organic carbon content and mineral constituents. These properties may affect sorption more or less depending on the chemical characteristics of the sorbate (Rowell *et al.*, 1999).

Sorption process is generally studied by plotting the equilibrium concentration of a compound in the sorbent as a function of its equilibrium concentration in a gas phase or in solution at a given temperature. Sorption isotherms are often non-linear. A sorbing system has a sorption capacity q_c defined as the ratio of the mass of sorbate to the unit mass of sorbent. The total sorption capacity is therefore $q_{c,m}$, in which m equals the mass of the sorbent. The rate of sorption is assumed to be proportional to the concentration of the oil C_o and to the difference between the total capacity $q_{c,m}$ and the amount sorbed q_m where q

is the actual concentration of the sorbate in the solid phase (Site, 2004). The sorption of a chemical on a solid from a water based solution may be seen as the result of a reversible reaction (sorption-desorption) which reaches a final equilibrium conditions between the concentration of the chemical in the two phases (Site, 2004). It would be definitely expected that factors such as the number of the reactive sites on the substrate and the bulkiness of substrate would affect the rate of sorption of adsorbate (Okoro *et al.*, 2007b).

1.4.10 Modification of Natural Sorbents for Oil Spillage Treatment

Application of agro-industrial residues represents an abundant, inexpensive and readily available source of renewable lignocellulosic biomass. Natural organic materials are widely used around the world and include; straw, hay, reeds, sea grass, husk peat, sawdust and gorse, together with other available local materials such as bagasse (dried sugarcane stalks) or dried palm fronds. These materials all appear to function by virtue of their having oleophilic surfaces and they trap the oil in the mat of crisscross strands of fibers rather than by actual capillarity (Zhang *et al.*, 2001). Many of these materials absorb water slowly so that if fibers are left lying in water, they will gradually float over and may finally sink altogether. These natural sorbents have the advantage of economy and biodegradability but also have been observed to have the disadvantage of poor buoyancy characteristics, relatively low sorption capacity and low hydrophobicity (Schatzberg, 1971).

Recent research and development is focused on the improvement of known products and synthesis paths as well as on new derivatives and alternative synthesis concepts (Heinze, 2005). Agricultural waste sorbents are abundantly available around the world and several different methods of development with or without catalyst have been developed. A number of natural sorbents have been modified and studied for use on oil spill cleanup, for

example; cotton (Johnson *et al.*, 1973; Choi *et al.*, 1993; Choi, 1996), wool (Radetic *et al.*, 2003), bark (Haussard *et al.*, 2003), barley straw (Amer *et al.*, 2007; Hussein *et al.*, 2008), kenaf (Lee *et al.*, 1999) and corn-cobs (Diya'udeen *et al.*, 2008). They were observed to be excellent oil sorbents because of their hydrophobic and oleophilic character.

Balernas and Vaisis, (2005) studied the thermal modification influence on sorption qualities of bio sorbents. Hussein *et al.*, (2008) and Diya'udeen *et al.*, (2008) also showed that carbonization of natural sorbents (pith bagasse and corn cobs respectively) had effect on oil sorption capacity. The characteristics of the sorbents were investigated and reported. Thermo gravimetric analysis and electro-scanning processes were used to monitor the behavior of the carbonized sorbents and the product tested under simulated field conditions. The main effect obtained by heat treatment is a reduced wood hygroscopicity. The foremost advantage of wood treated in this manner are its increased resistance to different biodegradation and its improved dimensional stability (Homan *et al.*, 2000).

Chemical modification of plant or wood materials to improve their dimensional stability has been the subject of research for many years. A wide variety of chemicals have been studied including anhydrides, acid chlorides, carboxylic acids, isocyanates, acetals, esters, acetyl chloride, β -propiolactone, acrylonitrile and epoxides. Cellulosic sorbents have been chemically treated (Sun *et al.*, 2005) and research into the use of their modified products as absorbents for the removal of crude oil from aqueous solutions have been on the increase (Okoro *et al.*, 2007b). Adebajo and Frost, (2004b) studied the acetylation of cotton in order to develop hydrophobic, biodegradable cellulosic materials for subsequent application for oil spill cleanup. Okoro and Ejike, (2007) discussed and investigated the chemical modification of cellulose and its sorption model as crude oil sorbents, using

treated wood pulp (newsprint). The procedure was carried out using toluene diisocyanate and benzoyl chloride in the presence of 10% ethanolic sodium hydroxide as catalyst, to show increased sorption capacity of the modified cellulose. Sugarcane bagasse was esterified, by Sun *et al.*, (2004), with acetic anhydride using N-Bromosuccinimide as a catalyst under mild conditions. The acetylation significantly increased the hydrophobic properties of bagasse and the oil sorption capacity of the acetylated bagasse obtained at 80°C for 6hours was 1.9 times higher than that of the commercial sorbent. The most studied of all the chemical modification chemistry is acetylation.

1.4.11 Acetylation of Natural Sorbents

Acetylation is the substitution of an acetyl radical for an active hydrogen. It is a reaction involving the replacement of the hydrogen atom of a hydroxyl group with an acetyl radical (CH_3CO) to yield a specific ester, the acetate (Stuart, 1989). Acetic anhydride is commonly used as an acetylating agent reacting with free hydroxyl groups. In the acetylation of natural fibers, the product obtained contains acetyl groups bonded to the hydroxyl (OH) sites in wood cell wall. It has been shown that the rate of reaction is diffusion dependent with rapid reaction of the anhydride molecule with the cell wall polymer OH site (Hill *et al.*, 1998). Reaction rates can be increased by raising the temperature and using catalysts. The extent of acetylation of acetic anhydride with wood is invariably reported as acetyl weight percent gain (WPG) (Hill, 2006a). Calculated as shown below:

$$\text{WPG}(\%) = [(W_{\text{mod}} - W_{\text{unmod}})/W_{\text{unmod}}] \times 100 \quad (1.3)$$

Where W_{mod} is the oven dry weight of the modified wood and W_{unmod} is the weight of the wood prior to reaction. Although the reaction can take place using ketene, acetic acid or

acetyl chloride, the most useful process is acetylation due to reaction with acetic anhydride.



In this reaction, acetic acid is produced as a byproduct and is important to remove this as well as unreacted anhydride at the end of the reaction. CELL-OH represents the hydroxyl site of the cellulosic natural sorbents (Tapio *et al.*, 1994). The common process for acetylation of cellulose is the reaction without solvents because the solvent will reduce the reaction rate by diffusion of modifiers and the use of solvents will require complicated separation processes to recover the chemicals after the reaction, which makes the process undesirable by increasing the production costs. In addition, the use of organic solvents is often harmful to humans and environment. Therefore a solvent free system is preferable to eliminate the use of organic solvents (Hill, 2006b).

1.4.11.1 Swelling of wood due to acetylation

Wood is swollen by acetylation because the chemically bonded acetyl groups occupy space within the cell wall. Invariably, the swelling is determined by measuring the external dimensions of oven dry wood samples before and after modification. The swellability of wood is calculated thus

$$S (\%) = [(V_{\text{wet}} - V_{\text{dry}}) / V_{\text{dry}}] \times 100 \quad (1.5)$$

where W_2 = wet weight of the sample after soaking in water; W_1 = oven dry weight after soaking.

1.4.11.2 Dimensional stability

When wood is acetylated, it is far less susceptible to shrinking and swelling in the presence of varying atmospheric conditions. The reason for this simply explained. The cell wall is

now filled with chemically bonded acetyl groups in swollen conditions, the extent of which depend upon the level of modification. There is very little residual swelling when wood is soaked in water. A very common method is the method of Rowell and Ellis, (1978), which is to soak the wood for five days in water and determine the swellability. Although this is a useful determination of the dimensional stability, a much better indicator is the anti shrinking efficiency (ASE) determined as shown below

$$ASE = [(S_0 - S) / S_0] \times 100 \quad (1.6)$$

S_0 = volumetric swelling of untreated samples and S = volumetric swelling of treated samples.

1.4.11.3 Catalysts for acetylation

The inability of acetic anhydride to acetylate natural fibers has received much attention from different research workers. It can be assumed that the energy of interaction between acetic anhydride and cellulose in the absence of a catalyst is insufficient to weaken the intermolecular action in cellulose.

Several different methods for acetylation of wood with or without catalyst have been developed and a number of various catalysts have been examined for accelerating the rate of reaction of acetic anhydride. A large number of substances have been proposed as catalyst for acetylation, of these, sulphuric acid and perchloric acid in cellulose acetylation was studied by measuring the conductivity of acetylation mixtures, with or without catalysts. The early work was done using acetic anhydride to catalyze with either zinc chloride (Ridgway and Wallington, 1946) or pyridine (Stamm and Tarkow, 1947). Through the years, many other catalyst have been tried both with liquid and vapor systems. Some of the catalysts used include urea-ammonium sulphate, dimethyl formamide, sodium

acetate, magnesium persulfate, trifluoroacetic acid, boron trifluoride and γ -rays. For many years, 4-dimethylamino pyridine (DMAP) has been used as an acetylation catalyst in chemical synthesis. Sun *et al.*, (2004), also demonstrated that acetylation of free hydroxyl groups in rice straw with acetic anhydride without solvent provided a suitable and effective method for the preparation of rice straw acetate that have a more hydrophobic characteristics and high sorption capacity. The reaction was performed at different reaction times and temperatures in the presence of different catalysts. Among the different catalyst used, 4-dimethyl amino pyridine was found to be the most effective.

Compared to pyridine, DMAP in chemical synthesis was found to be approximately over ten times more active when used as acylation catalyst (Hofle *et al.*, 1978). DMAP is too expensive and is not a commercially available reagent, which limits its industrial use. However from the standpoint of the so called green and sustainable chemistry, another approach to create cleaner and more selective catalytic systems for the organic transformations has become increasingly important in recent years (Karimi and Zareyee, 2008). More recently, based on the study of acetylation of alcohol under mild reaction condition, Karimi and Seradj, (2001) reported that N-Bromosuccinimide (NBS) is an inexpensive and commercially available reagent and is a novel and highly effective catalyst for the acetylation of free alcohols under mild conditions. Karimi and Zareyee (2008) introduced N-bromosuccinimide (NBS) as a mild and nearly neutral electrophilic catalyst for a variety of functional group transformations such as acetalization and acylation of carbonyl compounds, acetylation of alcohols, deoxygenation of sulfoxides and deprotection of 1,3-oxatioacetals. Sun *et al.*, (2004) successfully carried out the acetylation of sugarcane bagasse using N-Bromosuccinimide (NBS) as new catalyst in the presence of acetic anhydride under a solvent free system. The modification with acetic anhydride substituted

the hydroxyl groups modifying the properties of these polymers so that they become hydrophobic. Fourier-Transform infrared (FTIR) and solid state carbon 13 nuclear magnetic resonance spectroscopy were used to investigate the acetylation reaction. The acetylated products using NBS were able to absorb almost 20 times their weight.

1.4.12.1 Corn Cobs and its Availability As Agro Based Sorbent

Corn (Maize) is a major food crop in many parts of the world. In Nigeria, corn is processed to a variety of diets used for weaning. It is a major component of animal feeds and is consumed by many Nigerians as snack, either boiled or roasted (Bolanle and Alhassan, 2012). According to Food and Agriculture Organisation (FAO) data, 589 million tonnes of maize were produced worldwide in the year 2000 (FAO, 2002). The United States was the largest maize producer having about 43% of the world's production. Africa produced about 7% of the world's maize (IITA, 2002). Nigeria was the second largest producer of maize in Africa in the year 2001 with 4.62million metric tonnes (FAO, 2002). The capacity of corn production in Nigeria is high and efforts towards improvement are being made at various quarters. Currently, about eight million metric tonnes of corn are produced annually and a production forecast for 2010-2015 envisaged a 23% growth (Nwanma, 2009).The maize plant comprises of the stalks, husks, shanks, silks, leaf blades, leaf sheaths tassels and cobs (Bolanle and Alhassan, 2012). The corn cob carries the grains and together with associating husks, shanks and silks are harvested from the farm. The other parts are left on the farm to rot (Kludze *et al.*, 2010). Corn cob forms about 30% of maize agrowastes (Rangikuti and Djajanegara, 1983) of which application in biofuels industry are the focus of many researchers aimed at achieving an effective waste management scheme (Bolanle and Alhassan, 2012). It contains 32.3-45.6% cellulose, 39.8% hemicellulose- mostly pentosan and 6.7-13.9% lignin (Sun and Cheng, 2002). The two former components are hydrophilic

and the latter is hydrophobic. In other words the cellulose and hemicelluloses being more hydroscopic than lignin are mainly responsible for moisture uptake. These defects can be reduced considerably by chemical modification of its constituents (Sun *et al.*, 2004), for oil spill response. The microporous polymeric compounds can also be modified by attaching different functional groups to mimic activated carbon and to replace activated carbon for specific applications (Sun, 2010). One of the methods is that the hydroxyl groups which are mainly responsible for its hygroscopicity, attached to cellulose lignin and hemicelluloses can be changed to hydrophobic groups by chemical modification.

1.4.12.2 Mango kernel as an Agro waste sorbent

Mango (*Mangifera Indica*) is one of the most favoured and commercially valuable fruit growing throughout the tropics and is used in a variety of food product (Kaur *et al.*, 2004). Considerable amounts of mango kernel (seeds) are discarded as waste after industrial processing of mangoes (PuraVankara *et al.*, 2000). Approximately 40-60% waste is generated during processing of mangoes, 12-15% and 15-20% of which consists of peels and kernels respectively (Kaur *et al.*, 2004). Depending on the variety, mango kernel contains 6.0% protein, 11% fat, 77% carbohydrate, 2.0% crude fibre and 2.0% ash, based on dry weight average (Zeun *et al.*, 2005). Carbohydrates are the major component of mango kernel and contain several hydroxyl groups which makes it hydrophilic and hence limits its application as oil spill sorbent in aqueous environments. These defects can be reduced considerably by chemical modification of its constituents thereby improving on its hydrophobic properties.

1.4.13 Chemistry of Acetylation

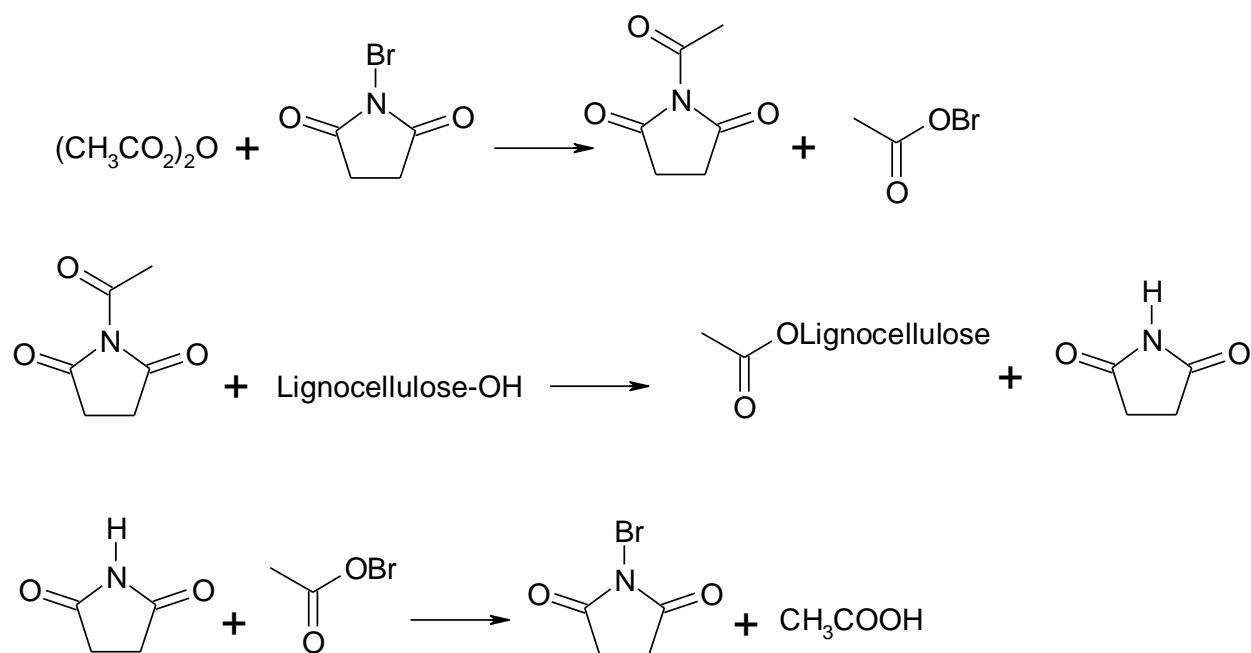


Figure 1.5: reaction mechanism for acetylation using N-Bromosuccinimide as catalyst (Source: Nwankwere, 2010)

The mechanism is one of free radical reactions. The first step involves the reaction of NBS with acetic anhydride to produce a strong acetylating agent. The splitting of the homolytic cleavage of the N-Br bond generates a Br radical, which abstracts an acetate group from the acetic anhydride (Fig 1.5).

The acyl carbon centre of the acetyl group forms an acetic succinimide, which is a very reactive and unstable acetylating agent, with the Nitrogen radical of the succinimide.

The second stage involves a nucleophilic attack on the acyl carbon centre of the acetylating agent by a lone pair of the hydroxyl group followed by the subsequent reduction of the acetylating agent to succinimide and thus generating the lignocellulosic acetates.

In the third stage, the succinimide produced reacts with the brominated acetate group, produced in step-1, resulting in the loss of acetic acid and the regeneration of the NBS catalyst.

The acetates are being washed with excess of acetone and ethanol to remove the by-products acetic acid, NBS and the unreacted acetic anhydride.

Chapter Two

2.1 Materials and Method

2.1.1 Sample Collection

Corn Cob and Mango Kernel (samples) used were collected from a local market in Enugu metropolis, Nigeria. The crude oil samples were collected from Nigerian National Petroleum Corporation (NNPC) Port-Harcourt, Nigeria.

2.1.2 Sample preparation

Corn cob and mango kernel (samples) used were collected from a local market in Enugu metropolis, Nigeria. They were thoroughly washed with water to remove dust, fungus, foreign materials and water soluble components. The washed samples were dried properly in sunlight for twelve hours (four hours for three days) and then left to dry at 65°C in the oven. They were size reduced and sieved through 20 and 25 British Standard Sieve (BSS Sieves). Reagents and chemicals used were from British Drug House (BDH) and include acetic anhydride, N-Bromosuccinimide (NBS), acetone, ethanol and n-Hexane, and were used without further purification.

2.1.3 Characterization of Corn Cob and Mango Kernel (samples)

Proximate analysis and physical characteristics of the materials was determined as follows;

Bulk and tapped Density: A portion (25g) of the samples was accurately weighed and poured into a 100ml graduated cylinder. The cylinder was stoppered and the bulk volume V_0 was recorded. For the tapped density, the cylinder was tapped on a hard surface to a constant volume (until no more settling of the material occurred). The final constant volume (V_1) was noted to be the tapped volume.

The bulk and tapped densities D_{bulk} and D_{tap} were determined as follows;

$$D_{\text{bulk}} = W/V_0 \quad 2.1$$

$$D_{\text{tap}} = W/V_1 \quad 2.2$$

True density: A portion (25g) of the samples was accurately weighed and poured into a 100ml graduated cylinder, and distilled water was carefully measured into the cylinder to the level of the material. The true density was calculated as follows;

$$\text{True density} = W/V \quad 2.3$$

Where W is the weight of the sample and water and V is the volume of the sample

Moisture Content: 2g each of the sorbents was measured into a wash glass. The samples were placed in the oven for 24 hours at 105°C. After 24 hours, the oven dried samples was reweighed and the moisture content was determined with the formula

$$Mc = [(W_0 - W_1)/W_0] \times 100$$

where Mc is the moisture content; W_1 is the new weight after drying; W_0 is the initial weight of the dry samples (ASTM, 1994).

Ash content: Ash content was determined using the methods employed by Dara, (1991) ; Aloko and Adebayo, (1997). Dry samples (2g) were placed in a pre-weighed porcelain crucible and transferred into a preheated muffle furnace set at a temperature of 600°C for 1 hour after which the crucible and its content were transferred to a desiccator and allowed to cool. The crucible and its content were reweighed and the new weight noted.

The percentage ash content was calculated with the formula

$$Ac (\%) = (W_a/W_0) \times 100 \quad 2.4$$

where Ac is the ash content in percentage; W_a is the weight of ash after cooling and W_0 is the original weight of dry sorbent.

Porosity: the porosity of the materials was calculated using the formula for porosity.

$$\text{Porosity} = 1 - (\text{BD}/\text{TD}) \quad 2.5$$

where BD is the bulk density and TD = true density

2.1.4. Characterization of crude oil

Viscosity: The viscosity of the oil samples was obtained using an NDJ-85 Digital rotary viscometer at 27°C. The samples were pre-warmed and placed in the sample chamber of the apparatus. The samples were brought to room temperature within 30 minutes and the motor started. The viscosity was automatically measured at 1 minute intervals. The mean of the viscosity was calculated and recorded.

Density: The density of the oil samples was obtained using the methods of (Hassan, et al., 2006) with a specific gravity bottle. The bottle was filled with the oil and weighed at 30°C in a thermostated water bath. The density of the oil was calculated using the formula

$$\rho = (\text{Ms}-\text{Mb})/\text{Vb} \quad 2.6$$

where Ms-Mb is the mass of the oil used and Vb is the volume of water used.

Specific gravity: The specific gravity (s.g) of the oil samples was calculated using the results obtained for density. The specific gravity being a more standard measurement was obtained by multiplying the density obtained with the density of water 0.998g/dm³.

The American Petroleum Institute (API)- Gravity: This was obtained using the formula API gravity given in (Nwankwere, 2010) and expressed thus:

$$\text{API}_o = (141.5/\text{S.g})-131.5 \quad 2.7$$

Where s.g is the specific gravity of the oil employed.

2.1.5 Soxhlet Extraction

To reduce the influence of the fibre extractives (oil, wax and fat) on acetylation, 10g of the sieved materials was extracted with a mixture of acetone and n-hexane (4:1 v/v) for 5hours. The extracted samples were dried in a laboratory oven for 16hours.

2.1.6 Acetylation of samples

The acetylation of the corn cob and mango kernel under mild conditions, in the presence of NBS, using acetic anhydride was carried out using the method of Sun *et al.*, (2004). The amount of substrate and reactant were combined in a ratio of 1:20 (g dried sorbent/ mL acetic anhydride). The reaction temperature, time and amount of catalyst were 30°C-130°C, 1-3hrs and 0-4% respectively. The mixture of raw sorbents, acetic anhydride and catalyst was placed in a round bottom flask fitted to a condenser. The flask was placed in an oil bath on top of a thermostatic heating device, thereafter, the flask was removed from the bath and the hot reagent was decanted off. The sorbents were thoroughly washed with ethanol and acetone to remove unreacted acetic anhydride and acetic acid as by-products. The new products were dried in an oven at 60°C for 16hours prior to analysis. The degree of acetylation was estimated from the infrared spectra by calculating the ratio (R) between the intensity of the acetyl C=O stretching band around 1740-1745 cm⁻¹ and the intensity of the C-O stretching vibrations of cellulose backbone at about 1020-1040 cm⁻¹ as shown below (Adebajo and Frost, 2004):

$$R = \frac{I_{1740}}{I_{1020}} \quad 2.8$$

2.1.7 Fourier transform infrared spectroscopic analysis

The properties of raw and acetylated samples were characterized using FT-IR Shimadzu 8400s spectrophotometer in the range of 4000-400 cm⁻¹. Samples were run

using the KBr pellet method at the National Research Institute for Chemical Technology (NARICT) Zaria, Kaduna-Nigeria.

2.1.8. Treatment protocol

The sorption of oil from water was carried out using the methods of Bannerjee *et al.*, (2006). A portion (1g) each of RCC and ACC was placed in a 250ml beaker containing a mixture of crude oil displaced in 100ml of water at 26°C. The samples were left in the mixture for about 3 minutes with little agitation. The sorbents were removed from the beakers using sieve nets. The nets were allowed to drain. The oil loaded sorbents were dried at 60°C for 30 minutes and reweighed. The oil sorption capacity was calculated by taking into account the weight of sorbent, weight of sorbent and oil and weight of sieve net.

2.1.9 X-ray Fluorescence (XRF)

The elemental composition of the raw corn cob (RCC) and raw Mango kernel (RMS) were characterized using Oxford Energy dispersive X-ray fluorescence. The scanning region was between 0 – 30 (KeV) energy region. Samples were run at Multipurpose Research Laboratory, Ahmadu Bello University, Zaria, Nigeria.

2.1.10 X-ray Diffraction (XRD)

The X-ray patterns of the raw and acetylated corn cob and mango kernel were obtained using Phillips analytical diffractometer at National Institute for Engineering research, Kaduna, Kaduna state, Nigeria. The scanning region of the diffraction angle (2θ) was from 5° to 45°. The crystallinity index (I_c) was determined using equation 2.9 below;

$$\text{Crystallinity Index (I}_c\text{)} = \frac{I_{(002)} - I_{(am)} \times 100}{I_{(002)}} \quad 2.9$$

Where $I_{(002)}$ is the counter reading at peak intensity at 2θ angle close to 22° , $I_{(am)}$ is the amorphous counter reading at 2θ angle of about 18° .

2.1.11 Kinetics and Thermodynamic considerations

2.2.11.1 Kinetics considerations

The kinetics was studied by fitting obtained data in rate curves- derived pseudo first-order, Lagergren pseudo first-order, Second order (Hill *et. al.*, 1998), pseudo second-order (Ho, 1995) and intra-particle diffusion.

Pseudo-first order equation used can be derived thus:

$$\text{Rate of acetylation (R}_1) = \frac{d\theta}{dt} = -k_1\theta \quad 2.10$$

Rearranging equation 2.10 gives

$$-\frac{d\theta}{\theta} = k_1 dt \quad 2.11$$

Solution can be obtained by integrating equation 2.11 as follows

$$\int_{\theta_0}^{\theta_t} -\frac{d\theta}{\theta} = k_1 \int_0^t dt \quad 2.12$$

Solution to equation 2.12 is

$$-[\ln \theta]_{\theta_0}^{\theta_t} = k_1 t \quad 2.13$$

Rearranging equation 2.13, gives the required pseudo-first order equation used

$$\ln \theta_t = \ln \theta_0 - k_1 t \quad 2.14$$

Oils are transported from the aqueous phase to the surface of the adsorbent and subsequently they can diffuse into the interior of the particles if they are porous. When the transport of the adsorbate from the liquid phase up to the solid phase plays a significant role in the sorption, liquid film diffusion may be applied. Equation representing liquid film diffusion kinetics is (Taffarel and Rubio, 2009);

$$\ln(1-F) = -k_{fd} \cdot t$$

2.23

Where F is the fractional attainment of equilibrium ($F = qt/q_e$) and k_{fd} is the rate constant.

Table 2.1 linear forms of the kinetic models used

Type		Linear form	Plot	Parameters
Derived kinetics	first-order	$\ln\Theta_t = \ln\Theta_0 - K_1t$	$\ln\Theta_t$ vs t	$K_1 = \text{slope},$ $\Theta_0 = \ln^{-1} \text{Intercept}$
Lagergren first-order kinetics	pseudo	$\ln(\Theta_0 - \Theta_t) = \ln\Theta_0 - k^1t$	$\ln(\Theta_0 - \Theta_t)$ vs t	$\Theta_0 = \ln^{-1} \text{slope},$ $K^1 = \text{slope}$
Hill kinetics	second order	$i/\Theta_t = i/\Theta_0 - k_2t$	i/Θ_t vs t	$\Theta_0 = 1/\text{intercept},$ $K_2 = \text{slope}$
Ho order kinetics	pseudo second-order	$t/\Theta_t = 1/k^2 \Theta_0^2 + 1/\Theta_0 t$	t/Θ_t vs t	$\Theta_0 = 1/\text{slope},$ $K^2 = \text{slope}^2/\text{intercept}$
Intra-particle diffusion		$\Theta = k_d t^{1/2} + C$	Θ vs $t^{1/2}$	$k_d = \text{slope},$ $c = \text{intercept}$

2.1.11.2 Thermodynamics consideration

The effect of temperature on the degree of acetylation was studied using

$$\ln \theta = A - \frac{B}{T} \quad 2.15$$

Considering that the anhydride reagent displaces surface -OH sites and these displacement reaction occurs when the pores of the substrate are covered appropriately, coverage is dependent on the concentration of -OH groups (Hill et al., 1998), which is proportional to

extent of acetylation. Therefore, θ represents surface coverage which is extent of acetylation.

There are two unknowns in equation 2.15 and these make it difficult to be used directly. However, careful observation enables one to observe that equation 2.15 is equivalent to the Clausius-Clapeyron equation

$$\ln \theta = -\frac{\Delta H}{RT} \quad 2.16$$

where $B = \frac{\Delta H}{R}$ and A is the intercept. Infact, equation 2.16 is the Gibbs-Helmholtz equation

$$\frac{d \ln \theta}{dT} = \frac{\Delta H}{RT^2} \quad 2.17$$

Integrating equation 2.17 is as shown

$$\int_{\theta_0}^{\theta_T} \ln \theta = \frac{\Delta H}{R} \int_{T_0}^T \frac{1}{T^2} dT \quad 2.18$$

Equation 2.18 gives

$$[\ln \theta]_{\theta_0}^{\theta_T} = -\frac{\Delta H}{R} [T^{-1}]_{T_0}^T \quad 2.19a$$

$$\ln \left(\frac{\theta_T}{\theta_0} \right) = -\frac{\Delta H}{RT} + \frac{\Delta H}{RT_0} \quad 2.19b$$

$$\ln \theta_T = -\frac{\Delta H}{RT} + \frac{\Delta H}{RT_0} + \ln \theta_0 \quad 2.19c$$

Equation 2.19c allows the plot of $\ln \theta_T$ versus T^{-1} such that $-\frac{\Delta H}{R}$ is the slope, intercept at/on Y axis ($\ln \theta$) gives $\ln \theta_0$ and intercept at/on x axis (T^{-1}) gives $\frac{\Delta H}{RT_0}$. ΔH is the heat of corn cob acetylation, T_0 is the critical temperature of acetylation (below which acetylation is not feasible), and θ_0 is the critical degree of acetylation.

The heat capacity (C_p) of acetylation at constant pressure was obtained using (Ibemesi, 2004)

$$\Delta H = \int_{T_1}^{T_2} C_p dT = C_p (T_2 - T_1) \quad 2.20$$

C_p represents the quantity of heat needed to acetylate the material whenever a degree rise in temperature occurs.

The change in entropy of acetylation (ΔS) was obtained from the equation (Ibemesi, 2004):

$$\Delta S = C_p \ln\left(\frac{T_2}{T_1}\right) \quad 2.21$$

An important thermodynamic parameter, change in Gibb's free energy (ΔG), was calculated thus: (Ibemesi, 2004)

$$\Delta G = \Delta H - T\Delta S \quad 2.22$$

Chapter Three

Results and Discussion

3.1 Result of Sample Characterization

3.1.1 Result of physical and mineral characterization of Samples

The results of the physical properties of the raw sorbents are presented in Table 3.1. The moisture content reported in this study is within acceptable limit of 5%. Moisture content (less than 5%) is needed for the best acetylation reaction. Values above this level will cause hydrolysis of anhydrides to corresponding carboxylic acid. This accounts for a 5.7% loss of anhydride for each 1% of water in the wood (Bodirlau and Teaca, 2009). The bulk and tapped densities measures the flowability of a material. A higher density indicates a better potential for a material to flow and re-arrange itself under compression. The results derived from this study are moderate and are consistent with findings elsewhere (Azubuike and Okhamafe, 2012). Hausner indices were estimated as the ratio of the difference between tapped and bulk densities. Hausner indices measures/estimates cohesion between particles (Carr, 1965; Wells, 1988). A value less than 1.20 indicates good flowability, whereas a value of 1.50 or higher suggests that the material will have poor flow properties (Azubuike and Okhamafe, 2012). In our findings, the hausner ratio for all the samples fell below 1.20, suggesting good flowability of the material.

Table 3.1: Physical properties of the sorbents

Property	Corn cob	Mango kernel
Moisture content (%)	5.680	5.890
Ash content (%)	4.230	3.880
Bulk density (tapped) (g/cm ³)	0.327	0.554
Bulk density (untapped) (g/cm ³)	0.293	0.514
Particle density (g/cm ³)	1.580	1.720
Hausner ratio	1.116	1.078
Porosity (%)	81.500	67.800

Results are average of 3 determinations.

The results of the Mineral analysis of the raw samples are presented in Table 3.2. Mineral analysis by x-ray fluorescence showed that corn cob and mango kernel contained essential minerals like potassium, magnesium, phosphorus, calcium and sodium in high proportion. Phosphorus is an essential nutrient and has an important role in the synthesis of amino acids and proteins (Zeun et al., 2005). Calcium and magnesium plays a significant role in photosynthesis, carbohydrate metabolism, nucleic acids and binding agents of cell wall (Scalbwet, 1998). Calcium assists in teeth development (Brody, 1994). Magnesium is essential mineral for enzyme activity like calcium chloride and plays a role in regulating the acid-alkaline balance in the body. Phosphorus is needed for bone growth, kidney function and cell growth. It also plays a role in maintaining the body's acid-alkaline balance (Fowomolo, 2010). The mineral contents of mango kernel and corn cob are in agreement with other lignocellulosic biomass (Ribeiro *et al.*, 2000; Fowomolo, 2010; Nzikou *et al.*, 2010; Banerjee *et al.*, 2006).

Table 3.2: Mineral composition of corn cob and mango kernel

Mineral	Corn cob (wt%)	Mango kernel (wt%)
Na ₂ O	0.000	0.000
MgO	0.456	1.495
Al ₂ O ₃	4.378	3.321
SiO ₃	58.205	35.429
P ₂ O ₅	4.677	9.389
SO ₃	3.863	7.386
Cl	3.789	1.984
K ₂ O	17.801	27.763
CaO	2.467	7.462
TiO ₂	0.358	0.263
Cr ₂ O ₃	0.346	0.227
Mn ₂ O ₃	0.123	0.786
Fe ₂ O ₃	3.317	4.494
ZnO	0.200	0.000
SrO	0.023	0.000

3.1.2 Result of Characterization of crude oil

The characterizing properties of crude oil carried out were viscosity, specific gravity, density and API gravity. The properties are shown in Table 3.3

Table 3.3; Result of characterization of crude oil

Property	Crude oil
Viscosity at 25°C (MPa.S)	67.5000
Specific gravity at 25°C	0.8825
Density (g/cm ³)	0.8956
API gravity (o)	28.8400

3.2 Acetylation of corn cob and mango kernel

3.2.1 Structural characteristics of corn cob

The x-ray diffraction spectra of the raw and acetylated corn cob are presented in Figure 3.1 and 3.2 respectively. The three broad peaks 12.36° , 17.76° and 19.37° that appeared in the crystalline pattern of raw corn cob are typical pattern of α -cellulose (Yu *et al.*, 2009). Significantly reduced intensity peaks are observed in the crystalline pattern of the acetylated corn cob. The crystallinity index recorded in this study was (83.39) for raw cob and (71.53) for acetylated cob, showing a slight reduction in crystallinity. High crystallinity indicates an ordered compact molecular structure, whereas lower crystallinity implies a more disordered structure, resulting in amorphous powder (Azubuike and Okhamafe, 2012). Acetylation of cellulose material often cause decrease in crystallinity (Kosaka *et al.*, 2005; Tserki *et al.*, 2005; Yang *et al.*, 2008). The major part of cellulose is in the crystalline form (about two third) due to intra and intermolecular hydrogen bonding of hydroxyl group (Chum *et al.*, 1985). These crystallites mainly have a hydrogen bonding with the hydroxyl group and are attacked by acetic anhydride to form acetylated cellulose in the amorphous structure. The substitution of an acetyl group for a hydroxyl group reduces the density of hydrogen bonding because an acetyl group offers a more bulky branch (lower ability to form hydrogen bonding) than a hydroxyl group (Yu *et al.*, 2007).

FT-IR spectroscopy has the ability to predict structural differences not seen by other physicochemical analysis. Structural units that undergo various changes are functional groups located on the glucose monomer of the cellulose, observable in the FTIR spectra (Bordilau and Teaca, 2009). As illustrated in Figs 3.3 and 3.4, the FTIR spectrum of the treated corn cob showed evidence of acetylation (Table 3.4). The presence of the band at $1750-1675\text{cm}^{-1}$ is characteristic absorption of carbonyl (C=O ester) stretching vibration of

acetate group in cellulose and uronic ester in hemicellulose. This band showed evidence of acetylation (Mohebbly, 2008; Nasar *et al.*, 2010; Indrayam *et al.*, 2000; Adebajo and Frost, 2004b). The peak absorption increased in the acetylated samples, indicating high level of acetyl gain (Yakubu *et al.*, 2013). The band at 1360-1320 cm^{-1} is attributed to aliphatic C-H deformation/bending vibrations of CH_3 in acetyl groups and this is evidence of the formation of ester band due to acetylation in cellulose and hemicellulose (Yakubu *et al.*, 2012; Mohebbly, 2008; Bordilau and Teaca, 2009; Indrayam *et al.*, 2000; Adebajo and Frost, 2004b). The band at 1264- 1256 cm^{-1} is assigned to the stretching of C-O and the deformation of C=O in the acetate bond formed during acetylation in xylan and lignin (Tuong and Li, 2010; Mohebbly, 2008; Indrayam *et al.*, 2000; Adebajo and Frost, 2004b). The bands at 1075-1036 cm^{-1} are assigned to C-O stretching vibrations in cellulose, hemicelluloses and that of primary alcohol (Yakubu *et al.*, 2012; Mohebbly, 2008; Bordilau and Teaca, 2009; Nasar *et al.*, 2010) is an evidence of acetylation. The band at 600 cm^{-1} can be linked to -OH out-of-plane bending (Bordilau and Teaca, 2009; Nasar *et al.*, 2010) and/or atmospheric CO_2 (deformation vibration) contamination. The following peak intensities 3887, 3431, 3770, 3781 cm^{-1} as reflected on the IR spectra of acetic anhydride treated samples are characteristics absorption of bonded -OH group stretching vibrations in cellulose and hemicelluloses. The intensity of the -OH absorption bands in the treated samples decreased. The decrease in the intensity of the treated samples indicated that some hydroxyl group contents of the corn cob were reduced during the reaction, indicating that some level of acetylation had taken place (Yakubu *et al.*, 2012; Mohebbly, 2008; Bordilau and Teaca, 2009). However, at some points a slight increase in the intensity of the OH stretching band indicating a gradual lowering of the extent of acetylation as the reaction time and temperature increased. Acetylation of cellulose is an equilibrium reaction

just like any other esterification reaction such that de-acetylation can take place under appropriate conditions (Adebajo and Frost, 2004). It is therefore possible for de-acetylation to occur in the presence of acetic acid by-product for the longer time reaction thereby leading to re-formation of the free hydroxyl groups of the corn cob (Adebajo and Frost, 2004b). The presence of absorption peaks at both 2150-2100 and 2980-2890 cm^{-1} assigned to the asymmetric stretching vibrations of aliphatic $-\text{CH}_3$ group is an evidence of acetylation (Yakubu *et al.*, 2012; Tuong and Li, 2010; Nasar *et al.*, 2010; Cetin and Ozmen, 2010). The absence of the absorption band at 1840-1760 cm^{-1} in all the treated samples indicated that the acetylated products were free of unreacted acetic anhydride (Adebajo and Frost, 2004b; Sun *et al.*, 2002, Yakubu *et al.*, 2013). The absence of the peak at 1700 cm^{-1} for a carboxylic group in all the spectra of acetylated samples also indicated that the acetylated products are free of acetic acid by-product. This indicated that FTIR is quite sensitive and a good technique for identifying contamination. Hence it is necessary to always ensure that the by-products are thoroughly washed with ethanol and acetone to avoid such contamination (Adebajo and Frost, 2004a).

/ Data >

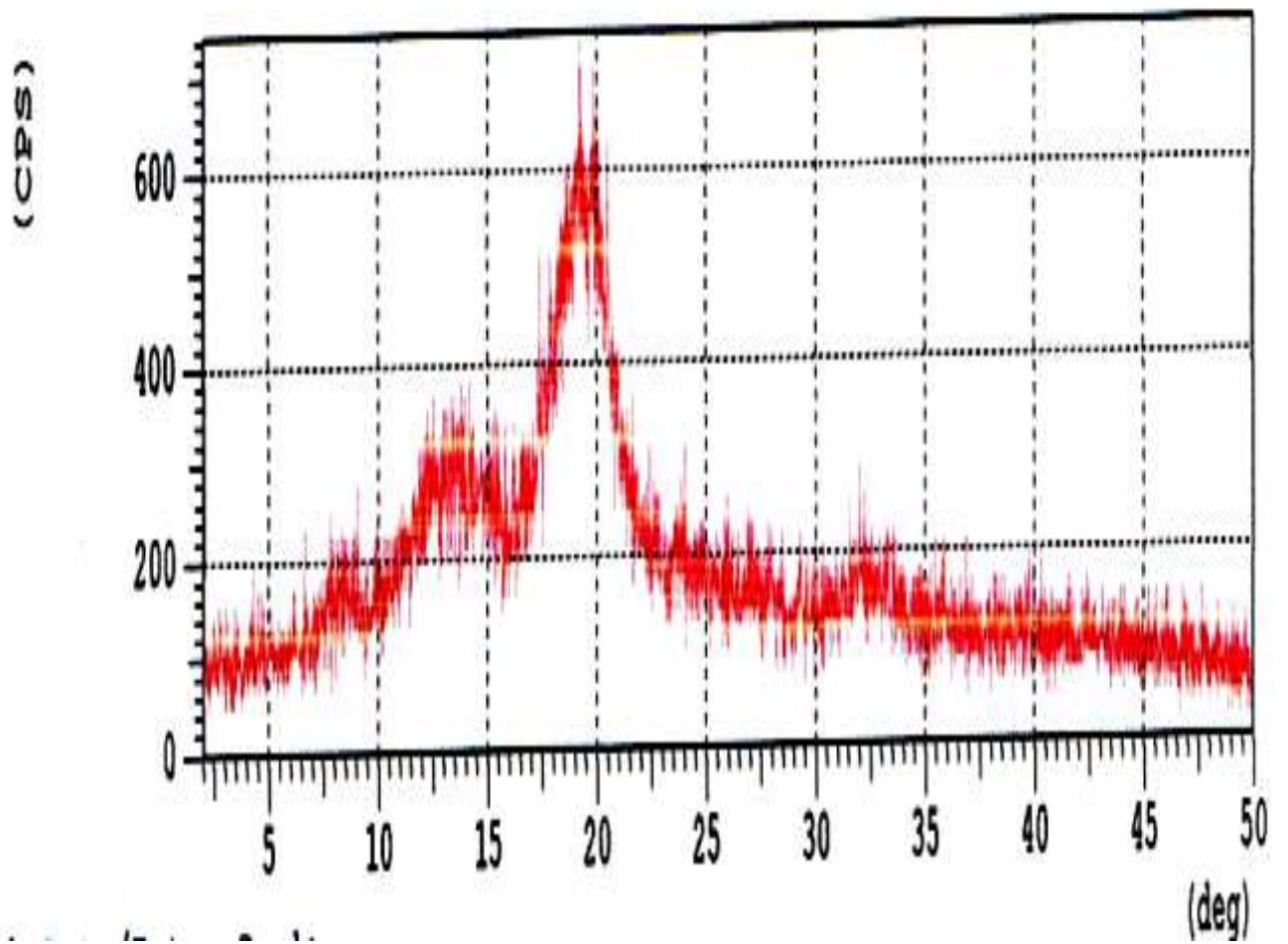
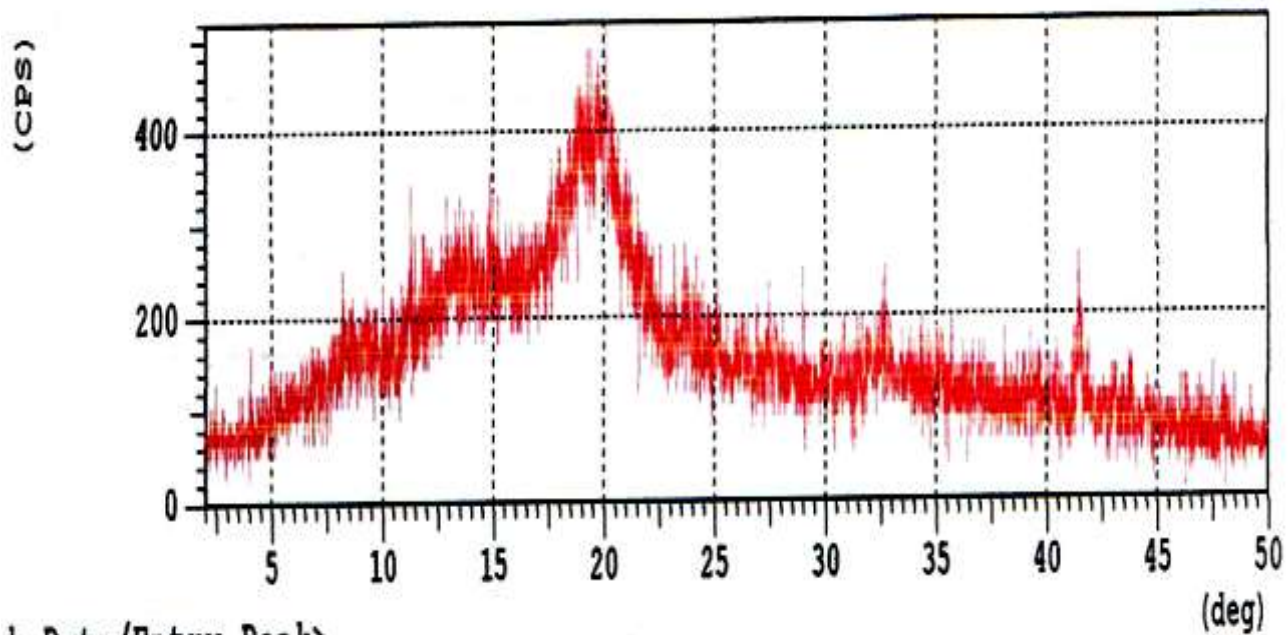


Figure 3.1 XRD pattern of raw corn cob



ik Data/Entry Peak>

Figure 3.2 XRD pattern of acetylated corn cob

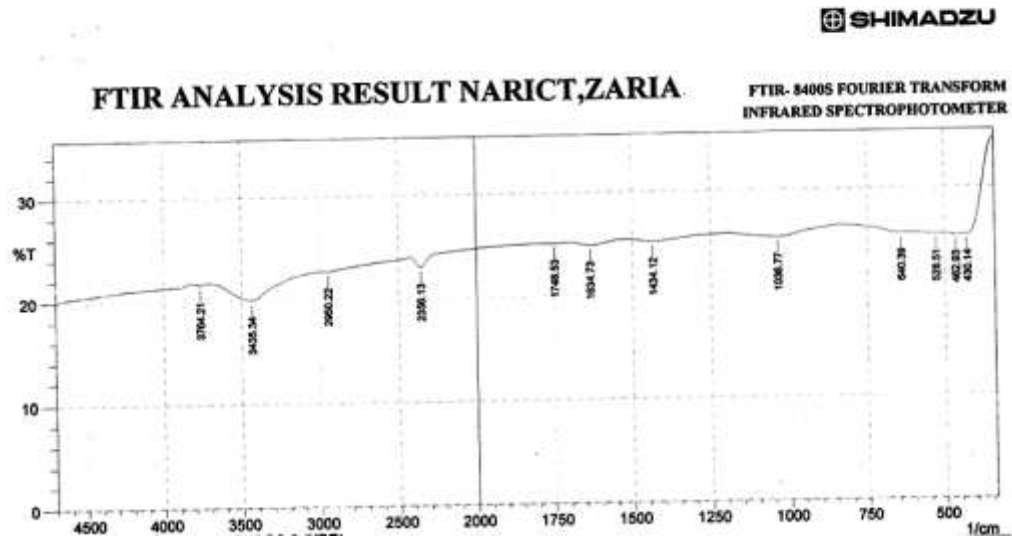


Figure 3.3: FTIR spectra of raw corn cob



Figure 3.4: FTIR spectra of acetylated corn cob (sample 11)

Table 3.4: Assignment of the IR spectra bands of functional groups in acetylated corn cob treated with acetic anhydride

Band position	Functional group
3978-3200	-OH stretching, hydroxyl group
2950-2880	-CH stretch, CH ₃ -O group cellulose
2356	CH ₃ group, stretching vibrations of aliphatic CH ₃ group
1750-1675	C=O, esters (ascribed to hemicellulose)
1660-1630	C=C alkanes and H-O-H bands of absorbed water
1440-1359	CH deformation in -O(C=O)-CH ₃ group
1257-1230	C=O stretch, acetyl group (lignin)
1075-1036	C-O stretching vibrations in cellulose, hemicellulose and primary alcohol
976-790	trisubstituted C-H bend, alkanes
700-600	Cis out of plane C-H band, alkanes
470-430	Si-O-Si bend, silica

3.2.2 Structural characteristics of mango Kernel

The x-ray diffraction spectra of the raw and acetylated mango kernel are presented in Figure 3.5 and 3.6 respectively. The three broad peaks 14.53° , 15.71° and 20.46° that appeared in the crystalline pattern of raw mango kernel are typical pattern of α -cellulose (Yuet *et al.*, 2009). Significantly reduced intensity peaks were observed in the crystalline pattern of the acetylated mango kernel. The crystallinity index recorded in this study was (33.25) for raw mango kernel and (-61.24) for acetylated mango kernel, showing that the crystallinity was lost after acetylation. High crystallinity indicated an ordered compact molecular structure, whereas lower crystallinity implied a more disordered structure, resulting in amorphous powder (Azupbuike and Okhamafe, 2012). This showed that acetylation reaction altered the structure of mango kernel.

Structural units that undergo various changes are functional groups located on the glucose monomer of the cellulose (Bodirlau and Teaca, 2009). Figure 3.7 and 3.8 illustrates the FTIR spectra of raw and treated mango kernel respectively. All the spectra of the treated mango kernel show evidence of acetylation (Table 3.4). The following peak intensities and band at 4393, 3853, $3200-3600\text{cm}^{-1}$ as reflected on the IR spectra of treated mango kernel are characteristic absorption of bonded $-\text{OH}$ group stretching vibrations in cellulose and hemicelluloses (Yakubu *et al.*, 2012). The $-\text{OH}$ absorption bands of the untreated mango kernel were predominantly detected at 4385, 4291, 3960, $3200-3600\text{cm}^{-1}$. The intensity of the $-\text{OH}$ absorption bands in the treated samples decreased. This decrease in the intensity of $-\text{OH}$ band is an indication that the hydroxyl content of the mango kernel reduced during the reaction, indicating that some levels of acetylation had taken place (Yakubu *et al.*,

2012). The presence of the band at $1750-1650\text{cm}^{-1}$ is characteristic absorption of carbonyl ($\text{C}=\text{O}$ ester) stretching vibration of acetate group in cellulose and uronic ester in hemicellulose. This band showed evidence of acetylation (Mohebbly, 2008; Nasar *et al.*, 2010; Adebajo and Frost, 2004b). The peak absorption increased in the acetylated samples, indicating high level of acetyl gain (Yakubu *et al.*, 2013). The increase in the peak absorptions at $1360-1320\text{cm}^{-1}$, attributed to aliphatic deformation/bending vibrations of $-\text{CH}_3$ in acetyl groups, is an evidence of the formation of ester bands due to acetylation in cellulose and hemicellulose (Mohebbly *et al.*, 2008; Yakubu *et al.*, 2013; bodirlau and Teaca, 2009). The band at $1264-1256\text{cm}^{-1}$ is assigned to the stretching of C-O and the deformation of $\text{C}=\text{O}$ in the acetate bond formed during acetylation in xylan and lignin (Tuong and Li, 2010; Mohebbly, 2008; Adebajo and Frost, 2004b). The band at $1075-1036\text{cm}^{-1}$ is assigned to C-O stretching vibrations in cellulose, hemicellulose and primary alcohol (Yakubu *et al.*, 2013; Bodirlau and Teaca, 2009; Nasar *et al.*, 2010). The band at 573cm^{-1} can be linked to $-\text{OH}$ out-of-plane bending (Bodirlau and Teaca, 2009). The presence of the absorption peak at 2134cm^{-1} assigned to the asymmetric stretching vibrations of aliphatic $-\text{CH}_3$ group is an evidence of acetylation (Cetin and Ozmen, 2010; Yakubu *et al.*, 2013; Tuong and Li, 2010). The absence of the band at $1840-1760\text{cm}^{-1}$ in all the treated samples showed that the acetylated samples were free of unreacted acetic anhydride (Sun *et al.*, 2002; Adebajo and Frost, 2004b). The absence of the peak at 1700cm^{-1} in all the treated samples also indicated that the acetylated products are free of acetic acid by-product. This indicated that FTIR is quite sensitive and good technique for identifying contamination. Hence it is always necessary to wash the treated samples with ethanol and acetone to prevent contamination (Adebajo and Frost, 2004b).

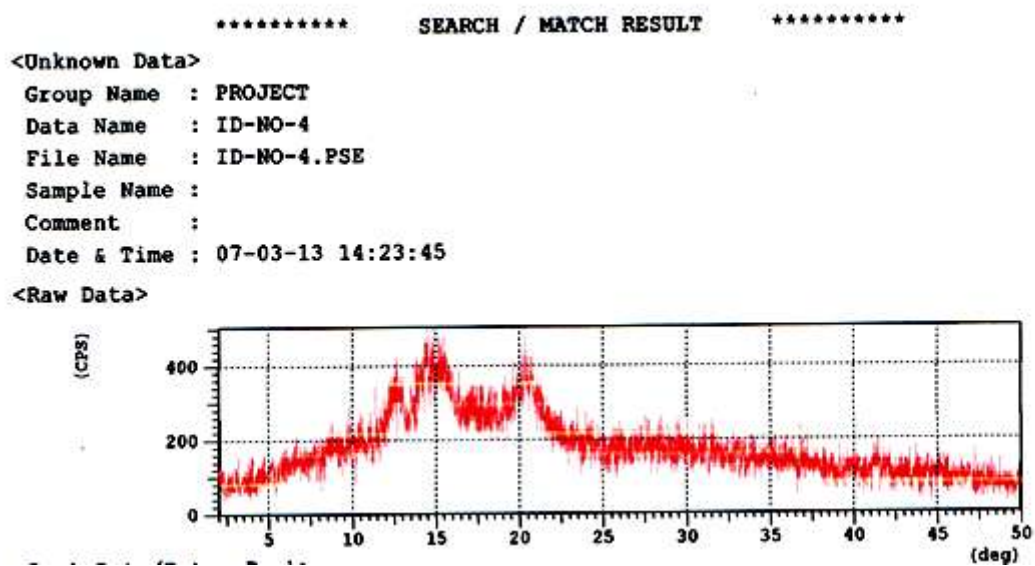


Figure 3.5 XRD pattern of raw Mango kernel

***** SEARCH / MATCH RESULT *****

<Unknown Data>
Group Name : PROJECT
Data Name : ID-NO-3
File Name : ID-NO-3.PKR
Sample Name :
Comment :
Date & Time : 07-03-13 14:43:06

<Raw Data>

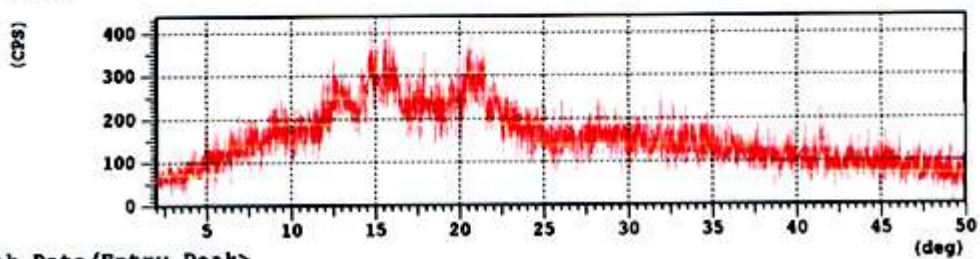
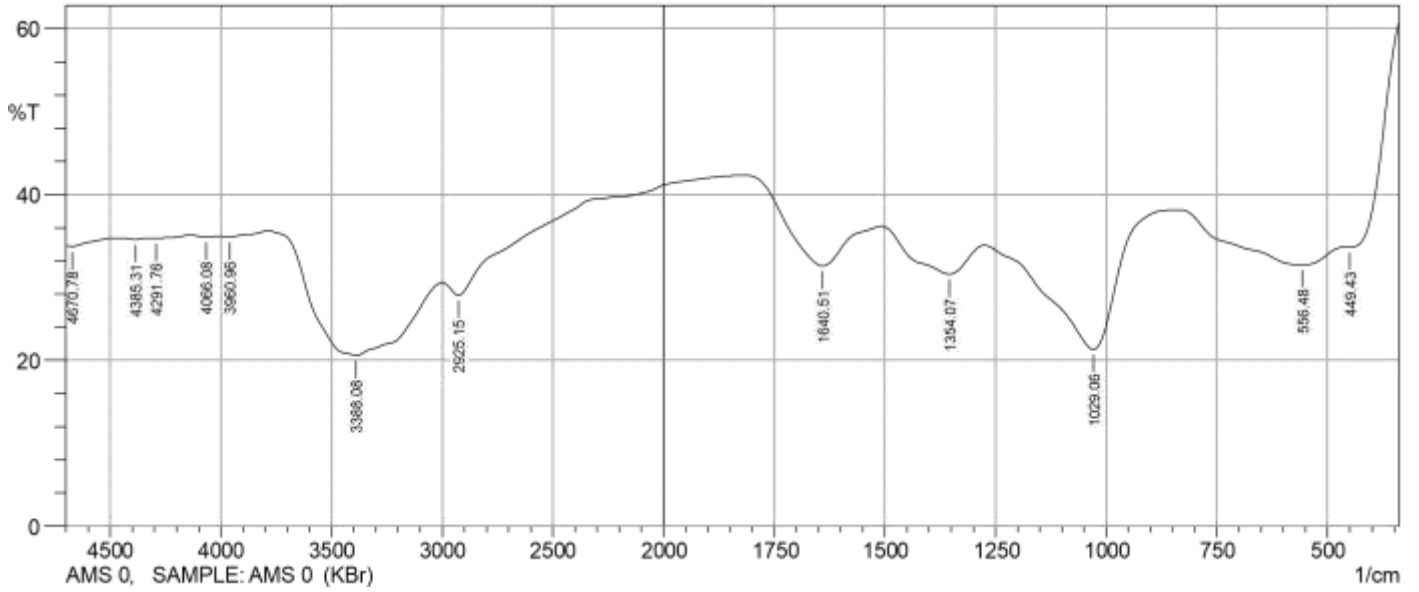


Figure 3.6 XRD pattern of acetylated mango kernel



FTIR ANALYSIS FTIR- 8400S FOURIER TRANSFORM

Figure 3.7 FTIR Spectra of raw Mango kernel

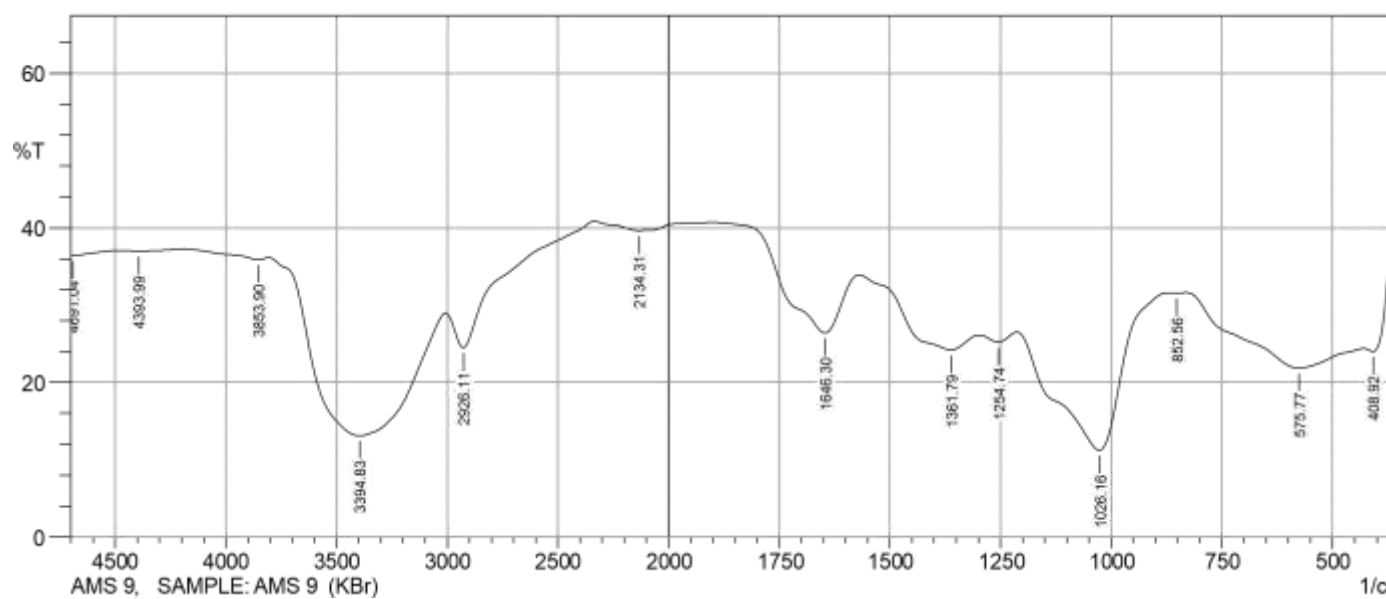


Figure 3.8 FTIR spectra of Acetylated Mango kernel (sample 9)

Table 3.5: Acetylation conditions for corn cob and the results obtained

Sample –ID	Solid-liquid ratio (g/ml)	Temperature (°C)	Time (min)	Catalyst (% g/mL)	Extent of acetylation
ACC1	1:20	30	60	1	1.02
ACC 2	1:20	60	60	1	0.99
ACC 3	1:20	80	60	1	1.00
ACC 4	1:20	100	60	1	1.08
ACC 5	1:20	130	60	1	1.01
ACC 6	1:20	100	90	1	1.03
ACC 7	1:20	100	120	1	1.06
ACC 8	1:20	100	150	1	1.00
ACC 9	1:20	100	180	1	1.10
ACC 10	1:20	100	60	2	1.11
ACC 11	1:20	100	60	3	1.50
ACC 12	1:20	100	60	4	1.10
ACC 13	1:20	100	60	0	1.06
ACC 14	1:20	30	90	1	0.99
ACC 15	1:20	30	120	1	1.01
ACC 16	1:20	30	150	1	1.09
ACC 17	1:20	60	90	1	0.97
ACC 18	1:20	60	120	1	0.98
ACC 19	1:20	60	150	1	0.98

3.3 Extent of Acetylation

3.3.1 Corn Cob-Extent of Acetylation

The effects of time, catalyst and temperature are shown in Figures 3.9, 3.10, 3.11 and Table 3.5. The trends observed in Figs 3.9, 3.10 and 3.11 are not steady (neither decreasing nor increasing) in the variations of the extent of acetylation with reaction time, catalyst and temperature and may be due to the complex nature of corn cob. Evidence, as reported by Sun and Cheng, (2002), revealed that cellulose is the major component of corn cob (about 45%), while other constituents in corn cob include lignin (6.7 – 13.9%), and hemicelluloses (39%). Furthermore, phenolic, benzylic or alcoholic (primary and secondary) hydroxyl groups are present in the lignin region while only the alcoholic hydroxyl groups are found in the carbohydrate. Phenolic hydroxyl groups are attached to aromatic rings containing various substituents (Hill *et al.*, 1998).

The different types of hydroxyl groups will react differently with acetic anhydride. For example, in the study of the acetyl distribution in acetylated (whole) wood and reactivity of isolated wood cell wall components to acetic anhydride, Rowell *et al.*, (1994) observed the order of reactivity to be lignin > hemicelluloses >>holocellulose (the remaining product after removal of lignin from wood). Cellulose was observed not to react with acetic anhydride in the absence of a catalyst.

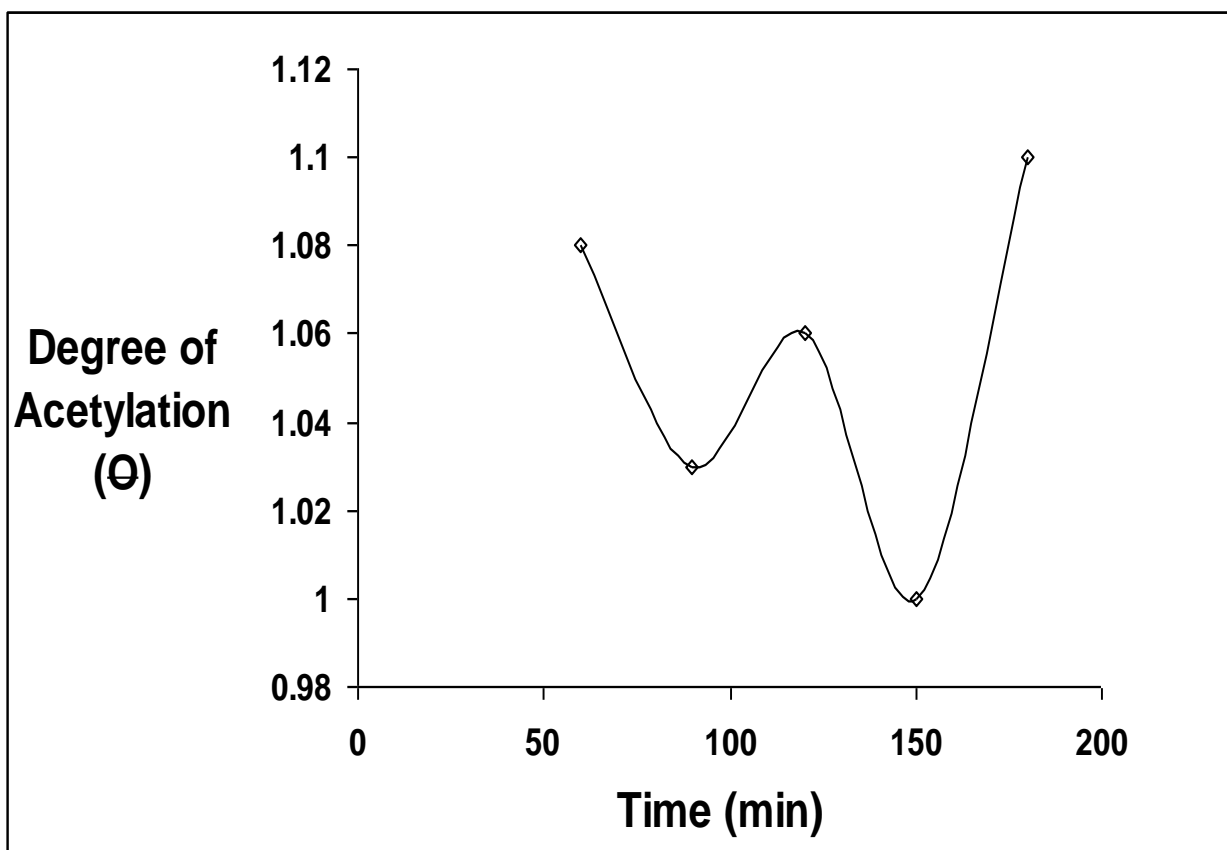


Figure 3.9: Effect of time on degree of acetylation of corn cob

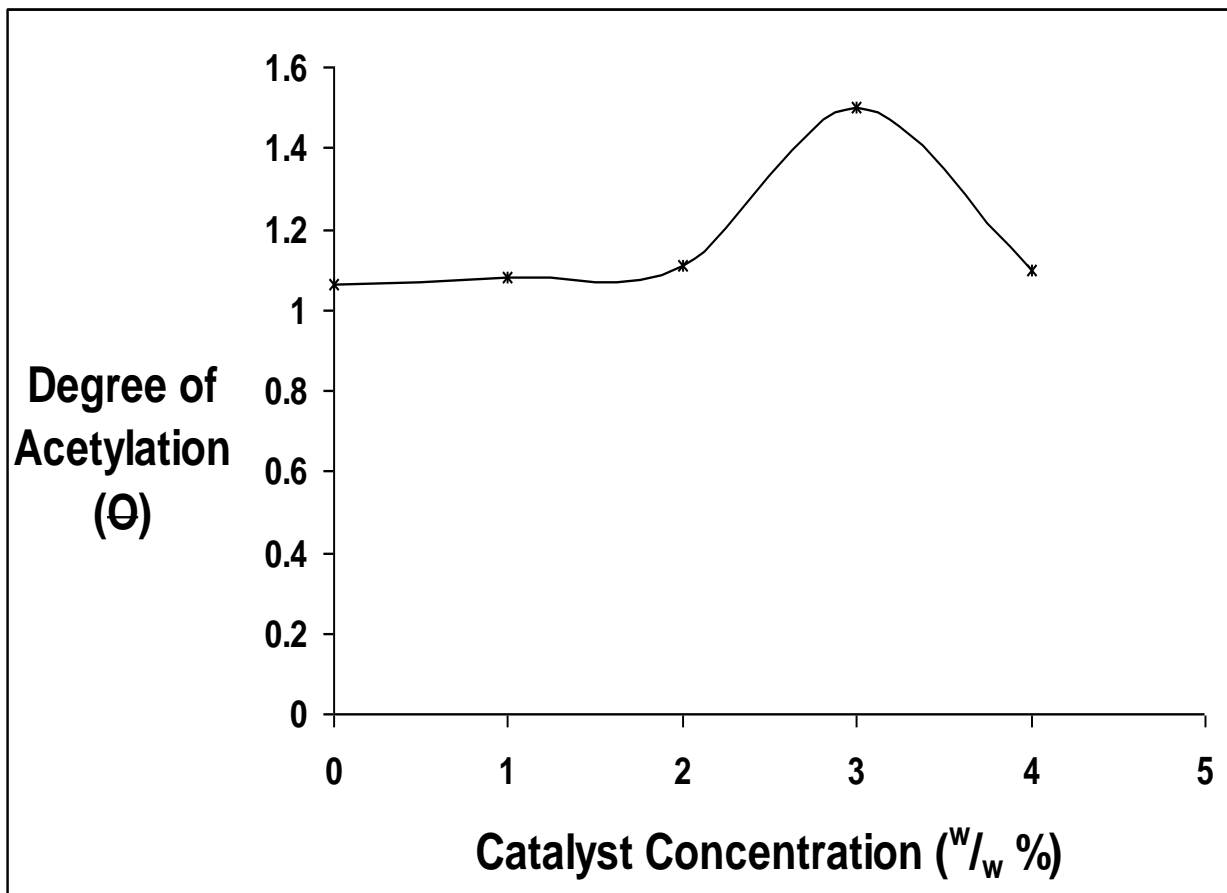


Figure 3.10: Effect of catalyst on degree of acetylation of corn cob

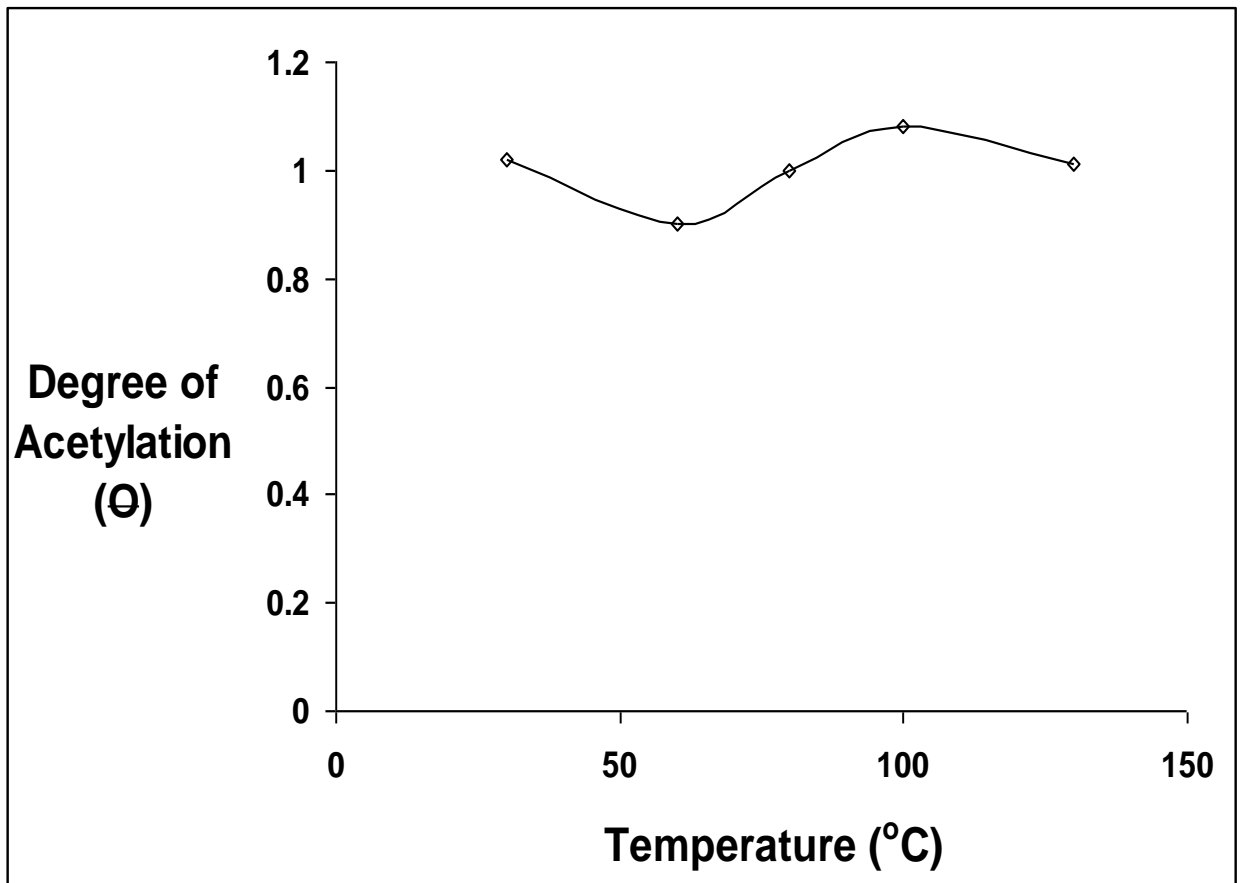


Figure 3.11: Effect of temperature on degree of acetylation of corn cob

The shown effects of time, catalyst and temperature on degree of acetylation of corn cob were tested for statistical difference. ANOVA results are presented in Table 3.6.

The null hypothesis (H_0), is that temperature, time and catalyst did not affect the acetylation of corn cob. Rejection of the hypothesis H_0 implies the acceptance of the alternative hypothesis (H_1), that temperature, time and catalyst affected the acetylation of corn cob. This statistic was performed at 5% significant level.

In this case we reject H_0 if p-value is less than 0.05 and conclude that there is significant difference in the performance of the variables. The results as presented in Table 3.6 indicated that the P-values (0.000) were less than 0.05. This therefore, implied that temperature, time and catalyst had significant effects on the acetylation of corn cob.

To understand the effects of the individual variables on the extent of acetylation (EA), their statistical relationship were tested. Correlation results are presented in Table 3.7. The results showed a positive correlation between the effects of temperature, time and catalyst on extent of acetylation. It also showed that time had a very weak relationship with EA, but temperature and catalyst had a moderate relationship. This showed that on increasing temperature and catalyst concentration, the extent of acetylation would as well increase.

Table 3.6: Anova results on corn cob extent of acetylation

		Sum of Squares	Df	Mean Square	F	Sig. P
Effect of Time	Between Groups	.006	4	.002	.000	.000
	Within Groups	.000	0	.000		
	Total	.006	4			
Effect of Temp	Between Groups	.005	4	.001	.000	.000
	Within Groups	.000	0	.000		
	Total	.005	4			
Effect of Catalyst	Between Groups	.138	4	.034	.000	.000
	Within Groups	.000	0	.000		
	Total	.138	4			

Table 3.7: Correlation for effect of time, temperature, catalyst on extent of acetylation of corn cob

	<i>TIME</i>	θ_1	<i>TEMP</i>	θ_2	<i>CATALYST</i>	θ_3
TIME	1					
θ_1	0.0397	1				
TEMP	0.9965	0.0660	1			
θ_2	0.3130	-0.5514	0.2414	1		
CATALYST	1	0.0397	0.9965	0.3130	1	
θ_3	0.4262	-0.7494	0.3681	0.9302	0.4262	1

Where θ_1 = EA for effect of time, θ_2 = EA for effect of temp, θ_3 = EA for effect of catalyst

The quantitative contributions of catalyst, time and temperature on extent of acetylation were determined using a statistical predictive tool- regression and the results are shown in Table 3.8,

Table 3.8 Regression analysis for the effect of catalyst, temperature and time on extent of acetylation

	Intercept	Slope	Standard error	t-stat	P-value
Catalyst	1.07	0.05	0.0613	0.816	0.474
Temperature	1.00	0.0002	0.0005	0.4309	0.6956
Time	1.05	0.000033	0.0005	0.0689	0.949

Equations 3.1, 3.2 and 3.3 were derived from the intercept and slope of the results presented in Table 3.8

$$EA = 1.05 + 0.00003TIME \quad . \quad 3.1$$

$$EA = 1.00 + 0.0002TEMP \quad 3.2$$

$$EA = 1.07 + 0.05C \quad 3.3$$

EA represents extent of acetylation, Time means time, Temp stands for temperature and C means catalyst. Equation 3.1, 3.2 and 3.3 showed that for every increase in acetylation reaction time brought about 0.003% increase in EA. Temperature rise by 1 Kel brought about 0.02% increase in EA, increase in the quantity of catalyst by 1%g/mL caused a 5.0% increase in EA.

3.3.2 Mango kernel Extent of Acetylation

The effects of time, catalyst and temperature are shown in Figures 3.12, 3.13, 3.14 and Table 3.9. The trends observed in Figs 3.12, 3.13 and 3.14 are not steady (neither decreasing nor increasing) in the variations of the extent of acetylation with reaction time, catalyst and temperature, might be as a result of de-acetylation mechanism attributed to lignocellulosic materials (Adebajo and Frost, 2004b) and/or differences in the reactivity of acetic anhydride and different hydroxyl group of the cell wall polymer of mango kernel (Hill *et al.*, 1996).

Table 3.9: Results of acetylation studies of mango seed kernel under several conditions

Sample –ID	Solid-liquid ratio (g/ml)	Temperature (°C)	Time (min)	Catalyst (% g/mL)	Extent of acetylation
AMSK1	1:20	30	60	1	1.14
AMSK2	1:20	60	60	1	1.30
AMSK3	1:20	80	60	1	1.58
AMSK4	1:20	100	60	1	1.50
AMSK5	1:20	130	60	1	1.79
AMSK6	1:20	100	90	1	1.67
AMSK7	1:20	100	120	1	1.50
AMSK8	1:20	100	150	1	1.65
AMSK9	1:20	100	180	1	2.36
AMSK10	1:20	100	60	0	1.23
AMSK11	1:20	100	60	2	1.02
AMSK12	1:20	100	60	3	1.05
AMSK13	1:20	100	60	4	1.93
AMSK14	1:20	30	90	1	1.48
AMSK15	1:20	30	120	1	1.59
AMSK16	1:20	30	150	1	1.34
AMSK17	1:20	60	90	1	1.54
AMSK 18	1:20	60	120	1	1.42
AMSK 19	1:20	60	150	1	1.45

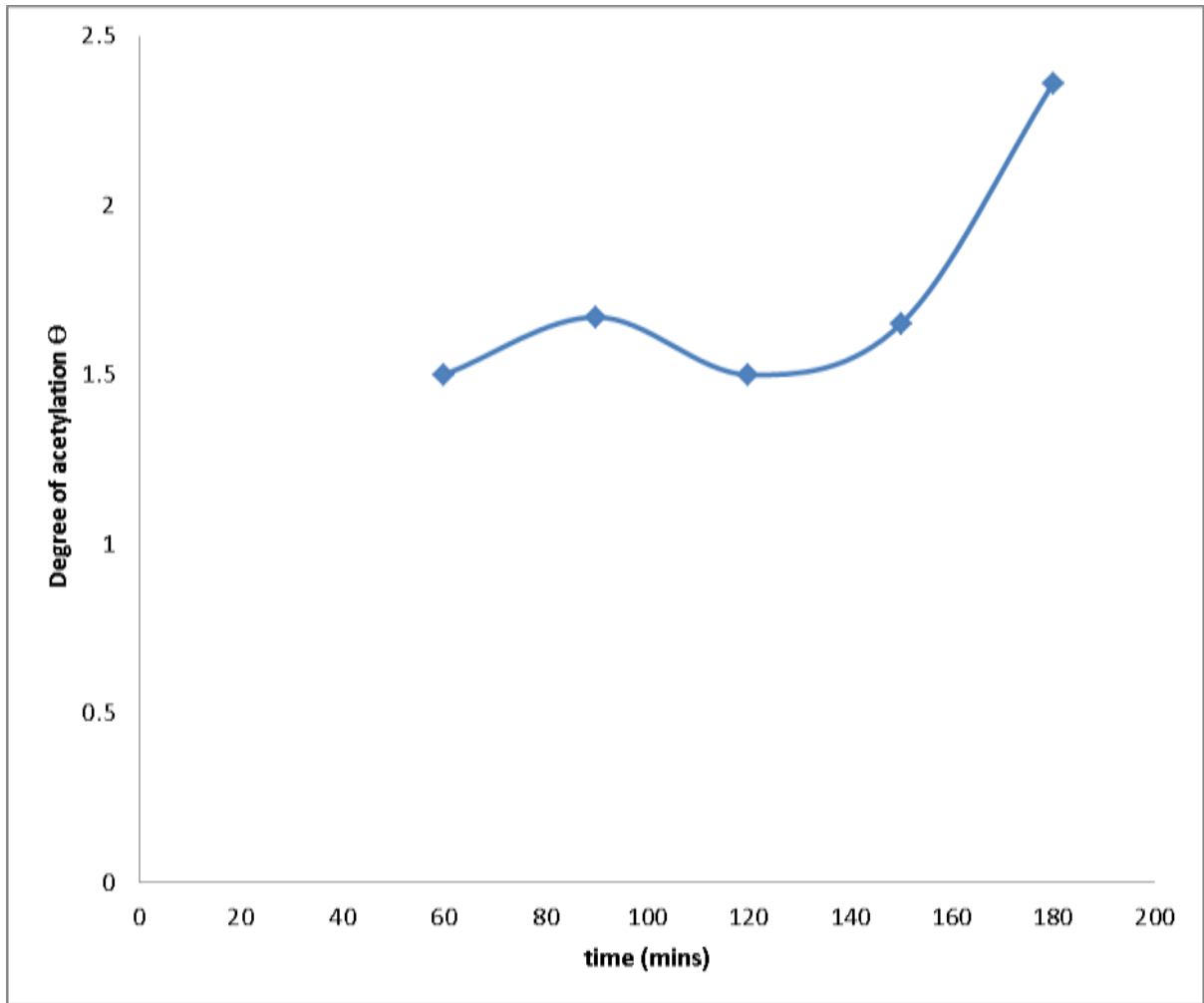


Figure 3.12: Effect of time on mango kernel extent of acetylation

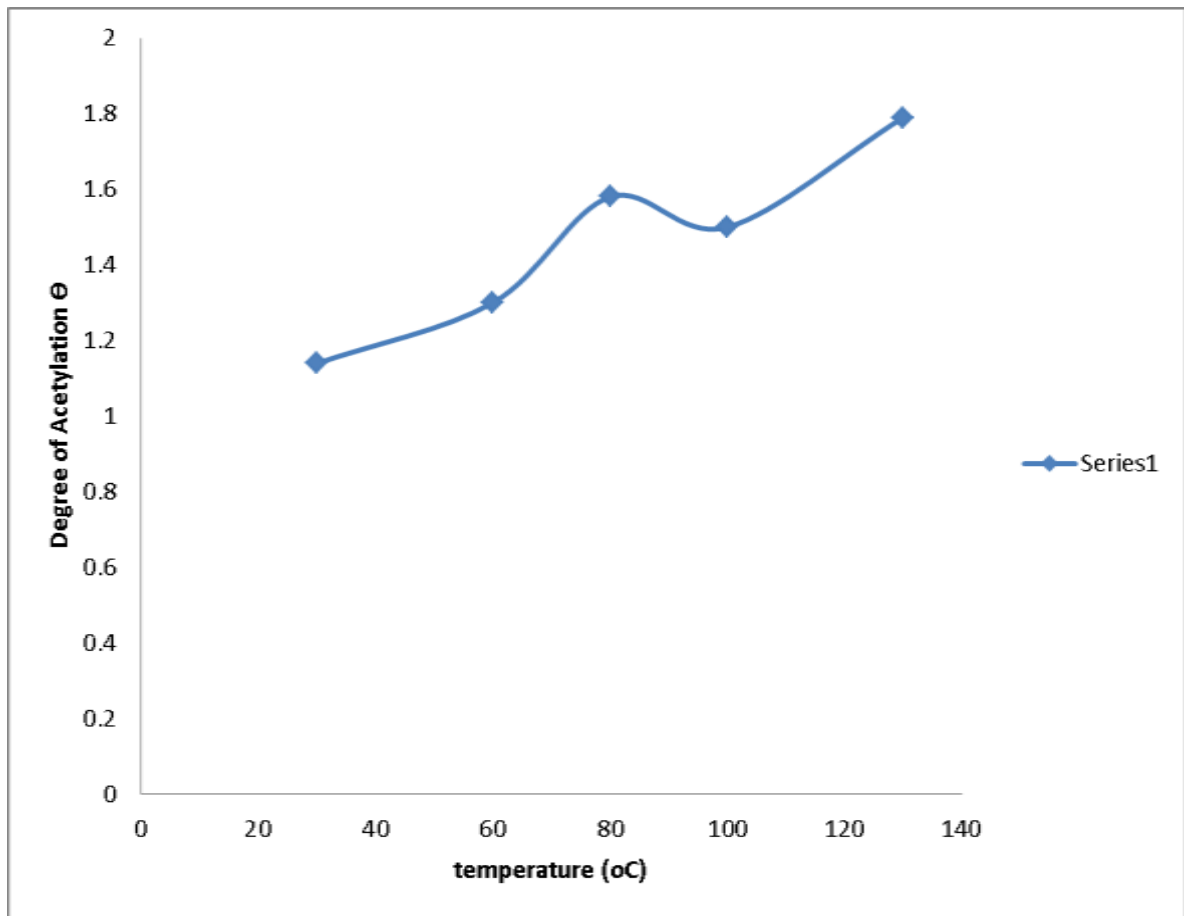


Figure 3.13: Effect of temperature on mango kernel extent of acetylation

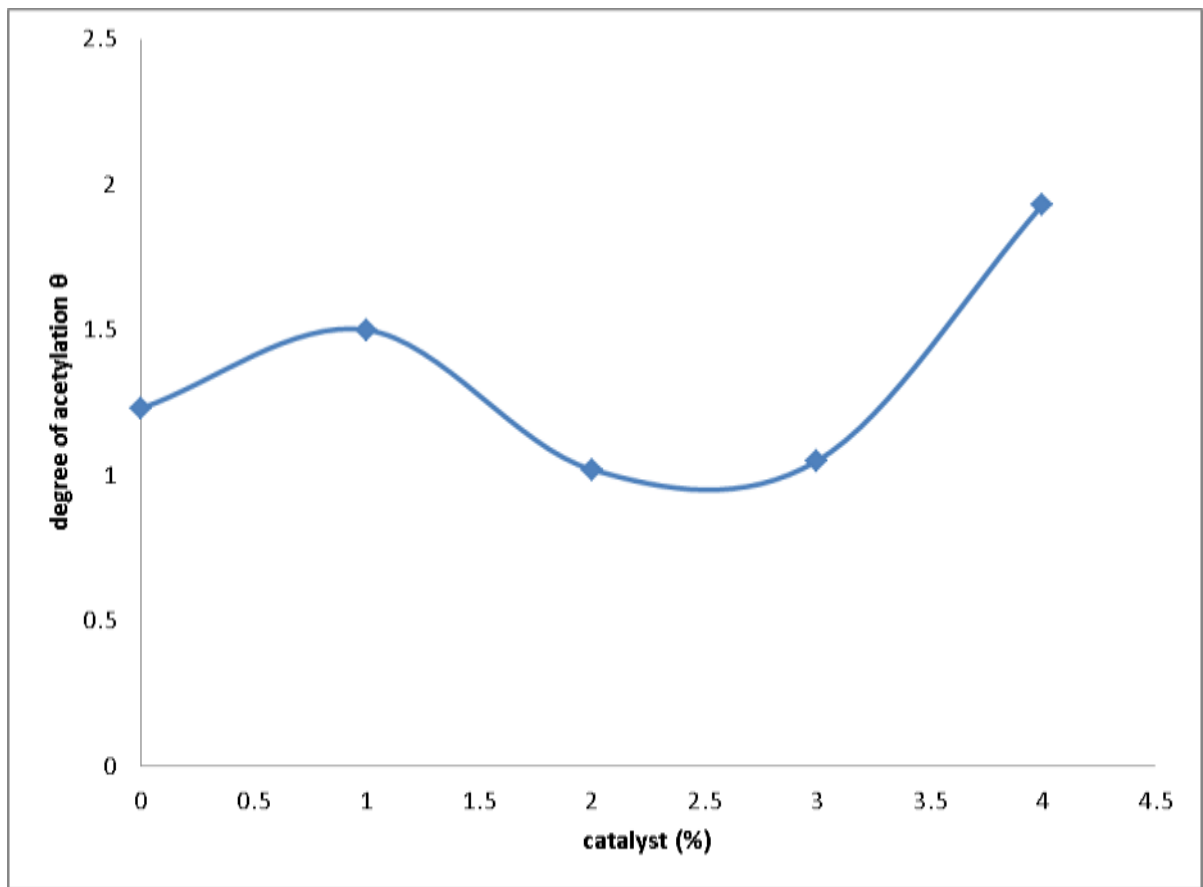


Figure 3.14: Effect of catalyst on mango kernel extent of acetylation

The shown effects of time, catalyst and temperature on degree of acetylation of mango kernel were tested for statistical difference. ANOVA results are presented in Table 3.10.

The null hypothesis (H_0), is that temperature, time and catalyst did not affect the acetylation of mango kernel. Rejection of the hypothesis H_0 implies the acceptance of the alternative hypothesis (H_1), that temperature, time and catalyst affected the acetylation of mango kernel. This statistic was performed at 5% significant level.

In this case we reject H_0 if p-value is less than 0.05 and conclude that there is significant difference in the performance of the variables. The results as presented in Table 3.10, indicated that the P-values (0.000) were less than 0.05. This therefore, implied that temperature, time and catalyst had significant effects on the acetylation of mango kernel.

To understand the effects of the individual variables on the extent of acetylation (EA), their statistical relationship were tested. Correlation results are presented in Table 3.11. The results showed that catalyst had moderate relationship with EA while temperature and time had a very strong relationship respectively. This showed that on increasing temperature, catalyst and time, the extent of acetylation would as well increase.

Table 3.10 Anova result on mango kernel extent of acetylation

		Sum of Squares	df	Mean Square	F	Sig. (p)
Effect of Time	Between Groups	0.513	4	0.128	0.000	0.000
	Within Groups	0.000	0	0.000		
	Total	0.513	4			
Effect of Temp	Between Groups	0.253	4	0.063	0.000	0.000
	Within Groups	0.000	0	0.000		
	Total	0.253	4			
Effect of Catalyst	Between Groups	0.572	4	0.143	0.000	0.000
	Within Groups	0.000	0	0.000		
	Total	0.572	4			

Table 3.11 correlation for effect of time, temperature, catalyst and mango kernel extent of acetylation

	<i>time</i>	<i>θ1</i>	<i>Temp</i>	<i>θ2</i>	<i>catalyst</i>	<i>θ3</i>
Time	1					
θ1	0.75092	1				
Temp	0.996546	0.78134	1			
θ2	0.943266	0.722872	0.953063	1		
catalyst	1	0.75092	0.996546	0.943266	1	
θ3	0.397173	0.893849	0.451352	0.405505	0.397173	1

The quantitative contributions of catalyst, time and temperature on extent of acetylation were determined using a statistical predictive tool-regression and the results are shown in Table 3.12,

Table 3.12 Regression analysis for the effect of catalyst on extent of acetylation

	Intercept	Slope	Standard error	t-stat	P-value
Catalyst	1.156	0.095	0.1267	0.7496	0.5079
Temperature	0.958	0.006	0.0012	5.4521	0.0121
Time	1.056	0.005	0.0029	1.9695	0.1435

The following expressions (equation 3.4, 3.5 and 3.6) were derived from the intercept and slope of the results of regression analysis presented in Table 3.12.

$$EA = 0.958 + 0.006TEMP \quad 3.4$$

$$EA = 1.056 + 0.005TIME \quad 3.5$$

$$EA = 1.156 + 0.095CAT \quad 3.6$$

Eqs 3.4, 3.5 and 3.6 showed that, temperature rise by 1 Kel brought about 0.6% rise in EA, increasing time by 1 minute caused a 0.5% rise in EA and increasing the amount of catalyst by 1%g/mL caused a 9.5% rise in EA.

3.4 Kinetics of Acetylation

3.4.1 Kinetics of Corn cob Acetylation

The kinetics of corn cob acetylation was studied by fitting obtained data in rate curves (Table 2.1). The predicted kinetics from the linear plots of derived pseudo first-order, lagergren first-order, second order model, pseudo second-order and intra-particle diffusion model are presented in Figures 3.15 - 3.19 respectively.

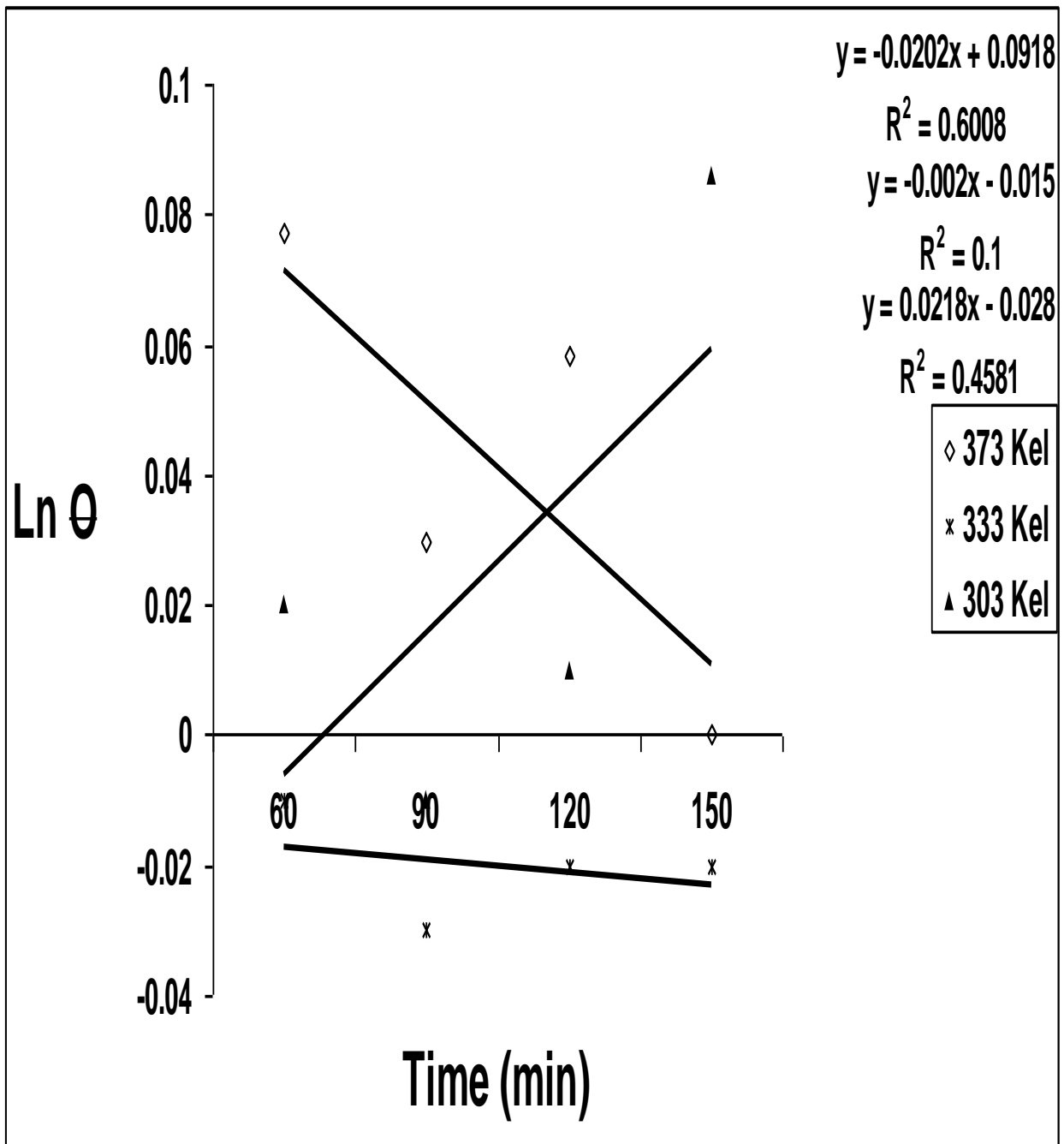


Figure 3.15: Pseudo-first order kinetics for acetylation of corn cob

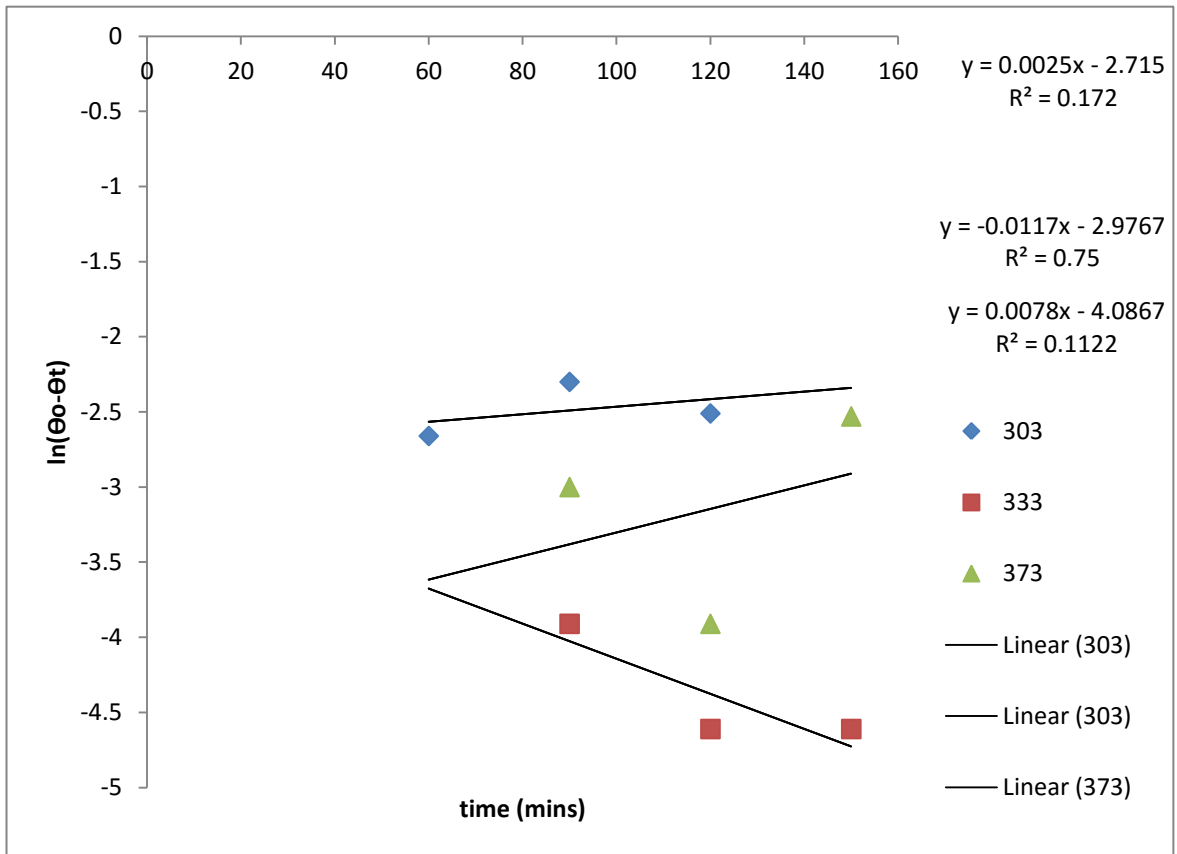


Figure 3.16 Lagergren pseudo first-order kinetics for corn cob acetylation

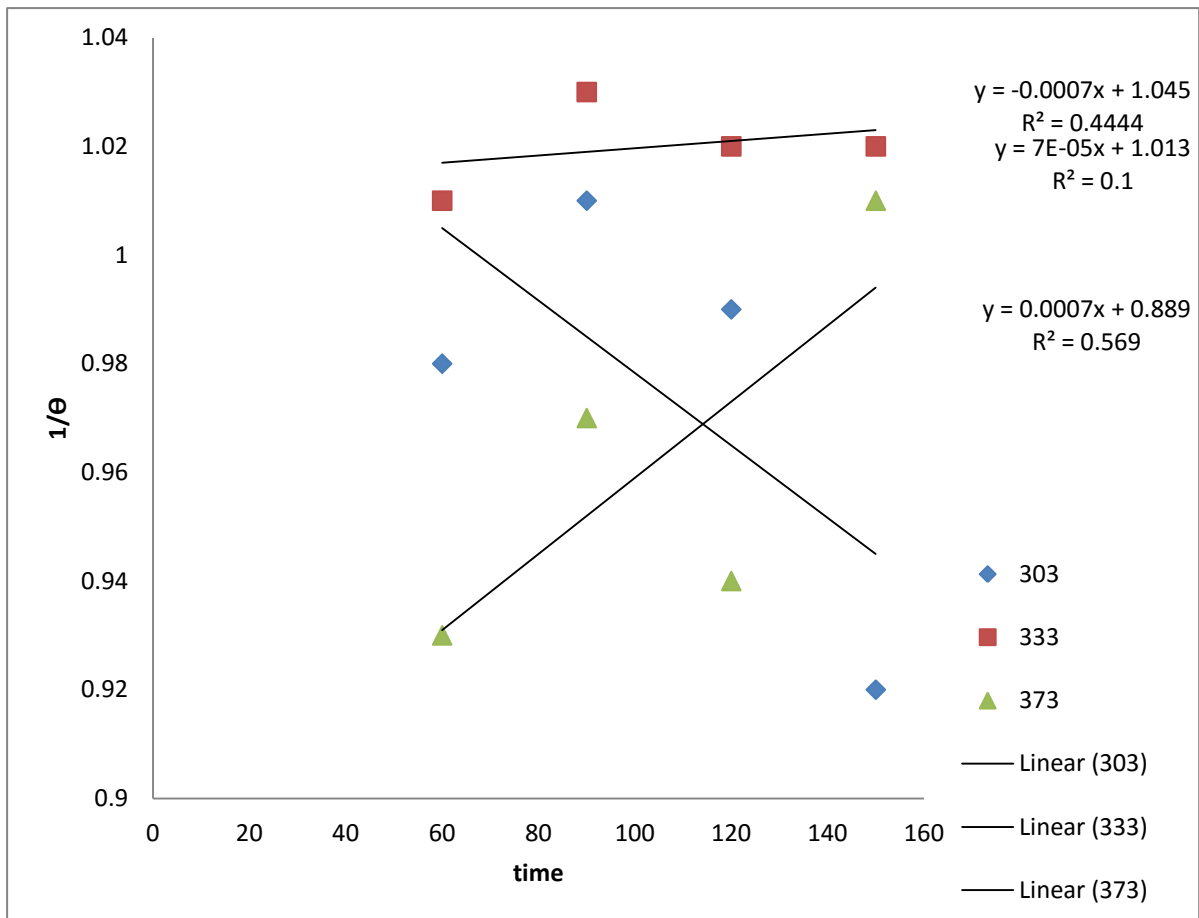


Figure 3.17:second order kinetics for corn cob acetylation

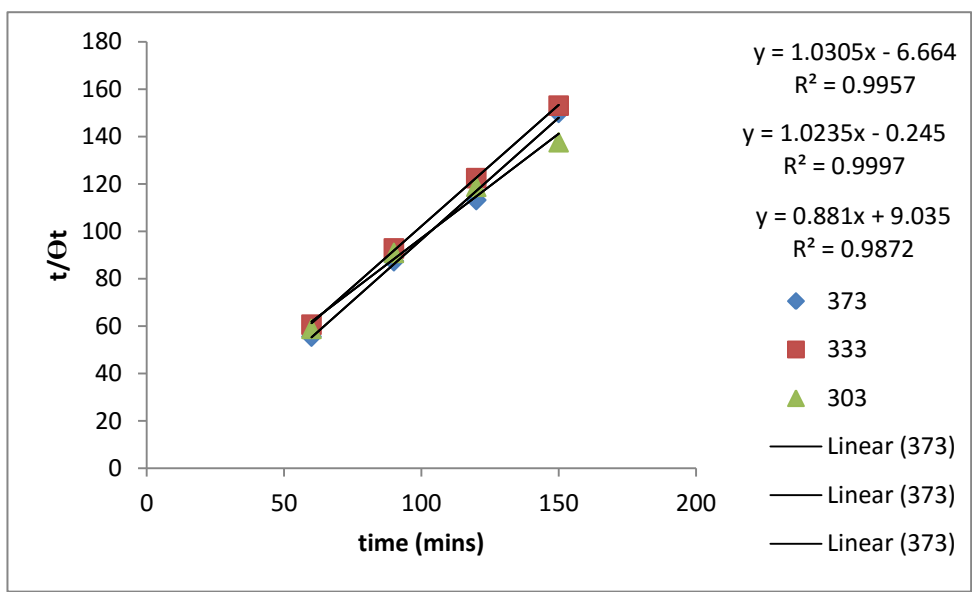


Figure 3.18 Ho Pseudo second-order kinetics for corn cob acetylation

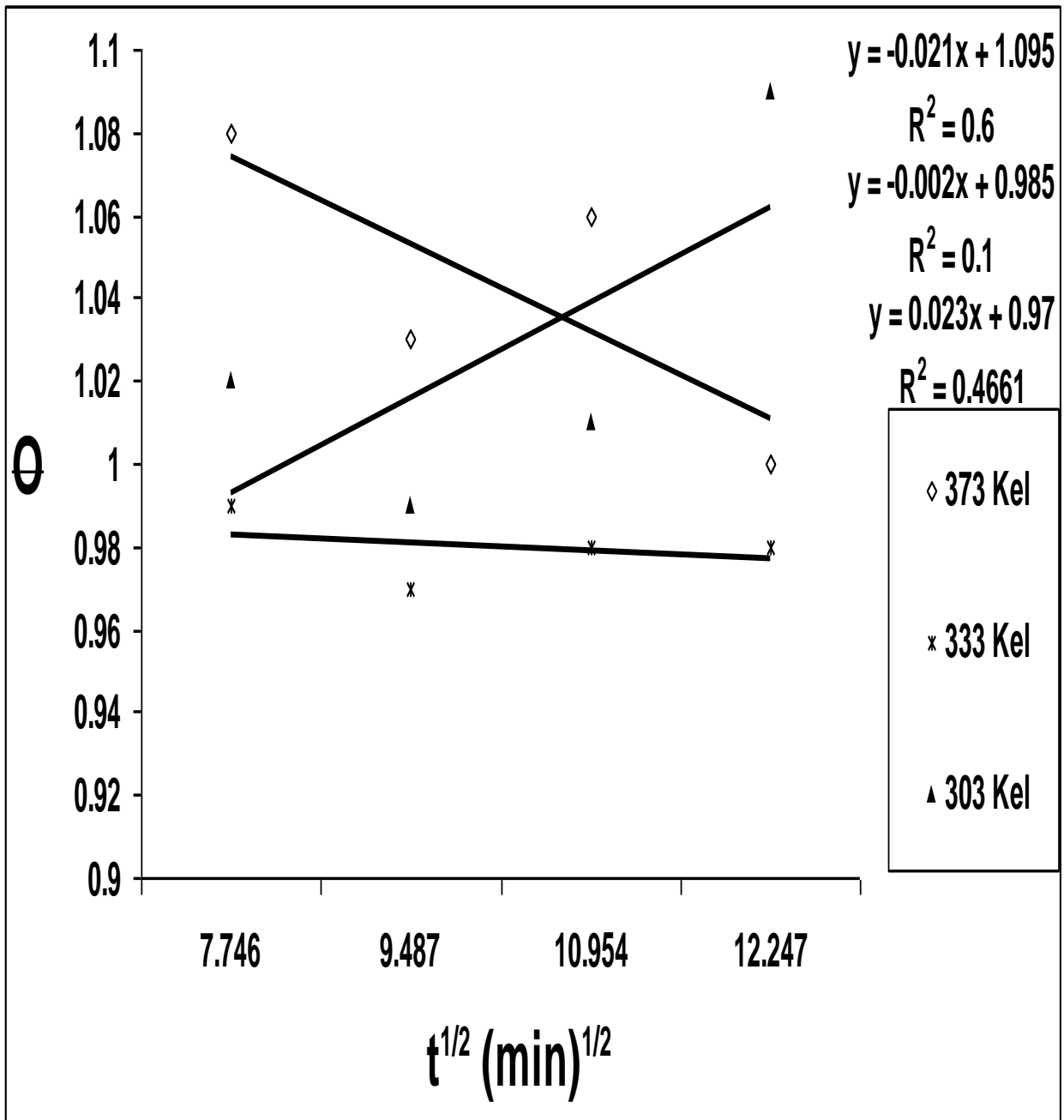


Figure 3.19: Intra-particle diffusion kinetics for acetylation of corn cob

Table 3.13 summary of kinetics derived from the plots for corn cob acetylation

	100°C	60°C	30°C
Θ_{exp}	1.08	0.99	1.09
Derived pseudo first-order			
$\Theta_{\text{o theo}}$	1.10	0.99	0.97
R^2	0.6008	0.1	0.4581
K_1	-2.0×10^{-2}	-2.0×10^{-3}	2.2×10^{-2}
Lagergren pseudo first-order			
$\Theta_{\text{o theo}}$	0.02	0.06	0.07
R^2	0.1122	0.75	0.172
K^1	7.8×10^{-3}	1.1×10^{-2}	2.5×10^{-3}
Hill second order			
Θ_{theo}	1.13	0.99	0.96
R^2	0.569	0.1	0.4444
K_2	7.0×10^{-4}	7.0×10^{-5}	-7.0×10^{-4}
Ho pseudo second order			
$\Theta_{\text{o theo}}$	0.97	0.98	1.14
K^2	-1.594×10^{-1}	-4.276	0.086
R^2	0.9957	0.9997	0.9872
Intra-particle diffusion			
k_d	-0.021	-0.002	0.023
R_2	0.6	0.1	0.4661
C	1.095	0.4661	0.97

The calculated kinetics derived from the constants are shown in Table 3.13. The very low values for the regression (R^2) for Lagergren pseudo first-order expression at studied temperature and the great difference between the theoretical and experimental active sites occupied suggests that it is inappropriate to use this kinetics to represent the acetylation of corn cob. From Table 3.13, it was also observed that the derived pseudo first-order and second order kinetics produced a theoretical value close to the experimental value, and the R^2 values for 100°C and 30°C were (0.6008 and 0.4581), (0.596 and 0.4444) respectively for the derived pseudo first-order and second order expression. These values are moderate and high (Dowine and Heath, 1974). However, the very higher R^2 values (> 0.98 in all cases) for Ho pseudo second-order expression at all temperatures studied suggests that this expression is the optimum expression to represent the acetylation of corn cob. It was also observed that as the temperature increased the theoretical number of sites occupied decreased. This suggests that effective acetylation could occur at low temperature and that high temperature is not favourable for the acetylation. Intra-particle diffusion model was also used to further study the mechanism of acetylation. Coefficient of regression values (R^2) are within $0.43 \leq R^2 \leq 0.83$ which are moderate and high (Dowine and Heath, 1974). This implies that corn cob acetylation at 30°C and 100°C are due to intra-particle diffusion. Data obtained at 60°C had low R^2 value, therefore, we cannot say for sure that diffusion mechanism is involved. It was expected that the plot of q_t versus $t^{1/2}$ would give linear relationship when intra-particle diffusion is involved in the acetylation processes and that intra-particle diffusion would be the controlling mechanism if the line passed through the origin [Hill *et al.*, 1998; Igwe and Abia, 2006; Krishnaiah *et al.*, 2008]. However for the case where the plots did not pass through the origin, the reason has been suggested that

the intra-particle diffusion was not the only mechanism involved in the acetylation process due to some degree of boundary layer control [Bulut *et al.*, 2008].

The larger, the intercept the greater the contribution of surface reaction in the rate controlling step (Dawodu and Akpomie, 2014). It was observed from our results presented in Table 3.13 that as temperature increased to 100°C the value of intercept also increased indicating a greater contribution of surface reactions. This explains better the results obtained in the pseudo second order expression on the non-favourability of high temperature on corn cob acetylation. Since diffusion is related to density and surface area through which the reagent diffuses. The surface area is not constant and may vary at different temperature. It may be deduced that corn cob being a light and porous material, at low temperature, the relative rates of diffusion and reaction of the anhydride and corn cob-OH are equal, but at high temperature, swelling of the material increases, thereby increasing the rate of diffusion of the anhydride at the expense of the reaction. This therefore, limits diffusion mechanism (Hill *et al.*, 1998).

Results from our kinetic studies revealed that, acetylation of corn cob is by surface reaction and diffusion into the pores of corn cob. This is in agreement with results elsewhere [Hill *et al.*, 1998].

3.4.2 Kinetics of Mango kernel Acetylation

The kinetics of mango kernel acetylation was studied using by fitting obtained data in rate curves- pseudo first-order model, lagergren pseudo first-order model, second order model (Hill *et al.*, 1998), pseudo second order (Ho, 1995) and intra-particle diffusion mechanism (Table 2.1). The predicted kinetics from the linear plots of derived pseudo first-order, lagergren first order, second order model, pseudo second-order and intra-particle diffusion model are presented in Figures 3.20 - 3.24 respectively

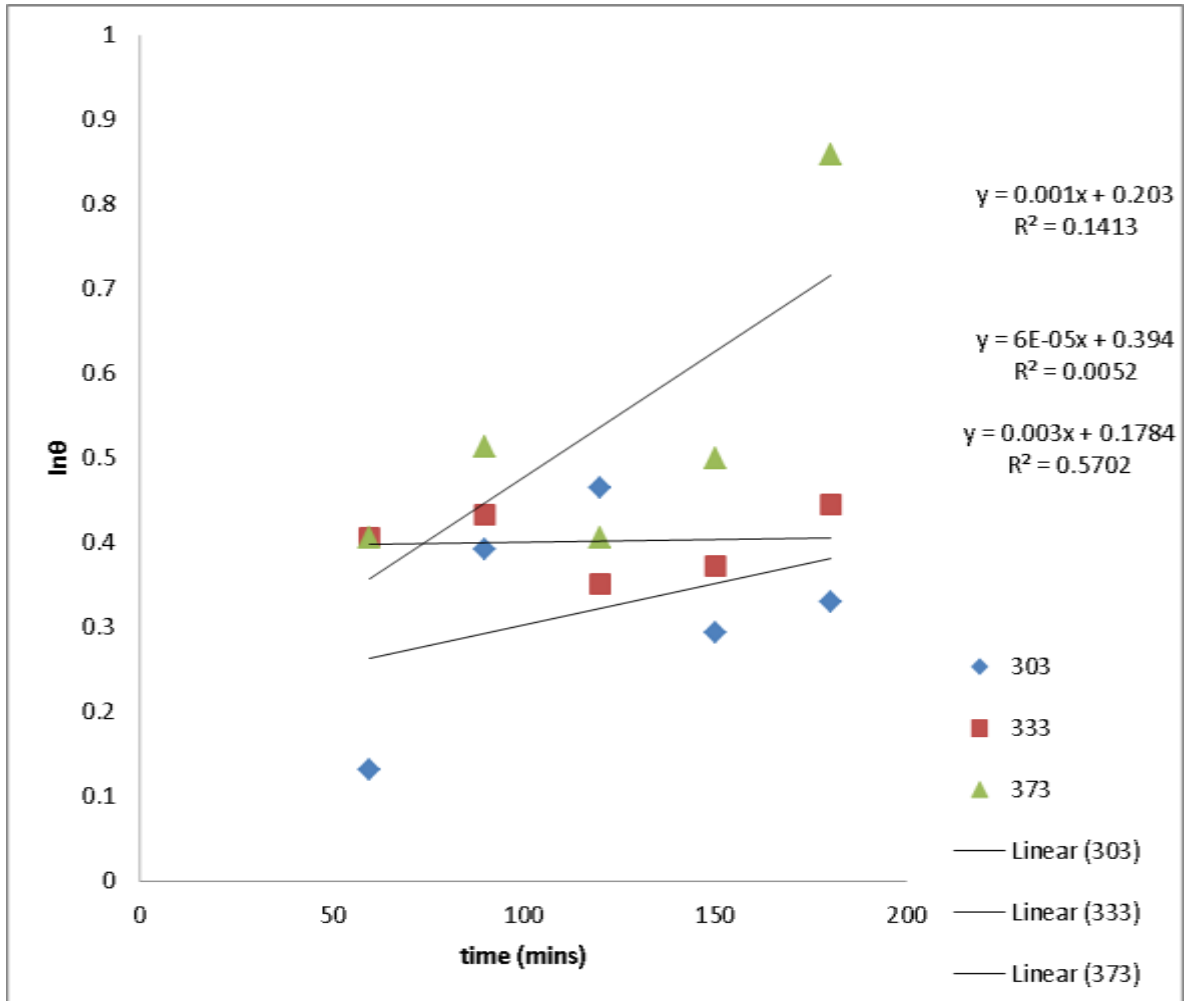


Figure 3.20: pseudo-first order kinetic model for mango kernel acetylation

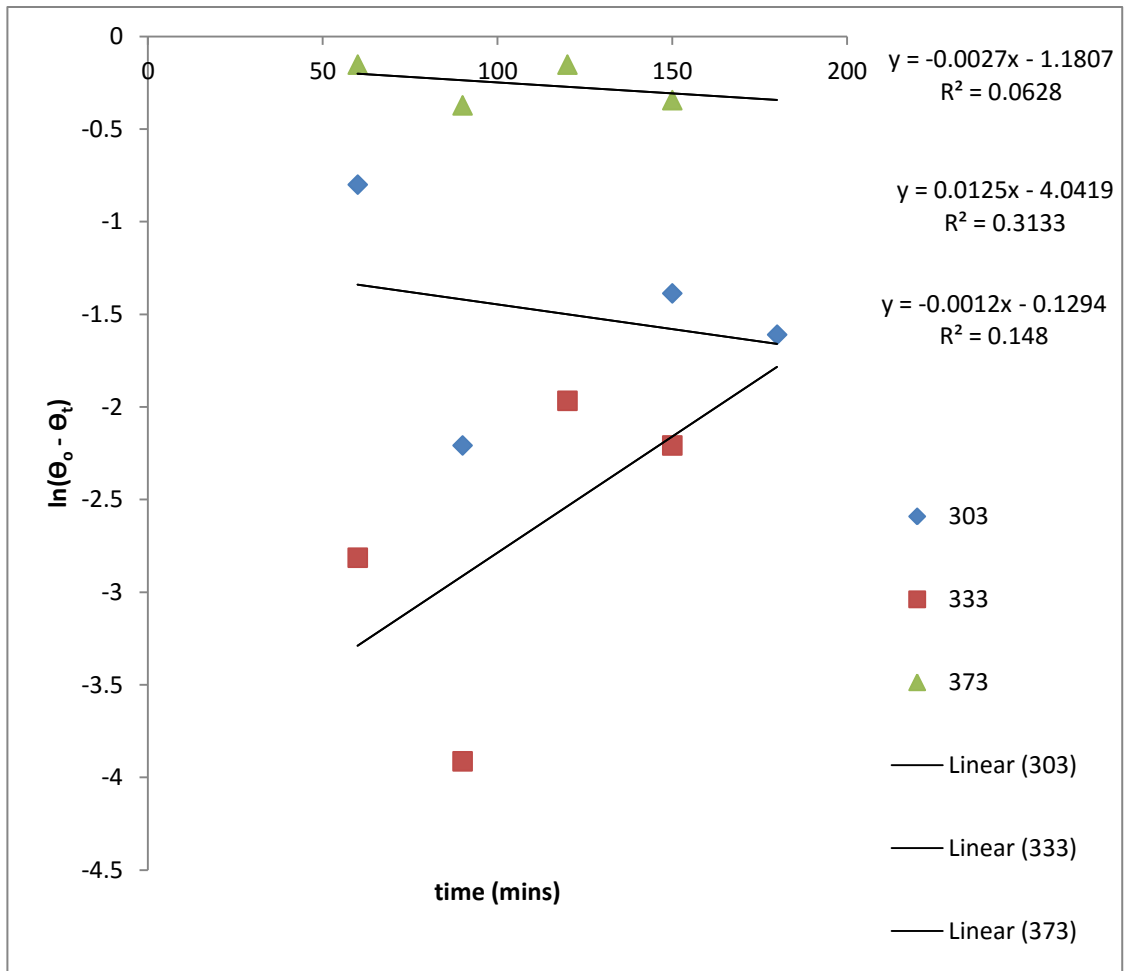


Figure 3.21 Lagergren pseudo first-order kinetics for mango kernel acetylation

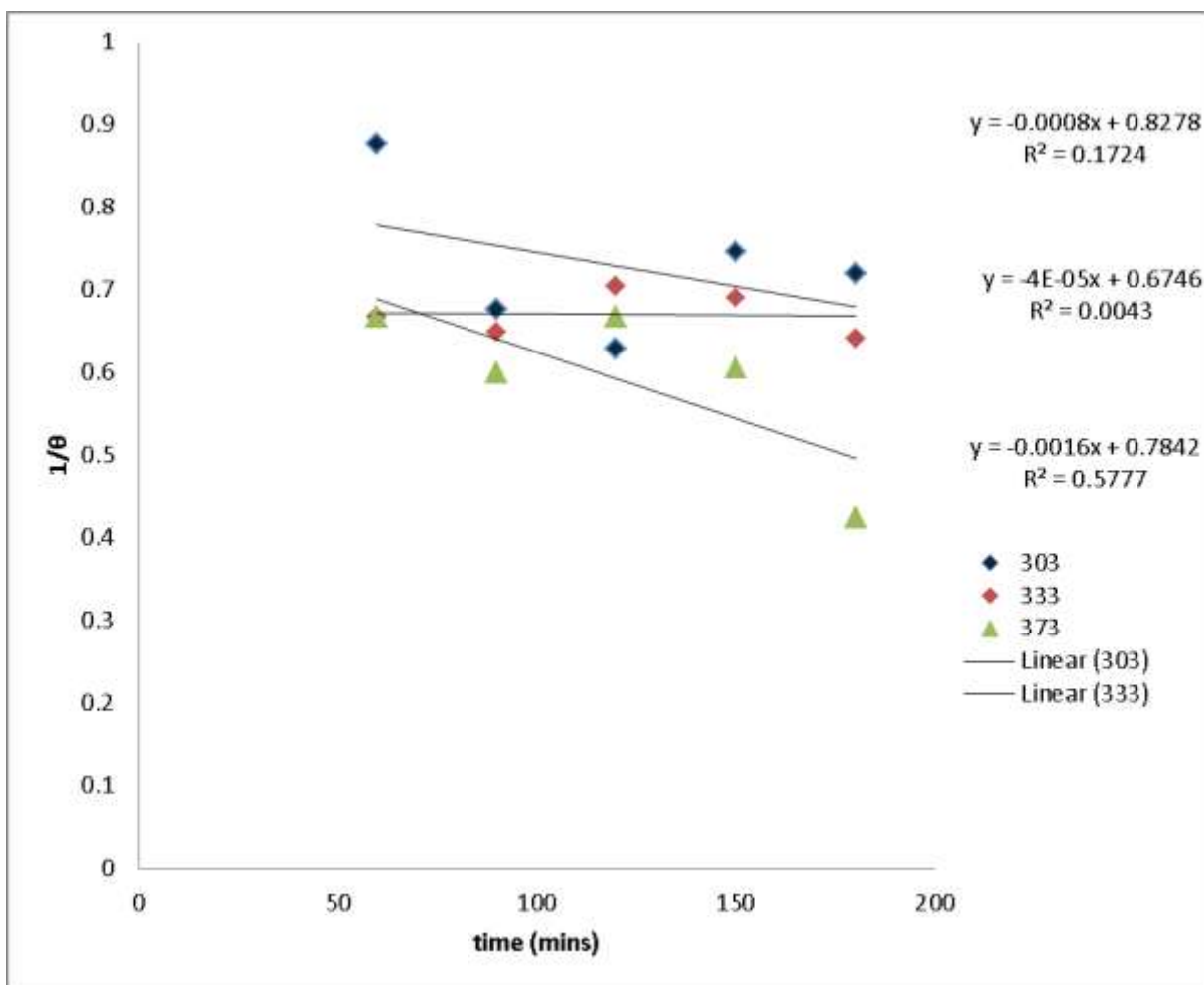


Figure 3.22: second order kinetic plot for mango kernel acetylation

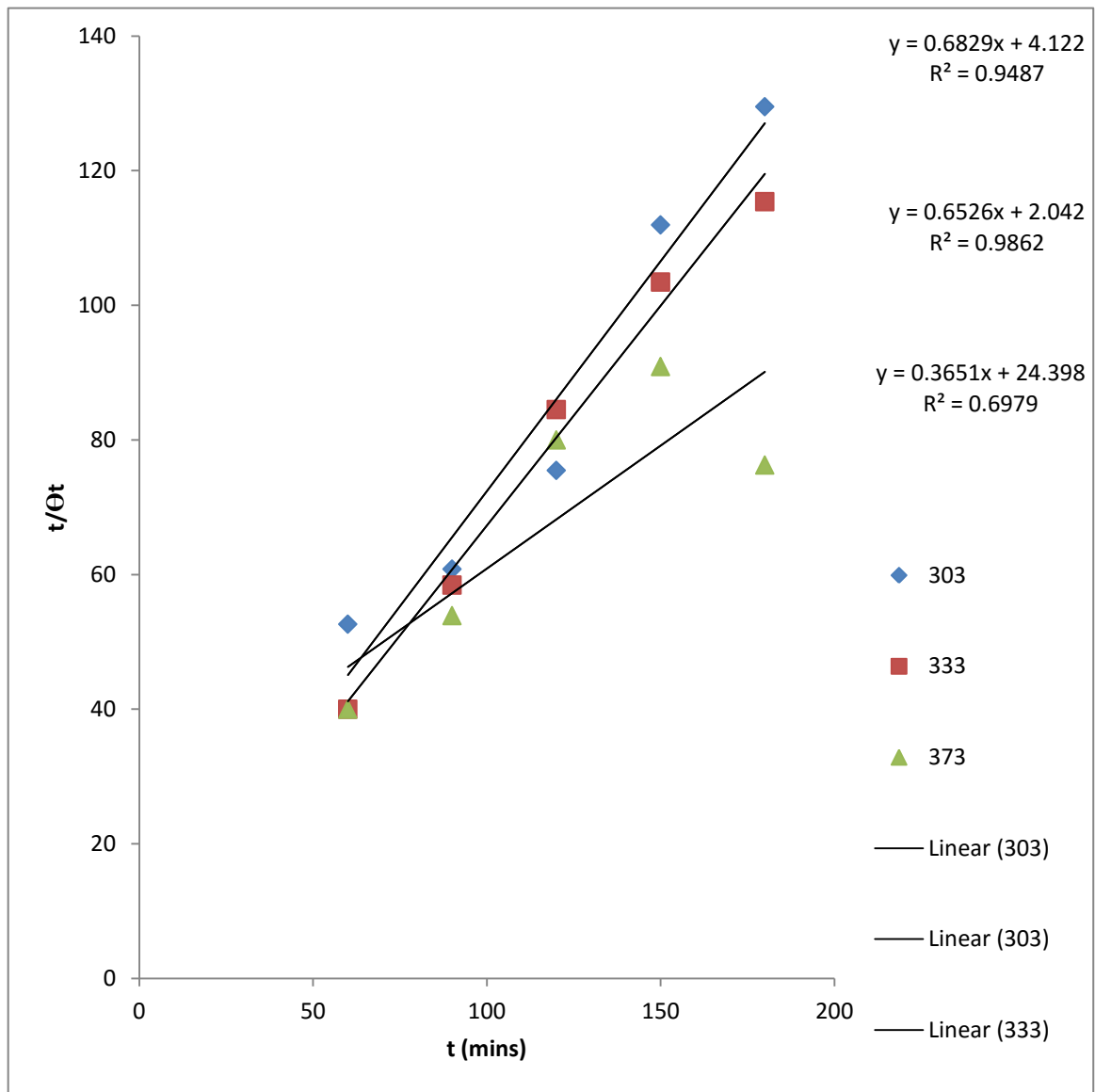


Figure 3.23 Ho Pseudo second-order kinetics for mango kernel acetylation

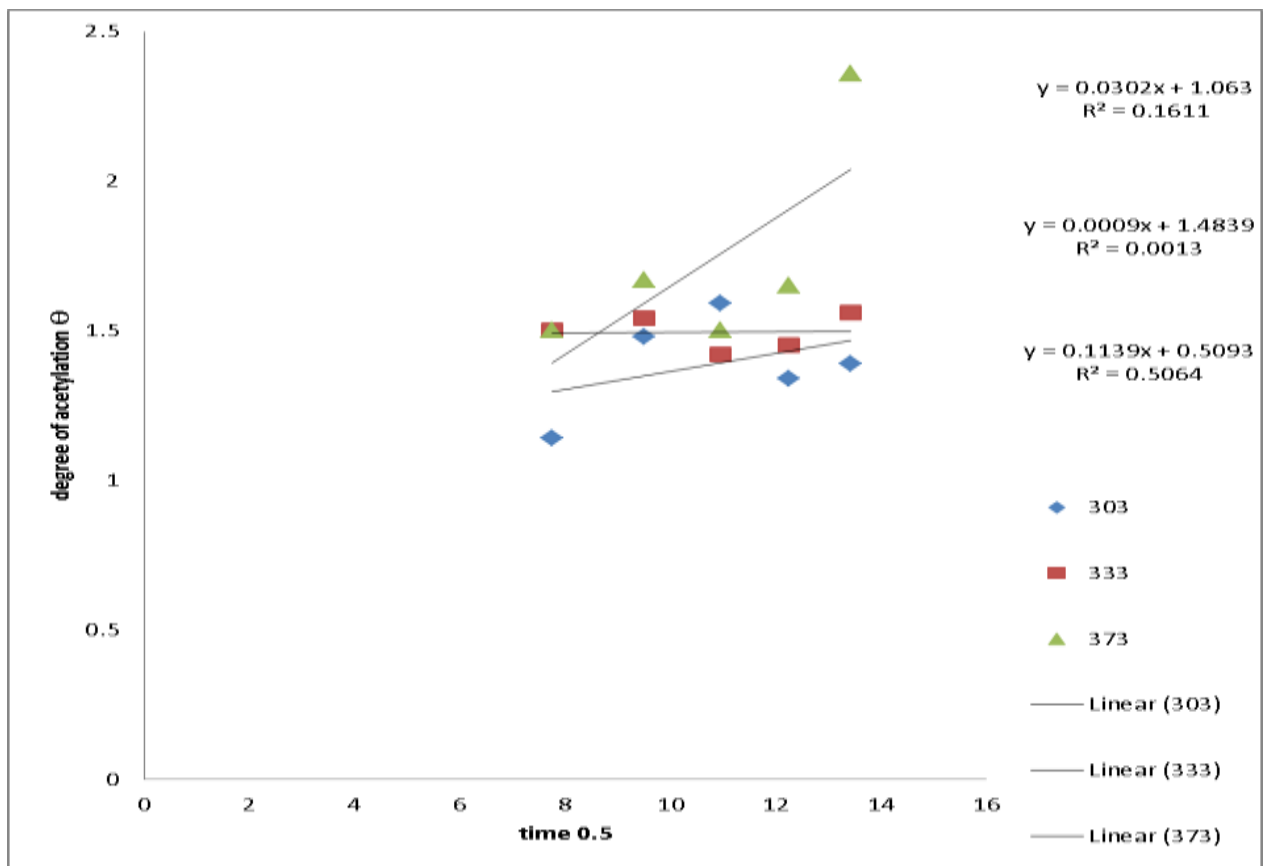


Figure 3.24: intra-particle diffusion kinetics for mango kernel acetylation

Table 3.14 Summary of the kinetics derived from the plots for Mango kernel acetylation

	100°C	60°C	30°C
$\Theta_o \text{ exp}$	2.36	1.56	1.59
Derived pseudo first-order			
$\Theta_o \text{ theo}$	1.195	1.482	1.225
R^2	0.5702	0.0052	0.1413
K_1	-3.0×10^{-3}	6.0×10^{-5}	1.0×10^{-3}
Lagergren pseudo first-order			
$\Theta_o \text{ theo}$	0.999	1.013	1.002
R^2	0.148	0.3133	0.0628
K^1	-1.2×10^{-3}	1.25×10^{-2}	2.7×10^{-3}
Hill second order			
Θ_{theo}	1.276	1.484	1.209
R^2	0.5772	0.004	0.172
K_2	-1.0×10^{-3}	-4.0×10^{-5}	-8.0×10^{-4}
Ho pseudo second order			
$\Theta_o \text{ theo}$	2.736	1.5323	1.4643
K^2	5.46×10^{-3}	2.08×10^{-1}	1.13×10^{-1}
R^2	0.6979	0.9862	0.9487
Intra-particle diffusion			
k_d	0.1139	0.0009	0.0302
R_2	0.5064	0.0013	0.1611
C	0.5093	1.4839	1.0639

The very low R^2 for Lagergren pseudo first-order expression at studied temperatures suggests that it is not appropriate to use this kinetics to represent the acetylation of mango kernel. It was observed that the pseudo first order and second order model (Table 3.14) was able to produce moderate fit to experimental data at 100°C. We cannot say for sure the mechanisms at 60°C and 30°C because of the very low R^2 values. However, the very higher R^2 values (> 0.6 in all cases) for Ho pseudo second-order expression in all temperature studied suggests that pseudo second-order kinetic expression is the optimum kinetic expression to represent the acetylation of mango kernel. It was also observed that as temperature increased the theoretical extent of acetylation also increased, showing the compatibility of the reaction ingredients with temperature.

Intra-particle diffusion model was also used to further study the mechanism of mango kernel acetylation. Likewise, coefficient of regression, values (R^2) are within $0.43 \leq R^2 \leq 0.83$ which are moderate and high (Dowine and Heath, 1974). This therefore implies that mango kernel acetylation mechanism at 100°C is due intra-particle diffusion. Data obtained at 30°C and 60°C had low R^2 value, therefore, we cannot say for sure if diffusion mechanism is involved. It was expected that the plot of Θ_t versus $t^{1/2}$ would give linear relationship when intra-particle diffusion is involved in the acetylation processes and that intra-particle diffusion would be the controlling mechanism if the line passed through the origin [Hill *et al.*, 1998; Igwe and Abia, 2006; Krishnaiah *et al.*, 2008]. However for the case where the plots did not pass through the origin, the reason has been suggested that the intra-particle diffusion was not the only mechanism involved in the acetylation process due to some degree of boundary layer control [Bulut *et al.*, 2008].

From the results of physicochemical analysis of mango kernel, it was observed that mango kernel has a high density and less pores. This indicates that the material is heavy and as a

result, requires more critical condition for acetylation. This might account for the reason why the mechanisms for 30°C and 60°C were not accounted.

Results, from our kinetic studies revealed that acetylation of mango kernel is by surface reaction and diffusion into the inner surfaces of mango kernel. This is in agreement with results elsewhere [Hill *et al.*, 1998].

3.5 Thermodynamics of acetylation

3.5.1. Thermodynamics of corn cob acetylation

The thermodynamics of corn cob acetylation was studied using the Clausius Clapeyron equation (Eq. 2.19). Figure 3.25 presents the plots using equation 2.19c.

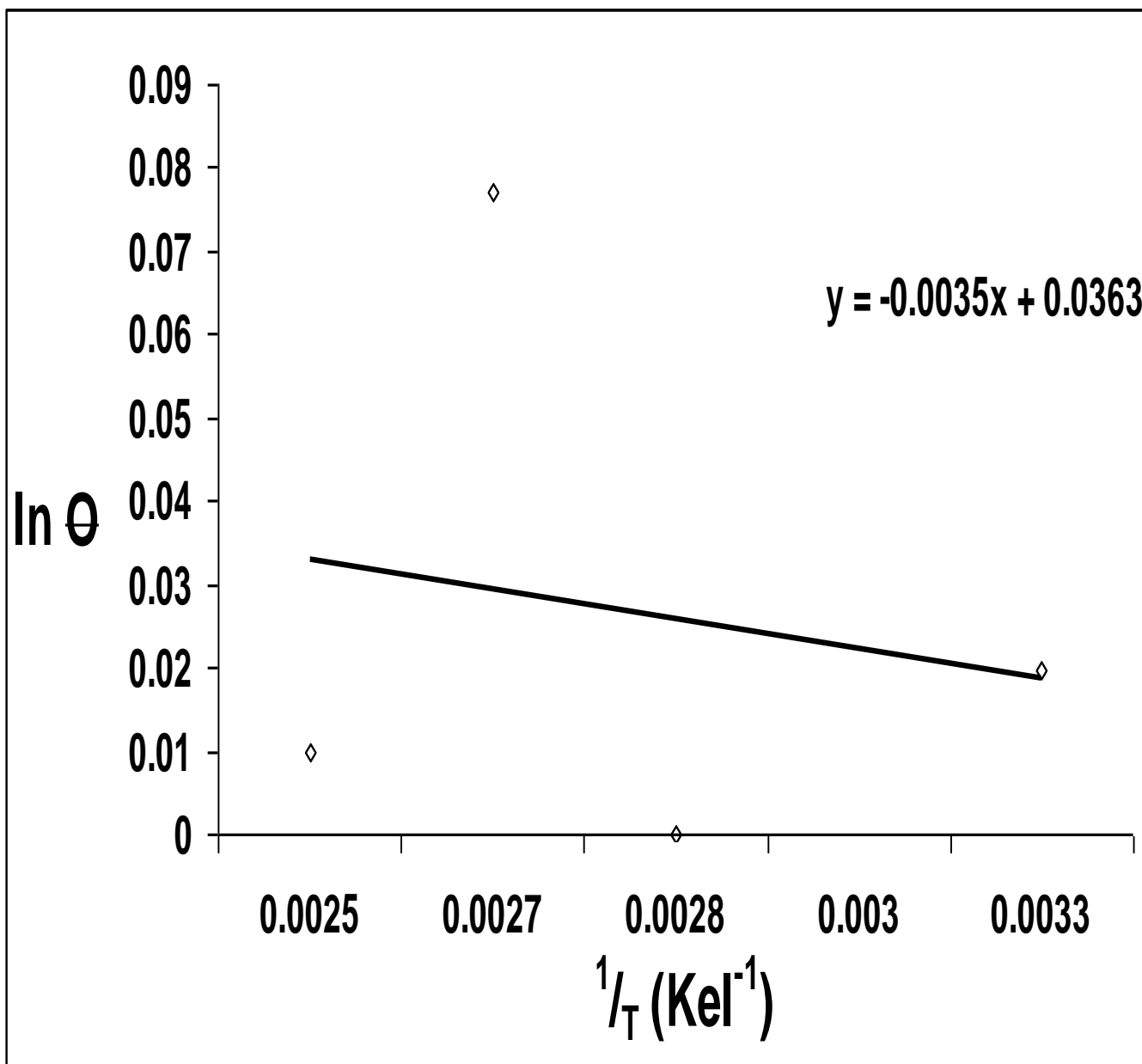


Figure 3.25: Clausius-Clapeyron plots for the acetylation of corn cob

It should be noted that we assumed the acetylation of corn cob to be an equilibrium surface reaction. Obtained value of slope allowed the calculation of heat of corn cob acetylation (0.0291 Jmol^{-1}). From intercepts on x and y axis, the critical temperature of acetylation (0.814 kel) and critical degree of acetylation (1.037) values were determined respectively. Positive value of heat of corn cob acetylation and very low critical temperature value suggested that corn cob acetylation is a process which proceeds easily (spontaneous) by absorbing heat from the environment. A general trend also exists such that high heat of acetylation of a substance/material means more difficulty in acetylating the material; therefore, very low heat of acetylation value implied the ease at which corn cob could be acetylated. The critical degree of corn cob acetylation represents values which obtained explains the mechanism of acetylation of corn cob (values above it suggest diffusion mechanism and vales below it suggest surface adsorption mechanism).

The heat capacity (C_p) of corn cob acetylation represents the quantity of heat needed to acetylate corn cob whenever a degree rise in temperature occurs. Value of C_p obtained was $4.157 \times 10^{-4} \text{ Jmol}^{-1}\text{K}^{-1}$.

The change in entropy (ΔS) for corn cob acetylation obtained is $5.005 \times 10^{-4} \text{ Jmol}^{-1}\text{K}^{-1}$. The value of ΔS is positive and suggested a degree of disorderliness during the acetylation process. Below is an equation which describes the acetylation of corn cob and showed that acetic anhydride (larger molecule) 'disintegrates' into acetic acid (smaller molecule). This accounts for the positive value of entropy change obtained.



An important thermodynamic parameter, change in Gibb's free energy (ΔG), were obtained at different temperature conditions, and values were -0.123 Jmol^{-1} (303 K), -0.138 Jmol^{-1} (333 K) and -0.158 Jmol^{-1} (373 K). The values are negative and suggested that, at all temperatures, corn cob acetylation was spontaneous.

3.5.2 Thermodynamics of Mango kernel acetylation

The effect of temperature on the extent of mango kernel acetylation was investigated through the plots of equation 2.19c. Figure 3.26 presents the plots of equation 2.19c

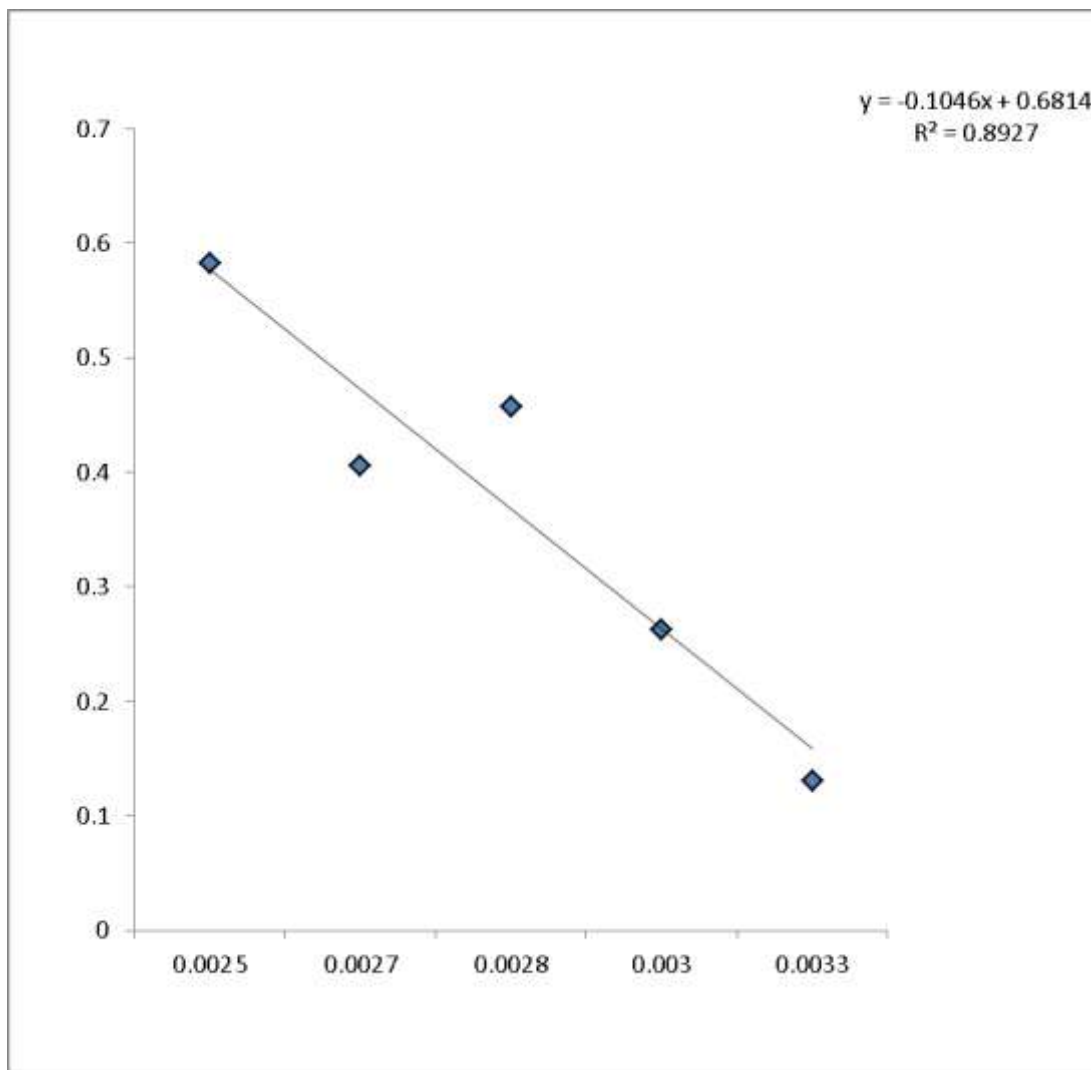


Figure 3.26 Clausius clapeyron plot for mango kernel acetylation

It should be noted that we assumed the acetylation of mango kernel to be an equilibrium surface reaction. Obtained value of slope allowed the calculation of heat of mango kernel acetylation (0.8696 Jmol^{-1}). From intercepts on x and y axes, the critical temperature of acetylation (0.016 K) and critical degree of acetylation (1.977) values were determined respectively. Positive value of heat of mango kernel acetylation and very low critical temperature value suggested that mango kernel acetylation is a process which proceeds easily (spontaneous) by absorbing heat from the environment. A general trend also exists such that high heat of acetylation of a substance/material means more difficulty in acetylating the material, therefore, very low heat of acetylation value implied the ease at which mango kernel could be acetylated. The critical degree of mango kernel acetylation represented values which were obtained and explains the mechanism of acetylation of mango kernel (values above it suggested diffusion mechanism and values below it suggested surface adsorption mechanism). This further explained why good acetylation results were obtained only at high temperature and longer reaction time.

The heat capacity (C_p) of mango kernel acetylation represents the quantity of heat needed to acetylate corn cob whenever a degree rise in temperature occurs. Value of C_p obtained was $1.242 \times 10^{-2} \text{ Jmol}^{-1}\text{K}^{-1}$.

The change in entropy (ΔS) for corn cob acetylation obtained is $1.495 \times 10^{-2} \text{ Jmol}^{-1}\text{K}^{-1}$. The value of ΔS is positive and suggested a degree of disorderliness during the acetylation process.

An important thermodynamic parameter, change in Gibb's free energy (ΔG), were obtained at different temperature conditions, and values were -3.66 Jmol^{-1} (303 K), -4.11 Jmol^{-1} (333 K) and -4.71 Jmol^{-1} (373 K). The values are negative and suggested that, at all temperatures, mango kernel acetylation was spontaneous.

3.6 Water absorption Capacity

3.6.1. Water Absorption Capacity of Corn Cob

The principal essence for studying corn cob acetylation is to observe whether the modification of corn cob (by acetylation) can alter its water absorption capacity. Figure 3.23 presents the results on water absorption capacity for modified and unmodified corn cob.

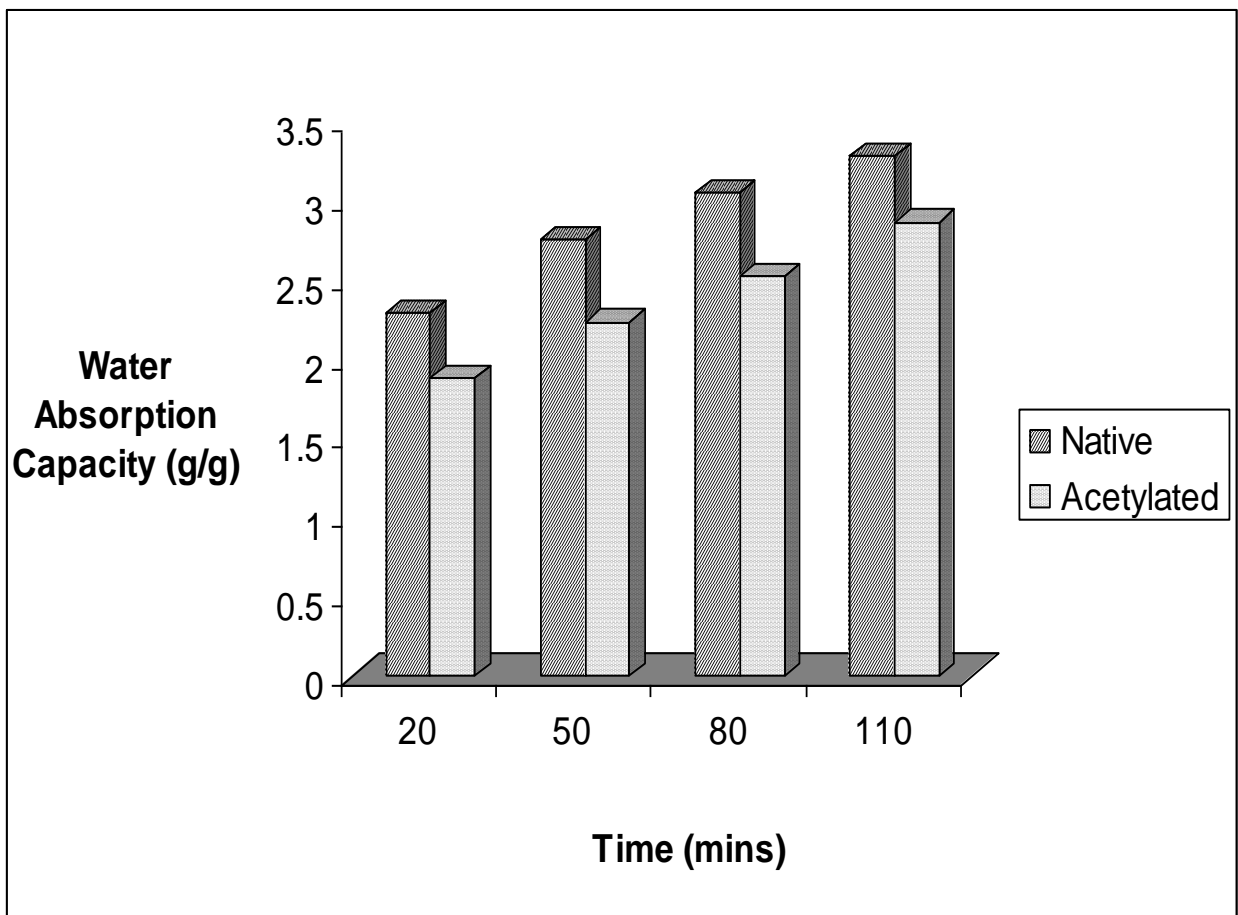


Figure 3.27: Variation of water absorption capacity with time for modified and unmodified corn cob

Raw corn cob can hold significant amount of water due to hydrogen bonding between hydroxyl group and water molecule. It has been established that when the accessible hydrogen of the hydroxyl group in the cell wall polymer have been substituted by acetyl group, reduction in water and moisture sorption are observed (Yakubu et al., 2012). Figure 3.27 revealed that at all times, the water absorption capacity of corn cob was highest for the native material and lowest for the acetylated material. It was also observed that the treated material reached saturation point faster than the untreated. This is due to an enhanced hydrophobicity. The reduction in water absorption capacity value was tested for significance. Table 3.15 presented results for the significant effects of time and acetylation on corn cob water absorption capacity.

Table 3.15: ANOVA Results on the effects of time on water absorption capacity of corn cob and mango kernel

	Mean	Std Deviation	Std. Error	t	Df	Sig (P)
			Mean			
ACC-RCC	-0.47000	0.06377	0.03189	-14.740	3	0.001
AMS_RMS	-0.33250	0.08057	0.04029	-8.254	3	0.004

The null hypothesis (H_0), is that acetylation have not reduced water absorption capacity of corn cob. Rejection of the hypothesis H_0 implies the acceptance of the alternative hypothesis (H_1), that acetylation have reduced the water absorption capacity. This statistic was performed at 5% significant level.

In this case we reject H_0 if p-value is less than 0.05 and conclude that there is significant difference in the performance of the two variables. The results as presented in Table 3.15

indicated that the P-value (0.001) is less than 0.05. This therefore, implied that time and acetylation has significant effects on water absorption capacity of corn cob.

To understand the direction of these effects, regression analysis was performed. Eq. (3.7 and 3.8) presents regression results for corn cob water absorption capacity. The (linear) regression equation for water absorption capacity of corn cob is:

$$\text{WAC} = 2.134 + 0.010\text{RCC} \quad 3.7$$

$$\text{WAC} = 1.672 + 0.010\text{ACC} \quad 3.8$$

Eq. 3.7 and 3.8 could be explained thus: for every increase in water absorption time would cause 1 % of water to be absorbed. It also reveals that if the corn cob used was acetylated, a 46.2% reduction/decrease in water absorption would be obtained.

3.6.2. Water absorption capacity of mango kernel

Raw mango kernel can hold significant amount of water due to hydrogen bonding between hydrogen bonding between hydroxyl groups and water molecule. The principal essence for studying mango kernel acetylation is to observe whether the modification (by acetylation) can alter its water absorption capacity, thereby increasing the hydrophobic properties. It has been established that when the accessible hydroxyl groups in the cell wall polymer have been substituted by acetyl group, reduction in water and moisture sorption are observed (Yakubu et al., 2012). Figure 3.28 presents the results of water absorption capacity of raw and treated mango kernel. Figure 3.28 revealed that at all times; the water absorption capacity of mango kernel was highest for the raw material and lowest for the

acetylated material. This may be attributed to the reduction of hydroxyl group contents of mango kernel by acetylation, thereby increasing the hydrophobic properties.

The reduction in water absorption capacity was tested for significance. Table 3.15 presents results for the significant effects of time and acetylation on mango kernel water absorption capacity. The null hypothesis (H_0), is that acetylation have not reduced water absorption capacity of mango kernel. Rejection of the hypothesis H_0 implies the acceptance of the alternative hypothesis (H_1), that acetylation have reduced the water absorption capacity. This statistic was performed at 5% significant level.

In this case we reject H_0 if p-value is less than 0.05 and conclude that there is significant difference in the performance of the two variables. The results as presented in Table 3.15 indicated that the P-value (0.004) is less than 0.05. This therefore, implied that time and acetylation has significant effects on water absorption capacity of mango kernel.

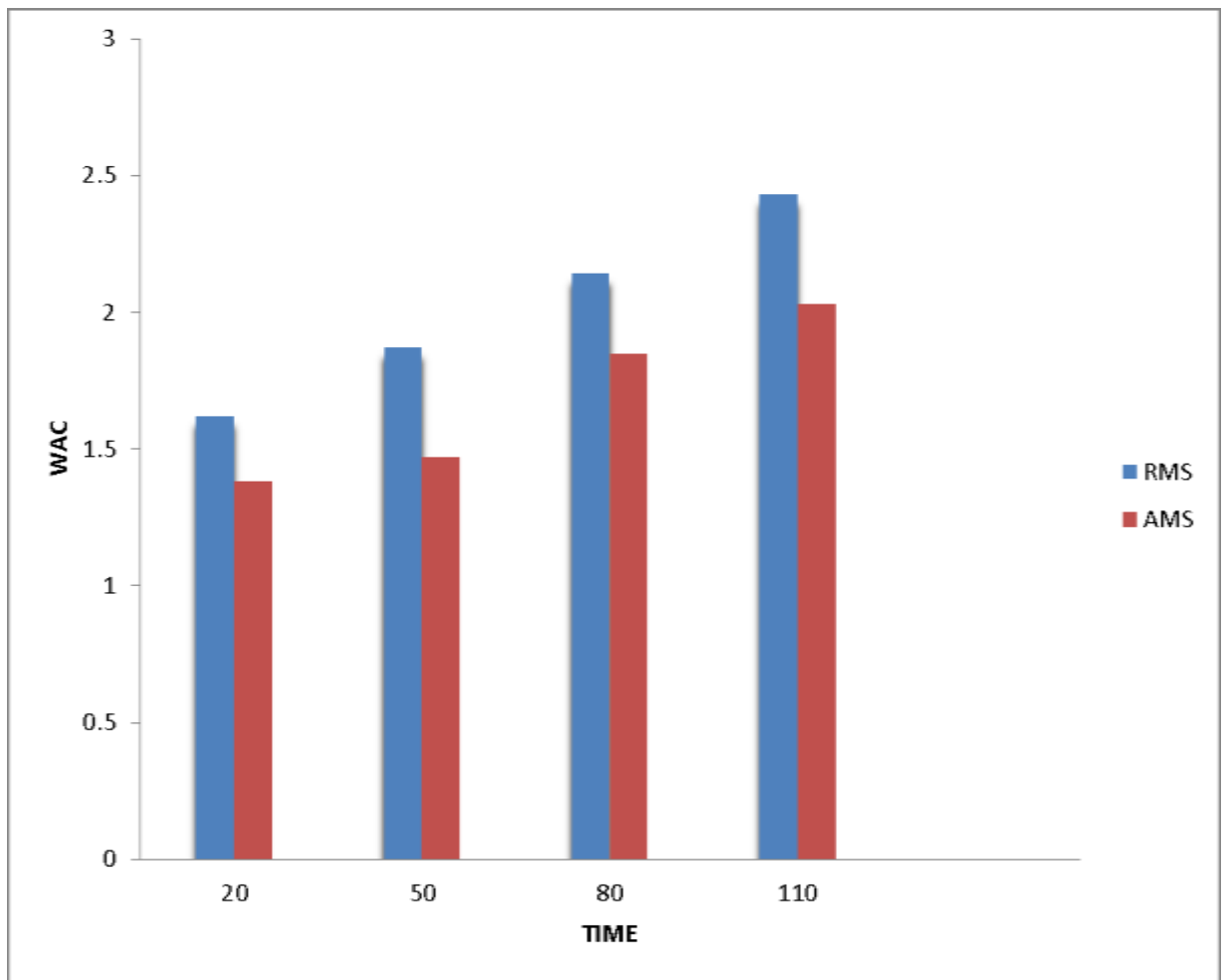


Figure 3.28 Variations of water absorption capacity with time for raw and acetylated mango kernel

To understand the direction of these effects, regression analysis was performed. Eq. 3.9 and 3.10 presents results of linear regression for mango kernel water absorption capacity.

$$WAC = 1.43 + 0.009RMS \quad 3.9$$

$$WAC = 1.17 + 0.007AMS \quad 3.10$$

Where (WAC) is water absorption capacity, RMS and AMS stands for raw and acetylated mango kernel. Eq. 3.9 and 3.10 showed that for every increase in water absorption time would cause 0.9% and 0.7% of water to be absorbed by RMS and AMS respectively. Also it

revealed that if the mango kernel used was acetylated, a 26% reduction/decrease in water absorption capacity would be obtained.

3.7 Sorption Studies of Crude Oil

3.7.1. Crude Oil Sorption Onto Corn Cob

Crude oil uptake was studied in batch experiments and the results are illustrated in Figure 3.29. The results from Figure 3.29 as expected increased with increase in sorption time from 30 to 120 seconds. 120 seconds showed the maximum oil sorption capacity of 2.50g/g for ACC and 2.03 for RCC. This might be due to initial adsorption onto the surface of the material and subsequent penetration into the inner microscopic voids (Amer *et al.*, 2007). The results also showed the fast and stable nature of the process as only a slight difference was observed between the initial and final contact time. The results are consistent with findings elsewhere (Hussein *et al.*, 2006; Nwankwere *et al.*, 2010). Results as presented in Fig 3.29 showed that acetylated corn cob absorbed higher amount of oil compared to the native corn cob. The effect of variation of material (modified and unmodified) was tested for statistical difference using ANOVA. Table 3.16 presents results for the significant effects of time and acetylation on corn cob oil sorption capacity. The null hypothesis (H_0) is that acetylation has not affected oil sorption capacity of corn cob. Rejection of the hypothesis H_0 implies the acceptance of the alternative hypothesis (H_1), that acetylation have reduced the water absorption capacity. This statistic was performed at 5% significant level.

In this case we reject H_0 if p-value is less than 0.05 and conclude that there is significant difference in the performance of the two variables. The results as presented in Table 3.16,

indicated that the P-value (0.075) is greater than 0.05. This therefore, implied that time and acetylation had no significant effects on corn cob oil sorption capacity. The statistical non difference may be attributed to the closeness of the means.

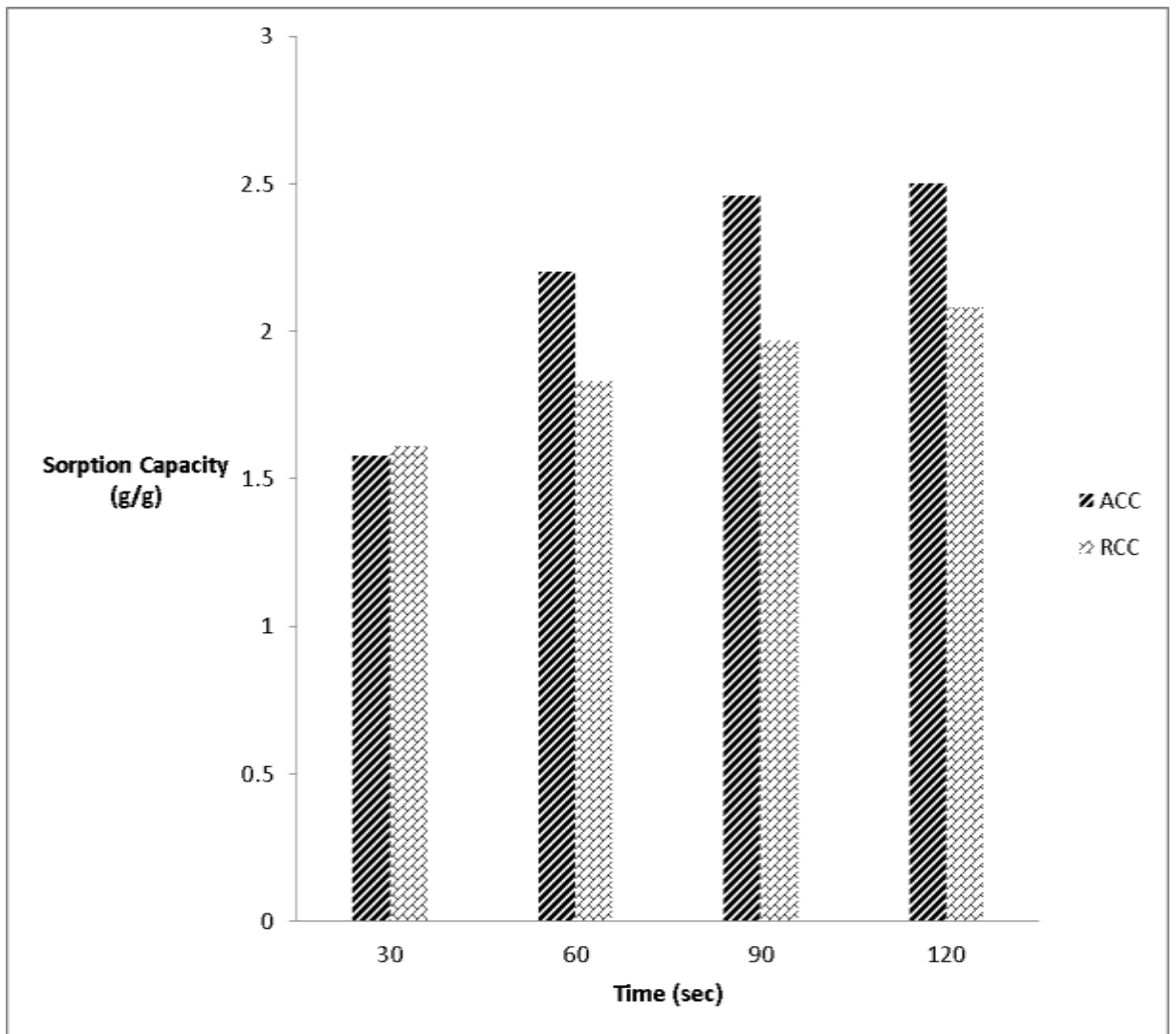


Figure 3.29: variation of oil sorption capacity (OSC) with time for modified and unmodified corn cob

Table 3.16 Summary of ANOVA results on the effect of time on sorption of oil onto corn cob and mango kernel

	Mean	Std Deviation	Std. Error	t	Df	Sig (P)
			Mean			
ACC-RCC	0.31250	0.23358	0.11679	2.676	3	0.075
AMS-RMS	0.23000	0.13880	0.06940	3.314	3	0.045

To understand the direction of these effects, regression analysis was performed. Eq. 3.11 and 3.12 presents the regression equation for oil sorption onto raw and acetylated corn cob.

$$\text{OSC} = 1.49 + 0.00517T \text{ RCC} \quad 3.11$$

$$\text{OSC} = 1.43 + 0.0101T \text{ ACC} \quad 3.12$$

OSC represents oil sorption capacity, T means time, while RCC stands for raw corn cob and ACC stands for acetylated corn cob. Equation 3.11 and 3.12 showed that for every increase in time by 1 sec, oil sorption capacity for raw corn cob increased by 0.5% while, the sorption capacity for acetylated corn cob increased by 1.0%. These findings, indicates that oil sorption capacity is affected by time, and that acetylation would cause a 50% rise on oil sorption capacity of corn cob for every increase in oil sorption time.

3.7.2 Kinetics of Crude Oil Sorption onto Corn Cob

The kinetics of sorption of crude oil onto corn cob was studied using by fitting obtained data in rate curves- derived pseudo first-order model, lagergren pseudo first-order model, second order model (Hill *et al.*, 1998) and pseudo second order (Ho, 1995), intra-particle diffusion mechanism and liquid film diffusion. The linear plots of this kinetics and how to obtain rate constants are presented in Table 2.1. The predicted kinetics from the linear plots of derived pseudo first-order, lagergren first order, second order model, pseudo second-order, intra-particle diffusion model and liquid film diffusion model are presented in Figures 3.30 - 3.35 respectively. The calculated kinetics derived from the constants are shown in Table 3.18.

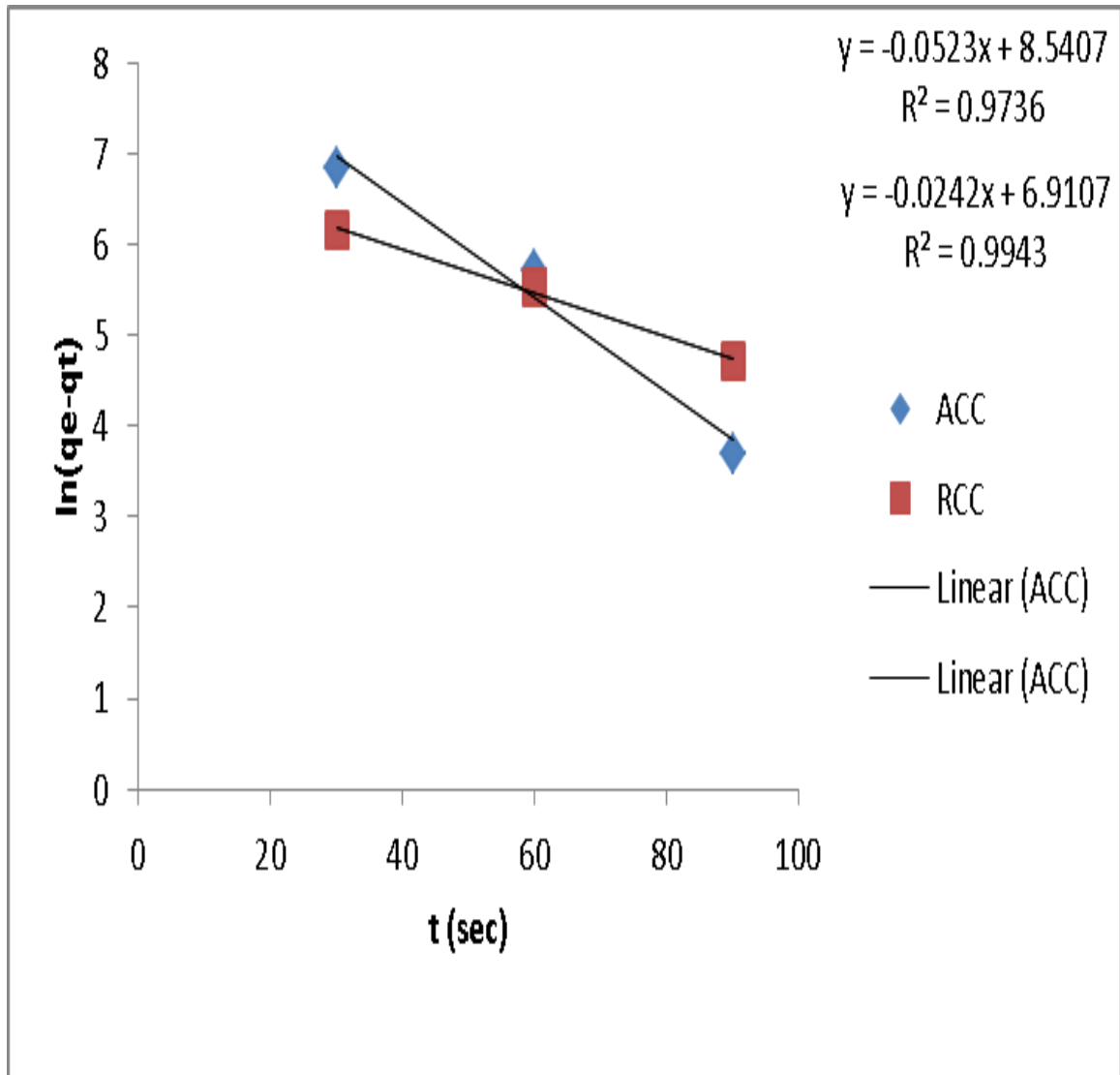


Figure 3.30: Lagergren pseudo-first order kinetic model for sorption of oil onto corn cob

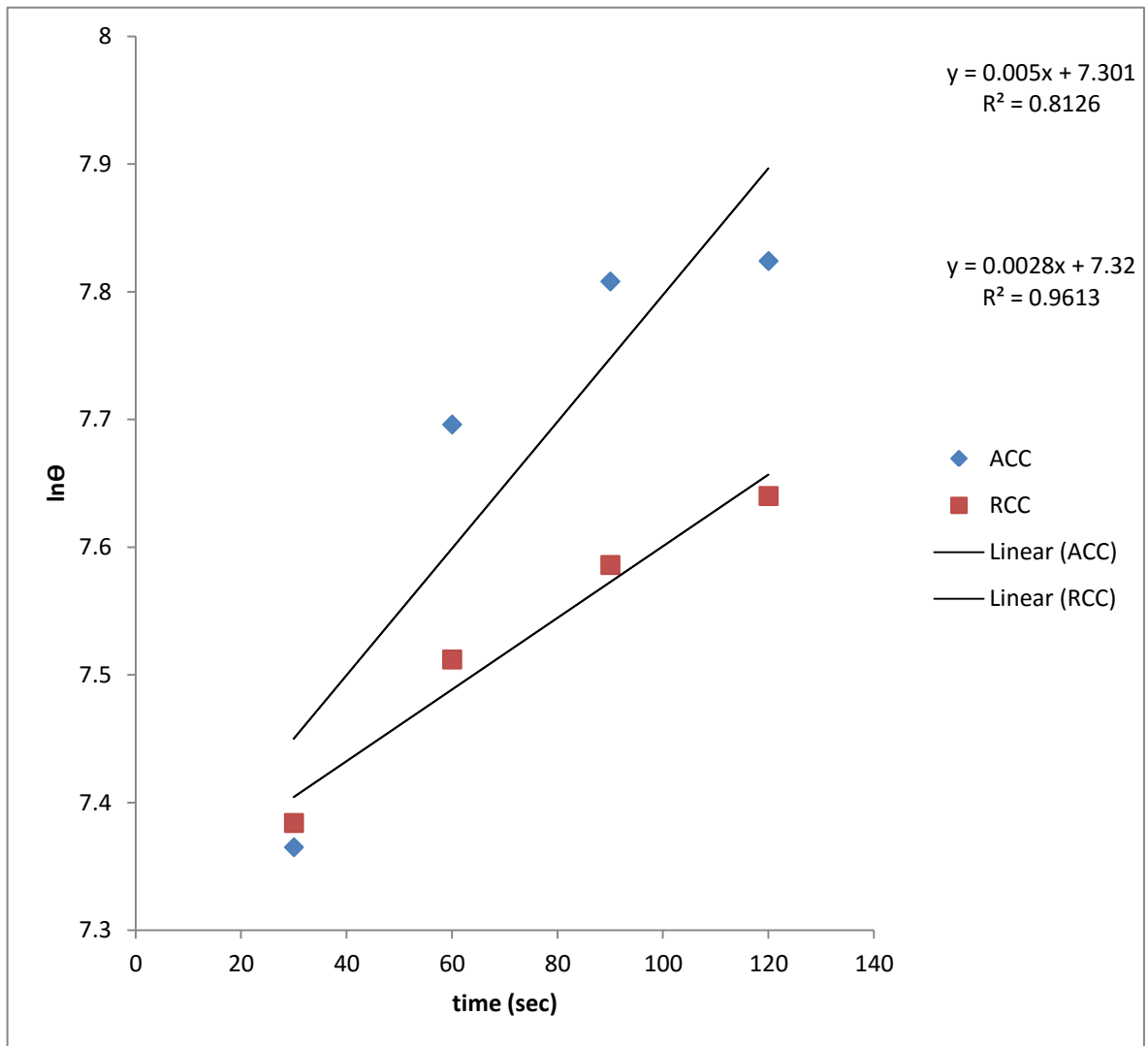


Figure 3.31. Derived Pseudo-first order kinetic model for the sorption of crude oil onto corn cob

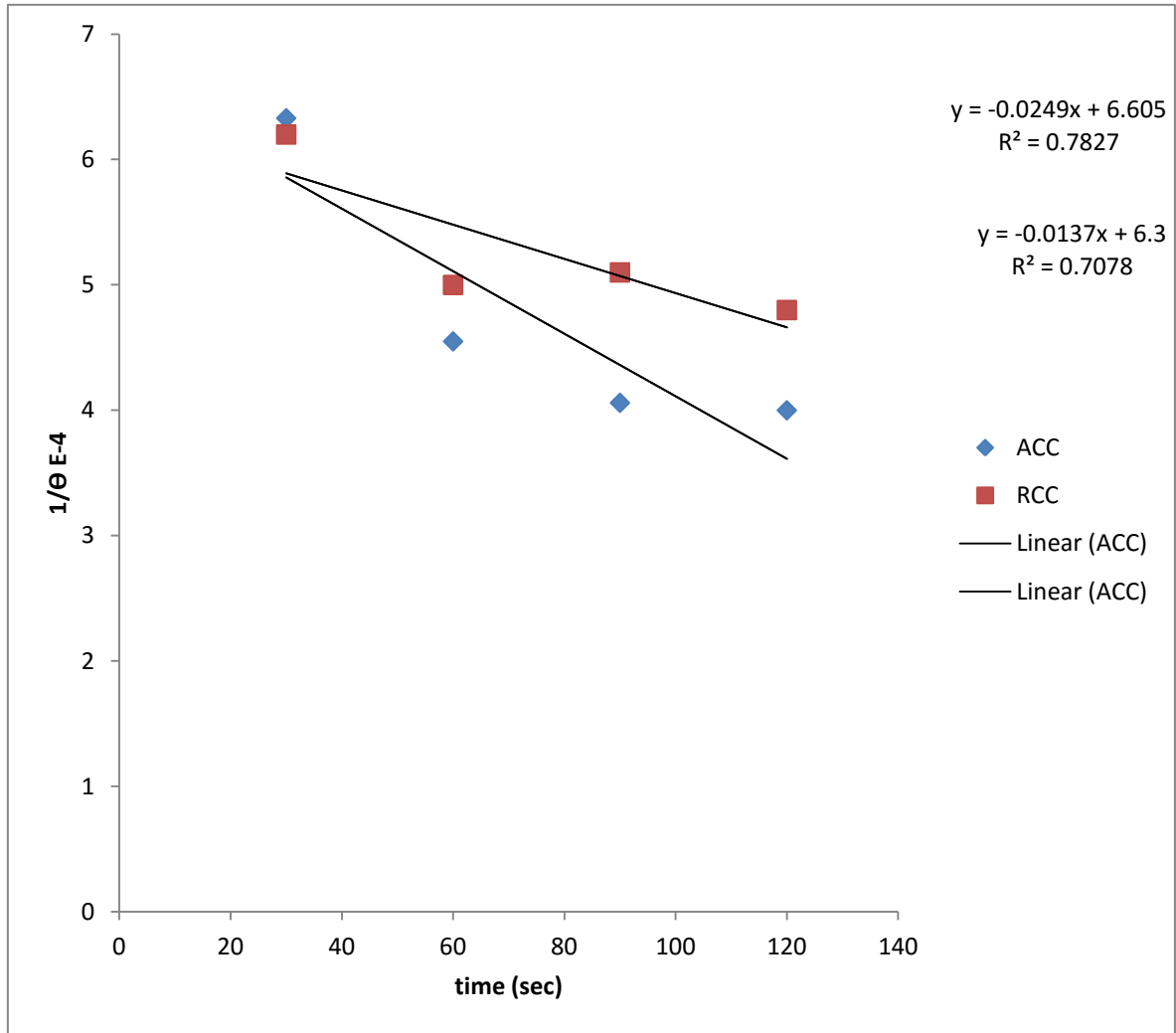


Figure 3.32: Hill second order kinetic model for sorption of oil

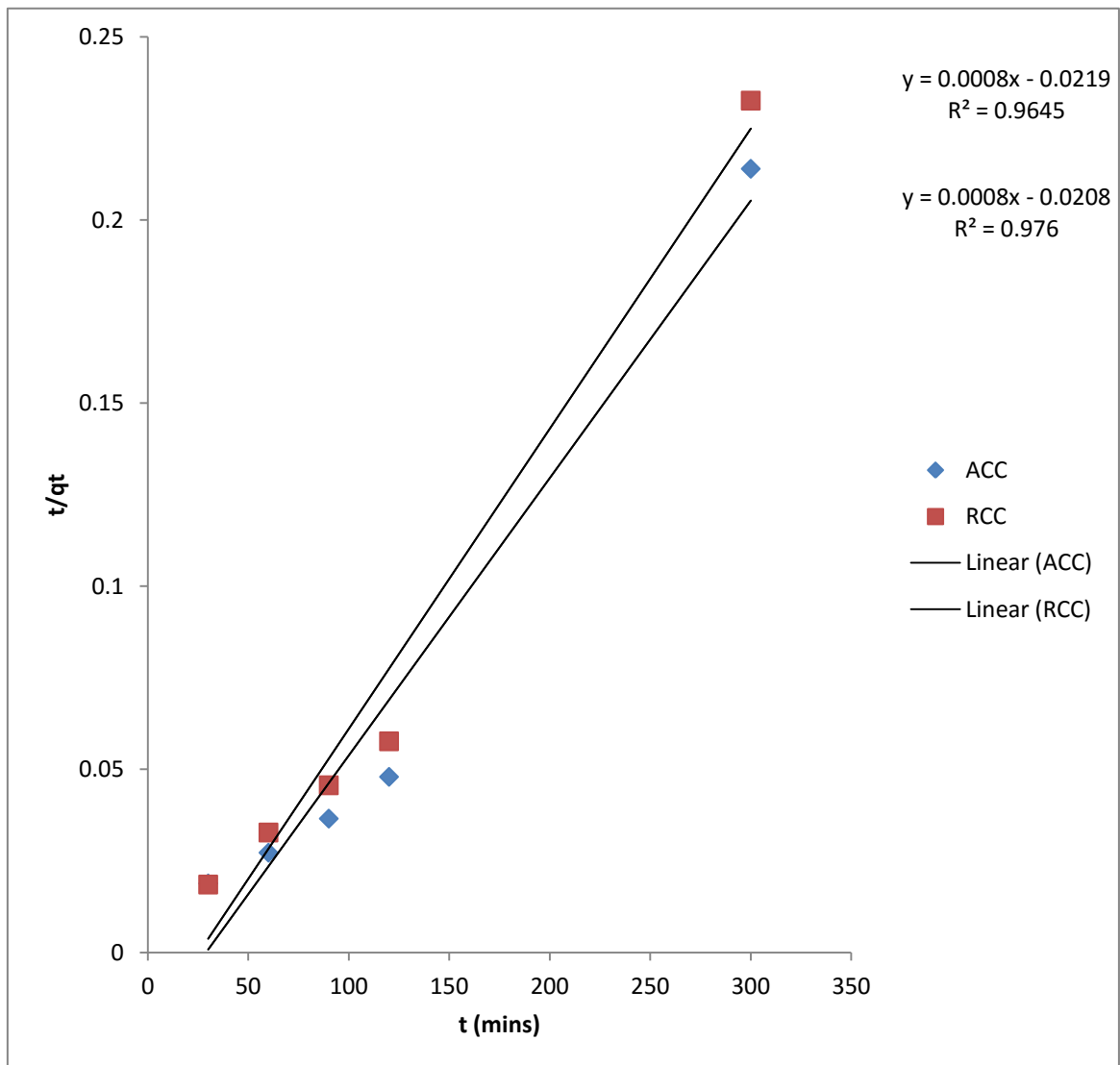


Figure 3.33 Ho pseudo second-order kinetics for the sorption of crude oil onto corn cob

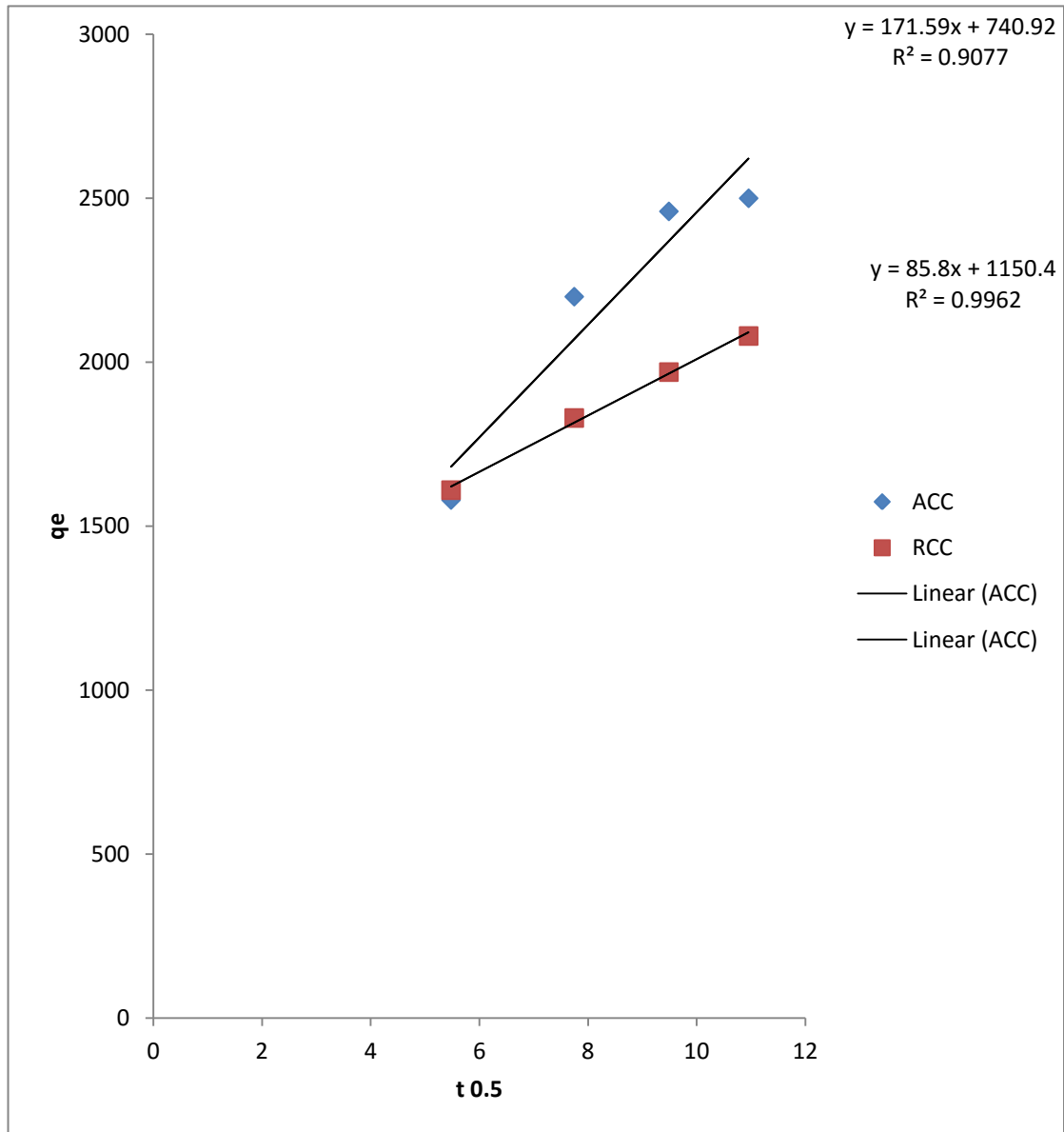


Figure 3.34. Intra-particle diffusion kinetics for the sorption of crude oil onto corn cob

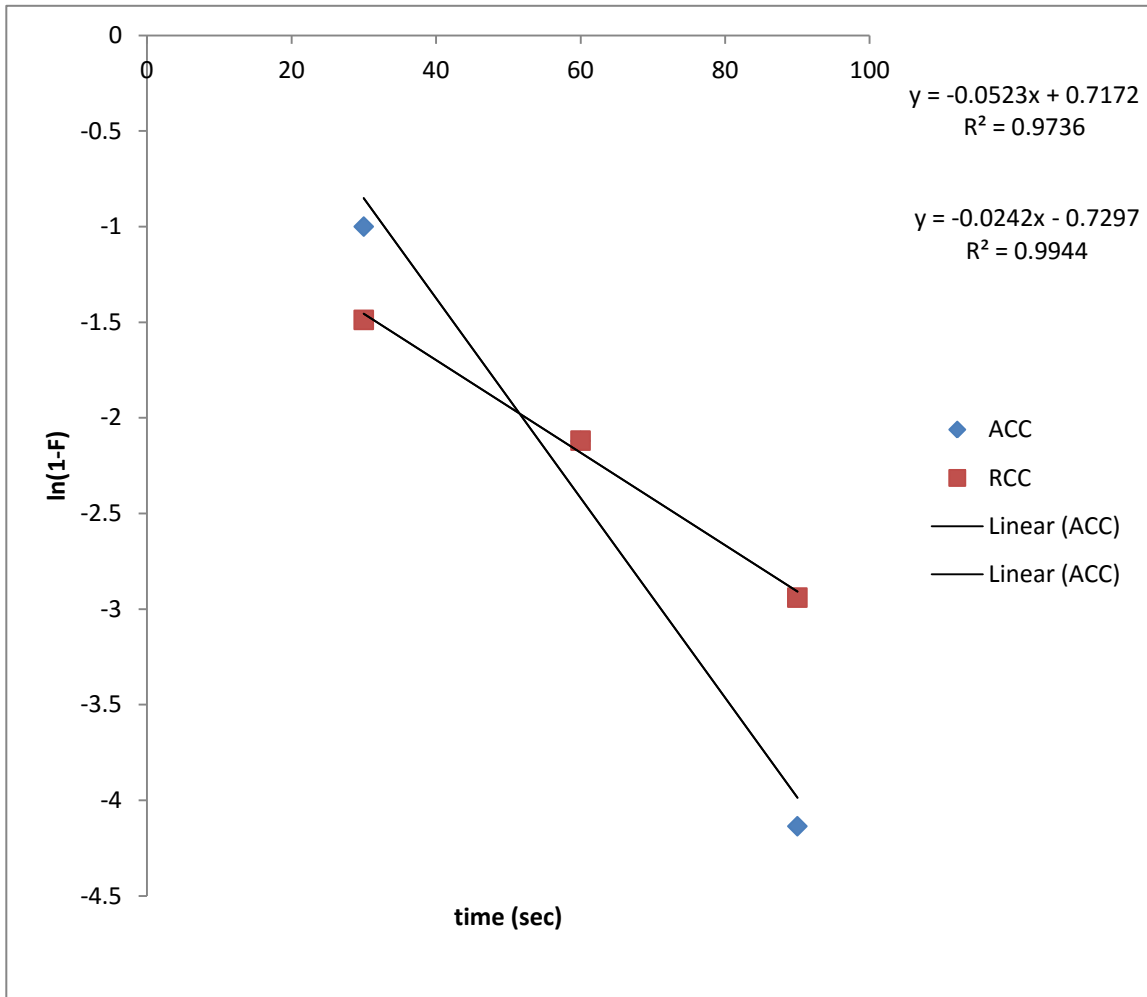


Figure 3.35 liquid film diffusion kinetics for sorption of oil onto corn cob

Table 3.17 summary of kinetics of crude oil sorption onto corn cob

Kinetic model	ACC	RCC
Θ_o exp (mg/g)	2500	2080
Lagergren pseudo first-order		
Θ_o calc (mg/g)	5118.92	1002.95
K_1 (sec ⁻¹)	-0.052	-0.024
R^2	0.9736	0.9943
Derived pseudo first-order		
Θ_o calc (mg/g)	1481.78	1510.20
K^1	0.005	0.0028
R^2	0.8126	0.9613
Hill second order		
Θ_o calc (mg/g)	0.1514	0.1587
K_2	-0.0249	-0.0137
R^2	0.7827	0.7078
Ho pseudo second-order		
Θ_o calc (mg/g)	1250	1250
K^2	2.92×10^{-5}	3.08×10^{-5}
R^2	0.9645	0.976
Intra-particle diffusion		
K_d (meq/g/sec)	171.59	85.8
C	740.92	1150.4
R^2	0.9077	0.9962
Liquid-film diffusion model		
Kf_d	-0.0523	-0.0242
R^2	0.9736	0.9944

A comparison of the coefficient of correlation results presented in Table 3.17, indicated that crude oil sorption unto raw and acetylated corn cob does not follow hill second order expression. The Θ_0 calculated values, obtained from this expression were not quite satisfactory and values are also fairly low when compared with Θ_0 experimental. The derived pseudo first-order and Ho pseudo second-order expression produced a fair fit to the data with coefficient of regression (R^2) values between 0.8126-0.976. Their Θ_0 calculated are satisfactory when compared with Θ_0 experimental value. The coefficient of correlation for the lagergren pseudo first-order expression were greater than 0.97 for both raw and acetylated corn cob and their Θ_0 calculated values agree well with the experimental value. This therefore, implied that the mechanism of sorption of crude oil unto corn cob conforms to pseudo first-order kinetic expression. Intra-particle diffusion and liquid-film diffusion models were also used to further study the mechanism of crude oil sorption unto corn cob. For the intra-particle diffusion model, the intercept of the plot indicated boundary layer effect. A large intercept implied greater contributions of the surface sorption in the rate-determining step. Intra-particle diffusion is the sole rate-determining step if the plots is linear, and passed through the origin. From Table 3.17, as indicated by high regression values for both raw and acetylated corn cob and also the presence of the intercept (c), it shows that the plot did not pass through the origin, but was close to it. The deviation from origin was due to the difference in mass transfer in the initial and final stages of the sorption process (Das and Mondal, 2011). The presence of boundary layer effect (c) showed the existence of surface sorption, indicating that intra-particle diffusion expression is not the only rate determining step. Similarly the application

of liquid film diffusion model gave high curve linearity (0.9736 (ACC) and 0.9944 (RCC)) indicating a high applicability of the model.

Results from our kinetic studies, revealed therefore that sorption of oil is by surface reaction and diffusion into the pores of corn cob. This is in agreement with results elsewhere [Uzoije *et al.*, 2011; Aisien *et al.*, 2011].

3.7.3. Crude oil sorption onto Mango kernel

Crude oil uptake was studied in batch experiments and the results are illustrated in Figure 3.36. The results from Figure 3.36 as expected increased with increase in sorption time from 30 to 120 seconds. 120 seconds showed the maximum oil sorption capacity of 1.34g/g for AMS and 1.13 for RMS, this may be due to initial adsorption onto the surface of the material and subsequent penetration into the inner microscopic voids (Amer *et al.*, 2007). The results also showed the fast and stable nature of the process as only a slight difference was observed between the initial and final contact time. The results are consistent with findings elsewhere (Hussein *et al.*, 2006; Nwankwere *et al.*, 2010). In all the period studied, acetylated mango kernel absorbed higher amount of oil compared to the native mango kernel. The effect of variation of material (modified and unmodified) on oil sorption was tested for statistical difference using ANOVA. Table 3.16 presents results for the significant effects of time and acetylation on mango kernel oil sorption capacity. The null hypothesis (H_0), is that acetylation have not affected oil sorption capacity of mango kernel. Rejection of the hypothesis H_0 implies the acceptance of the alternative hypothesis (H_1), that acetylation have affected the oil sorption capacity. This statistic was performed at 5% significant level.

In this case we reject H_0 if p-value is less than 0.05 and conclude that there is significant difference in the performance of the two variables. The results as presented in Table 3.16 indicated that the P-value (0.045) is less than 0.05. This therefore, implied that time and acetylation has significant effects on oil sorption capacity of mango kernel.

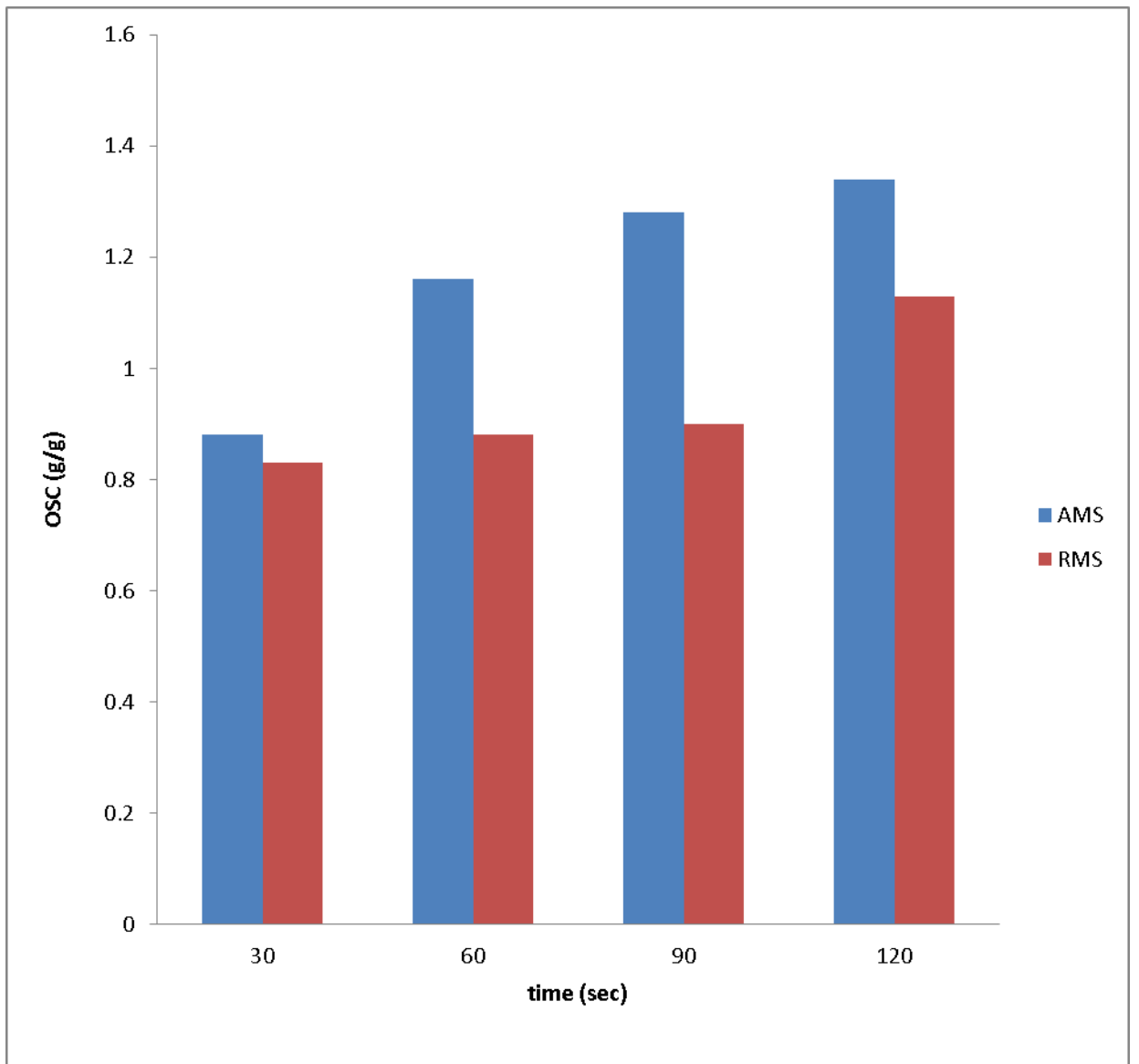


Figure 3.36: variation of OSC with time for modified and unmodified mango kernel

To understand the direction of these effects, regression analysis was performed. Eq. 3.13 and 3.14 presents regression equation.

$$\text{OSC} = 0.735 + 0.00277T \text{ RMS} \quad 3.13$$

$$\text{OSC} = 0.790 + 0.00500T \text{ AMS} \quad 3.14$$

RMS and AMS represents raw and acetylated mango kernel. Equation 3.13 and 3.14 showed that for every increase in oil sorption time, oil sorption capacity for mango kernel increased by 0.277% while, the sorption capacity for acetylated corn cob increased by 0.5%. These findings, indicates that oil sorption capacity is affected by time, and that acetylation would cause a 50% rise on oil sorption capacity of mango kernel for every increase in oil sorption time.

3.7.4 Kinetics of crude oil sorption onto mango kernel

The kinetics of sorption of crude oil onto mango kernel was studied by fitting obtained data in rate curves- derived pseudo first-order model, Lagergren pseudo first-order model, second order model (Hill *et al.*, 1998) and pseudo second order (Ho, 1995), intra-particle diffusion mechanism and liquid film diffusion. The linear plots of this kinetics and how to obtain rate constants are presented in Table 2.1. The predicted kinetics from the linear plots of Lagergren pseudo first order, derived pseudo first order, second order model, Ho pseudo second-order, intra-particle diffusion model and liquid film diffusion model are presented in Figures 3.37, 3.38, 3.39, 3.40, 3.41, 3.42 respectively. The calculated kinetics derived from the constants is shown in Table 3.118.

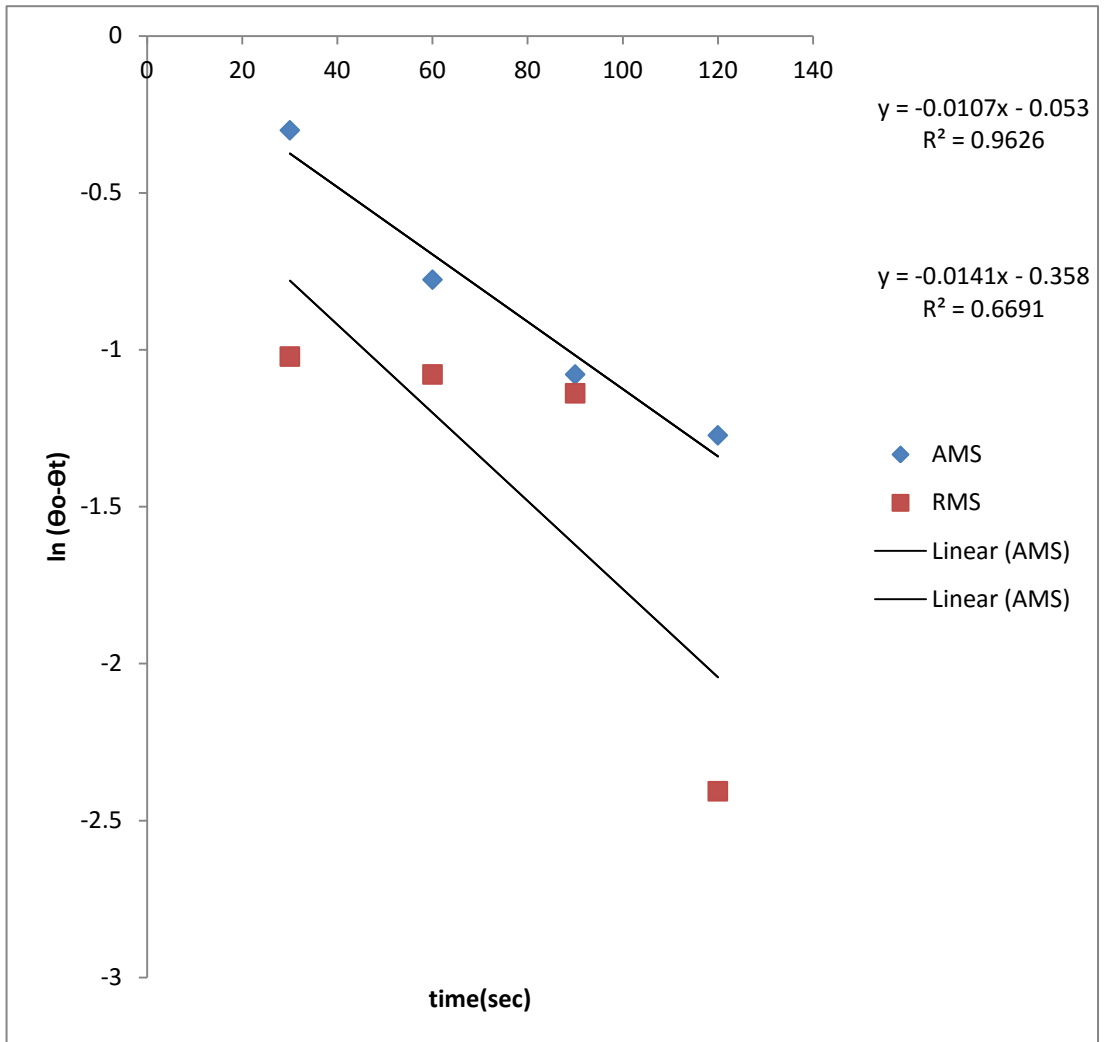


Figure 3.37 Lagergren pseudo-first order kinetics for sorption of oil onto mango kernel

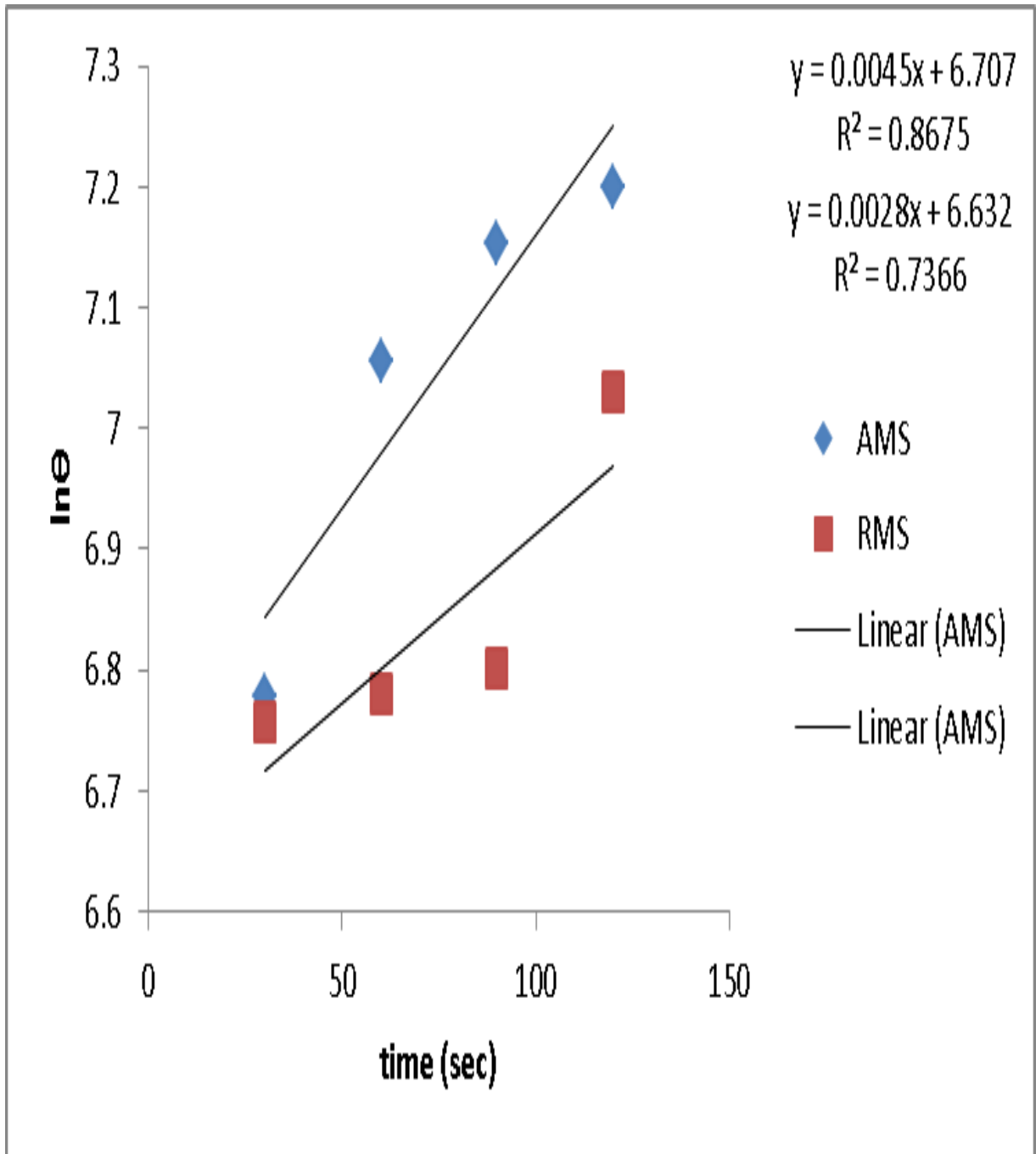


Figure 3.38 derived pseudo first-order kinetics for sorption of oil onto mango kernel

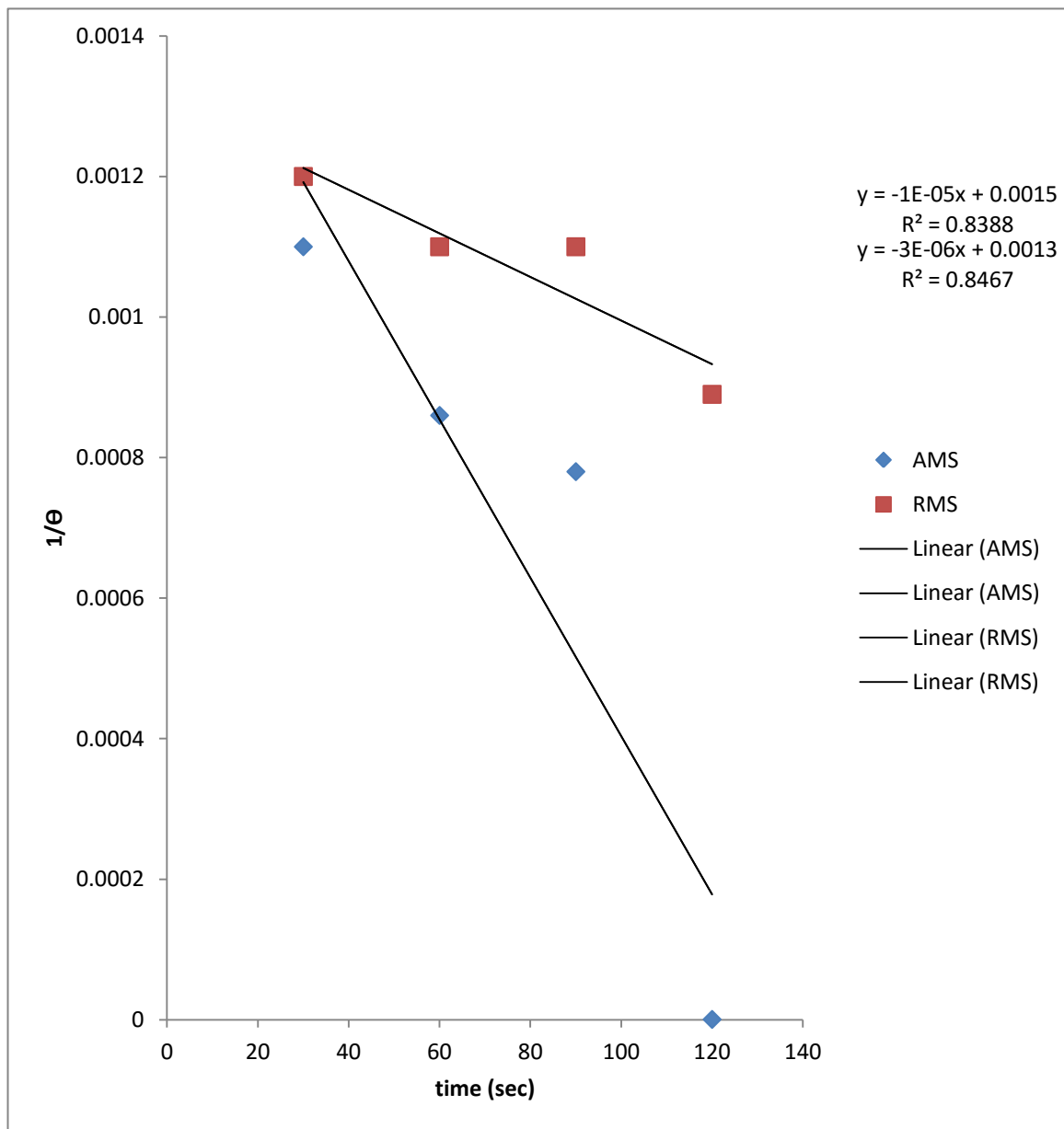


Figure 3.39 Hill second order kinetics for sorption of oil onto mango kernel

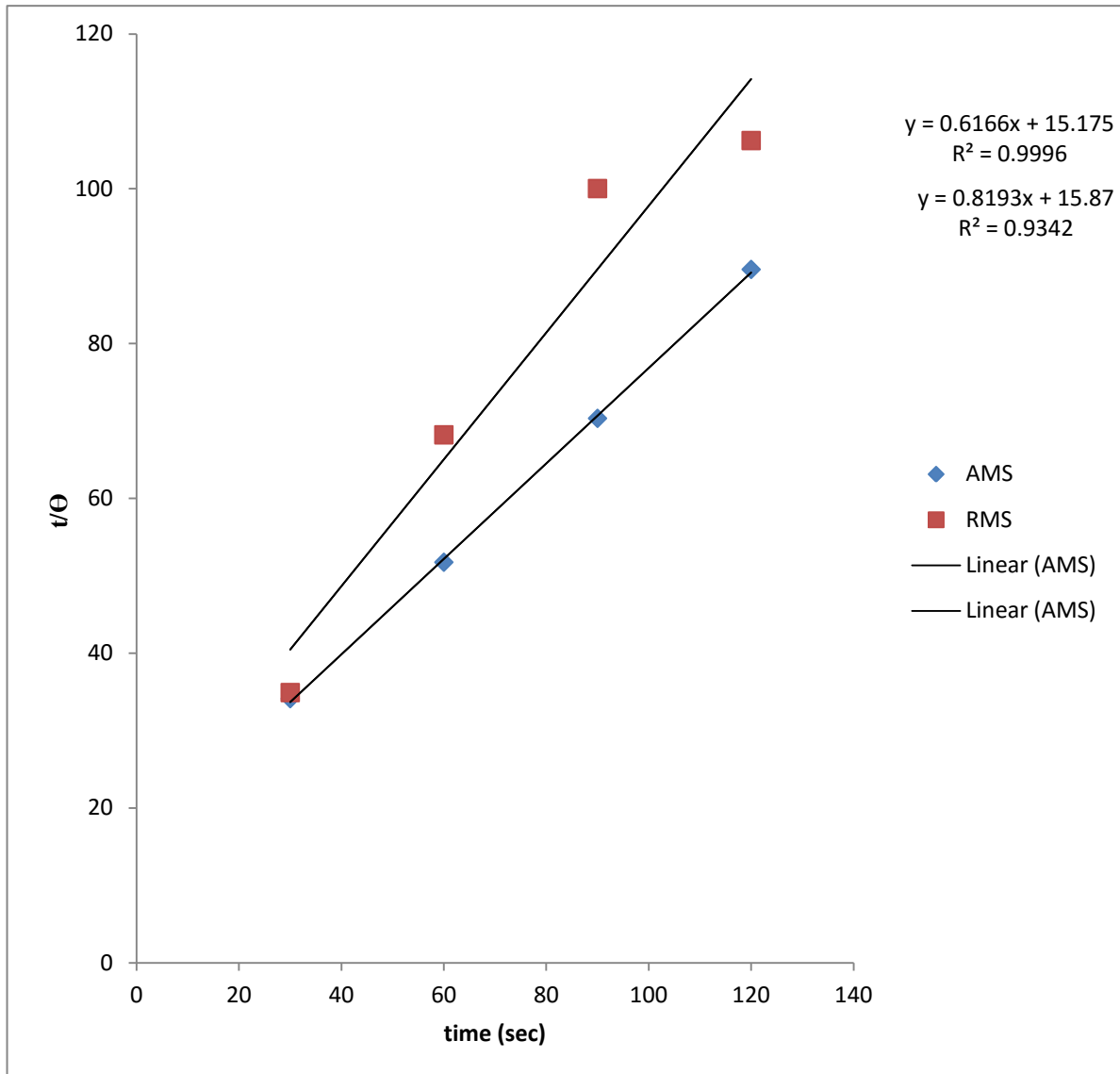


Figure 3.40 Ho pseudo second order kinetics for the sorption of oil onto mango kernel

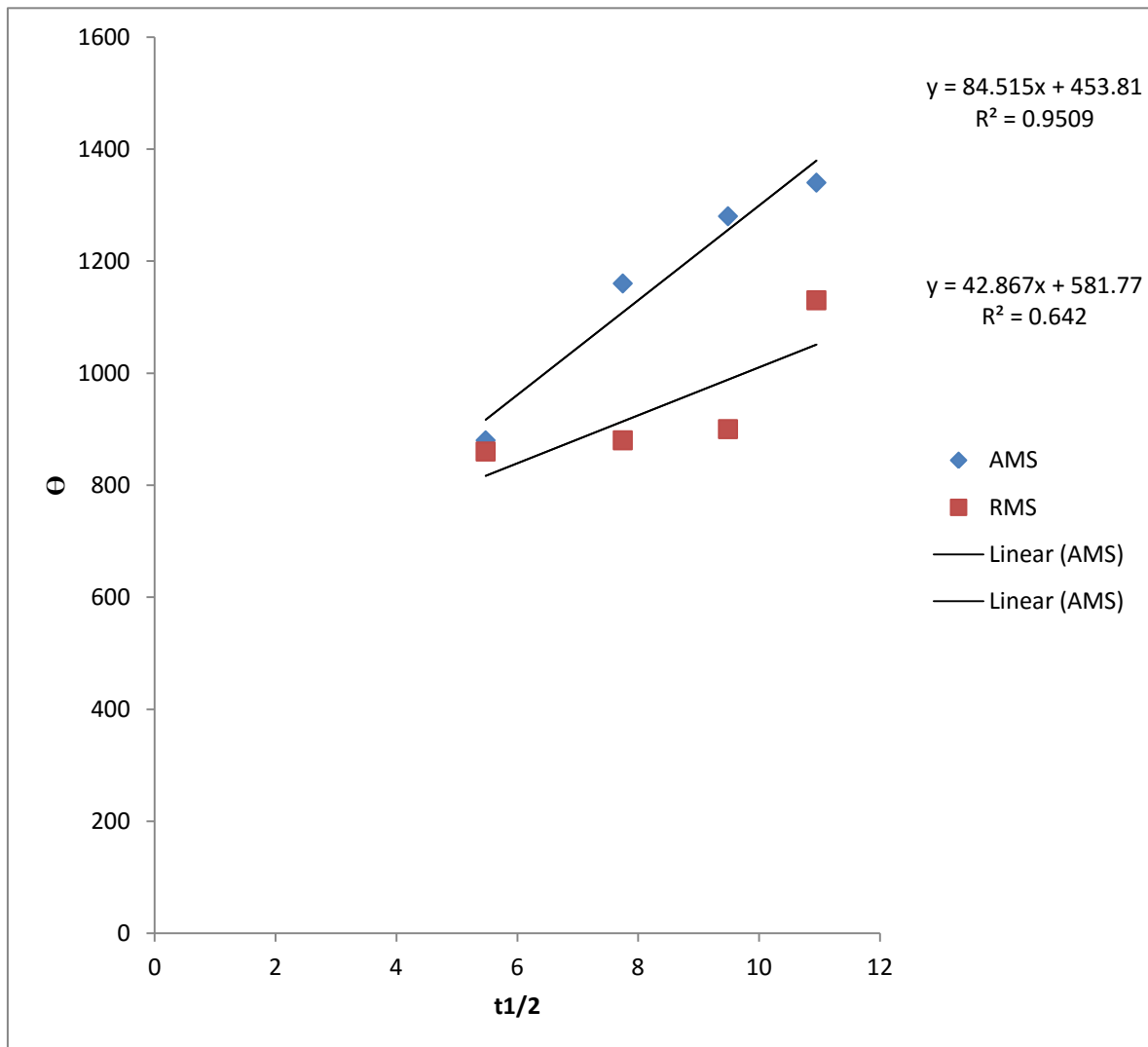
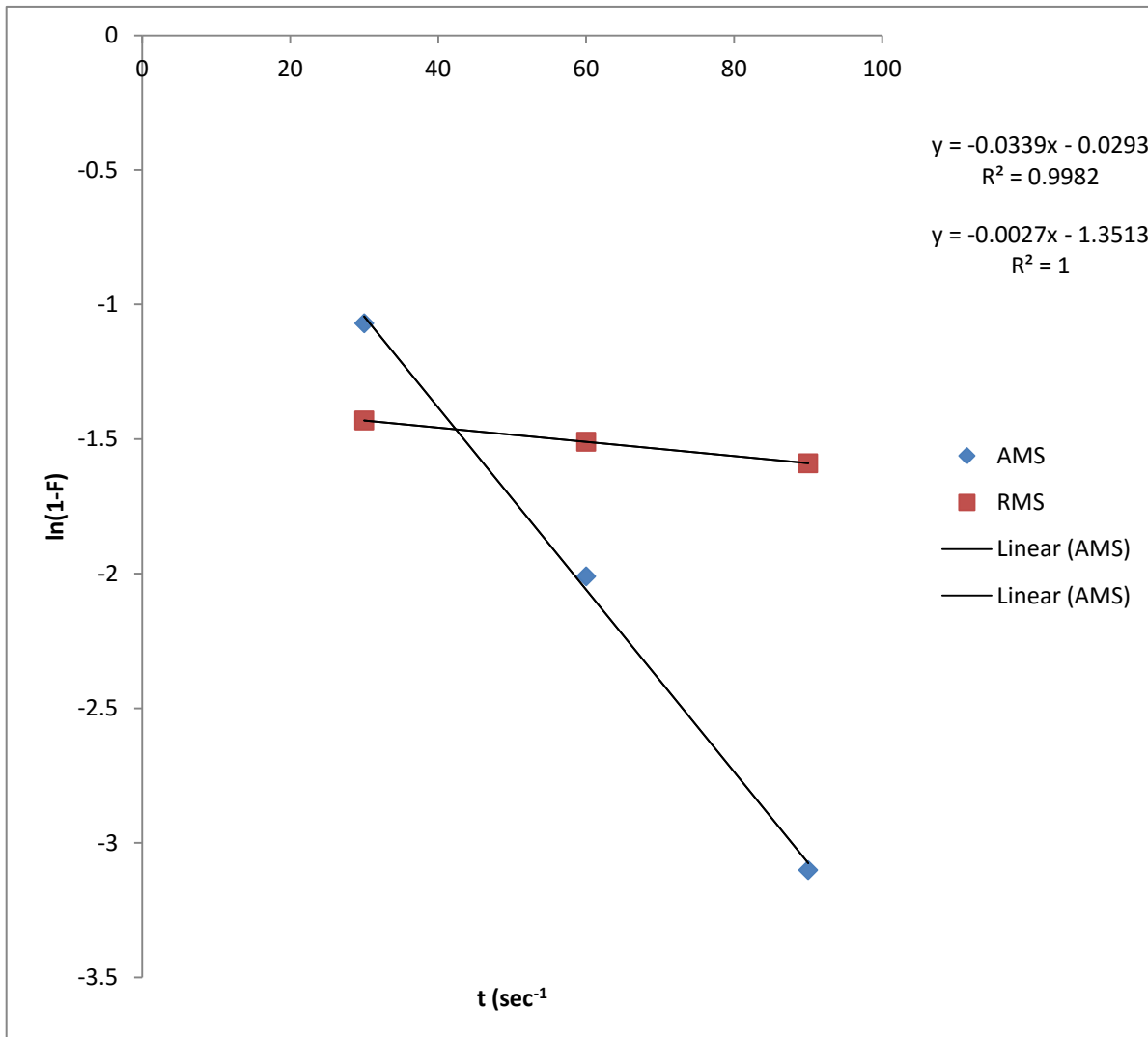


Figure 3.41 intra-particle diffusion kinetics for sorption of oil onto mango kernel



A comparison of the correlation coefficients results presented in Table 3.18 indicated that Lagergren pseudo first-order, derived pseudo first-order and Hill second order expressions produced R^2 within $0.43 \leq R \leq 0.89$ which are moderate and high (Dowine and Heath, 1974). The derived pseudo first-order and Hill second order expressions produced Θ_0 calculated values reasonably close to the experimental value. However, the very high R^2 value produced by the Ho pseudo second-order expression indicates that is the optimum kinetic expression to explain the sorption of crude oil unto mango kernel.

Intra-particle diffusion and liquid-film diffusion models were also used to further study the mechanism of crude oil sorption unto mango kernel. For the intra-particle diffusion model, the intercept of the plot indicated boundary layer effect. A large intercept indicated a greater contribution of the surface sorption in the rate-determining step. Intra-particle diffusion is the sole rate-determining step if the plot is linear, and passed through the origin. From Table 3.18, as indicated by high regression values for both raw and acetylated mango kernel and also the presence of the intercept (c), it shows that the plot did not pass through the origin, but was close to it. The deviation from origin was due to the difference in mass transfer in the initial and final stages of the sorption process (Das and Mondal, 2011). The presence of boundary layer effect (c) showed the existence of surface sorption, indicating that intra-particle diffusion expression is not the only rate determining step. Similarly the application of liquid film diffusion model gave high curve linearity (0.9982 (AMS) and 1.0 (RMS) indicating a high applicability of the model. The R^2 values for the liquid film diffusion model are higher than the intra-particle diffusion model, indicating that sorption of crude oil unto mango kernel occurred more at the surface.

Results from our kinetic studies revealed, therefore that sorption of oil is by surface reaction and diffusion into the pores of mango. This is in agreement with results elsewhere [Uzoijeet *al.*, 2011; Aisienet *al.*, 2011].

Table 3.18 Summary of kinetics derived from the plot for mango kernel OSC

Kinetic model	AMS	RMS
Θ_o exp (mg/g)	1340	1130
Lagergren pseudo first-order		
Θ_o calc (mg/g)	0.948	0.699
K_1 (sec ⁻¹)	-1.07×10^{-2}	-1.41×10^{-2}
R^2	0.9626	0.6691
Derived pseudo first-order		
Θ_o calc (mg/g)	818.11	759.00
K^1	4.5×10^{-3}	2.8×10^{-3}
R^2	0.8675	0.7366
Hill second order		
Θ_o calc (mg/g)	666.67	769.23
K_2	-1.0×10^{-5}	-3.0×10^{-6}
R^2	0.8388	0.8467
Ho pseudo second-order		
Θ_o calc (mg/g)	1.134	1.221
K^2	8.5×10^{-2}	9.4×10^{-2}
R^2	0.9996	0.9342
Intra-particle diffusion		
K_d (meq/g/sec)	84.515	42.967
C	453.81	581.77
R^2	0.9509	0.642
Liquid-film diffusion model		
Kf_d	-0.0339	-0.0293
R^2	0.9982	1.0

Chapter Four

Conclusion and Recommendation

4.1 Conclusion

This work showed that corn cob acetylation has been affected by temperature and catalyst (NBS) while mango kernel acetylation has been affected by temperature, time and catalyst (NBS). The acetylation has been found to occur by surface reaction and intra-particle diffusion mechanism, involving substitution of hydrogen of hydroxyl ($-OH$) group by acetate groups at $30^{\circ}C$ and $100^{\circ}C$ for corn cob and $100^{\circ}C$ for mango kernel. Heat of acetylation and critical temperature of acetylation values were found to be (0.029 Jmol^{-1} and 0.814 K) and (0.8696 Jmol^{-1} and 0.016 K) for corn cob and mango kernel respectively suggest that the acetylation of corn cob and mango kernel can take place under mild conditions. Results from XRD and FTIR suggested alteration in the chemical structure and subsequent increase in hydrophobicity of the acetylated corn cob and mango kernel. The sorption behavior of mango kernel and corn cob was greatly enhanced when modified with acetic anhydride. Sorption of oil was found to be controlled by pseudo first order kinetics, intra-particle diffusion and liquid-film diffusion mechanism for corn cob, while for mango kernel, it was Ho pseudo second order, intra-particle diffusion and liquid film diffusion mechanism. The rapid uptake of oil and high absorption capacity of the acetylated materials made them a very promising alternative sorbents for crude oil, considering that they are cheap, readily available and are biodegradable.

4.2 Recommendations

The acetylation of corn cob and mango kernel using NBS as catalyst under mild conditions is therefore technically feasible and the products recommended as materials that could be used for cleansing aquatic environments, mangroves and wetlands of spilled oil films arising from oil exploration and exploitation of crude and refined petroleum products. The economy of the procedure using mild reaction conditions and the availability of the materials makes acetylated corn cob and mango kernel a good substitute for commercial synthetic sorbents. Further research and development on the storage effect and reusability of acetylated corn cob and mango kernel should be developed as it is beneficial in oil spill cleanup operations. The research for more efficient methods to improve the sorption capacity of these acetylated materials should be encouraged. Research should also be carried out by exploring more commercially available and environmentally friendly catalysts; investigating more stringent acetylation conditions and using other cellulose based products.

It is also recommended that more work be done on development of scale up industrial processes for the continuous mass production of acetylated materials for subsequent application.

REFERENCES

- Aboul-Gheit, A-K., Khalil, F.H., Abdoul-Moghny, T., (2006). Adsorption of spilled oil from sea water by waste plastic. *Oil and Gas Technology Revolution- IFP*, 61(2): 259-268.
- Adebajo, M.O., Frost, R.L., Klopprogge, J.T. and Carmody, O., (2003). Porous materials for oil spill cleanup: A review of synthesis and absorbing properties. *Porous Materials*, 10: 159-170.
- Adebajo, M.O. and Frost, R.L., (2004a). Acetylation of raw cotton for oil spill cleanup application: an FTIR and ¹³C MAS NMR spectroscopic investigation. *Spectrochimica Acta, Part A: Molecular and Biomolecular Spectroscopy*, 60(10): 2315-2321.
- Adebajo, M.O. and Frost, R.L., (2004b). Infrared and ¹³C-MAS Nuclear Magnetic Resonance Spectroscopic study of acetylation of cotton. *Spectrochimica Acta, Part A: Molecular and Biomolecular Spectroscopy*, 60(1-2): 449-453.
- Adonis, M., Martinez, V., Riguelme, R., Ancic, P., Gonzalez, G. and Tapia, R., (2003). Susceptibility and exposure biomarkers in people exposed to PAHs from diesel exhaust. *Toxicology Letters*, 144(1): 3-15.
- Agency for Toxic Substances and Diseases Registry (ASTDR) (1996). *Polycyclic Aromatic Hydrocarbons (PAHs): ToxFAQs*. US Department of Health and Human Service, Public Health Service. Atlanta GA. Pp 12-17.
- Agency for Toxic Substances and Diseases Registry (ASTDR) (1997). *Toxicological Profile for Benzene, Update (Final Report)*, NTIS Accession NO PB 78-101157. United States Agency for Toxic Substances and Disease Registry, P. 459.

Agency for Toxic Substances and Diseases Registry (ASTDR), (2008a). *Toxicological Profile for Toluene Update*. US department of health and human service, public health service. Atlanta GA. Pp 7-25.

Agency for Toxic Substances and Diseases Registry (ASTDR), (2008b). *Toxicological Profile for Cresols*. US department of health and human services, public health service. Atlanta GA. Pp 9-15.

Aisien, F.A., Ebewele, R.O and Hymore, F.K., (2011). Mathematical model of sorption kinetics of crude oil by rubber particles from scrap tyres, *Leonardo Journal of Science* 18:85-96

Aloko, D.F. and Adebayo, G.A., (1997). Production and characterization of activated carbon from agricultural wastes (Rice husk and corn cob), *Journal of Engineering and Applied Sciences*, 2(2): 440-444.

Alther, G.R., (2001). How to remove emulsified oil from wastewater with organoclays, *Water Engineering and Management.*, 148(7): 27-29.

Amer, A.A., El-Maghray, A., Malash, G.F. and Nahla, T.A., (2007). Extensive characterization of raw barley straw and study of the effect of steam pretreatment. *J. Applied Science Resources*, 3(1): 1336-1342.

American Standards for Testing and Materials (ASTM) (1994). D4442-84: Standard Test Method For Direct Moisture Content of Wood and Wood Based Materials. *ASTM*, 04-09: 514-518.

- Annunciado, T.R., Sydenstricker, T.H.D. and Amico, S.C., (2005). Experimental investigation of various vegetable fibers as sorbents materials for oil spills. *Marine Pollution Bulletin*, 50(11): 1340-1346.
- Anonymous, (2008). Article: NOSDRA Detects 1150 Oil Spill Sites. *Newspaper This Day*, Jan. 25.
- Armstrong, B., Hutchinson, E., Unwin, J., and Fletcher, T., (2004). Lung cancer risk after exposure to poly cyclic hydrocarbons: a review and meta-analysis. *Environment Health Perspective* 112(9): 970-978.
- Aynechi, N., (2004). *Oil Spill Response*, <http://www.darwin.bio.uci.edu/-sustain/global.html>.Retrived: 30 June 2012.
- Azubuikwe, C.P and Okhamafe, A.O., (2012). Physicochemical, spectroscopic and thermal properties of microcrystalline cellulose derived from corn cobs, *International journal of recycling organic waste in agriculture*, 1:9.
- Badejo, O.T. and Nwilo, P.C., (2004). *Management of Oil Spill Dispersal Along the Nigerian Coastal Areas*. ISPRS Congress, Istanbul, Turkey.
- Balernas, P. and Vaisis, V., (2005).Experimental Investigation of Thermal Modification Influence on Sorption Qualities of Biosorbents. *Environmental Engineering Landscape Management*, 13(1): 3-8.
- Banerjee, S.S., Joshi, M.V. and Jayaram, R.V., (2006). Treatment of oil spills using organo-fly ash. *Desalination*, 195:32-39

- Bayat, A., Aghamiri, S.F., Moheb, A. and Vakili-Nezhaad, G.R., (2005). Oil spill cleanup from seawater by sorbent materials. *Journal of Chemical Engineering Technology*, 28: 1525-1528.
- Bodîrlău, R. and Teacă, C.A., (2009). Fourier Transform Infrared Spectroscopy and thermal analysis of lignocellulose fillers treated with organic anhydrides. *Romanian Journal of Physics*, Bucharest, 54(1-2): 93-104.
- Bolanle, K.S. and Alhassan, S., (2012). Bioethanol potentials of corn cob hydrolysed using celluloses of aspergillus niger and penicillium decumbens *EXCLI Journals*, 11:468-479.
- Breitenbeck, G.A., Grace, B., Holiday, M. and Assoc. (1997). Louisiana applied oil spill research and development program, OSTRADP Technical Report series 96-001.
- Brody, T., (1994). Nutritional biochemistry, New York academic press, pp 450-459.
- Buist, I., McCourt, J., Potter, S., Ross, S. and Trudel, K., (1999). In situ burning. *Pure Applied Chemistry*, 71(1): 43-65.
- Bukowski, J.A., (2001). Review of the epidemiological evidence relating toluene to reproductive outcomes. *Regulation and Toxicological pharmacology*. 33: 147-156.
- Bulut, E., Ozacar, M. and Sengil, I.A., (2008), Adsorption of malachite green onto bentonite: equilibrium and kinetic studies and process design. *Micro.Meso. Material* 115:234-246.
- Burgeir, J., Tseng, F., Jessup, D. and Clapp, R., (2002). *Oil: A Life Cycle Analysis of Its Health and Environmental Impacts*, the Center for Health and the Global Environment. Harvard medical School. Pp. 1-79.

- Burns, K.A., Codi, S., Pratt, C., Swannell, R.J.P. and Duke, N.C., (1999). Assessing the oil degrading potential of endogenous micro-organisms in tropical marine wetlands. *Mangroves and Salt Marshes*, 3: 67-83.
- Carr, R.L. Jr., (1965). Evaluating flow properties of solids, *Chemical Engineering*, 72: 163-168.
- Cetin, N.S. and Ozmen, N., (2010). Acetylation of wood composites and fourier transform infrared spectroscopic studies, *African Journal of Biotechnology*, 40:31-40.
- Chen Y. and Cheng X., (2008). Preparation and characterization analysis of rice husk high boiling solvent lignin. *Journal of Forestry Research*, 19(2): 159-163.
- Choi, H.M. and Cloud, R.M., (1992). Natural sorbent in oil spill cleanup. *Environmental Science and Technology*, 26 (4): 772-776.
- Choi, H.M. and Moreau, J.P., (1993). Oil sorption behavior of various sorbents studied by sorption capacity measurement and environmental scanning electron microscopy. *Journal of Microscopic Research Technology*, 25(5-6): 447-455.
- Choi, H.M., Kwon, H. and Moreau, J., (1993). Cotton nonwovens as oil spill cleanup sorbents *Textile Research Journal.*, 63(4): 211-218.
- Choi, H.M., (1996). Needle punched cotton nonwovens and other natural fibers as oil cleanup sorbents. *Environment Science and Health*, 31(6): 1441-1457.
- Christodoulou, N.C., (2002). *Porous and Magnetic Inorganic Based Composite Materials Used as a Sorbent for Cleaning Water and the Environment from Oil Spill*, International patent: PCT/CY00/00003.

- Chum, H.L., Douglas, J., Feinberg, D.A. and Schroeder, H.A.,(1985), Evaluation of pretreatments of biomass for enzymatic hydrolysis of cellulose, *Solar energy research institute Golden CO*,
- Chung and Vennosa, A.D., (2008). Effect of sand particle size, oil contamination and water table level on the effectiveness of sorbents in wicking oil from contaminated wetland.*Intl Oil Spill Conference*, Ohio, Pp. 537-540.
- Coxeter, R., (1994). Hope for oil spills is a thing with feathers. *Business Week*, 76.http://www.businessweek.com/archives/1994/b338184.arc.htm?campaign_id=search. Retrieved: 30 June 2012
- Das, B. and Mondal, N.K., (2011). Calcerous soil as a new adsorbent to remove lead from aqueous solution: Equilibrium, Kinetics and Thermodynamics study. *Universal Journal of Environmental Research and Technology*, 1(4):515-530.
- Dara, S.S., (1991). *Experiments and calculations in engineering chemistry*, S. Chand and Co. Ltd., New Delhi, pp. 185-191.
- Deschamps, G., Carvel, H., Bonedom, M., Bonnin, C. and Vigroles, C., (2003). Oil removal from water by selective sorption on hydrophobic cotton fibers: study of sorption properties and comparism with cotton fiber-based sorbents. *Environmental Science Technology*, 37(5): 1013-1015.
- Delaune, R.D. Lindau, C.W. and Jugsujinda, A., (1999). Effectiveness of "Nochar" solidifier polymer in removing oil from open water in coastal wetlands.*Spill Science and Technology Bulletin*, 5(5-6): 357-359.

- Diya'uddeen, B.H., Mohammed, I.A., Ahmed, A.S. and Jibril, B.T., (2008). Production of activated carbon and its utilization in crude oil spillage cleanup. *Agricultural Engineering International: the Cigr Ejournal*, Pp. 1-9.
- Dowine, N.M and Heath, R.W., (1974) Basic Statistical Methods, fourth ed. Harper and Row, New York.
- Duke, N.C., Burns, K.A., Swanell, R.P.J, Dalhause, O. and Ropp, R.J., (2000). Dispersant used and a bioremediation strategy as alternate means of reducing impacts of large oil spills on mangroves: The Gladstone field trials. *Marine Pollution Bulletin*, 41(7-12): 403-412.
- Eka, O. U. and Udotong, I. R., (2003). A case study of effects of incessant oil spills from Mobil producing Nigeria unlimited on human health in Akwa-Ibom State. *In: E. N. Ainna, O. B. Ekop and Attah V.I. (Eds), Environmental Pollution and Management in the Tropics*, SNAAP Press Limited Enugu, pp. 204-229.
- English, B., (1997). Filters, sorbents and geotextiles. *In: Rowell, R.M., Young, R.A and Rowell J.K. (Eds), Paper and Composites from Agro-Based Resources*, CRC press, Lewis publishers, Boca Raton, pp. 403-425.
- European Commission (2002). Polyaromatic hydrocarbons-occurrence in food. *Dietary Exposure and Health Effects*, scientific committee on food. 4 December 2002.
- Eyong, E.U., Umoh, B., Ebong, P.E., Eteng, M.U., Antai, A.B. and Akpa, A.O., (2004). Haematotoxic effects following ingestion of Nigerian crude oil and crude oil polluted shellfish by rats. *Nigerian Journal of Physiological Sciences*, 19(1-2): 1-6.

- Fingas, M. and Charles, J., (2001). *Basics of Oil Spill Clean Up*, Second Edition, Lewis publishers, CRC Press. Pp 122-128.
- Food and Agricultural Organization (FAO)., (2002). Available at: <http://apps.fao.org/default.htm>. Retrieved 31 July, 2013
- Folasegun, A.D. and Kovo, G.A., (2014). Simultaneous Adsorption of Ni(II) and Mn(II) ions from Aqueous Solution onto a Nigerian Kaolinite Clay. *Journal of Materials Research and Technology*, 3(2): 129-141.
- Fowomola, M.A., (2010). Some nutrients and anti-nutrients contents of mango (*mangifera indica*) seed. *African Journal of Food Science*, 4:472-476.
- French, J.E., Lacks, G.D., Trempus, C., Dunnick, J.K., Foley, J., Mahler, J., Tice, R.R. and Tennant, R.W., (2001). Loss of heterozygosity frequency at trp 53 locus in p53 deficient (+/-) mouse tumors in carcinogens and tissue deficiency. *Carcinogenesis*, 22910: 99-106.
- Friends of the Earth Netherlands (FEN), (2009). Oil Spills in the Niger Delta in Nigeria. *Milieu Defensie*, 1-2.
- Frost, R., Camody, D., Yunfei, X., Kokot, S., (2007). Adsorption of hydrocarbons on organo-clays - implications for oil spill remediation. *Journal of Colloid and Interface Science*, 305(1): 17-24.
- Ghalambhor, A., (1995). Evaluation and characterization of sorbents in removal of oil spills. *Louisiana Applied Oil Spill Research and Development Program OSRADP*

Technical Report Series, Louisiana Oil Spill Coordinators Office, Baton Rouge-Louisiana.

Greene, G., Mackary, D. and Overall, J., (1975). Cleanup after territorial oil spills in arctic. *Short Papers*, 140-142.

Hassan, A.B., Abolarin, M.S. and Ratchel, U., (2006). Investigation on the use of palm oil as lubricating oil. *Leonardo Electronic Journal of Practices and Techniques*, 8: 1-8.

Haussard, M., Gaballah, I., Kanari, N., De Donato, P., Barrés, O. and Villieras, F., (2003). Separation of hydrocarbons and lipid from water using treated bark. *Water Resources*, 37(2): 362–374.

Heinze, T., (2005). *Carboxyl Methyl Esters of Cellulose and Starch- A Review*, Centre of Excellence for Polysaccharide Research, Friedrich Schiller University of Jera, Humboldtstrasse, 3: 13–29.

Hill, C A S., Jones, D., Strickland, G., and Cetin, N S., (1998). Kinetics and mechanistic aspects of the acetylation of wood with acetic anhydride. *Holzforschung*, 52: 623-629.

Hill, C.A.S., (2006a). *Acetylated wood: The science behind the material*. <http://www.accoya.com/download.asp>. Retrieved 03/06/2012.

Hill, C.A.S., (2006b). *Wood Modification: Chemical, Thermal and Other Processes*. John Wiley and Sons, Chichester Sussex, Uk. P 35-47.

Hitzman, D.O. and Okia, B., (1968). Method of removing oil from polluted water using expanded vermiculite. *US Patent, No.3414511*.

- Ho, Y.S.,(1995). Adsorption of Heavy Metals from waste streams by peat. PhD thesis, University of Birmingham, UK.
- Hofle, G., Steglich, W. and Vorbroggen, H., (1978).4-Dimethylamino pyridines as highly active acylation catalyst. *Angew Chemical, International Edition England*. 17: 569-583.
- Homan, W., Tjeerdsma, B., Beckers, E. and Joessen, A., (2000). *Structural and other properties of modified wood*. Congress WCTE, Whistler, Canada. Pp 433-441.
- Hulla, L.E., French, J.E. and Dunnick, J.K., (2001). Chromosome 11 allotropes reflect a mechanism of chemical carcinogenesis in heterozygous p-53 deficient mice. *Carcinogenesis*, 22(10): 69-98.
- Hussein, M., Amer, A.A. and Sawsan, I.I., (2008). Oil spill sorption using carbonized pith bagasse: trial for practical application. *International Journal of Environmental Science and Technology*, 5(2): 233-242.
- Ibemesi, J.A. (2004). Physical chemistry for tertiary institutions, Part 1. SAN Press Enugu, Second Edition, pp 189-210.
- Igwe, J.C., Abia, A.A., (2006). A bioseparation process for removing heavy metals from wastewater using biosorbents. *African Journal of Biotechnology*, 5 (12), 1167-1179.
- Indrayam, Y., Yusuf, S., Hadi, Y.S., Nandika, D. and Ibach, R.E., (2000). Dry wood termite resistance of acetylated and polymerized tributyltin acrylate (TBTA) Indonesian and USA wood, in proceedings of the 3rd international wood science symposium, core university programme in the field of wood science.

- International Annual Report on Carcinogens (IARC), (2005). Benzene. *Substance Profile Report on Carcinogens*, CAS: NO 71-43-2.
- International Institute of Tropical agriculture (IITA), (2002). Available at: <http://intranet/iita4/crops/maize.htm>. Retrieved: 7 July, 2013.
- International Tankers Owners pollution Federation limited (ITOPF), (2004). *Containment and recovery of floating oil*, <http://www.itopf.com/containment.html>. Retrieved 12 November 2012.
- Johnson, R.F., Manjrekar, T.G. and Halligan, J.E., (1973). Removal of oil from water surface by sorption on un-structural fibers. *Environmental Science Technology*, (7): 439-443.
- Kanoh, T., Fukuda, M., Itayemi, E., Kinouchi, T., Nishifiyi, K. and Ohnishi, Y., (1990). Nitro-reaction in mice injected with pyrene during exposure to Nigerian dioxide. *Mutat. Resources*, 275: 1-4.
- Kaur, M., Singh, N., Sandhu, K.S. and Guray, H.S., (2004). Physicochemical, thermal, morphological and rheological properties of some starches prepared from kernels of some Indian mango cultivars (*Mangifera Indica* L.) *Food Chemistry*, 85: 131-140
- Karimi, B. and Seradj, H., (2001). N-Bromosuccinimide (NBS): A novel and highly effective catalyst for acetylation of alcohols under mild conditions. *Synletters*, 4: 510-519.
- Karimi, B. and Zareyee, D., (2008). Selective metal- free oxidation of sulphides to sulfoxides catalyzed with n- bromosuccinimide (NBS) under neutral buffered reaction conditions. *Journal of the Iran Chemical Society*, 5: 5103-5107.

- Kludze, H., Deen, B., Weersink, A., Van Acker, R., Janovicek, K. and De Laporte, A., (2010). Assessment of the availability of agricultural biomass for heat and energy production in ontario. Available on http://www.uoguelph.ca/plant/research/agronomy/publications/pdf/ontario_biomass_availability_project_final_report_2011.01.27.pdf. Retrieved: 12 october 2012.
- Kosaka, P.M., Kawano, Y., Salvadori, M.C. and Petri, D.F.S., (2005), *Cellulose* 12:351-359.
- Kumar, S. (1994). Chemical modification of wood. *Wood Fibre Sci.* 26: 270-280.
- Lee, B., Hans, J.S. and Rowell, R.M., (1999). Oil sorption by lignocellulosic fibers. *In: Kenaf Properties, Processing and Product*, Mississippi State University- Ag and Bio Engineering, Pp. 432-533.
- Louise W-H., (1997). Teratogen update: Toluene. *Teratology*, 55: 145-151.
- Mobbs, P., (1996). *The Sea Empress Spill: the Potential for Human Health Effects*, Mobbs Environmental Investigations, Cymro, pp. 1-13.
- Mohebbi, B., (2008). Application of ATR infrared spectroscopy in wood acetylation, *Journal of Agricultural Science and Technology*, 10(3) 253-259.
- Mohebbi, B. and Hadjihassani, R., (2008). Moisture repellent effect of acetylation on poplar fiber. *Journal Agricultural Science and Technology*, 10: 157-163
- Mullin, J V. and Champ, M A., (2003). Introduction/overview to in-situ burning of oil spills. *Spill Science and Technology Bulletin*, 8(4): 323-330.

- Nasar, M., Emam, A., Sultan, M. and Abdul-Hakim, A.A., (2010). Optimization of Characterization of Sugarcane Bagasse Liquefaction, *Indian Journal of Science and Technology*, 13(12) 207-212.
- National Oceanic Atmospheric Administration (NOAA), (2004). *Dispersants*.<http://www.response.restoration.noaa.gov/oilaid/response/pdfs/methods/disperse.pdf>. Retrieved: 21 January, 2013.
- Nenkova, S., Garvanska, R. and Jelev, S., (2004). Fibrous wood sorbent for eliminating oil pollution. *Aulex Research Journal*, 4(30): 157-163.
- Nordvick, A.B., Simmons, J.L., Bitting, K.R., Lewis A. and Strøm-Kristiansen T., (1996). Oil and water separation in marine oil spill clean-up operations. *Spill Science and Technology Bulletin*, 3(3): 107-122.
- Nwankwere, E.T., (2010). Acetylation of rice husks for oil spillage treatment. MSc. Thesis, Ahmadu Bello University Zaria, Nigeria.
- Nwankwere, E.T., Gimba, C.E., Kagbu, J.A., Nale, B.Y.,(2010). Sorption studies of crude oil on acetylated rice husks. *Advances in Applied Science Research*, 2(5): 141-151.
- Nwanma, V., (2009). Nigerian corn study shows production could be more than double: A report presented to government by IITA. Bloomberg. Available on <http://www.bloomberg.com/apps/news?pid=newsarchive&sid=orgf2xjGoSoM>. Retrieved: 31 January 2013.
- Nzikou, J.M., Kimbonguila, A., Matos, L., Loumouamou, O., Dambou-Tobi, N.P.G., Ndangui, C.B, Abene, A.A., Silou, T.L., Scher, J., and Desoby, S., (2010). Extraction and

- characterization of seed oil from mango (*mangifera indica*). *Research Journal of Environmental and Earth Sciences*, 2(1): 231-238.
- Okoro, A., Ejike, E.N., and Anunoso, C., (2007a). Sorption model of modified cellulosic as crude oil sorbent. *Journal of Engineering and Applied Sciences*, 2(2): 282-285.
- Okoro, I.A. and Ejike, E.N., (2007). Chemical modification of cellulose pulp as crude oil absorbents. *Research Journal of Applied Sciences*, 2(1): 75-76.
- Okoro, I.A., Okwu, D.E. and Emeka, U.S., (2007b). Sorption kinetics and intra-particulate diffusivity of crude oil on kenaf (*Hibiscus CannabinusL.*) Plant Parts. *Journal of Engineering and Applied Sciences*, 2(1): 170-173.
- Proffitt, E., (1997). *Managing Oil Spills in Mangrove Ecosystems; Effects, Remediation, Restoration and Modeling*, OCS Study MMS 97-0003, New Orleans U.S Department of Interior, Minerals Management Service, Gulf of Mexico OCS Region Pp. 76.
- Puravankara, D., Bohgra, V. and Sharma, R.S., (2000). Effects of antioxidant principles isolated from from mango (*mangifera indica* l) seed kernels on oxidative stability of buffalo glee (butter fat) *Journal of the Science of Food and Agriculture*, 80: 522-526
- Radetic, M., Jovic, D., Jovenic, P., Petrovic, Z. and Thomas H., (2003). Recycled wood based nonwoven materials as oil sorbents. *Environmental Science and Technology*, 37(5): 1008-1012.
- Ramos-Vianna, M.M.G., Frano, J.H.R., Pinto, C.A., Valenzuela-Diaz F.R. and Buchler P.M., (2004). Sorption of oil pollution by organoclays and a coal mineral complex. *Brazilian Journal of Chemical Engineering*, 21(20): 239-295.

- Rangikuti, M. and Djajanegara, A., (1983). The utilization of agricultural byproducts and wastes (as animal feeds) in Indonesia. In: the use of organic residues in rural communities as animal feed in south east asia. Proceedings, workshop on organic residues in rural communities Denpasar (Indonesia); pp. 11-25.
- Refaat, A.A. and Sheltawy, E.L., (2008). Time factor in microwave-enhanced biodiesel production. *Environment and Development*, 4(4): 279-287.
- Reynolds, J.G., Coronado, P.R. and Hrubesh, L.W., (2001). Hydrophobic aerogels for oil spill cleanup-synthesis and characterization. *Non-Crystalline Solids*, 292 (1-3): 127-137.
- Ribeiro, T., Smith, R. and Rubio, J., (2000). Sorption of oils by the nonliving biomass of a *salvinia* sp. *Environmental Science Technology*, 34: 5201-5205.
- Ridgway, W.B. and Wallington, H.T., (1946). *Esterification of wood*. British patent 579255.
- Roulia, M. Chassapis, K. Fotinopoulos, C. Savvidis, T. Katakis, D., (2003). Dispersion and sorption of oil spills by emulsifier-modified expanded perlite. *Spill. Science Technology Bulletin*, 8(5-6): 425-431.
- Rowell, R.M. and Ellis, W.N., (1978). Determination of dimensional stabilization of wood using the water soak method. *Wood and Fiber*, 10(4): 104-111.
- Rowell, R.M. Simonson, S., Hess, S., Placket, D.V., Cronshaw, D. and Dunningham, I.O., (1994). Swelling of acetylated wood in organic solvent. *Wood Fiber Science*, 26: 11.
- Rowell, R.M., Young, R.A and Rowell J.K., (1999). *Paper and Composites from Agro-Based Resources*, CRC press, Lewis publishers, Boca Raton, pp. 249-266.

- Sayed, S.A., El Sayed, A.S., El kareish, S.M. and Zayed, A.M., (2003). Treatment of liquid oil spill by untreated and treated aswanly clay from Egypt. *Journal of Applied Science and Environmental Management.*, 7(1): 23-33.
- Sayed, S.A., El-Sayed, A.S. and Zayed, M.A., (2004). Removal of oil spills from salt water by magnesium, calcium carbonates and oxides. *Journal of Applied Science and Environmental Management*, 8(1): 71-78.
- Scalbwet, A., (1998). Antimicrobial properties of tannins. *Phytochemistry*, 30: 3875-3883.
- Shatzberg, P., (1971). *Us Coastal Guard Rep No 724110.1/2/1*. US Coastal Guard headquarters, Washington DC. P. 32-49.
- Shell Petroleum Development Company (SPDC), (2004). Protecting the environment. *In : Shell Nigeria Annula Report*, pp 16.
- Shell Petroleum Development Company (SPDC), (2006). People and the environment. *In: Shell Nigeria Annual Report*, pp 8-9.
- Shigenaka, G., (2002). Oil toxicity in mangroves. *In: Hoff, R. (Ed.) Oil Spills in Mangroves- Planning and Response Consideration*. National oceanic and atmospheric administration, Seattle, Washington, pp. 23-35.
- Site, A.D., (2004). Factors affecting sorption of organic compounds in Natural sorbents/water systems and sorption coefficients for selected pollutants: A review. *Journal of Physics and Chemical Reference Data*, 30(1): 187-439.
- Smith, J.W., (1983). *The control of oil pollution*, Graham and Trotman limited, London, UK. pp. 243-249.

- Snyder, R. and Hedlim, C.C. (1996).An overview of benzene metabolism (Review). *Environmental Health Perspective*,104(6): 1165-1171.
- Stamm, A.J and Tarkow, H, (1947). *Acetylation of Wood and Boards*, US patents 2417995.
- Stanly, E., (1996). Oil spill response techniques: A review. *Emergency and Response Bulletin*, 1: 18-22.
- Stuart, M.L., (1989). *Dictionary of Composite Material Technology*. Lewis publishers, CRC press,p. 3.
- Sun, Y. and Cheng, J., (2002). Hydrolysis of lignocellulosic materials for ethanol production: a review. *Bioresource Technolnology*, 83:1-11.
- Sun, X-F., Sun, R. and Sun, J.X., (2002).Acetylation of Rice Straw for Oil Sorption; With or Without Catalysts.*Journal of Agriculture and Food Chemistry*, 50: 6428.
- Sun, X.F., Sun, R.C. and Sun, J.X., (2004). Acetylation of sugarcane bagasse using NBS as a catalyst under mild reaction conditions for the production of oil sorption-active materials. *Bioresource Technology*, 95(3): 343-350.
- Sun, J.X., Xu, F., Geng, Z.C., Sun, X.F., and Sun, R.C., (2005). Comparative study of cellulose isolated by totally chlorine-free method from wood and cereal straw.*Journal of Applied Polymer Science*, 97: 322–335.
- Sun, R.C., (2010). Cereal straw as a resource for sustainable biomaterials and biofuels.First edition, Elsevier, Linacre house, Jordan hill, Oxford OX2 8DP, UK, pp 10-25.

- Taffarel, R.S. and Rubio, J.R., (2009). On the removal of Mn(II) ions by adsorption onto natural and activated Chilean zeolite. *Minerals Engineering*, 22: 336-343.
- Tapio, S., Daniel, V., Erkki, P., Bjarne, H. and Rainer, S., (1994). Kinetic study of the carboxymethylation of cellulose. *Industrial and Engineering Chemistry Research*, 33 (6): 1454–1459.
- Teas, C., Kalligeros, S., Zanikos, F., Stournas, S., Lois, E. and Anastopoulos, G., (2001). Investigation of the effectiveness of absorbent materials in oil spills clean up. *Desalination*, 140(3): 259-264.
- Tronc, E.C., Hernandez-Escobar, C.A., Ibarra-Gomez, R., Estrada-Monje, a., Navarette-Bolanos, J., Zaragoza-Contreras, E.A. (2006). Mechanical and thermal properties of chemical treated kenaf fibres, *Carbohydrate Polymers*, 67:245-252.
- Tsutsumi, H., Kono, M., Takai, K., Manabe, T., Haraguchi, M., Yamamoto, I. and Oppenheimer, C., (2000). Bioremediation on the shore after an oil spill from the Nakhodka in the sea of Japan III Field tests of a bioremediation agent with microbiological cultures for the treatment of an oil spill, Marine. *Pollution Bulletin*, 40(4): 320-324.
- Tserki, V., Zaferopoulos, N.E., Simon, F. and Panayiotou, C., (2005). *Composites Part A*, 36:1110.
- Tuong, V.M. and Li, J., (2010), Effect of Heat Treatment on the Change in Colour and Dimensional Stability of Acacia hybrid Wood, *BioResources*, 5(2) 1257-1267.

- Udoette, U.B., (1997). *Effects of Administration of Qua Iboe Light Crude Oil on Biochemical Parameters in Albino Wister Rats*. Unpublished M.Sc Thesis, Biochemistry Department, University of Calabar.
- United Nation Development Program (UNDP), (2006). *Niger Delta Human Development Report 2006*, Abuja, Nigeria, pp. 19-73.
- United States Army Corps of Engineering (USACE), (2005). Incidences and environmental effects of oil and gas releases. *In: Known and Potential Environmental Effects of Oil and Gas Drilling Activity in the Great Lakes*. Final report. www.lrc.usace.army.mil/GrtLakes/OilGas/Chapter3.pdf, pp. 26-38. Retrieved 21 July 2013.
- United States Department of Agriculture (USDOA), (2008). *Design Guide for Oil Spill Prevention and Control at Substations*. Rural development utilities programs, bulletin 1724E-302, pp. 73-108.
- United States Environmental Protection Agency (USEPA), (1994). *Chemicals in the environment: Toluene*. OPPT chemical fact sheet. EPA 749-F-54-021.
- United States Environmental Protection Agency (USEPA), (1999). Shoreline cleanup of oil spill. *In: Understanding Oil Spills and Oil Spill Response*. Office of Emergency and Remedial Response, bulletin Pp1934F-312, pp 17-20.
- United States Environmental Protection Agency (USEPA), (2004a). *Booms*, <http://www.epa.gov/oilspill/boom.htm>. Retrieved: 31 July 2012.

- United States Environmental Protection Agency (USEPA) (2004b). *Dispersing agents*, <http://www.epa.gov/oilspill/disperse.htm>. Retrieved: 24 August 2013.
- United States Environmental Protection Agency (USEPA), (2004c). NRT fact sheet. *Bioremediation in oil spill response*, <http://www.epa.gov/oilspill/pdfs/biofact.pdf>. Retrieved: 24 August 2014.
- Uzoije, A.P., Onunkwo, A., Egwuonwu, N., (2011). Crude oil sorption onto groundnut shell activated carbon: kinetics and isothermal studies. *Research journal of environmental and earth sciences*, 3(5): 552-563.
- Vee Gee scientific, (2004). *Toluene*. Material and safety Data sheet, M10003.
- Venkata Subbaiah, M., Kalyani, S., Sankara Reddy, G., Veera M. Boddu, Krishnaiah, A., (2008) Biosorption of Cr (VI) from aqueous solutions using trametes vesicolor polyporous fungi, *Electronic Journal of Chemistry*, 5:3 499-510.
- Vennosa, A.D., Lee, K., Suldán, M.T., Gracia-Planco, S., Cobanlı, S., Moteleb, M. and King, O.W., (2002). Bioremediation and bio restoration of crude oil contaminated fresh wetland on the Saint Lawrence River. *Bioremediation Journal*, 6(3): 266.
- Ventikos, N.P., Vergetis, E., Psaratifs, H.N. and Triantafyllou, G., (2004). A high level synthesis of oil spill response equipment and countermeasures. *Journal of Hazardous Materials*, 107: 51-58.
- Wang, W. Zappi, M., Singletary, J., Hall, N. and Karr, L., (2001). *Using chemical priming as a means of enhancing the performance of bio-cells for treating petroleum products*

containing recalcitrant chemical species, Environmental technology research and applications laboratory, Mississippi State University. Pp 22-37.

Wardrop, J.A., Wagstaff, B., Pfennig, P., Leeder, J. and Connoly, R., (1996). *The distribution, persistence and effects of petroleum hydrocarbons in mangroves impacted by the "era" oil spill (September, 1992)*. Final phase one report, Adelaide office of the environmental protection agency, south australian department of environmental and natural resources.

Wei, Q.F., Mather, R.R., Fotheringham, A.F. and Yang, R.D., (2003). Evaluation of non-woven polypropylene oil sorbents in marine oil-spill recovery. *Marine Pollution Bulletin*, 46(6): 780–783.

Wells, J., (1988). Pharmaceutical preformulation: the physicochemical properties of drug substances. 1st edn, John Wiley and Sons, New York. In: Azubuike, C.P and Okhamafe, A.O., (2012). Physicochemical, spectroscopic and thermal properties of microcrystalline cellulose derived from corn cobs, *International journal of recycling organic waste in agriculture*, 1:9.

Yakubu, A., Olatunji, A.G., Mohammed, C., Mamza, P.A., (2013) acetylation of wood flour from four wood species grown in Nigeria using vinegar and acetic anhydride. *International Journal of Carbohydrate Chemistry*. Article ID 141034.

Yang, Z., Xu, S., Ma, S. and Wang S. (2008), *wood Sci Technol* 42:621-629.

Yender, R. (2002). Response Oil Spills in Mangroves. *In: Hoff, R. (Ed.), Oil Spills in Mangroves- Planning and Response Consideration*. National oceanic and atmospheric administration, Seattle, Washington, pp. 36-47.

- Yu, C.T., Chen, W.H., Men, L. and Hwang, W.C., (2009), *Industrial Crops and Products*, 29: 308-316.
- Yui, T., Taki, N., Sugiyama, J. and Hayashi, S., (2007), *Internal Journal of Biological Macromolecule* 40(4)336-341.
- Zeun, R.E., El-bagoury, A.A. and Kassab, H.E., (2005). Chemical and nutritional studies on mango seed kernel, *Journal of agricultural Sciences*, 30: 3285-3299
- Zhang, J., Zhang, L., Li, Z., Xie, X., Li, J. and Luo, P., (2001). Interaction between the hydrophobically modified water soluble amphoteric cellulose graft copolymer and clay. *Acta Physica Chimica Sinica*, 18(04): 315-320.

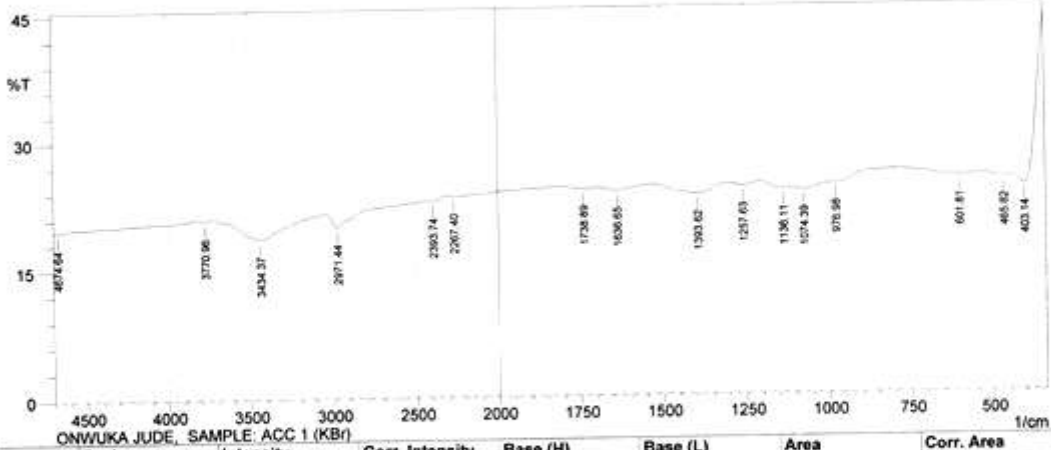
List of Appendices

Appendix 1: Spectrograph of acetylated corn cob (sample 1)



FTIR ANALYSIS RESULT NARICT,ZARIA

FTIR- 8400S FOURIER TRANSFORM
INFRARED SPECTROPHOTOMETER



ONWUKA JUDE, SAMPLE: ACC 1 (KBr)

Peak	Intensity	Corr. Intensity	Base (H)	Base (L)	Area	Corr. Area	
1	403.14	23.944	8.143	440.75	339.48	55.208	6.829
2	465.82	24.872	0.185	537.19	441.71	57.419	0.155
3	601.81	25.034	0.4	797.59	538.16	154.385	0.787
4	976.98	24.353	0.089	987.59	798.56	112.802	0.089
5	1074.39	23.661	0.299	1115.86	988.55	79.081	0.335
6	1136.11	23.75	0.194	1206.51	1116.82	55.517	0.211
7	1257.63	24.195	0.311	1302.96	1207.48	58.576	0.273
8	1393.62	23.291	1.149	1533.46	1303.92	142.96	2.517
9	1636.65	23.838	0.439	1700.31	1634.42	102.518	0.633
10	1738.89	24.093	0.115	1817.97	1701.27	71.955	0.111
11	2267.4	23.314	0.169	2312.73	1818.93	308.332	0.9
12	2393.74	22.831	0.208	2426.53	2313.69	71.933	0.231
13	2971.44	19.934	1.752	3046.67	2427.5	409.342	4.58
14	3434.37	18.614	2.624	3720.81	3047.63	469.78	17.29
15	3770.96	20.771	0.218	3818.22	3721.77	65.607	0.22
16	4674.64	19.651	0.05	4700.68	3819.18	611.603	1.278

Comment:
ONWUKA JUDE, SAMPLE: ACC 1 (KBr)

User: Administrator

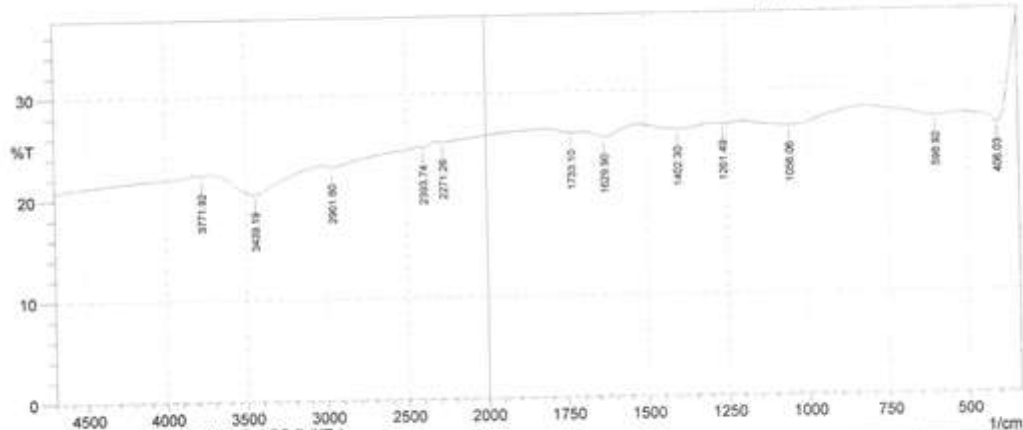
No. of Scans;
Date/Time; 6/10/2013 10:45:13 AM
Resolution;

APPENDIX 2: Spectrograph of acetylated corn cob (sample 2)

SHIMADZU

FTIR ANALYSIS RESULT NARICT,ZARIA

FTIR- 8400S FOURIER TRANSFORM INFRARED SPECTROPHOTOMETER



Peak	Intensity	Corr. Intensity	Base (H)	Base (L)	Area	Corr. Area	
1	406.03	26.298	6.956	516.94	339.48	97.404	8.979
2	598.92	27.044	0.492	820.74	517.9	169.783	0.963
3	1056.06	28.326	0.951	1200.73	821.7	215.743	2.793
4	1281.49	26.575	0.083	1288.49	1201.69	49.851	0.066
5	1402.3	26.08	0.54	1524.78	1289.46	136.341	1.084
6	1629.9	25.491	0.778	1695.49	1525.74	99.369	1.023
7	1733.1	25.92	0.214	1814.11	1696.45	68.637	0.188
8	2271.26	25.23	0.137	2308.87	1815.08	291.065	0.709
9	2393.74	24.722	0.178	2423.64	2309.83	68.639	0.184
10	2961.8	23.025	0.294	3026.41	2424.6	374.484	0.91
11	3439.19	20.397	2.368	3717.92	3027.38	457.406	14.36
12	3771.92	22.297	0.147	3813.4	3718.88	61.452	0.134

Comment:
ONWUKA JUDE, SAMPLE: ACC 2 (KBr)

User; Administrator

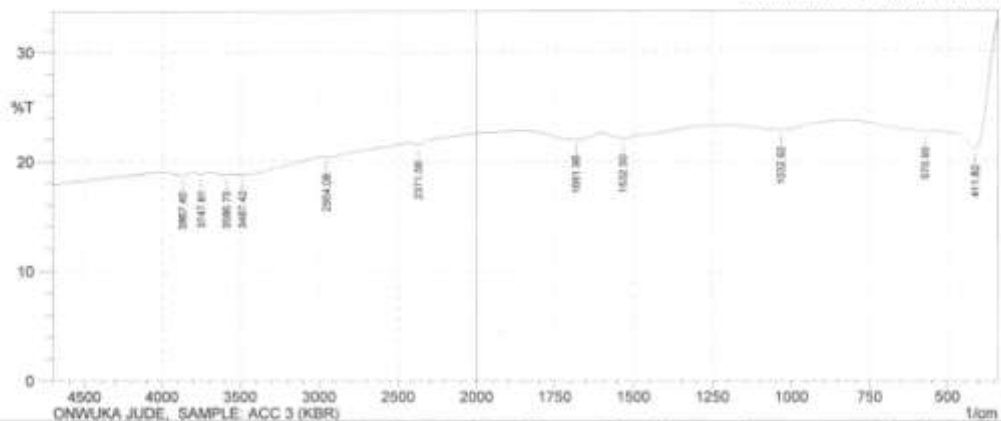
No. of Scans;
Date/Time; 6/10/2013 10:48:00 AM
Resolution;

Appendix 3: Spectrograph of acetylated corn cob (sample 3)



FTIR ANALYSIS RESULT NARICT,ZARIA

FTIR-8400S FOURIER TRANSFORM INFRARED SPECTROPHOTOMETER



ONWUKA JUDE, SAMPLE: ACC 3 (KBR)

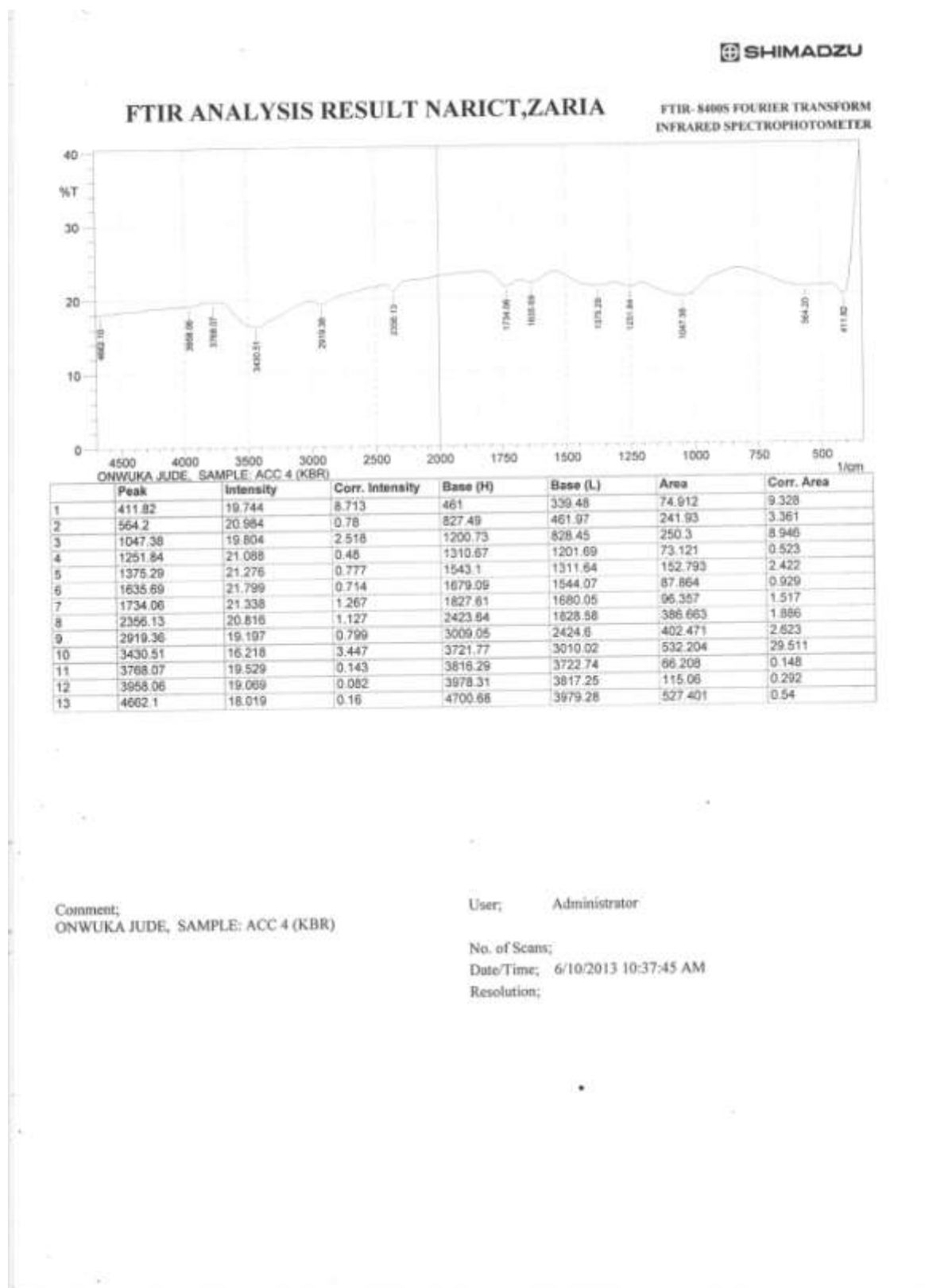
Peak	Intensity	Corr. Intensity	Base (H)	Base (L)	Area	Corr. Area	
1	411.82	21.038	8.573	561.3	339.48	140.089	15.253
2	570.95	22.683	0.034	623.63	562.27	166.204	0.313
3	1032.92	22.758	0.683	1199.76	824.6	238.313	2.11
4	1532.92	21.993	0.633	1597.11	1200.73	255.656	1.725
5	1681.98	21.956	0.604	1869.08	1598.08	176.608	1.546
6	2371.56	21.451	0.307	2429.42	1870.05	366.924	0.397
7	2954.08	20.336	0.069	2981.08	2430.39	373.603	0.261
8	3487.42	18.805	0.094	3519.24	2982.05	381.675	1.198
9	3566.75	18.771	0.106	3694.77	3520.21	126.558	0.245
10	3747.81	18.821	0.202	3798.93	3695.73	74.615	0.239
11	3867.4	18.694	0.335	4000.5	3799.89	145.279	0.665

Comment:
ONWUKA JUDE, SAMPLE: ACC 3 (KBR)

User: Administrator

No. of Scans;
Date/Time; 6/10/2013 10:10:58 AM
Resolution;

Appendix 4: Spectrograph of Acetylated corn cob (sample 4)

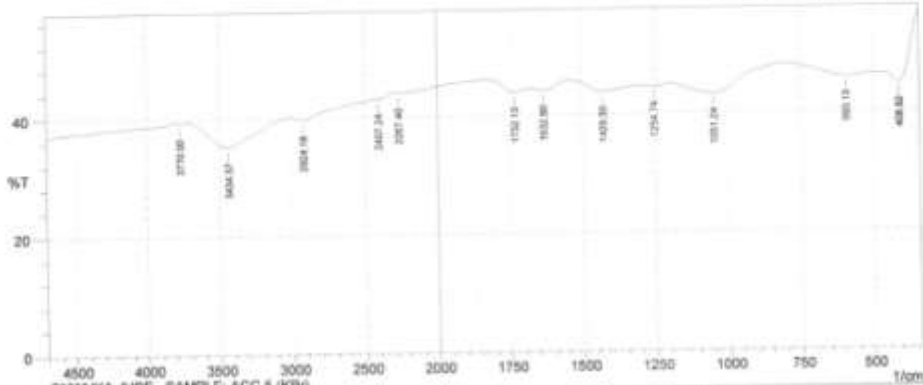


Appendix 5: Spectrograph of Acetylated Corn cob (sample 5)



FTIR ANALYSIS RESULT NARICT,ZARIA

FTIR-8400S FOURIER TRANSFORM INFRARED SPECTROPHOTOMETER



Peak	Intensity	Corr. Intensity	Base (H)	Base (L)	Area	Corr. Area
1	406.92	44.62	6.594	470.55	339.48	4.132
2	593.13	45.788	1.158	806.2	471.61	1.711
3	1051.24	43.18	2.937	1197.83	809.17	4.806
4	1254.74	44.409	0.383	1302.96	1198.8	0.195
5	1429.3	43.719	1.486	1539.25	1303.92	1.763
6	1632.8	44.026	0.814	1680.05	1540.21	0.563
7	1732.13	43.782	1.15	1828.58	1681.02	0.716
8	2267.4	43.888	0.219	2305.98	1829.54	0.923
9	2407.24	42.981	0.066	2416.89	2306.94	0.101
10	2924.18	39.517	0.992	3017.73	2417.85	1.634
11	3434.37	35.181	4.553	3715.99	3018.7	17.501
12	3770	39.207	0.21	3800.54	3718.95	0.111

Comment:
ONWUKA JUDE, SAMPLE: ACC 5 (KBr)

User: Administrator

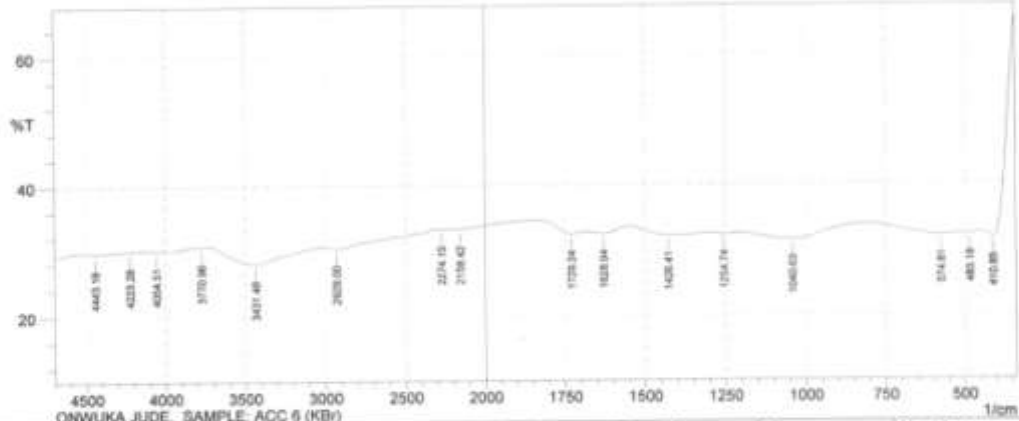
No. of Scans:
Date/Time: 6/10/2013 10:54:27 AM
Resolution:

Appendix 6: Spectrograph of Acetylated Corn cob (sample 6)



FTIR ANALYSIS RESULT NARICT,ZARIA

FTIR-8400S FOURIER TRANSFORM INFRARED SPECTROPHOTOMETER



ONWUKA JUDE, SAMPLE: ACC 6 (KBr)

Peak	Intensity	Corr. Intensity	Base (H)	Base (L)	Area	Corr. Area	
1	410.85	31.571	11.582	444.81	339.48	42.562	7.459
2	483.18	32.181	0.142	513.08	445.57	33.174	0.072
3	574.81	32.102	0.451	810.13	514.05	143.544	0.99
4	1040.63	31.549	1.495	1206.51	811.09	193.555	3.904
5	1254.74	32.348	0.159	1301.03	1207.48	45.756	0.102
6	1426.41	32.183	0.86	1548.89	1301.99	120.422	1.649
7	1628.94	32.519	0.584	1681.02	1549.86	63.381	0.55
8	1728.24	32.445	0.859	1846.9	1681.98	78.571	0.721
9	2158.42	33.291	0.193	2202.78	1847.87	167.041	0.601
10	2274.15	33.242	0.038	2304.05	2203.75	47.934	0.026
11	2929	30.357	0.628	3012.91	2305.01	353.538	2.725
12	3431.48	28.041	2.734	3721.77	3013.87	376.785	14.333
13	3770.96	30.644	0.146	3816.29	3722.74	47.955	0.099
14	4054.51	30.171	0.143	4107.55	3817.25	150.446	0.659
15	4223.28	30.087	0.019	4239.68	4108.51	68.296	0.013
16	4443.18	29.688	0.204	4511.65	4240.84	142.247	0.378

Comment;
ONWUKA JUDE, SAMPLE: ACC 6 (KBr)

User; Administrator

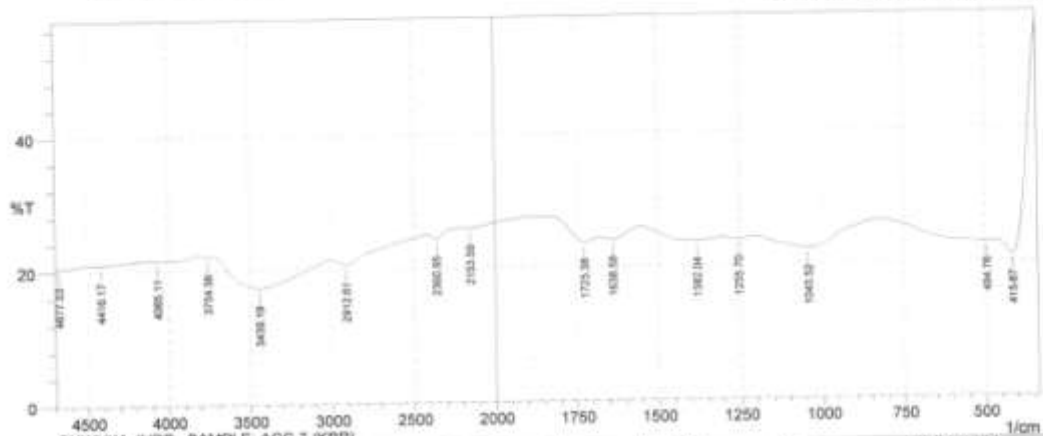
No. of Scans;
Date/Time; 6/10/2013 10:57:36 AM
Resolution;

Appendix 7: Spectrograph of Acetylated Corn con (sample 7)



FTIR ANALYSIS RESULT NARICT,ZARIA

FTIR-8400S FOURIER TRANSFORM INFRARED SPECTROPHOTOMETER



ONWUKA JUDE, SAMPLE: ACC 7 (KBR)

Peak	Intensity	Corr. Intensity	Base (H)	Base (L)	Area	Corr. Area
1	415.67	20.967	15.263	467.75	339.48	13.313
2	494.76	22.947	0.317	824.6	468.72	3.215
3	1043.52	22.222	2.827	1204.59	825.56	9.134
4	1255.7	23.707	0.318	1304.89	1205.55	0.292
5	1382.04	23.569	0.974	1553.71	1305.65	3.108
6	1638.58	23.931	0.783	1677.16	1554.68	0.875
7	1725.38	23.619	1.515	1848.63	1678.13	1.656
8	2153.59	25.92	0.245	2197.66	1849.8	0.696
9	2360.95	24.351	0.942	2422.67	2198.92	1.087
10	2912.61	20.676	1.298	3008.09	2423.64	4.284
11	3439.19	17.284	4.546	3724.67	3009.05	40.164
12	3754.56	22.071	0.136	3812.43	3725.63	0.123
13	4085.11	21.483	0.258	4133.59	3813.4	1.695
14	4416.17	21.011	0.081	4457.64	4134.55	0.329
15	4677.53	20.473	0.068	4700.68	4458.61	0.163

Comment:
ONWUKA JUDE, SAMPLE: ACC 7 (KBR)

User: Administrator

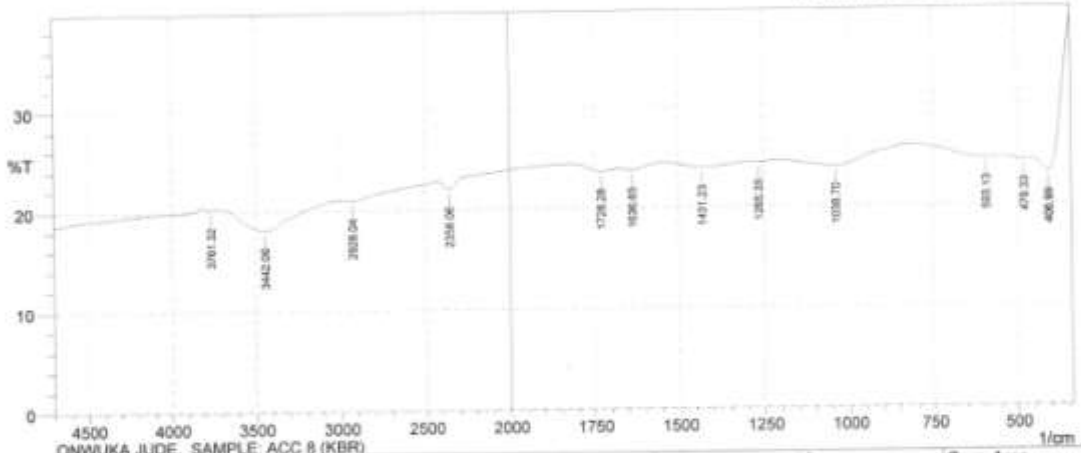
No. of Scans;
Date/Time; 6/10/2013 10:22:50 AM
Resolution;

Appendix 8: Spectrograph of Acetylated Corn cob (sample 8)



FTIR ANALYSIS RESULT NARICT,ZARIA

FTIR- 8400S FOURIER TRANSFORM INFRARED SPECTROPHOTOMETER



ONWUKA JUDE, SAMPLE: ACC 8 (KBR)

	Peak	Intensity	Corr. Intensity	Base (H)	Base (L)	Area	Corr. Area
1	406.99	23.153	7.332	456.18	339.48	66.742	7.134
2	479.33	24.404	0.105	549.73	457.14	56.506	0.073
3	593.13	24.648	0.257	612.06	550.7	156.425	0.663
4	1038.7	23.976	1.203	1201.69	813.02	235.894	3.814
5	1265.35	24.414	0.056	1289.46	1202.66	53.061	0.051
6	1431.23	23.932	0.525	1543.1	1290.42	155.799	1.246
7	1636.65	23.804	0.263	1675.23	1544.07	81.151	0.312
8	1728.28	23.665	0.423	1822.79	1676.2	90.914	0.5
9	2358.06	22.078	0.97	2429.42	1823.76	380.616	1.428
10	2928.04	21.001	0.348	2999.41	2430.39	375.072	1.295
11	3442.09	18.134	2.529	3712.13	3000.37	504.262	18.166
12	3761.32	20.259	0.134	3810.5	3713.09	67.403	0.141

Comment;
ONWUKA JUDE, SAMPLE: ACC 8 (KBR)

User; Administrator

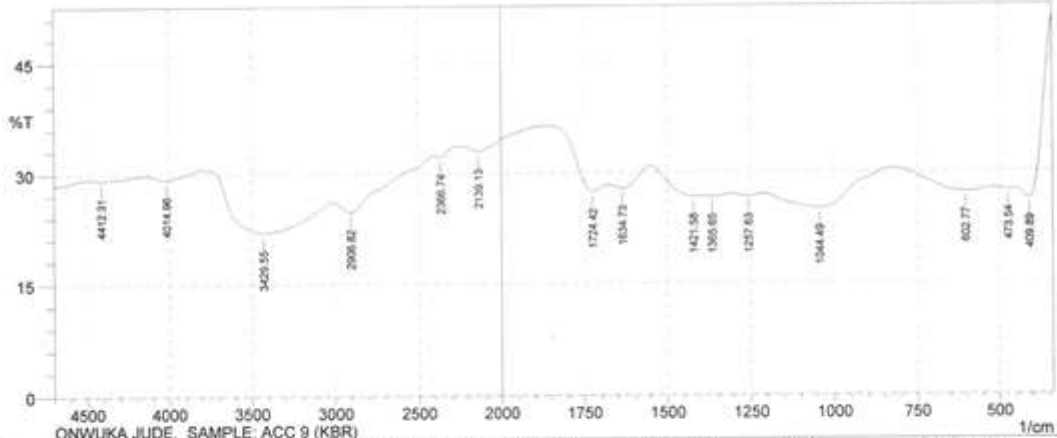
No. of Scans;
Date/Time; 6/10/2013 10:26:05 AM
Resolution;

Appendix 9: Spectrograph of Acetylated Corn cob (sample 9)



FTIR ANALYSIS RESULT NARICT,ZARIA

FTIR- 8400S FOURIER TRANSFORM INFRARED SPECTROPHOTOMETER



Peak	Intensity	Corr. Intensity	Base (H)	Base (L)	Area	Corr. Area	
1	409.89	26.308	10.27	453.29	339.48	56.324	8.062
2	473.54	27.474	0.145	518.87	454.25	36.134	0.065
3	602.77	27.251	1.233	822.67	519.83	165.714	3.19
4	1044.49	25.085	3.416	1209.41	823.63	219.28	10.166
5	1257.63	26.891	0.35	1305.85	1210.37	54.504	0.273
6	1365.65	26.674	0.156	1397.47	1306.82	51.858	0.122
7	1421.58	26.712	0.655	1550.82	1398.44	83.938	1.43
8	1634.73	27.863	1.35	1677.16	1551.78	67.668	1.406
9	1724.42	27.461	2.853	1867.16	1678.13	94.488	2.451
10	2136.13	32.97	1.531	2265.47	1868.12	185.009	3.763
11	2366.74	32.201	0.538	2405.31	2266.43	67.211	0.413
12	2906.82	24.789	2.44	3010.98	2408.28	332.511	8.465
13	3429.55	21.981	6.55	3802.79	3011.95	483.023	49.785
14	4014.96	29.312	0.855	4149.99	3803.75	182.207	2.438
15	4412.31	29.18	0.263	4497.18	4150.95	183.923	0.774

Comment;
ONWUKA JUDE, SAMPLE: ACC 9 (KBR)

User; Administrator

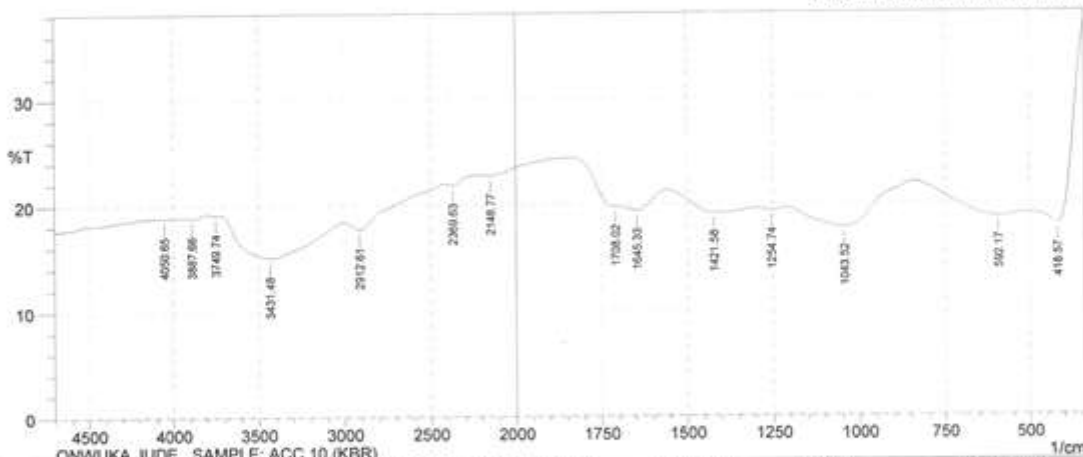
No. of Scans;
Date/Time; 6/10/2013 10:34:16 AM
Resolution;

Appendix 10: Spectrograph of Acetylated Corn cob (sample 10)

SHIMADZU

FTIR ANALYSIS RESULT NARICT,ZARIA

FTIR- 8400S FOURIER TRANSFORM INFRARED SPECTROPHOTOMETER



Peak	Intensity	Corr. Intensity	Base (H)	Base (L)	Area	Corr. Area	
1	418.57	17.893	10.559	505.37	339.48	110.862	15.449
2	592.17	18.729	1.059	839.06	506.33	233.936	4.616
3	1043.52	17.769	2.908	1210.37	840.03	264.567	11.744
4	1254.74	19.371	0.221	1301.03	1211.34	63.721	0.225
5	1421.58	19.13	1.274	1557.57	1301.99	180.037	3.802
6	1645.33	19.395	0.916	1693.56	1558.54	94.145	1.315
7	1708.02	19.731	0.426	1845.94	1694.52	99.479	0.691
8	2148.77	22.759	0.305	2204.71	1846.9	225.353	1.068
9	2369.63	21.833	0.361	2414.96	2205.67	136.072	0.406
10	2912.61	17.722	1.251	3004.23	2415.92	413.51	4.186
11	3431.48	15.053	3.791	3718.88	3005.2	559.404	40.884
12	3749.74	19.071	0.114	3798.93	3719.85	56.787	0.105
13	3887.66	18.836	0.236	3971.56	3799.89	124.048	0.528
14	4050.65	18.813	0.039	4092.12	3972.53	86.686	0.05

Comment:
ONWUKA JUDE, SAMPLE: ACC 10 (KBR)

User; Administrator

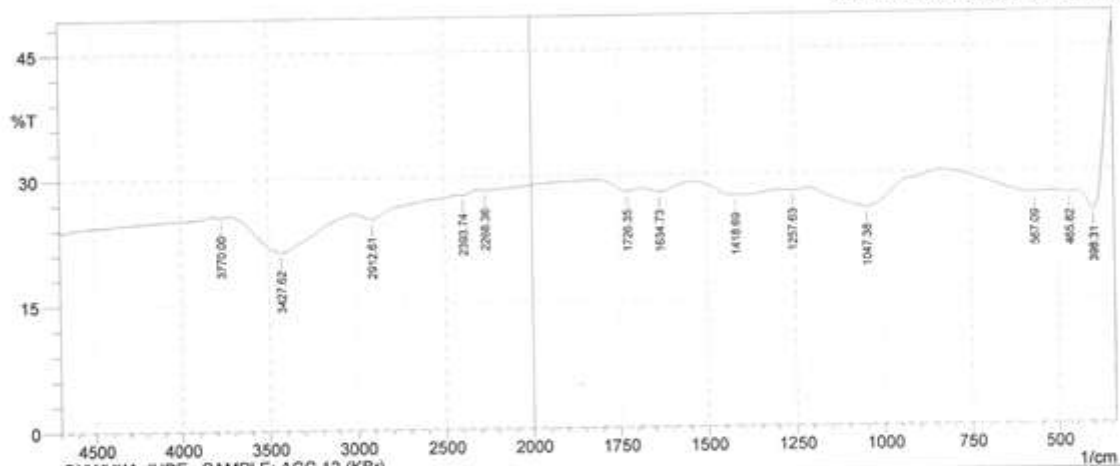
No. of Scans;
Date/Time; 6/10/2013 10:15:00 AM
Resolution;

Appendix 11: Spectrograph of Acetylated corn cob (sample 12)



FTIR ANALYSIS RESULT NARICT,ZARIA

FTIR- 8400S FOURIER TRANSFORM INFRARED SPECTROPHOTOMETER



ONWUKA JUDE, SAMPLE: ACC 12 (KBr)

Peak	Intensity	Corr. Intensity	Base (H)	Base (L)	Area	Corr. Area	
1	398.31	25.289	10.902	442.68	339.48	53.486	8.085
2	465.82	27.354	0.133	512.12	443.64	38.455	0.066
3	567.09	27.434	0.556	831.35	513.08	173.328	1.473
4	1047.38	25.909	3.141	1210.37	832.31	210.605	8.332
5	1257.63	27.899	0.206	1295.24	1211.34	46.379	0.141
6	1418.69	27.446	1.132	1537.32	1296.21	133.452	2.242
7	1634.73	27.955	0.683	1682.95	1538.28	78.997	0.702
8	1726.35	28.06	0.677	1817.97	1683.91	72.766	0.574
9	2268.36	28.388	0.166	2310.8	1818.93	265.494	0.814
10	2393.74	27.805	0.214	2423.64	2311.76	61.745	0.191
11	2912.61	25.164	0.958	3012.91	2424.6	338.501	2.089
12	3427.62	21.224	4.49	3720.81	3013.87	444.667	27.783
13	3770	25.451	0.196	3814.36	3721.77	54.867	0.153

Comment;
ONWUKA JUDE, SAMPLE: ACC 12 (KBr)

User; Administrator

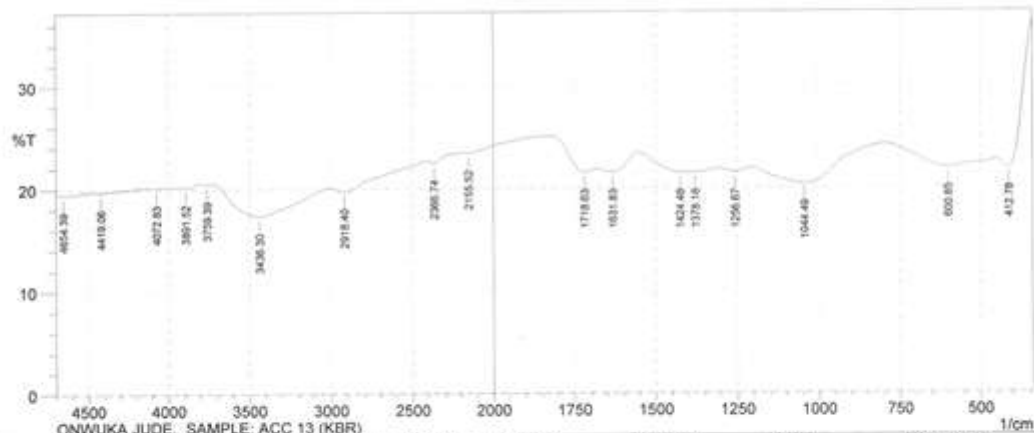
No. of Scans;
Date/Time; 6/10/2013 10:51:38 AM
Resolution;

Appendix 12: Spectrograph of Acetylated Corn cob (sample 13)



FTIR ANALYSIS RESULT NARICT,ZARIA

FTIR- 8400S FOURIER TRANSFORM INFRARED SPECTROPHOTOMETER



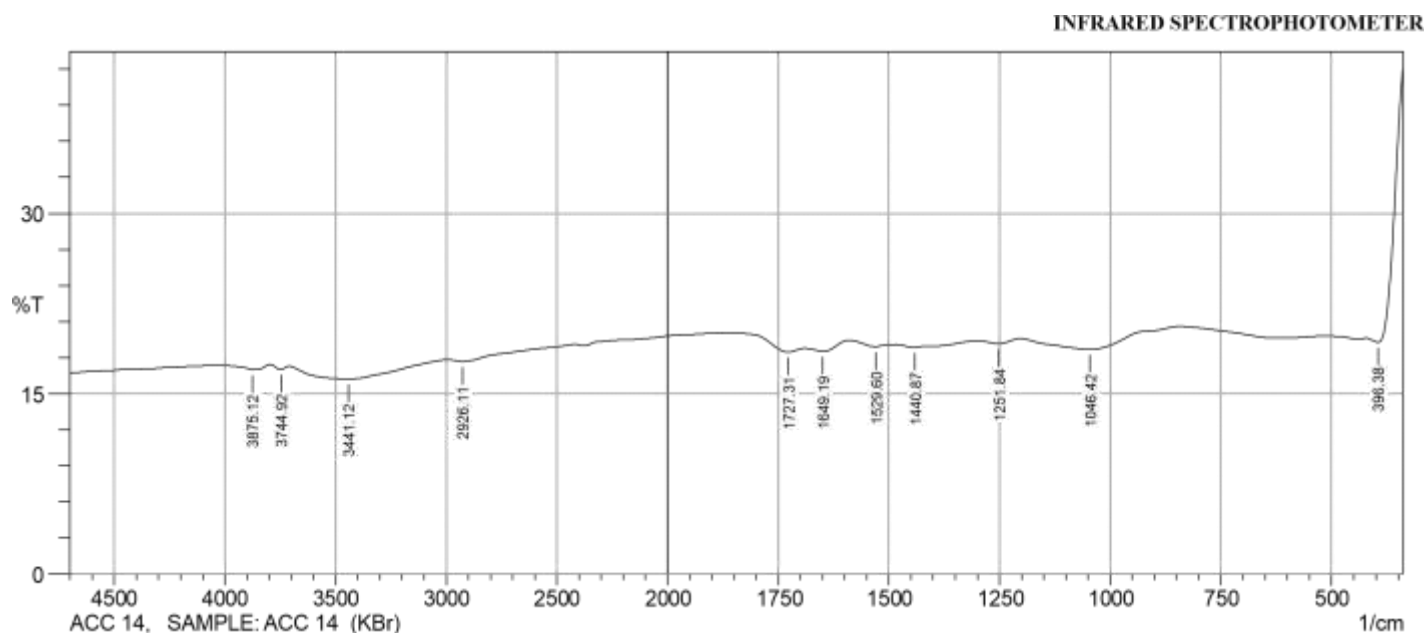
Peak	Intensity	Corr. Intensity	Base (H)	Base (L)	Area	Corr. Area
1	412.78	21.847	5.491	451.36	68.318	5.689
2	600.85	21.889	1.428	794.7	220.736	4.809
3	1044.49	20.369	2.444	1205.55	270.467	9.125
4	1256.67	21.479	0.368	1308.75	67.881	0.406
5	1378.18	21.494	0.052	1389.76	53.228	0.069
6	1424.48	21.464	0.437	1550.62	104.957	1.031
7	1631.83	21.522	0.873	1677.16	82.133	1.18
8	1718.63	21.511	1.159	1831.47	97.958	1.395
9	2155.52	23.42	0.174	2190.24	220.831	0.693
10	2366.74	22.459	0.38	2413.99	142.187	0.421
11	2918.4	19.689	0.771	3007.12	400.555	3.281
12	3436.3	17.305	3.059	3720.81	520.669	27.293
13	3759.39	20.456	0.103	3798.93	53.094	0.089
14	3891.52	20.147	0.208	3965.78	115.04	0.429
15	4072.83	20.114	0.047	4122.02	108.061	0.094
16	4419.06	19.688	0.112	4467.29	241.348	0.298
17	4654.39	19.428	0.116	4700.68	164.696	0.298

Comment:
ONWUKA JUDE, SAMPLE: ACC 13 (KBR)

User; Administrator

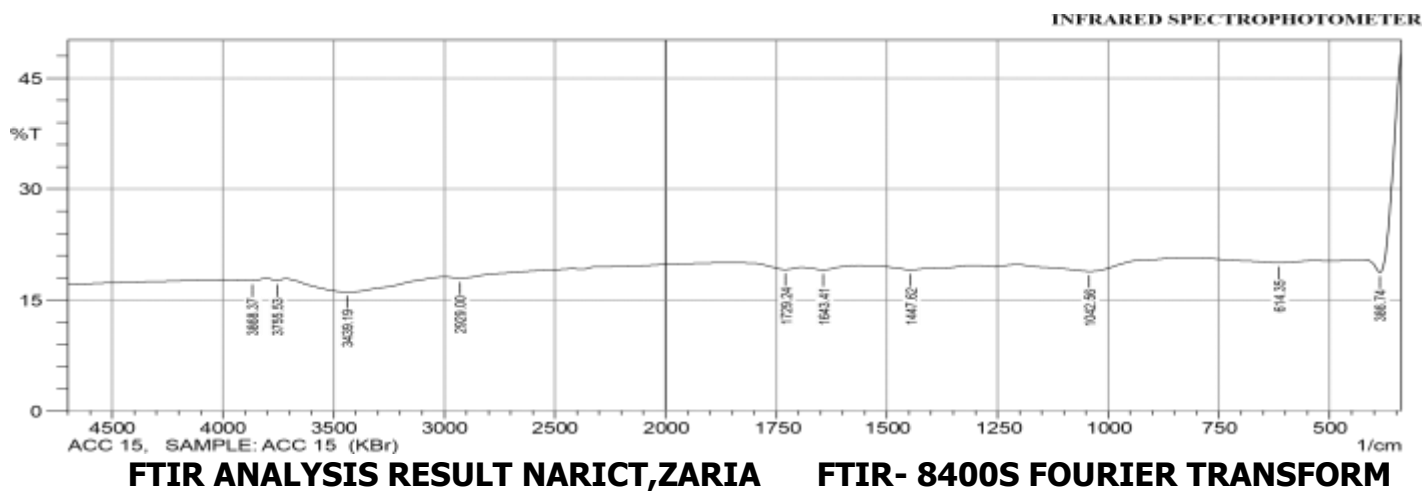
No. of Scans;
Date/Time; 6/10/2013 10:18:55 AM
Resolution;

Appendix 13: Spectrograph of Acetylated Corn cob (sample 14)



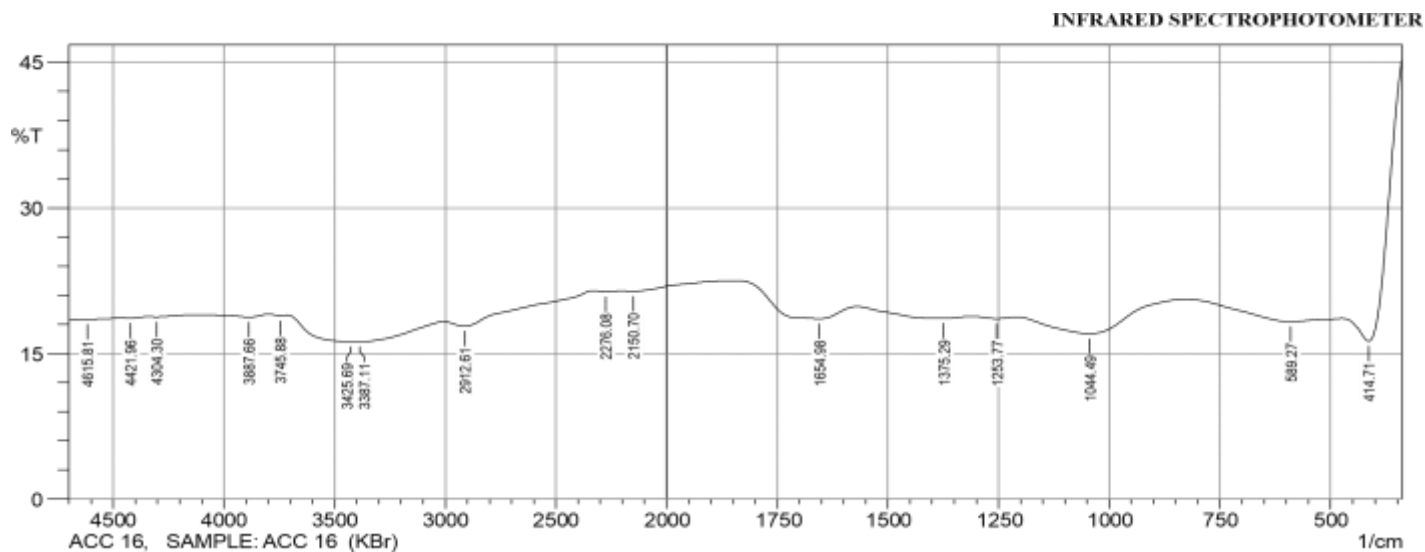
	Peak	Intensity	Corr. Intensity	Base (H)	Base (L)	Area	Corr. Area
1	396.38	19.29	7.44	422.42	339.48	51.48	6.63
2	1046.42	18.66	1.37	1202.66	842.92	255.92	5.11
3	1251.84	19.16	0.34	1299.10	1202.66	68.85	0.36
4	1440.87	18.85	0.01	1442.80	1414.83	20.23	-0.01
5	1529.60	18.91	0.29	1588.43	1499.7	63.77	0.28
6	1649.19	18.53	0.50	1688.73	1588.43	72.69	0.58
7	1727.31	18.44	0.62	1840.15	1692.59	105.67	0.55
8	2926.11	17.68	0.29	2990.73	2420.74	419.32	1.10
9	3441.12	16.21	0.16	3480.66	2990.73	377.98	1.13
10	3744.92	17.02	0.01	3745.88	3708.27	28.79	-0.01
11	3875.12	16.99	0.03	3921.41	3869.33	39.96	0.02

Appendix 14: Spectrograph of acetylated corn cob (sample 15)



	Peak	Intensity	Corr. Intensity	Base (H)	Base (L)	Area	Corr. Area
1	386.74	18.71	12.19	414.71	339.48	45.264	7.53
2	614.35	20.02	0.41	817.85	533.34	196.947	1.148
3	1042.56	18.86	1.30	1205.55	817.85	273.257	4.199
4	1447.62	19.06	0.09	1478.49	1438.94	28.383	0.046
5	1643.41	19.06	0.43	1689.70	1579.75	78.55	0.50
6	1729.24	19.10	0.45	1819.90	1694.52	88.98	0.48
7	2929.00	17.93	0.31	2998.44	2416.89	424.78	0.99
8	3439.19	16.05	0.01	3584.82	3437.26	116.15	0.39
9	3755.53	17.63	0.04	3771.92	3748.78	17.43	0.01
10	3868.37	17.62	0.01	3870.30	3856.80	10.17	0.00

Appendix 15: Spectrograph of Acetylated corn Cob sample 16

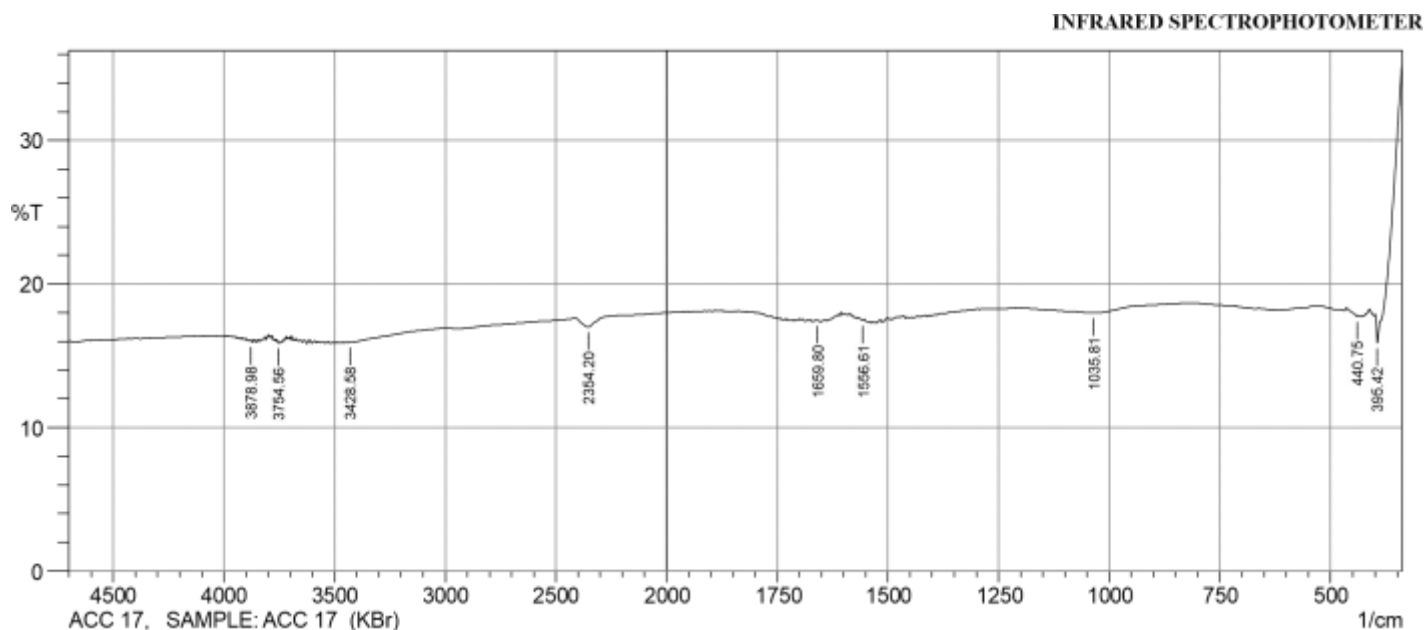


FTIR ANALYSIS RESULT NARICT,ZARIA FTIR- 8400S FOURIER TRANSFORM

	Peak	Intensity	Corr. Intensity	Base (H)	Base (L)	Area	Corr. Area
1	414.71	16.26	13.97	472.58	339.48	86.94	15.66
2	589.27	18.26	0.99	828.45	473.54	255.18	3.76
3	1044.49	17.03	2.52	1208.44	829.42	277.96	10.18
4	1253.77	18.58	0.21	1308.75	1209.41	72.37	0.24
5	1375.29	18.62	0.46	1569.14	1309.71	187.33	2.07
6	1654.98	18.57	2.10	1843.04	1570.11	191.94	7.72
7	2150.70	21.40	0.20	2204.71	1844.01	238.13	0.78
8	2276.08	21.35	0.10	2330.09	2205.67	83.31	0.12
9	2912.61	17.79	0.92	3006.16	2331.05	479.63	4.91
10	3387.11	16.18	0.12	3410.26	3007.12	310.16	2.02

11	3425.69	16.18	0.13	3713.09	3411.22	232.63	4.19
12	3745.88	18.88	0.10	3797.96	3714.06	60.63	0.10
13	3887.66	18.74	0.29	4144.20	3798.93	249.88	0.94
14	4304.30	18.76	0.06	4343.84	4145.16	143.98	0.14
15	4421.96	18.62	0.09	4468.25	4344.8	89.94	0.12
16	4615.81	18.50	0.04	4644.74	4469.21	128.40	0.15

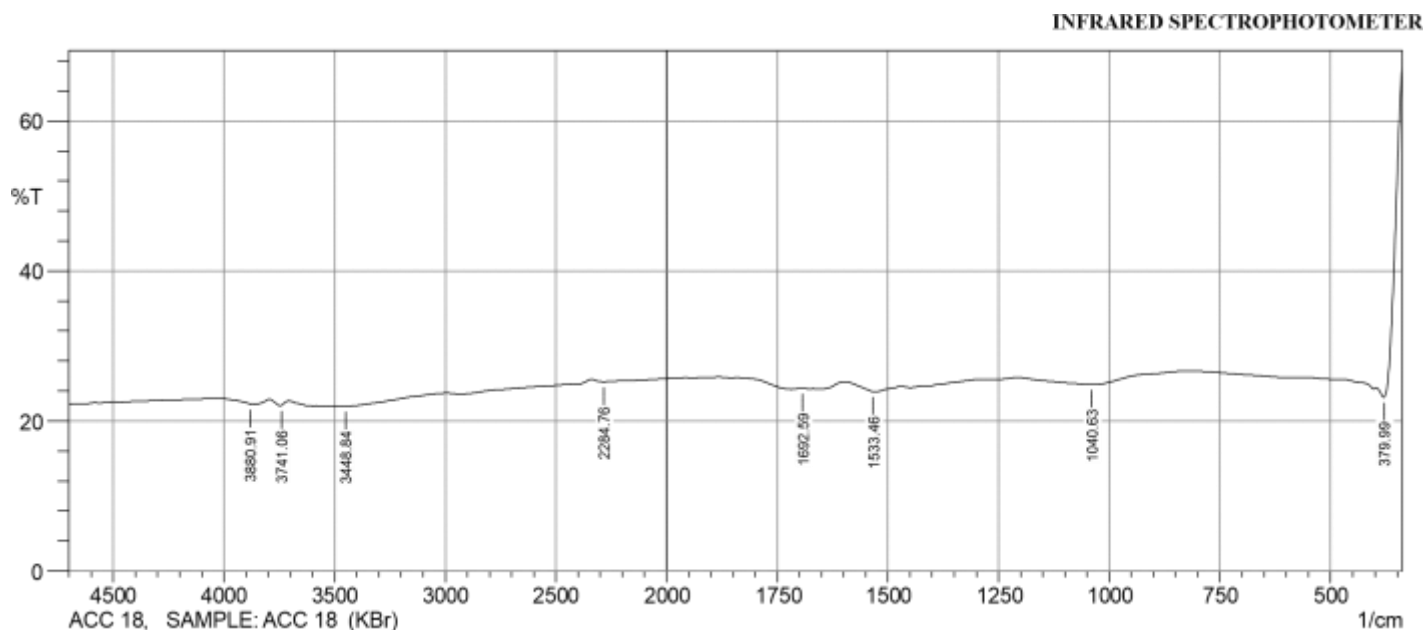
Appendix 16: Spectrograph of Acetylated Corn Cob (Sample 17)



FTIR ANALYSIS RESULT NARICT,ZARIA FTIR- 8400S FOURIER TRANSFORM

	Peak	Intensity	Corr. Intensity	Base (H)	Base (L)	Area	Corr. Area
1	395.42	15.92	1.83	399.28	388.67	8.21	0.23
2	440.75	17.75	0.13	462.93	437.86	18.66	0.03
3	1035.81	17.99	0.49	1204.59	862.21	252.86	1.78
4	1556.61	17.47	0.11	1563.36	1552.75	8.03	0.02
5	1659.80	17.44	0.05	1662.69	1656.91	4.38	0.00
6	2354.20	17.00	0.69	2413.99	2196.99	164.19	1.17
7	3428.58	15.93	0.01	3430.51	3418.94	9.23	0.00
8	3754.56	15.92	0.04	3758.42	3753.60	3.84	0.00
9	3878.98	16.00	0.05	3883.80	3877.05	5.36	0.00

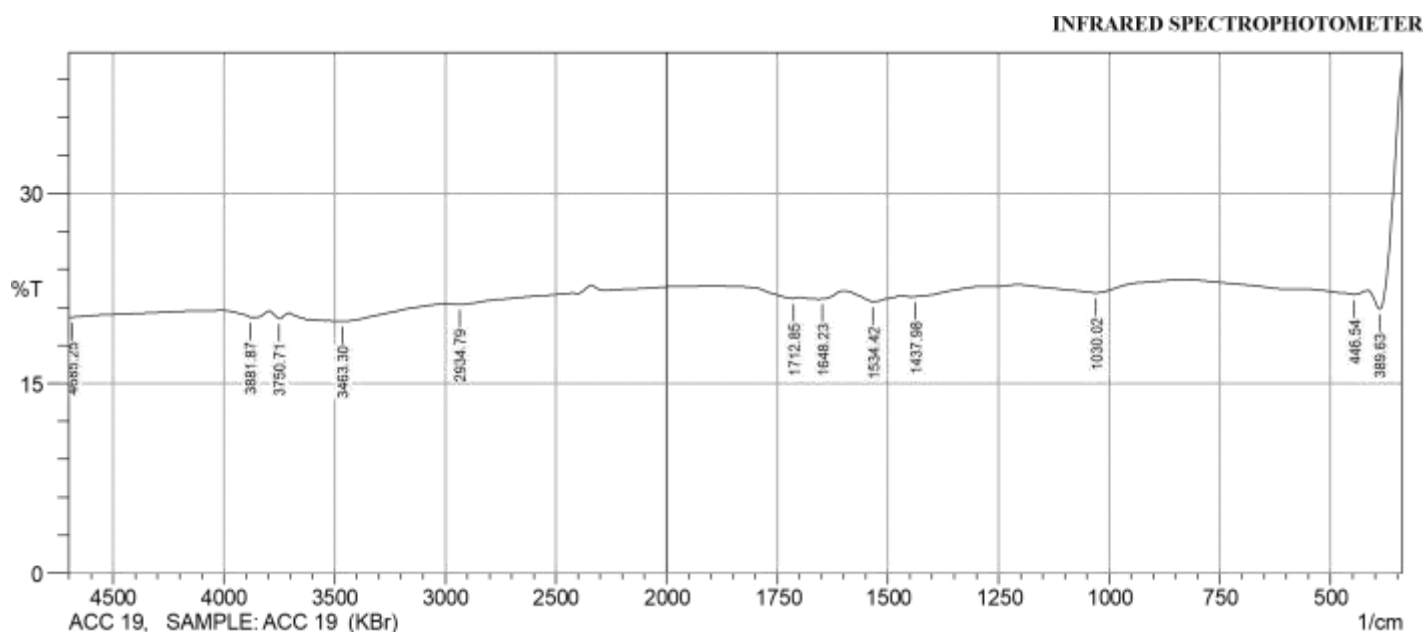
APPENDIX 17: Spectrograph of Acetylated Corn cob (sample 18)



FTIR ANALYSIS RESULT NARICT,ZARIA FTIR- 8400S FOURIER TRANSFORM

	Peak	Intensity	Corr. Intensity	Base (H)	Base (L)	Area	Corr. Area
1	379.99	23.19	14.03	397.35	339.48	27.90	5.18
2	1040.63	24.83	1.33	1205.55	823.63	225.81	3.77
3	1533.46	23.92	0.08	1595.18	1530.57	39.379	-0.01
4	1692.59	24.34	0.00	1693.56	1690.66	1.78	0.00
5	2284.76	25.22	0.37	2337.80	1955.88	226.96	1.39
6	3448.84	21.97	0.15	3481.63	2991.69	314.59	0.43
7	3741.06	22.08	0.019	3742.03	3705.38	23.78	-0.03
8	3880.91	22.24	0.08	3915.63	3875.12	26.32	0.012

Appendix 18: Spectrograph of Acetylated Corn cob (sample 19)

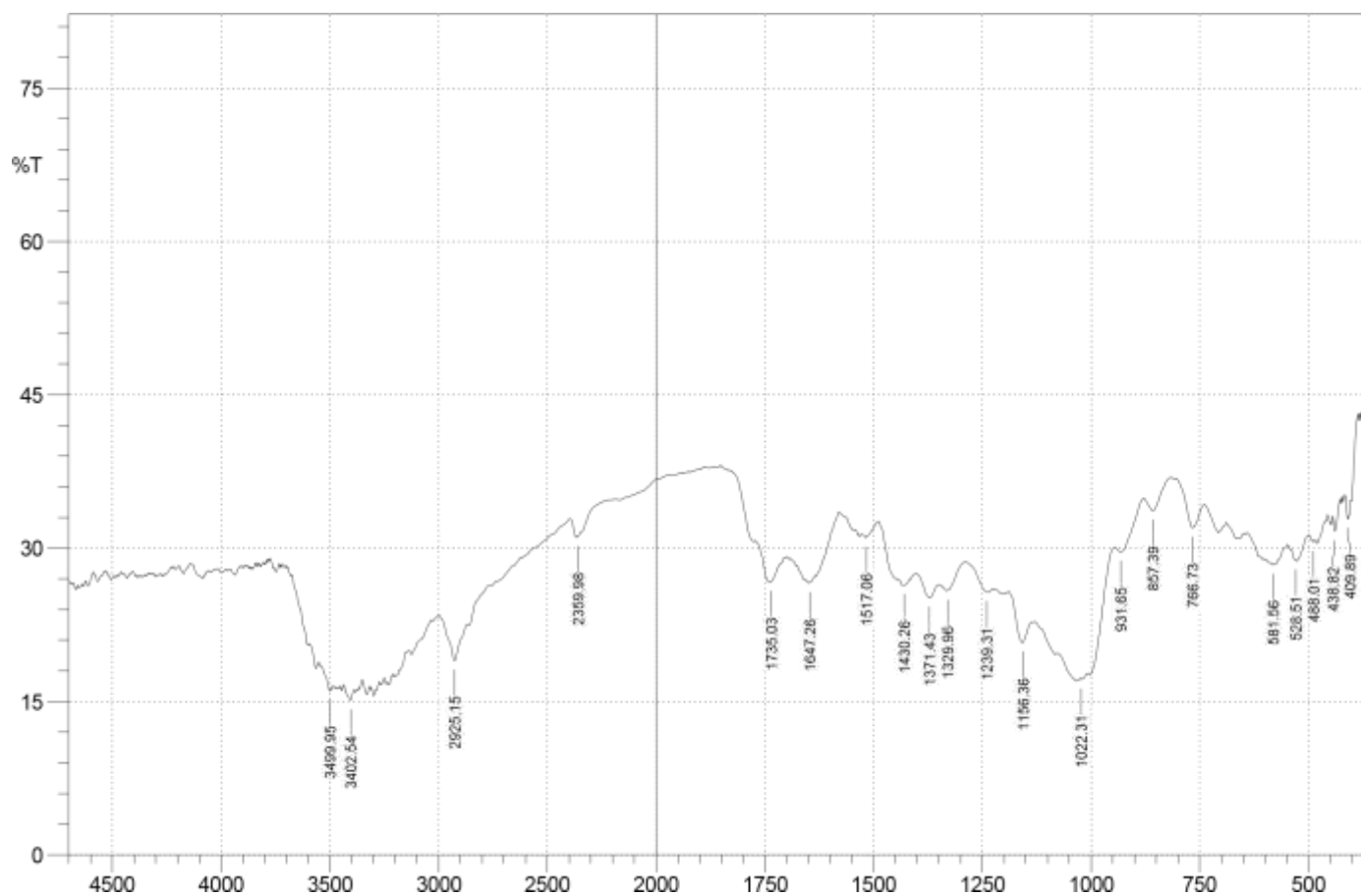


FTIR ANALYSIS RESULT NARICT,ZARIA FTIR- 8400S FOURIER TRANSFORM

	Peak	Intensity	Corr. Intensity	Base (H)	Base (L)	Area	Corr. Area
1	389.63	20.85	7.59	415.67	339.48	45.11	5.23
2	446.54	22.01	0.32	560.34	420.50	91.30	0.39
3	1030.02	22.16	0.83	1204.59	832.31	240.05	2.42
4	1437.98	21.85	0.00	1438.94	1405.19	22.25	-0.01
5	1534.42	21.44	0.55	1597.11	1491.02	70.23	0.55
6	1648.23	21.66	0.04	1651.12	1597.11	35.56	0.03
7	1712.85	21.71	0.18	1837.26	1696.45	92.11	0.11
8	2934.79	21.23	0.16	2990.73	2421.71	377.85	0.45

9	3463.30	19.91	0.00	3473.91	3461.38	8.79	0.00
10	3750.71	20.13	0.01	3792.18	3749.74	29.30	0.02
11	3881.87	20.22	0.05	3913.70	3876.08	26.02	0.01
12	4685.25	20.24	0.01	4695.86	4436.42	179.26	0.01

Appendix 19: Spectrograph of Acetylated Corn cob (sample 21)



NAME: NWADIOGBU ONYEBUCHI,

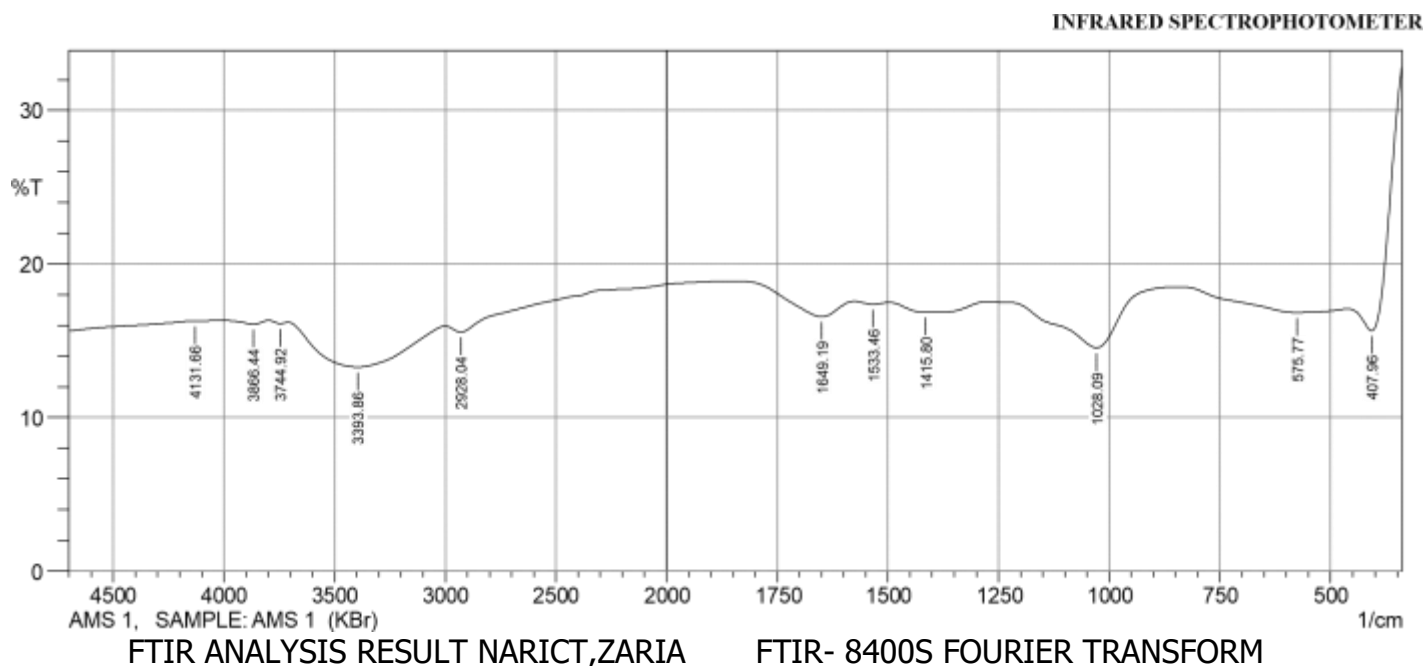
SAMPLE: ACC21 (KBr)

1/

No.	Peak	Intensity	Corr. Intensity	Base (H)	Base (L)	Area	Corr. Area
1	409.89	32.84	2.12	416.64	402.17	6.80	0.19
2	438.82	31.63	2.03	443.64	427.25	7.91	0.23
3	488.01	30.61	0.23	490.90	483.18	3.96	0.02
4	528.51	28.80	0.11	538.16	527.55	5.69	0.04
5	581.56	28.38	0.14	586.38	578.66	4.21	0.01
6	766.73	32.00	3.37	803.38	738.76	30.30	1.25

7	857.39	33.65	1.93	878.60	817.85	27.72	0.66
8	931.65	29.65	0.03	945.15	930.68	7.60	0.01
9	1022.31	17.16	0.11	1025.20	1019.41	4.42	0.01
10	1156.36	20.76	3.08	1189.15	1138.04	32.96	1.48
11	1239.31	25.69	0.14	1287.53	1237.38	28.31	-0.09
12	1329.96	25.85	1.29	1349.25	1287.53	35.13	0.55
13	1371.43	25.13	1.79	1399.40	1349.25	29.28	0.74
14	1430.26	26.36	0.11	1432.19	1415.80	9.44	0.04
15	1517.06	31.04	0.35	1521.89	1500.67	10.68	0.06
16	1647.26	26.57	0.21	1649.19	1632.80	9.35	0.03
17	1735.03	26.68	0.09	1735.99	1721.53	8.18	0.03
18	2359.98	31.10	0.07	2361.91	2342.62	9.72	0.00
19	2925.15	18.96	3.845	2983.98	2869.21	77.81	4.14
20	3402.54	15.09	0.408	3408.33	3388.08	16.38	0.09
21	3499.95	16.10	0.274	3513.45	3497.06	12.80	0.07

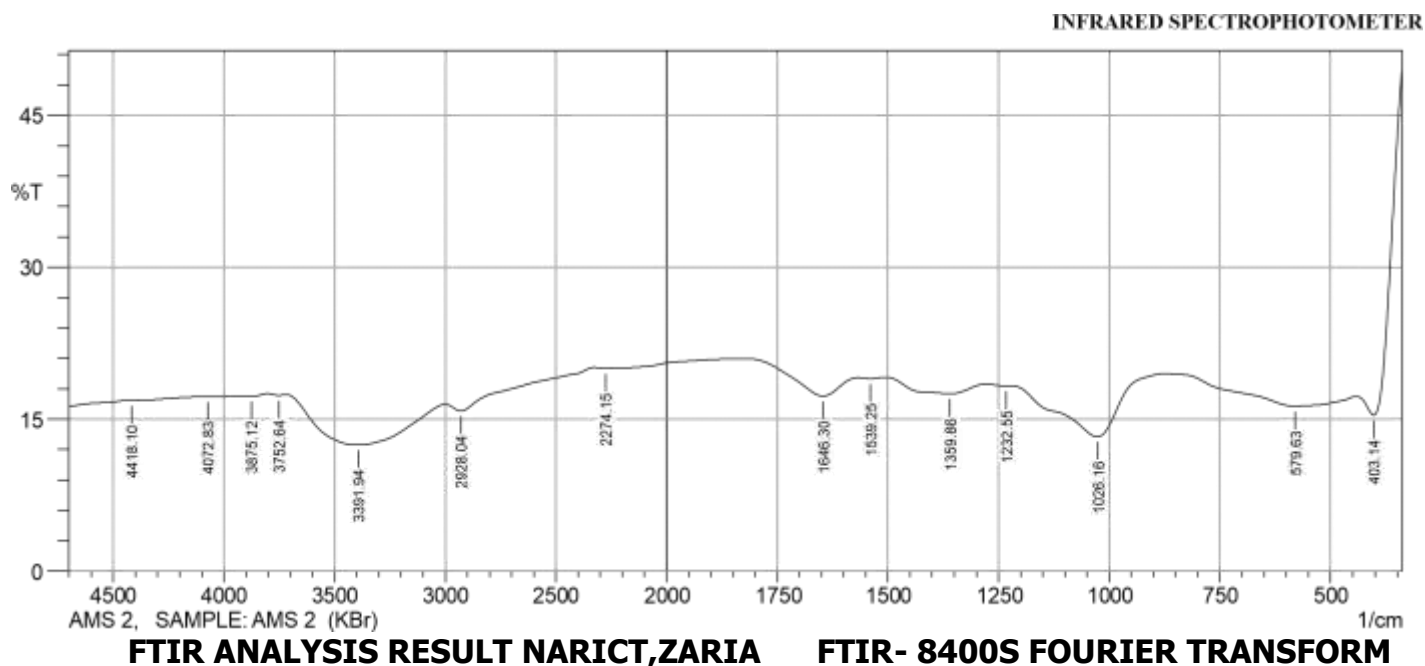
Appendix 20: Spectrograph of Acetylated Mango kernel (sample 1)



	Peak	Intensity	Corr. Intensity	Base (H)	Base (L)	Area	Corr. Area
1	407.96	15.65	8.27	460.04	339.48	85.83	10.63
2	575.77	16.84	0.68	837.13	461.00	285.94	3.79
3	1028.09	14.54	3.54	1272.1	838.10	336.63	13.70
4	1415.8	16.85	0.67	1495.85	1273.06	170.84	2.34
5	1533.46	17.37	0.16	1574.93	1496.81	59.23	0.16
6	1649.19	16.57	1.36	1843.04	1575.89	201.18	3.68
7	2928.04	15.56	0.57	2999.41	1844.01	871.45	1.35
8	3393.86	13.28	2.80	3709.24	3000.37	597.60	34.81
9	3744.92	16.12	0.12	3798.93	3710.20	70.15	0.15
10	3866.44	16.08	0.25	4012.07	3799.89	167.62	0.60

11	4131.66	16.27	0.01	4151.91	4013.03	109.43	0.02
----	---------	-------	------	---------	---------	--------	------

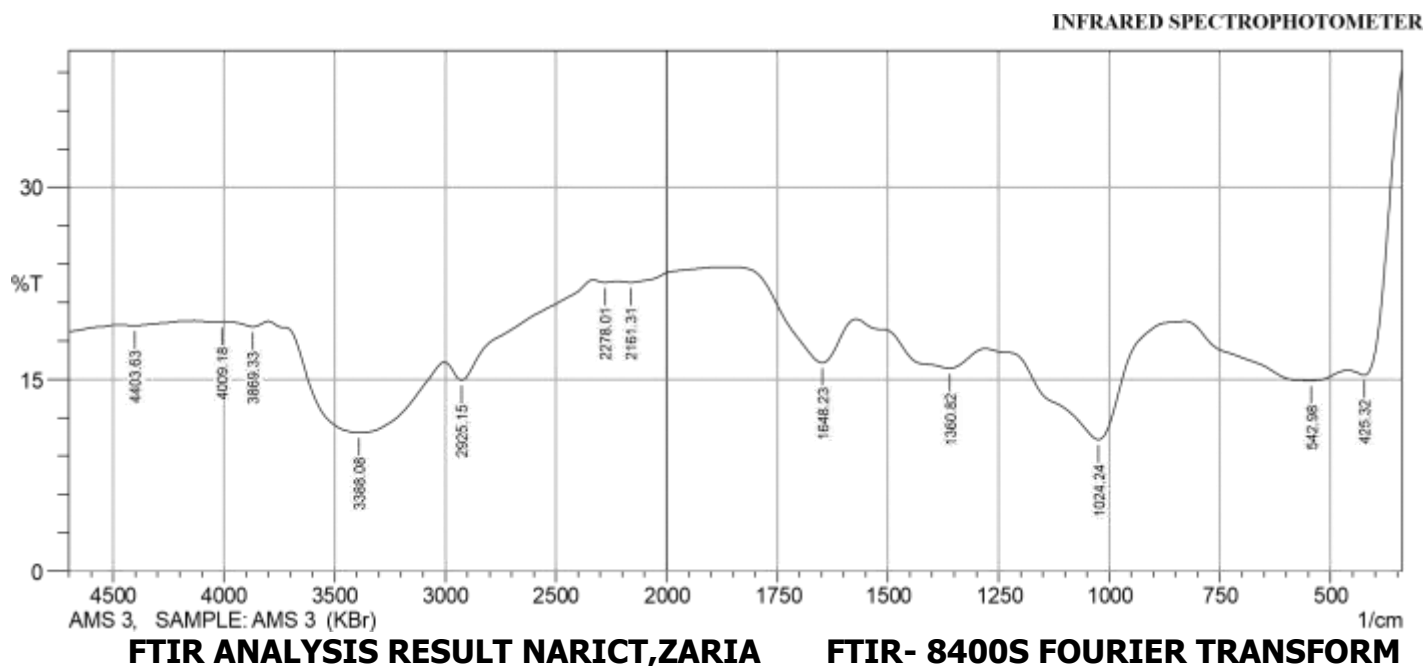
Appendix 21: Spectrograph of Acetylated Mango kernel (sample 2)



	Peak	Intensity	Corr. Intensity	Base (H)	Base (L)	Area	Corr. Area
1	403.14	15.39	14.05	441.71	339.48	66.78	12.40
2	579.63	16.28	1.68	873.78	442.68	326.47	8.99
3	1026.16	13.27	5.71	1224.84	874.75	274.88	21.51
4	1232.55	18.30	0.02	1276.92	1225.80	37.63	0.03
5	1359.86	17.51	1.20	1504.53	1277.88	168.70	4.20
6	1539.25	19.01	0.11	1566.25	1505.49	43.73	0.08
7	1646.30	17.29	2.39	1826.65	1567.21	186.79	5.63
8	2274.15	20.00	0.20	2326.23	1827.61	344.33	1.67

9	2928.04	15.81	1.06	2999.41	2327.19	500.18	3.04
10	3391.94	12.46	4.54	3718.88	3000.37	610.93	57.04
11	3752.64	17.36	0.11	3801.82	3719.85	62.22	0.12
12	3875.12	17.26	0.12	3919.48	3802.79	88.81	0.21
13	4072.83	17.22	0.01	4099.83	3920.45	136.92	0.04
14	4418.10	16.85	0.01	4426.78	4100.80	250.63	0.14

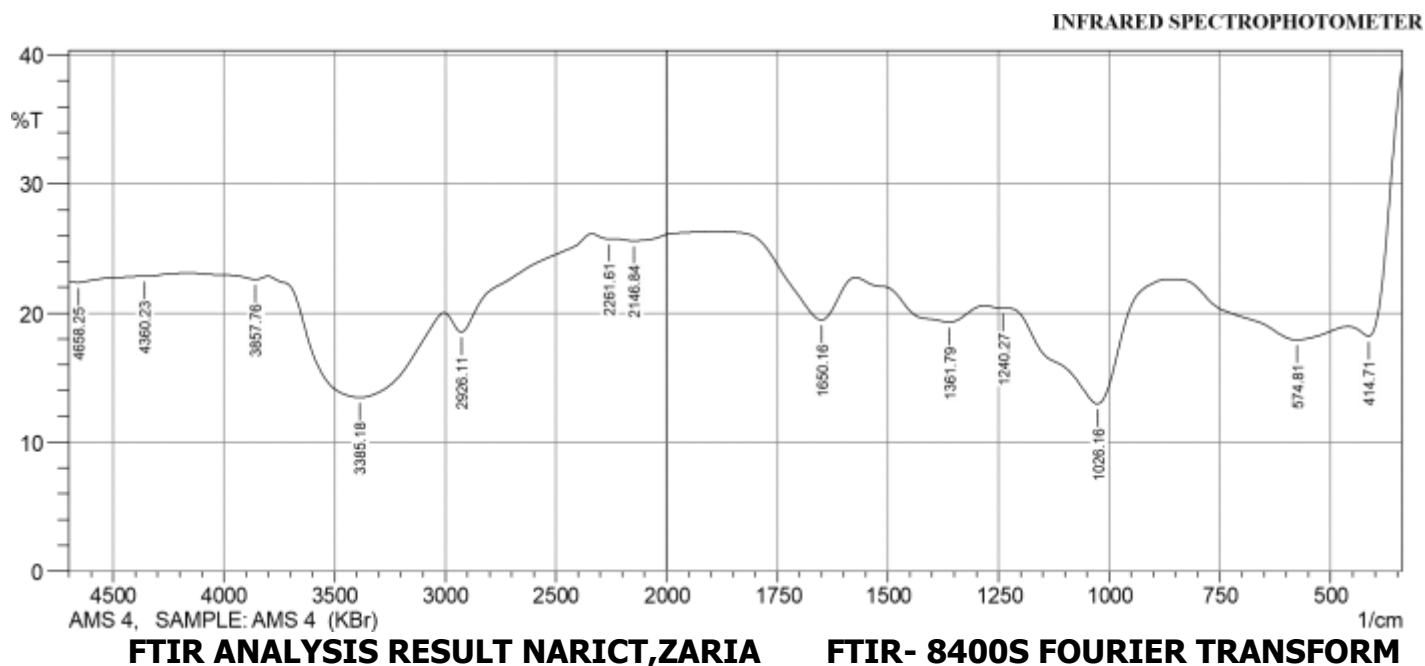
Appendix 22: Spectrograph of Acetylated Mango kernel (sample 3)



	Peak	Intensity	Corr. Intensity	Base (H)	Base (L)	Area	Corr. Area
1	425.32	15.32	7.04	459.07	339.48	81.75	9.62
2	542.98	14.90	1.67	828.45	460.04	290.54	11.83
3	1024.24	10.28	8.33	1278.85	829.42	369.78	39.82
4	1360.82	15.86	2.18	1572.04	1279.81	222.90	8.78
5	1648.23	16.28	4.44	1872.94	1573.00	209.87	11.29
6	2161.31	22.57	0.27	2221.11	1873.91	221.15	0.98
7	2278.01	22.57	0.14	2331.05	2222.07	70.32	0.15

8	2925.15	14.93	2.16	3002.30	2332.02	485.54	6.64
9	3388.08	10.81	7.07	3798.93	3003.27	691.18	95.97
10	3869.33	19.11	0.38	3967.71	3799.89	119.90	0.70
11	4009.18	19.43	0.05	4132.63	3968.67	116.49	0.11
12	4403.63	19.20	0.14	4475.00	4133.59	243.41	0.44

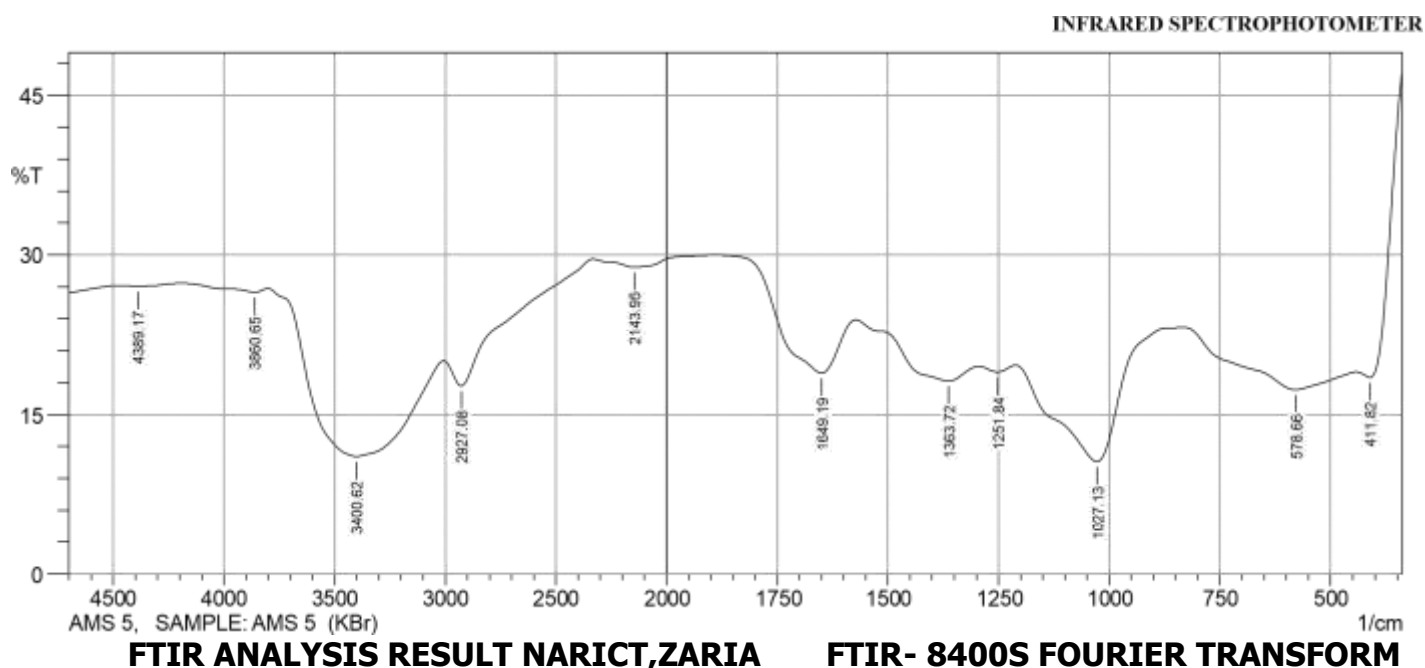
Appendix 23: Spectrograph of Acetylated Mango kernel (sample 4)



	Peak	Intensity	Corr. Intensity	Base (H)	Base (L)	Area	Corr. Area
1	414.71	18.21	8.30	460.04	339.48	77.61	9.62
2	574.81	17.93	2.08	861.24	461	283.05	9.56
3	1026.16	12.97	8.65	1228.70	862.21	276.68	31.90
4	1240.27	20.37	0.05	1281.74	1229.66	35.90	0.03
5	1361.79	19.30	1.88	1572.04	1282.71	198.57	6.28
6	1650.16	19.46	4.18	1890.30	1573.00	201.77	8.72
7	2146.84	25.60	0.32	2239.43	1891.27	204.30	0.93

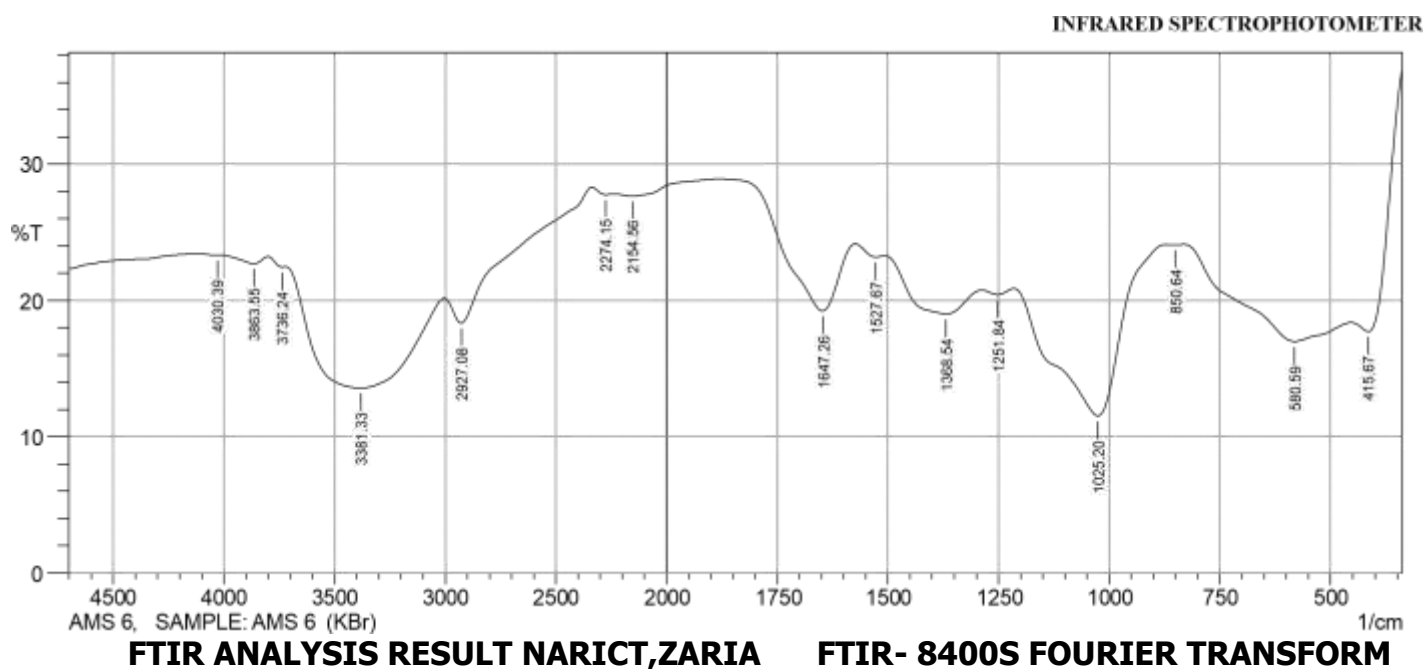
8	2261.61	25.76	0.09	2336.84	2240.39	56.6	0.12
9	2926.11	18.54	2.21	3004.23	2337.80	431.01	4.98
10	3385.18	13.45	7.92	3799.89	3005.2	620.47	88.18
11	3857.76	22.61	0.29	4160.59	3800.86	230.29	0.63
12	4360.23	22.84	0.04	4385.31	4161.56	142.91	0.06
13	4658.25	22.38	0.11	4700.68	4386.27	202.83	0.15

Appendix 24: Spectrograph of Acetylated Mango kernel (sample 5)



	Peak	Intensity	Corr. Intensity	Base (H)	Base (L)	Area	Corr. Area
1	411.82	18.47	8.76	441.71	339.48	61.71	8.36
2	578.66	17.32	3.14	832.31	442.68	279.32	15.09
3	1027.13	10.56	10.80	1210.37	833.28	293.90	41.27
4	1251.84	18.98	0.60	1293.31	1211.34	58.63	0.57
5	1363.72	18.14	2.47	1572.04	1294.28	192.70	7.79
6	1649.19	18.89	6.47	1888.37	1573.00	195.51	16.11
7	2143.95	28.83	0.94	2331.05	1889.34	235.19	2.96
8	2927.08	17.68	3.49	3006.16	2332.02	418.81	7.38
9	3400.62	11.05	12.37	3800.86	3007.12	641.69	137.97
10	3860.65	26.49	0.44	4191.46	3801.82	222.30	1.34
11	4389.17	27.04	0.15	4475.97	4192.42	160.54	0.40

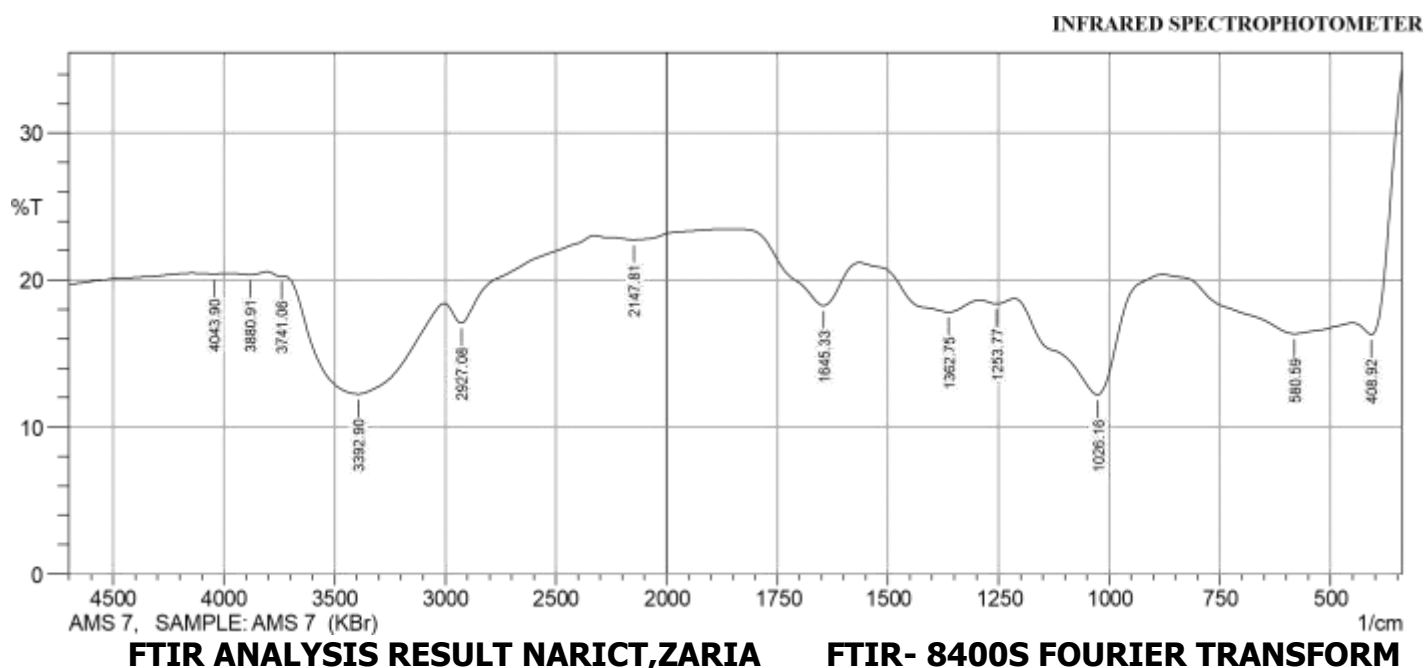
Appendix 25: Spectrograph of Acetylated Mango kernel (sample 6)



	Peak	Intensity	Corr. Intensity	Base (H)	Base (L)	Area	Corr. Area
1	415.67	17.72	6.81	453.29	339.48	74.38	8.08
2	580.59	17.00	3.32	830.38	454.25	269.71	15.25
3	850.64	24.08	0.04	869.92	831.35	23.84	0.02
4	1025.20	11.54	11.12	1214.23	870.89	265.24	42.46
5	1251.84	20.44	0.38	1286.56	1215.19	48.94	0.30
6	1368.54	19.02	2.69	1506.46	1287.53	151.93	7.92
7	1527.67	23.20	0.37	1573.00	1507.42	41.23	0.26
8	1647.26	19.24	6.06	1880.66	1573.97	189.41	13.05
9	2154.56	27.66	0.42	2234.61	1881.62	194.29	1.21
10	2274.15	27.78	0.24	2335.87	2235.57	55.57	0.22

11	2927.08	18.34	2.76	3003.27	2336.84	420.96	6.86
12	3381.33	13.58	7.81	3720.81	3004.23	571.33	89.99
13	3736.24	22.46	0.16	3799.89	3721.77	50.23	0.15
14	3863.55	22.71	0.55	4014.96	3800.86	136.58	1.04
15	4030.39	23.33	0.02	4115.27	4015.93	62.71	0.02

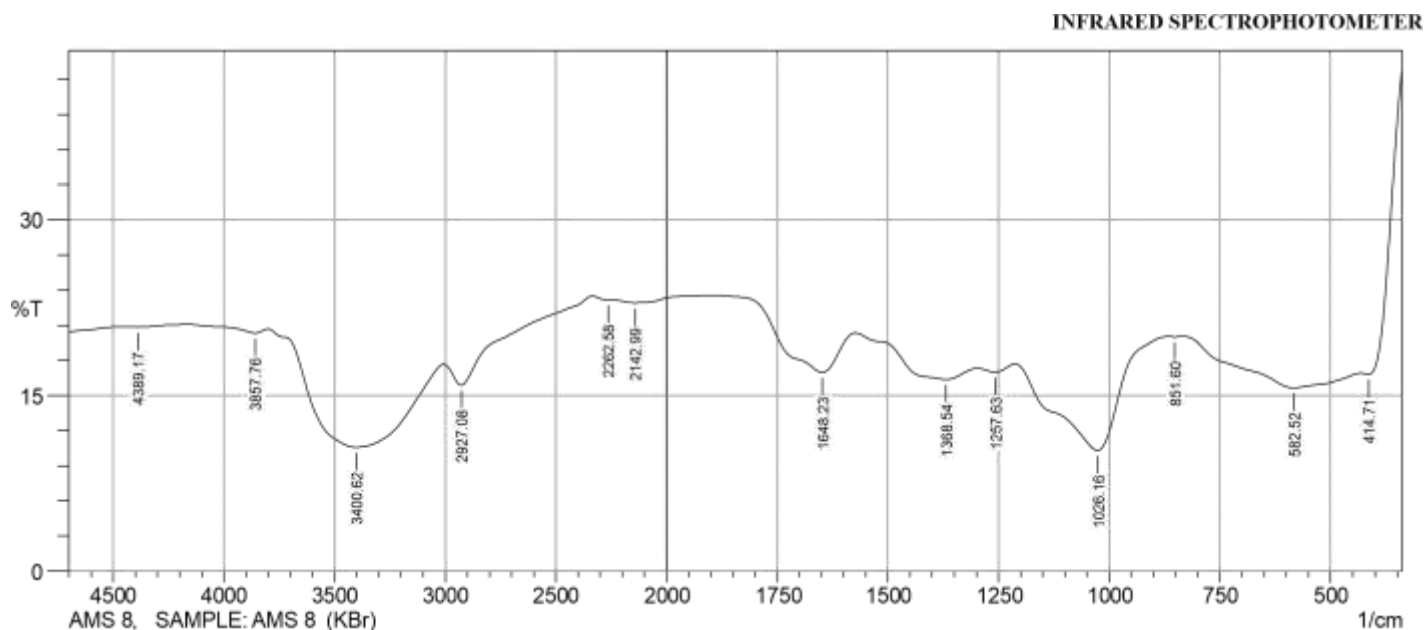
Appendix 26: Spectrograph of Acetylated Mango kernel (sample 7)



	Peak	Intensity	Corr. Intensity	Base (H)	Base (L)	Area	Corr. Area
1	408.92	16.29	7.26	450.39	339.48	76.91	8.78
2	580.59	16.35	1.73	878.60	451.36	320.32	9.00
3	1026.16	12.20	7.46	1213.27	879.57	264.98	28.43
4	1253.77	18.38	0.31	1292.35	1214.23	57.20	0.29
5	1362.75	17.82	1.47	1564.32	1293.31	195.06	4.97
6	1645.33	18.26	3.53	1866.19	1565.29	204.37	8.62
7	2147.81	22.74	0.46	2326.23	1867.16	292.92	2.03
8	2927.08	17.06	1.87	3003.27	2327.19	466.11	4.19
9	3392.90	12.25	7.15	3728.53	3004.23	602.07	84.81
10	3741.06	20.25	0.05	3803.75	3729.49	51.31	0.06
11	3880.91	20.37	0.14	3977.35	3804.72	119.06	0.27

12	4043.90	20.42	0.04	4144.20	3978.31	114.38	0.07
----	---------	-------	------	---------	---------	--------	------

Appendix 27: Spectrograph of acetylated Mango kernel (sample 8)

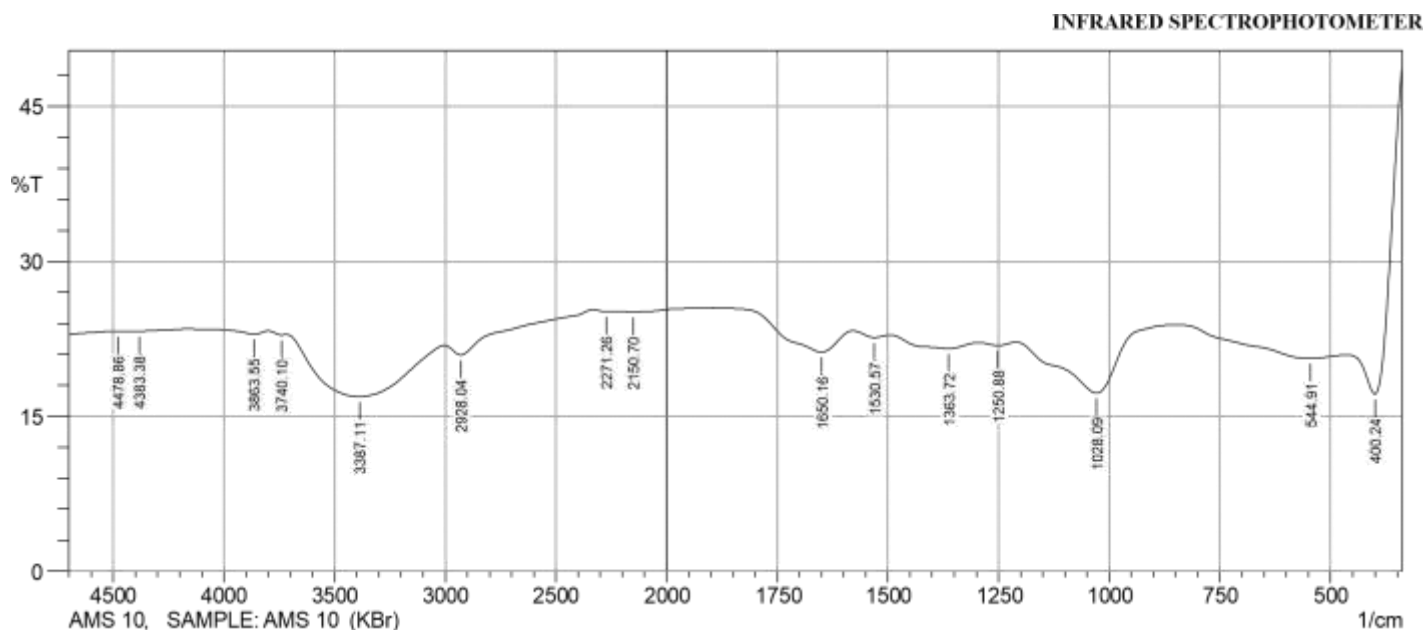


FTIR ANALYSIS RESULT NARICT,ZARIA FTIR- 8400S FOURIER TRANSFORM

	Peak	Intensity	Corr. Intensity	Base (H)	Base (L)	Area	Corr. Area
1	414.71	16.81	4.96	432.07	339.48	58.62	6.06
2	582.52	15.66	2.43	831.35	433.03	306.47	13.69
3	851.60	20.02	0.02	867.03	832.31	24.25	0.01
4	1026.16	10.31	8.65	1211.34	868.00	285.74	36.77
5	1257.63	16.99	0.51	1297.17	1212.30	64.79	0.56
6	1368.54	16.37	1.73	1573.00	1298.14	206.03	6.34
7	1648.23	16.97	4.12	1896.09	1573.97	223.46	11.73

8	2142.99	22.92	0.38	2255.83	1897.05	227.79	1.25
9	2262.58	23.18	0.02	2334.91	2256.79	49.44	0.06
10	2927.08	15.89	2.46	3005.20	2335.87	467.23	6.05
11	3400.62	10.58	8.59	3799.89	3006.16	681.50	111.10
12	3857.76	20.34	0.41	4166.38	3800.86	249.59	0.96
13	4389.17	20.84	0.09	4446.07	4167.35	189.20	0.20

Appendix 28: Spectrograph of acetylated Mango kernel (sample 10)



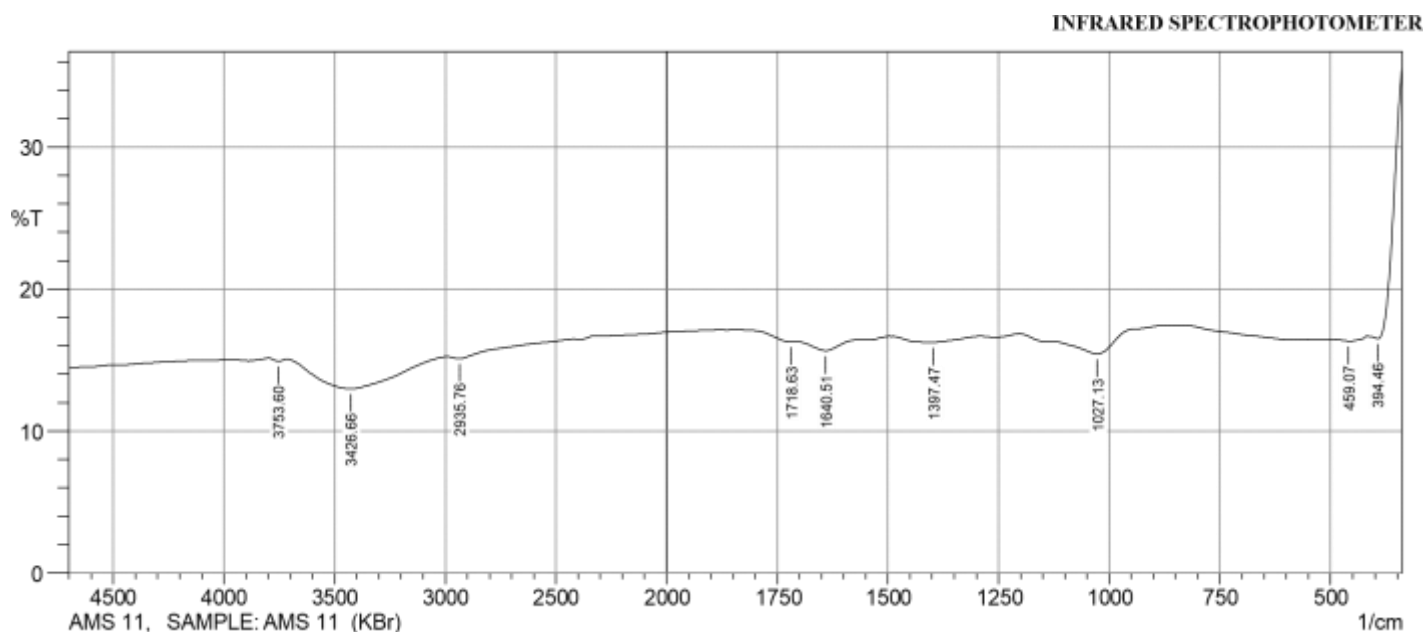
FTIR ANALYSIS RESULT NARICT,ZARIA

FTIR- 8400S FOURIER TRANSFORM

	Peak	Intensity	Corr. Intensity	Base (H)	Base (L)	Area	Corr. Area
1	400.24	17.17	17.72	461.00	339.48	76.45	16.48
2	544.91	20.61	0.98	838.10	461.97	249.28	4.53
3	1028.09	17.24	5.76	1209.41	839.06	252.44	16.17
4	1250.88	21.86	0.30	1294.28	1210.37	55.17	0.26
5	1363.72	21.56	0.83	1494.88	1295.24	131.52	2.19
6	1530.57	22.63	0.42	1578.79	1495.85	53.16	0.34
7	1650.16	21.21	2.57	1894.16	1579.75	198.33	5.99
8	2150.70	25.11	0.13	2231.71	1895.12	201.17	0.44

9	2271.26	25.14	0.08	2332.02	2232.68	59.47	0.08
10	2928.04	20.94	1.30	3003.27	2332.98	423.41	2.65
11	3387.11	16.91	5.52	3717.92	3004.23	515.56	51.55
12	3740.10	22.88	0.13	3798.93	3718.88	51.06	0.11
13	3863.55	22.95	0.35	4160.59	3799.89	228.38	0.63
14	4383.38	23.24	0.05	4425.82	4161.56	167.03	0.15
15	4478.86	23.23	0.01	4500.08	4426.78	46.45	0.01

Appendix 29: Spectrograph of acetylated Mango kernel (sample 11)

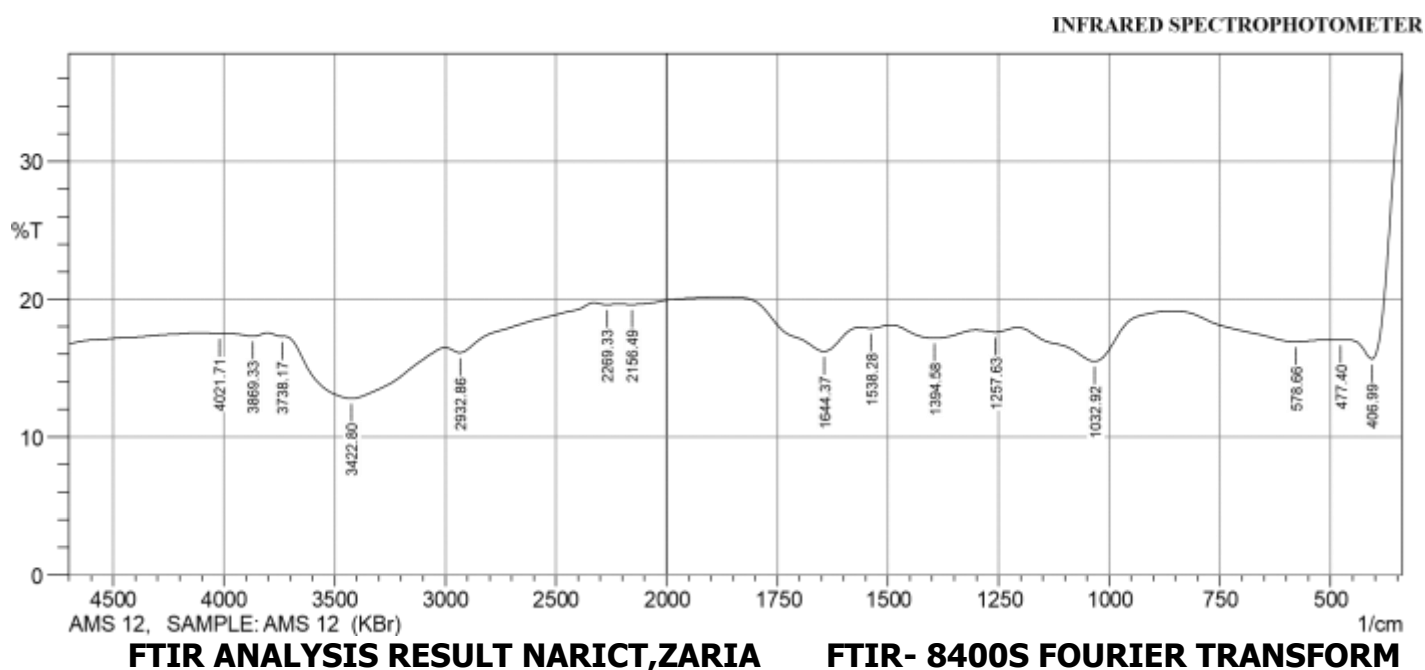


FTIR ANALYSIS RESULT NARICT,ZARIA FTIR- 8400S FOURIER TRANSFORM

	Peak	Intensity	Corr. Intensity	Base (H)	Base (L)	Area	Corr. Area
1	394.46	16.50	5.94	418.57	339.48	54.37	5.87
2	459.07	16.34	0.01	495.72	457.14	30.29	0.00
3	1027.13	15.43	1.31	1125.5	877.64	194.52	2.78
4	1397.47	16.24	0.00	1398.44	1290.42	84.67	0.02
5	1640.51	15.66	0.69	1700.31	1566.25	106.58	1.16
6	1718.63	16.28	0.06	1838.22	1711.88	97.95	-0.24
7	2935.76	15.08	0.27	2990.73	2418.82	457.57	0.01

8	3426.66	12.96	2.18	3713.09	2990.73	618.02	26.10
9	3753.60	14.90	0.21	3797.00	3713.09	69.12	0.25

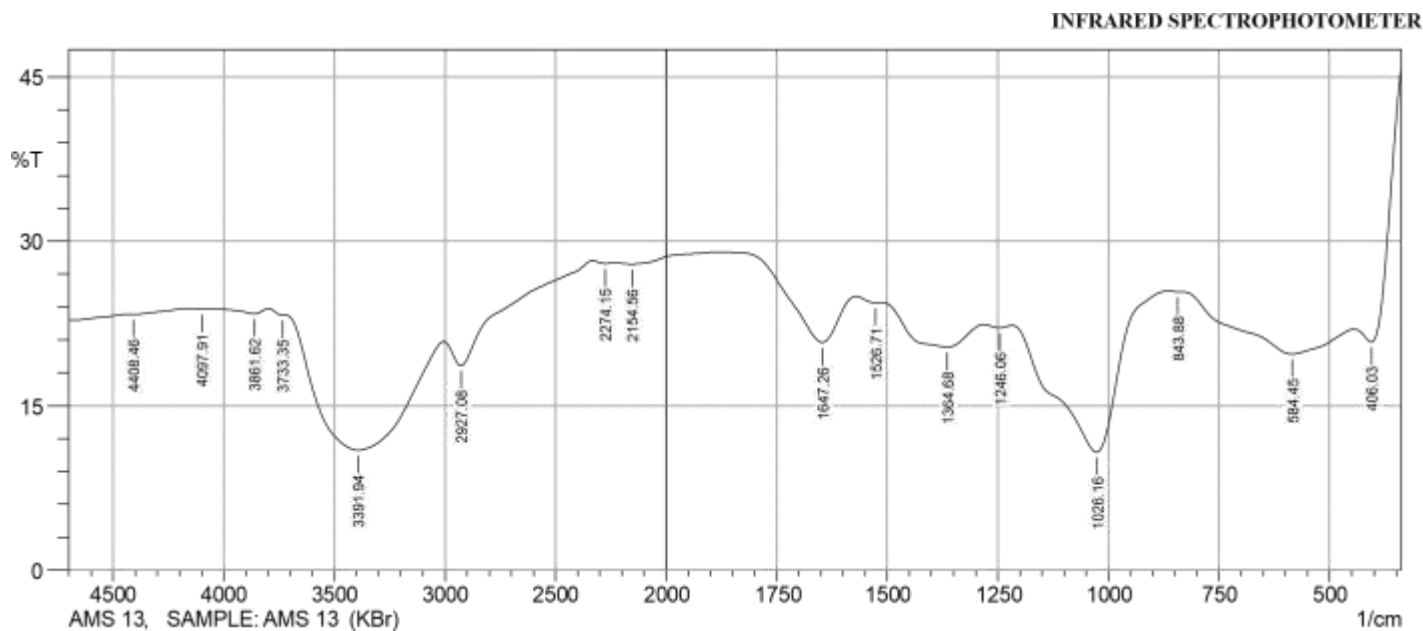
Appendix 30: Spectrograph of acetylated Mango kernel (sample 12)



	Peak	Intensity	Corr. Intensity	Base (H)	Base (L)	Area	Corr. Area
1	406.99	15.67	9.82	458.11	339.48	82.93	11.64
2	477.40	17.03	0.02	506.33	459.07	36.32	0.02
3	578.66	16.91	0.57	858.35	507.30	263.60	2.86
4	1032.92	15.49	3.06	1205.55	859.32	263.73	10.36
5	1257.63	17.62	0.23	1299.10	1206.51	69.54	0.27
6	1394.58	17.18	0.77	1491.99	1300.07	145.22	2.06
7	1538.28	17.89	0.13	1564.32	1492.95	53.19	0.12

8	1644.37	16.21	2.30	1881.62	1565.29	234.63	7.11
9	2156.49	19.62	0.12	2215.32	1882.59	233.77	0.51
10	2269.33	19.61	0.08	2327.19	2216.28	78.38	0.11
11	2932.86	16.12	0.69	2999.41	2328.16	500.30	1.84
12	3422.80	12.79	4.17	3726.60	3000.37	610.90	50.00
13	3738.17	17.30	0.04	3801.82	3727.56	56.39	0.06
14	3869.33	17.31	0.24	3998.57	3802.79	148.51	0.54
15	4021.71	17.52	0.01	4124.91	3999.53	94.80	0.01

Appendix 31: Spectrograph of Acetylated Mango kernel (sample 13)



FTIR ANALYSIS RESULT NARICT,ZARIA

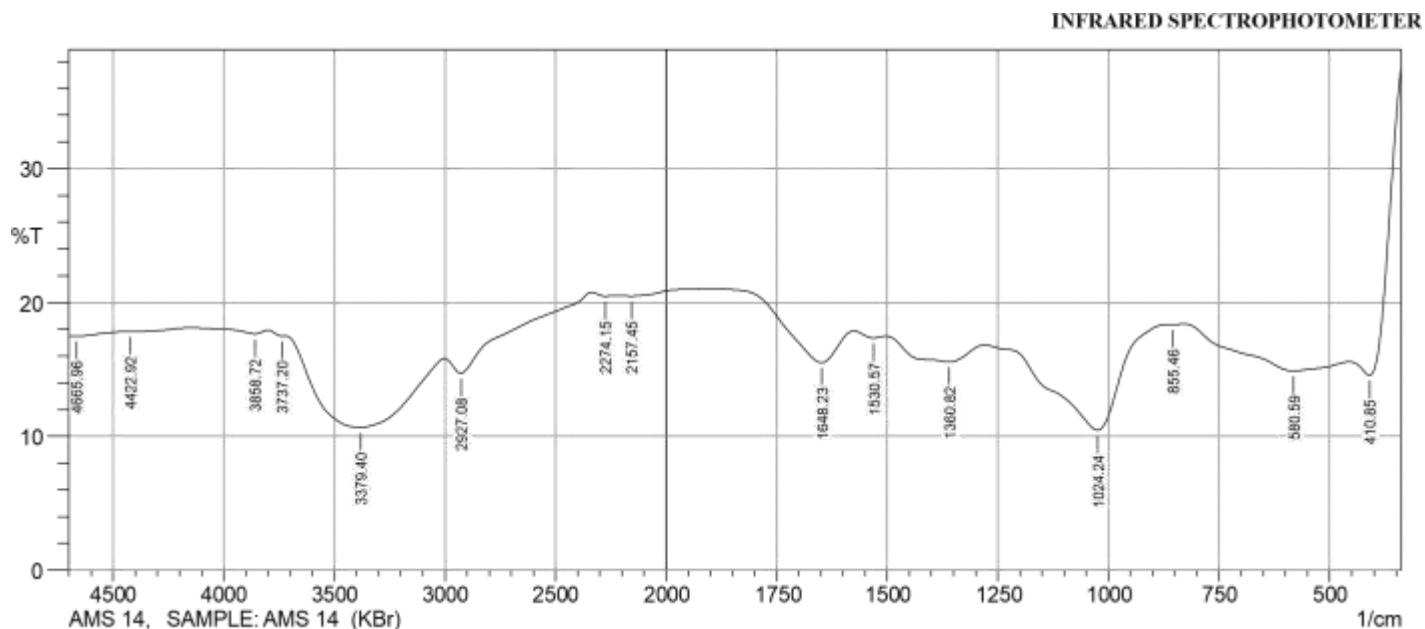
FTIR- 8400S FOURIER

TRANSFORM

	Peak	Intensity	Corr. Intensity	Base (H)	Base (L)	Area	Corr. Area
1	406.03	20.81	9.90	444.61	339.48	60.93	8.65
2	584.45	19.71	3.48	838.10	445.57	260.73	14.82
3	843.88	25.42	0.01	866.07	839.06	16.06	0.00
4	1026.16	10.76	13.27	1217.12	867.03	264.49	46.48
5	1246.06	22.11	0.25	1280.78	1218.09	40.94	0.16
6	1364.68	20.34	2.79	1512.24	1281.74	153.46	8.02
7	1526.71	24.40	0.16	1570.11	1513.21	34.67	0.11
8	1647.26	20.78	5.20	1878.73	1571.07	183.92	9.39

9	2154.56	27.92	0.31	2229.79	1879.69	191.62	0.89
10	2274.15	27.98	0.13	2332.02	2230.75	55.90	0.11
11	2927.08	18.65	3.06	3004.23	2332.98	416.82	6.14
12	3391.94	10.93	11.23	3721.77	3005.20	594.90	124.19
13	3733.35	23.27	0.09	3797.00	3722.74	46.70	0.10
14	3861.62	23.39	0.48	4080.55	3797.96	176.82	0.94
15	4097.91	23.84	0.01	4161.56	4081.51	49.83	0.01
16	4408.46	23.34	0.05	4430.64	4162.52	168.24	0.18

Appendix 32: Spectrograph of Acetylated Mango kernel (sample 14)

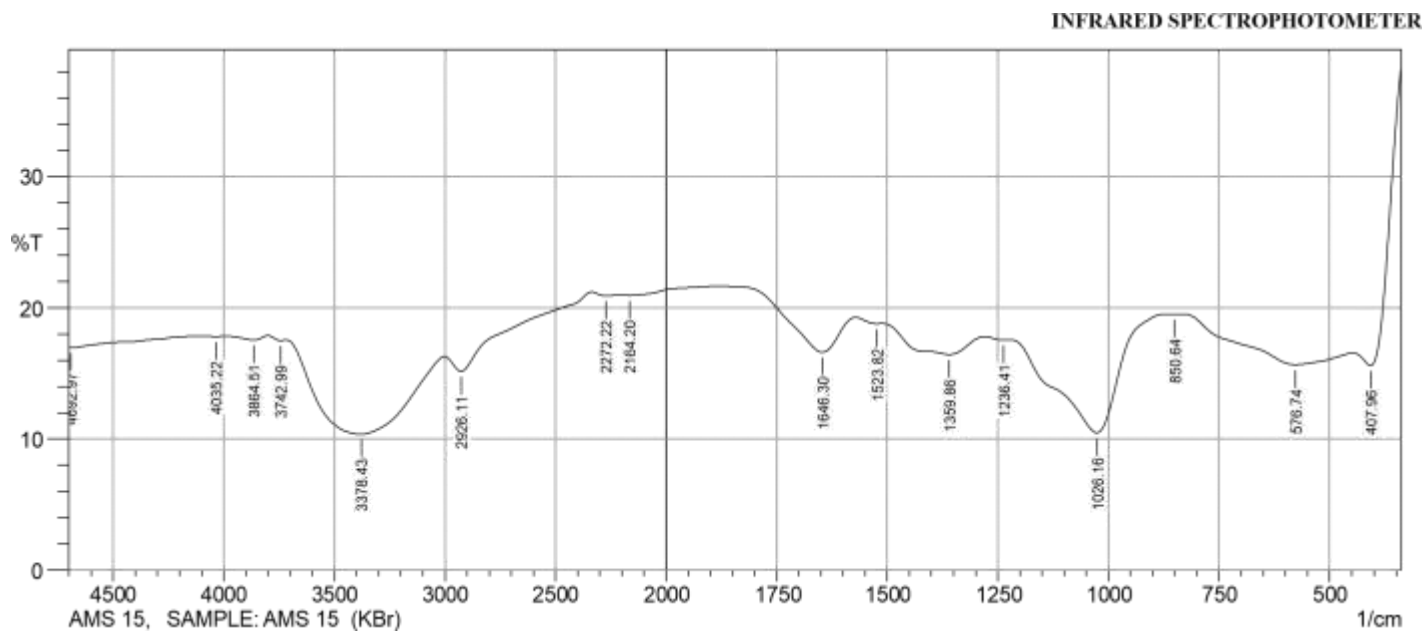


FTIR ANALYSIS RESULT NARICT,ZARIA FTIR- 8400S FOURIER TRANSFORM

	Peak	Intensity	Corr. Intensity	Base (H)	Base (L)	Area	Corr. Area
1	410.85	14.55	9.44	455.22	339.48	82.81	11.63
2	580.59	14.87	1.64	828.45	456.18	296.65	9.38
3	855.46	18.35	0.01	866.07	829.42	26.98	0.01
4	1024.24	10.45	7.31	1278.85	867.03	345.69	34.7
5	1360.82	15.55	1.52	1502.60	1279.81	176.37	5.77
6	1530.57	17.35	0.28	1574.93	1503.56	53.98	0.27
7	1648.23	15.51	3.08	1894.16	1575.89	233.67	7.91
8	2157.45	20.47	0.14	2219.18	1895.12	221.59	0.50
9	2274.15	20.47	0.17	2335.87	2220.14	79.53	0.22

10	2927.08	14.71	1.65	3001.34	2336.84	498.06	5.21
11	3379.40	10.66	6.04	3720.81	3002.30	643.06	83.35
12	3737.20	17.50	0.10	3798.93	3721.77	58.10	0.12
13	3858.72	17.65	0.32	4144.20	3799.89	257.01	0.76
14	4422.92	17.81	0.03	4449.93	4145.16	227.50	0.24
15	4665.96	17.48	0.07	4700.68	4450.89	188.29	0.22

Appendix 33: Spectrograph of Acetylated Mango kernel (sample 15)



FTIR ANALYSIS RESULT NARICT,ZARIA

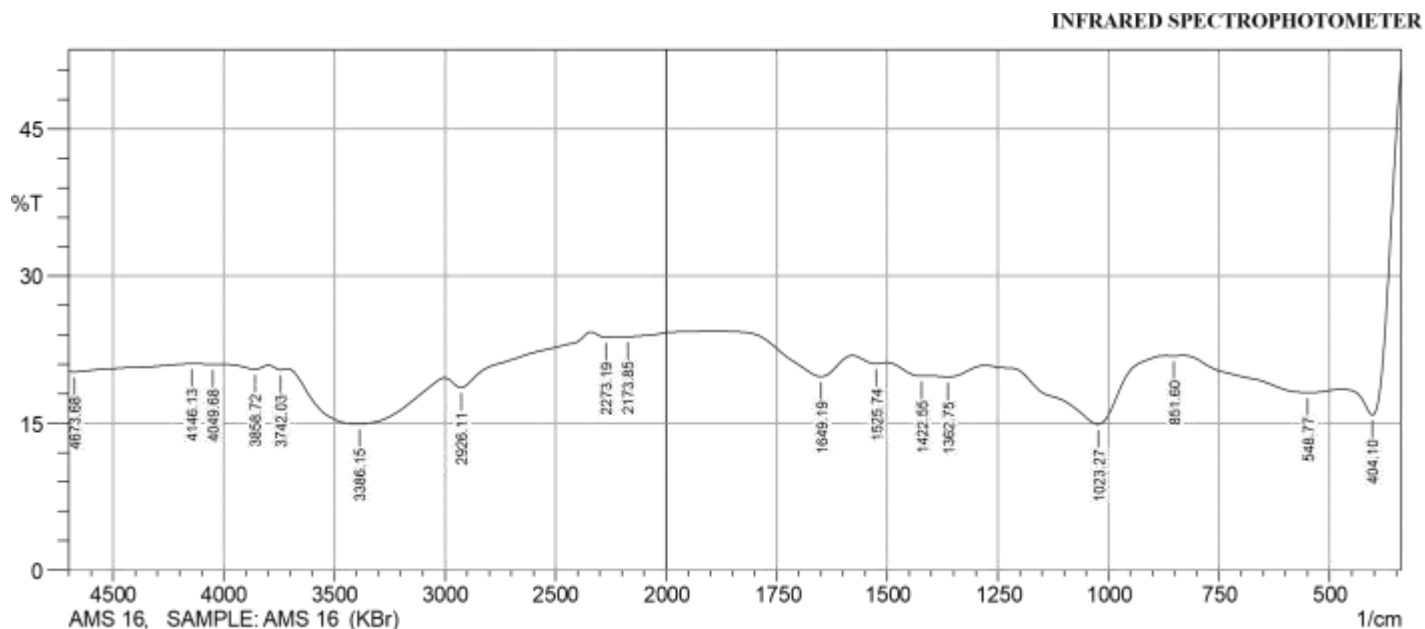
FTIR- 8400S FOURIER

TRANSFORM

	Peak	Intensity	Corr. Intensity	Base (H)	Base (L)	Area	Corr. Area
1	407.96	15.60	9.03	448.46	339.48	75.24	10.13
2	576.74	15.66	1.88	831.35	449.43	294.91	10.24
3	850.64	19.51	0.02	868.96	832.31	26.00	0.01
4	1026.16	10.48	8.17	1220.98	869.92	291.35	34.24
5	1236.41	17.54	0.08	1278.85	1221.95	42.89	0.07
6	1359.86	16.44	1.71	1511.28	1279.81	176.97	6.25
7	1523.82	18.79	0.10	1571.07	1512.24	42.49	0.10
8	1646.30	16.6	3.23	1880.66	1572.04	220.13	7.81

9	2164.20	20.95	0.12	2213.39	1881.62	223.24	0.52
10	2272.22	20.91	0.18	2334.91	2214.35	81.73	0.24
11	2926.11	15.15	1.69	3001.34	2335.87	490.66	4.834
12	3378.43	10.35	6.60	3717.92	3002.30	641.97	89.56
13	3742.99	17.51	0.14	3799.89	3718.88	61.05	0.15
14	3864.51	17.53	0.34	3986.99	3800.86	139.98	0.74
15	4035.22	17.81	0.03	4134.55	3987.96	109.78	0.05
16	4692.97	16.95	0.01	4700.68	4135.52	428.80	0.03

Appendix 34: Spectrograph of Acetylated Mango kernel (sample 16)

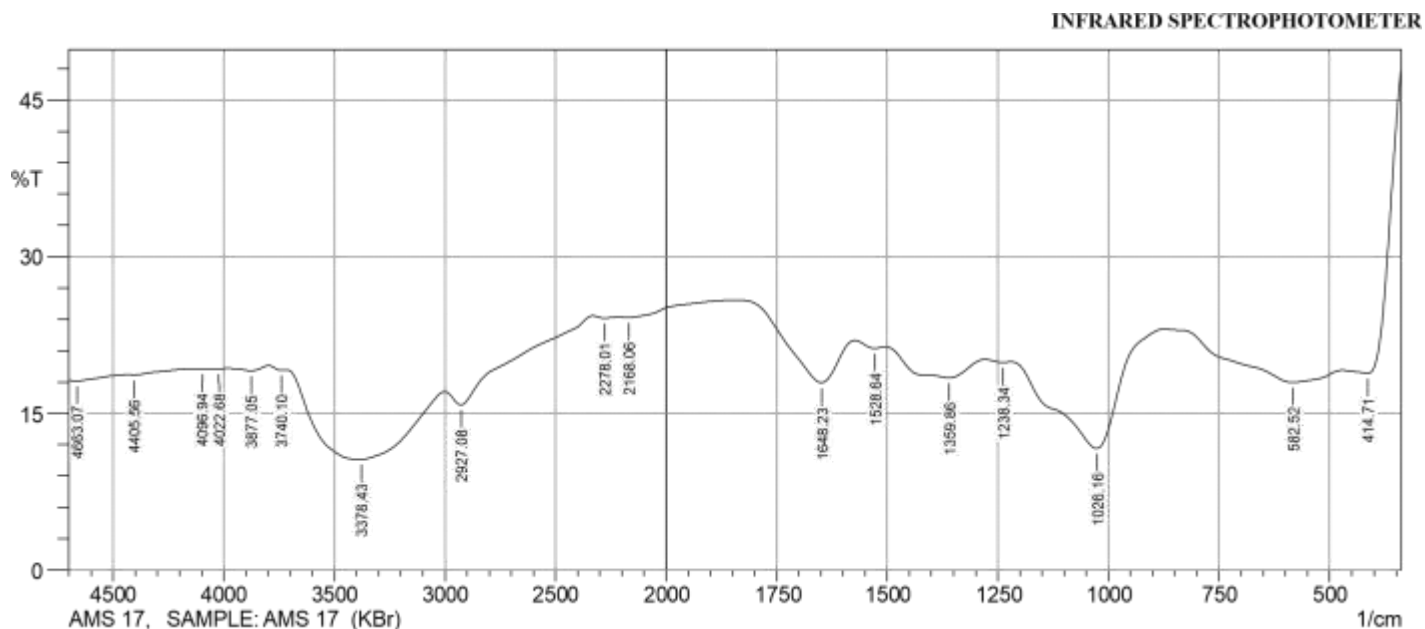


FTIR ANALYSIS RESULT NARICT,ZARIA FTIR- 8400S FOURIER TRANSFORM

	Peak	Intensity	Corr. Intensity	Base (H)	Base (L)	Area	Corr. Area
1	404.10	15.82	19.41	471.61	339.48	87.22	19.80
2	548.77	18.12	1.07	830.38	472.58	254.97	5.66
3	851.60	21.87	0.02	868.00	831.35	24.19	0.00
4	1023.27	14.88	6.63	1278.85	868.96	298.82	24.21
5	1362.75	19.71	0.46	1402.30	1279.81	85.34	0.67
6	1422.55	19.80	0.28	1500.67	1403.26	67.45	0.39
7	1525.74	21.07	0.33	1578.79	1501.63	51.75	0.28
8	1649.19	19.74	2.71	1889.34	1579.75	202.17	5.80
9	2173.85	23.82	0.08	2215.32	1890.30	201.00	0.30

10	2273.19	23.76	0.29	2338.77	2216.28	76.13	0.35
11	2926.11	18.62	1.51	3000.37	2339.73	442.34	5.63
12	3386.15	14.88	5.23	3711.17	3001.34	551.50	56.36
13	3742.03	20.43	0.24	3797.00	3712.13	58.24	0.22
14	3858.72	20.50	0.43	4013.03	3797.96	146.77	0.80
15	4049.68	21.00	0.02	4118.16	4014.00	70.57	0.02
16	4146.13	21.04	0.00	4150.95	4119.12	21.55	0.00
17	4673.68	20.24	0.06	4700.68	4151.91	376.05	0.15

Appendix 35: Spectrograph of Acetylated Mango kernel (sample 17)

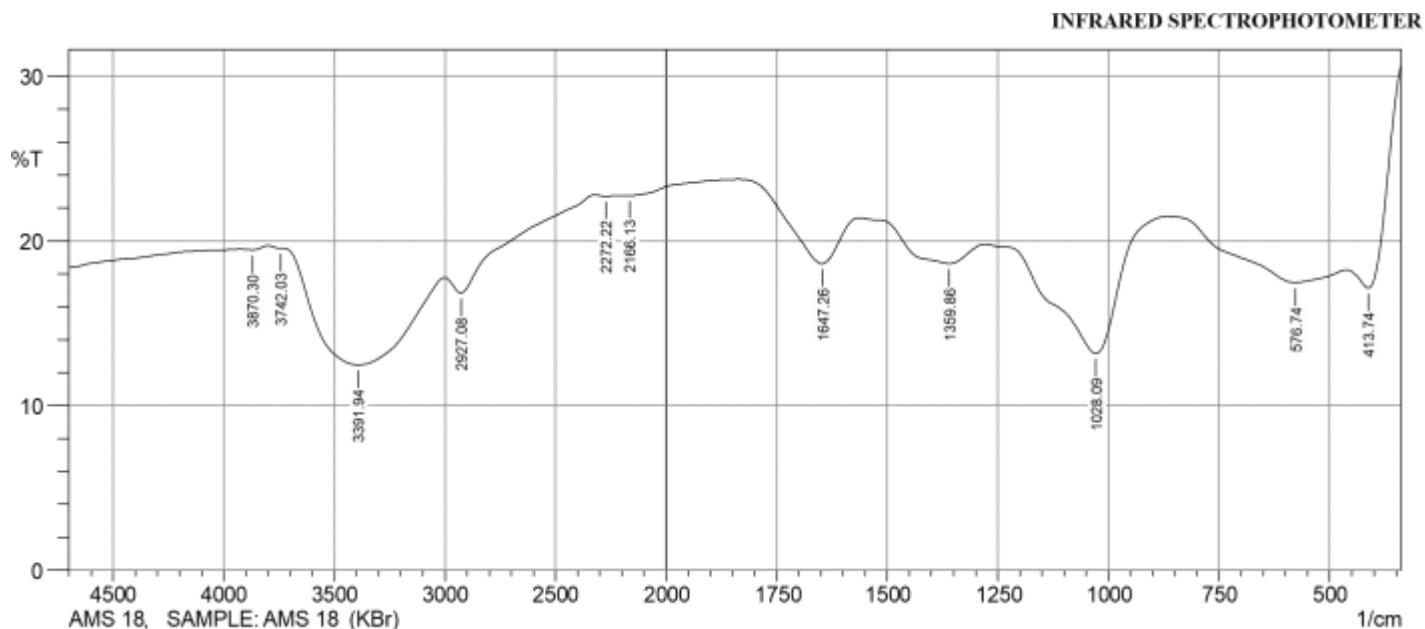


FTIR ANALYSIS RESULT NARICT,ZARIA FTIR- 8400S FOURIER TRANSFORM

	Peak	Intensity	Corr. Intensity	Base (H)	Base (L)	Area	Corr. Area
1	414.71	18.83	12.48	469.68	339.48	81.51	14.17
2	582.52	17.95	2.27	872.82	470.65	282.50	10.22
3	1026.16	11.63	10.05	1219.05	873.78	268.14	37.29
4	1238.34	19.89	0.12	1277.88	1220.02	40.47	0.09
5	1359.86	18.40	2.20	1503.56	1278.85	160.52	7.10
6	1528.64	21.23	0.37	1573.00	1504.53	45.74	0.28
7	1648.23	17.94	5.14	1837.26	1573.97	175.37	11.58
8	2168.06	24.19	0.23	2214.35	1838.22	226.95	0.88
9	2278.01	24.11	0.17	2331.05	2215.32	71.33	0.18

10	2927.08	15.81	2.07	3000.37	2332.02	466.46	5.42
11	3378.43	10.61	7.57	3715.02	3001.34	630.80	100.95
12	3740.10	19.12	0.18	3797.00	3715.99	57.91	0.17
13	3877.05	19.09	0.37	3975.42	3797.96	126.98	0.76
14	4022.68	19.29	0.01	4057.40	3976.39	57.89	0.01
15	4096.94	19.29	0.01	4128.77	4058.36	50.31	0.01
16	4405.56	18.68	0.08	4436.42	4129.73	221.25	0.13
17	4663.07	18.09	0.15	4700.68	4437.39	193.66	0.35

Appendix 36: Spectrograph of Acetylated Mango kernel (sample 18)

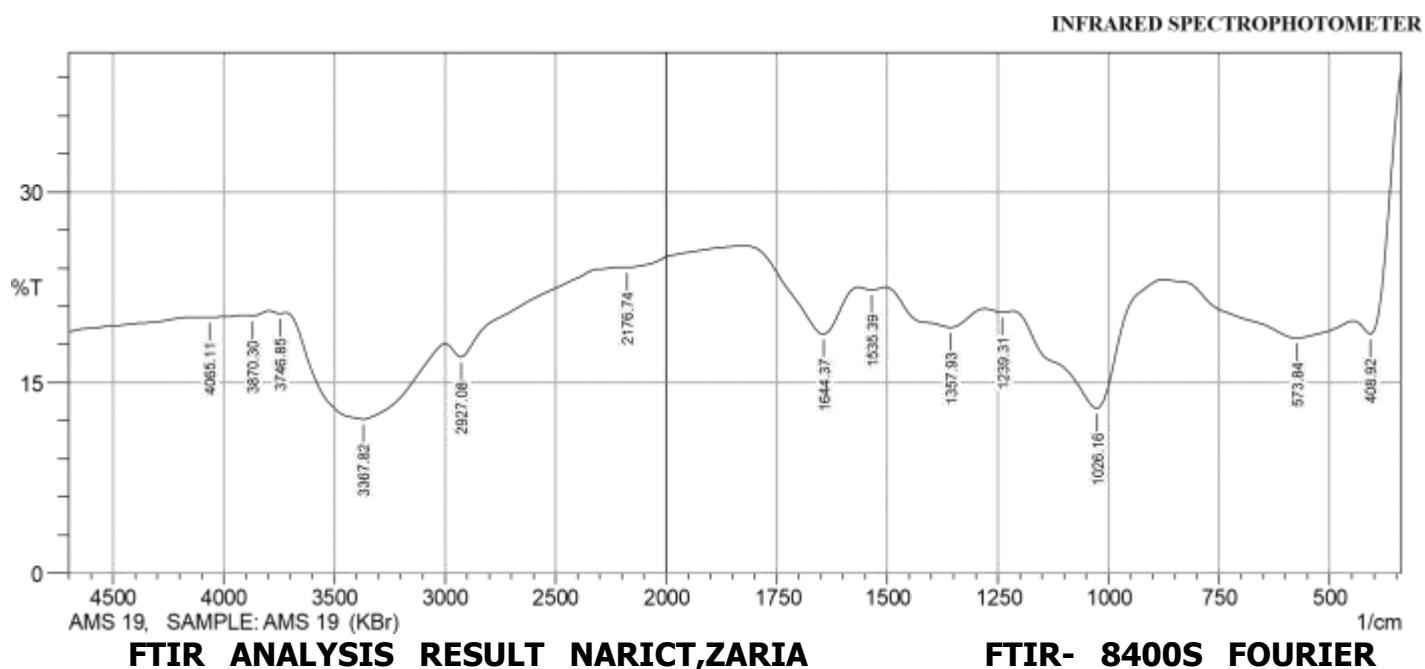


FTIR ANALYSIS RESULT NARICT,ZARIA FTIR- 8400S FOURIER TRANSFORM

	Peak	Intensity	Corr. Intensity	Base (H)	Base (L)	Area	Corr. Area
1	413.74	17.15	5.96	461.00	339.48	83.74	7.82
2	576.74	17.478	1.69	866.07	461.97	292.18	8.16
3	1028.09	13.16	7.67	1277.88	867.03	311.07	29.47
4	1359.86	18.63	1.63	1562.39	1278.85	199.75	5.23
5	1647.26	18.62	3.51	1836.29	1563.36	184.57	8.13
6	2166.13	22.76	0.13	2210.50	1837.26	236.77	0.54
7	2272.22	22.72	0.07	2322.37	2211.46	71.31	0.08
8	2927.08	16.85	1.49	3000.37	2323.34	472.99	3.44
9	3391.94	12.48	6.26	3727.56	3001.34	604.86	75.17

10	3742.03	19.55	0.04	3797.96	3728.53	49.13	0.04
11	3870.30	19.44	0.14	3925.27	3798.93	89.59	0.21

Appendix 37: Spectrograph of Acetylated Mango kernel (sample 19)



TRANSFORM

	Peak	Intensity	Corr. Intensity	Base (H)	Base (L)	Area	Corr. Area
1	408.92	18.83	7.97	446.54	339.48	67.09	8.14
2	573.84	18.51	2.32	875.71	447.50	297.48	11.13
3	1026.16	12.97	9.05	1215.19	876.68	254.83	31.19
4	1239.31	20.54	0.16	1278.85	1216.16	42.96	0.12
5	1357.93	19.35	2.06	1503.56	1279.81	155.05	6.35
6	1535.39	22.29	0.22	1565.29	1504.53	39.49	0.14

7	1644.37	18.82	4.68	1824.72	1566.25	169.90	10.16
8	2176.74	24.07	0.14	2206.64	1825.68	230.60	0.81
9	2927.08	17.02	1.57	2997.48	2207.60	533.71	3.29
10	3367.82	12.12	7.19	3717.92	2998.44	601.01	86.02
11	3746.85	20.44	0.12	3796.04	3718.88	53.08	0.10
12	3870.30	20.26	0.17	3909.84	3797.00	77.94	0.24
13	4065.11	20.15	0.06	4123.95	3910.8	148.09	0.20